ALFRED-WEGENER-INSTITUT
HELMHOLTZ-ZENTRUM FÜR POLAR-
UND MEERESFORSCHUNG

697
2016

Berichte
zur Polar- und Meeresforschung

Reports on Polar and Marine Research

Studies of Polygons in Siberia and Svalbard

Edited by

Lutz Schirrmeister, Liudmila Pestryakova, Andrea Schneider

and Sebastian Wetterich

HELMHOLTZ
GEMEINSCHAFT

Die Berichte zur Polar- und Meeresforschung werden vom Alfred-Wegener-Institut, Helmholtz-Zentrum für Polar- und Meeresforschung (AWI) in Bremerhaven, Deutschland, in Fortsetzung der vormaligen Berichte zur Polarforschung herausgegeben. Sie erscheinen in unregelmäßiger Abfolge.

Die Berichte zur Polar- und Meeresforschung enthalten Darstellungen und Ergebnisse der vom AWI selbst oder mit seiner Unterstützung durchgeführten Forschungsarbeiten in den Polargebieten und in den Meeren.

Die Publikationen umfassen Expeditionsberichte der vom AWI betriebenen Schiffe, Flugzeuge und Stationen, Forschungsergebnisse (inkl. Dissertationen) des Instituts und des Archivs für deutsche Polarforschung, sowie Abstracts und Proceedings von nationalen und internationalen Tagungen und Workshops des AWI.

Die Beiträge geben nicht notwendigerweise die Auffassung des AWI wider.

The Reports on Polar and Marine Research are issued by the Alfred Wegener Institute, Helmholtz Centre for Polar and Marine Research (AWI) in Bremerhaven, Germany, succeeding the former Reports on Polar Research. They are published at irregular intervals.

The Reports on Polar and Marine Research contain presentations and results of research activities in polar regions and in the seas either carried out by the AWI or with its support.

Publications comprise expedition reports of the ships, aircrafts, and stations operated by the AWI, research results (incl. dissertations) of the Institute and the Archiv für deutsche Polarforschung, as well as abstracts and proceedings of national and international conferences and workshops of the AWI.

The papers contained in the Reports do not necessarily reflect the opinion of the AWI.

Herausgeber
Dr. Horst Bornemann

Redaktionelle Bearbeitung und Layout
Birgit Reimann

Editor
Dr. Horst Bornemann

Editorial editing and layout
Birgit Reimann

Alfred-Wegener-Institut
Helmholtz-Zentrum für Polar- und Meeresforschung
Am Handeshafen 12
27570 Bremerhaven
Germany

www.awi.de
www.reports.awi.de

Alfred-Wegener-Institut
Helmholtz-Zentrum für Polar- und Meeresforschung
Am Handeshafen 12
27570 Bremerhaven
Germany

www.awi.de
www.reports.awi.de

Titel: Tundra mit Polygontümpeln am Ufer des Naumskoe See im Kolymadelta in Nordostsibirien (Foto: F. Kienast, Senckenberg Weimar).
Cover: Tundra with merging polygon ponds at the Naumskoe Lake shore in the Kolyma Delta in northeastern Siberia (photograph: F. Kienast, Senckenberg Weimar).

Studies of Polygons in Siberia and Svalbard

Edited by

Lutz Schirrmeister, Liudmila Pestryakova, Andrea Schneider

and Sebastian Wetterich

The expeditions Kytalyk – Pokhodsk 2012, Pokhodsk 2013 and Adventdalen 2013

Please cite or link this publication using the identifiers

hdl:10013/epic.47333 or http://hdl.handle.net/10013/epic.47333 and

doi:10.2312/BzPM_0697_2016 or or http://doi.org/10.2312/BzPM_0697_2016

ISSN 1866-3192

Contents

Joint Russian - German Polygon Project East Siberia 2011 - 2014

ARCTIC CIRCLE

AWI EMAU MSU StPSPU UHH YSU

June 30 – September 05, 2012
July 14 – August 05, 2013
Kytalyk, Indigirka Lowland, eastern Siberia
Pokhodsk, Kolyma Delta, eastern Siberia

Russian expedition leaders:

Prof. Lyudmila Pestryakova
Yakutsk Federal University
Belinsky st., 58, 677000 Yakutsk, Russia

Dr. Vladimir Tumskoy
Department of Geocryology, Faculty of Geology,
Moscow State University
Vorob`evy Gory, 119992 Moscow, Russia,

German expedition leader:

Dr. Lutz Schirrmeister
Alfred Wegener Institute for Polar and Marine Research
Department of Periglacial Research
Telegrafenberg A5, 14473 Potsdam, Germany

CONTENT

1. INTRODUCTION

Lyudmila Pestryakova & Lutz Schirrmeister

1.1 Scientific motivation

Polygonal tundra, thermokarst basins and pingos are common and characteristic periglacial features of arctic lowlands underlain by permafrost in Northeast Siberia. Modern polygonal mires are in the focus of biogeochemical, biological, pedological, and cryolithological research with special attention to their carbon stocks and greenhouse-gas fluxes, their biodiversity and their dynamics and functioning under past, present and future climate scenarios. Within the frame of the joint German-Russian DFG-RFBR project *Polygons in tundra wetlands: state and dynamics under climate variability in Polar Regions (POLYGON)* field studies of recent and of late Quaternary environmental dynamics were carried out in the Indigirka lowland and in the Kolyma River Delta in summer 2012 and summer 2013.

Using a multidisciplinary approach, several types of polygons and thermokarst lakes were studied in different landscapes units in the Kolyma Delta in 2012 around the small fishing settlement Pokhodsk (Fig. 1-1). The floral and faunal associations of polygonal tundra were described during the fieldwork (chapters 4, 10). Ecological, hydrological, meteorological, limnological (chapters 3, 4, 5), pedological (chapter 7) and cryological (chapters 8, 9) features were studied in order to evaluate modern and past environmental conditions and their essential controlling parameters. The ecological monitoring and collection program of polygonal ponds (chapter 3) were undertaken as in 2011 in the Indigirka lowland by a former POLYGON expedition (Schirrmeister et al. [eds.] 2012). Exposures, pits and drill cores in the Kolyma Delta were studied to understand the cryolithological structures of frozen ground and to collect samples for detailed paleoenvironmental research of the late Quaternary past (chapters 8, 9). Dendrochronological and ecological studies were carried out in the tree line zone south of the Kolyma Delta (chapter 11). Based on previous work in the Indigirka lowland in 2011 (Schirrmeister et al. [eds.] 2012), the environmental monitoring around the Kytalyk research station was continued until the end of August 2012 (chapter 12; Fig. 1-1). In addition, a classical exposure of the late Pleistocene permafrost at the Achchaygy Allaikha River near Chokurdakh was studied (chapter 12). The ecological studies near Pokhodsk were continued in 2013 (chapter 13). Other fieldwork took place at the Pokhodsk-Yedoma-Island in the northwestern part of the Kolyma Delta (chapter 14).

Our studies were realized in co-ordination with Dutch groups from the Vrije Universiteit, Faculty of Earth and Life Sciences in Amsterdam, and the North-Eastern Federal University Yakutsk. This report contains the systematic description and documentation of field data and observations with all basic information for future analysis of sample collections and interpretation of field data.

Fig. 1-1: Position of the study areas Kytalyk in the Indigirka lowland and Pokhodsk in the Kolyma Delta - marked by red stars. DEM compiled by G. Grosse (AWI Potsdam).

1.2 Expedition itinerary and general logistics

The first period of fieldwork from July 2nd to July 11th 2012 in the vicinity of the Kytalyk station and at the Achchagy Allaikha River was performed by V. Tumskoy (Moscow State University), A. Schneider and L. Schirrmeister (both AWI Potsdam). The expedition group started in Moscow and reached Chokurdakh via Yakutsk by airplane. From Chokurdakh the travel to the Kytalyk research station was continued by motorboat. The second field period from July 13th to August 31st 2012 to Pokhodsk was performed by a large group of in total 10 German and 8 Russian colleagues (Tab. 1-1, Fig. 1-2, A 1-1), who worked in different groups and periods there. Parallel to the field work of the POLYGON project a larger group from the Institute of Biological Problems of the Cryolithosphere (IBPC, RAS SB) and of the North-Eastern Federal University Yakutsk lead by Mikhail Cherosov worked on modern flora and fauna.
The third field period was carried out between July 17th and August 1st 2013 in Pokhodsk and the Kolyma Delta by S. Wetterich and L. Schirrmeister (Tab. 1-2, Fig. 1-3).
The expedition would not have been successfully without the support of several Russian and German institutions and authorities. In particular, we would like to thank the Committee of Nature Conservation in Chokurdakh (Tatyana Gavrilovna), the ladies from the Pokhodsk administration, the famous Arbatsky family in Pokhodsk, the North-Eastern Federal University (Mikhail Cherosov), the colleagues from the Northeast Science Station in Cherskii and Alexey Pestryakov, our most important logistic support in Yakutsk.

Tab. 1-1: Time table of the expedition *Kytalyk - Pokhodsk 2012*.

Date	Location	Activity
30.06. 2012	Moscow	Departure of the 1st group
01.07. 2012	Yakutsk	Arrival of the 1st group
01./02.07. 2012	Yakutsk	Expedition preparation
02.07. 2012	Yakutsk to Chokurdakh	Travel by airplane
02./03.07. 2012	Chokurdakh	Expedition preparation
03.07.2012	Chokurdakh to Kytalyk	Travel by motor boat
03. to 09.07. 2012	Kytalyk	Field work around the Kytalyk Station
09.07.2012	Kytalyk to Chokurdakh	Travel by boat
10.07.2012	Achagy Alaykha	Work at the exposure
11.07.2012	Chokurdakh to Yakutsk	Travel by airplane
12.07.2012	Berlin – Moscow - Yakutsk	Arrival of the 2nd group
13.07. 2012	Yakutsk to Cherskii	Travel of the 1st and the 2nd group by airplane
13.07. 2012	Cherskii to Pokhodsk	Travel by a river vessel
13.07. to 29. 08. 2012	Pokhodsk	Field work around Pokhodsk and Cherskii
01.08. to 03.08. 2012	Moscow – Yakutsk – Cherskii - Pokhodsk	Arrival of the 3rd group by airplane and motor boats
13.08. to 18.08. 2012	Pokhodsk – Cherskii – Yakutsk – Moscow - Berlin	Departure of the first expedition members
29.08. 2912	Pokhodsk to Cherskii	Return of the last group, travel by motor boat
29.08. to 31. 08. 2012	Cherskii	Expedition post processing
31.08. 2012	Cherskii to Yakutsk	Travel by airplane
01.09. to 04.09. 2012	Yakutsk	Expedition post processing
05.09. 2012	Yakutsk – Moscow – Berlin	Departure of the last group

Fig. 1-2: The participants of the expedition *Kytalyk-Pokhodsk 2012*

Tab. 1-2: Time table of the expedition “Pokhodsk 2013”.

Date	Location	Activity
14.07. to 16.07 2013	Berlin – Moscow – Yakutsk – Cherskii	Departure, travel by airplane
16.07. 2013	Cherskii – Pokhodsk	Travel by motor boat
17.07. to 01.08. 2013	Pokhodsk and Pokhodsk Yedoma	Field work
02.08. 2013	Cherskii – Yakutsk	Departure, Travel by airplane
02. to 05.07. 2013	Yakutsk	Expedition post preparation

Fig. 1-3: The participants of the expedition *Pokhodsk 2013*

1.3 Data management

The data and samples collected during the fieldwork are summarized in appendix chapters and referred in the respective report chapters. Field data are prepared for submission to the PANGEA data base (http://www.pangaea.de/) while still ongoing analytical work on samples and following publications will contribute data to PANGEA before submission of the separate papers.

2. STUDY AREA, GEOLOGICAL AND GEOGRAPHICAL CHARACTERISTICS

Vladimir Tumskoy & Lutz Schirrmeister

The study areas of the expeditions *Kytalyk – Pokhodsk 2012* and *Pokhodsk 2013* were predominantly located in the region of the Kolyma Delta (chapters 3 to11 and 13 to 14) and the Lower Kolyma, south of Cherskii (Fig. 2-1). Additionally, the Kytalyk study site near Chodurdakh in the Indigirka lowland from 2011 was revisited in 2012 (see Schirrmeister et al. [eds.], 2012), and the Achchagyi–Allaikha site about 20 km west of Chokurdakh was also studied (chapter 12).

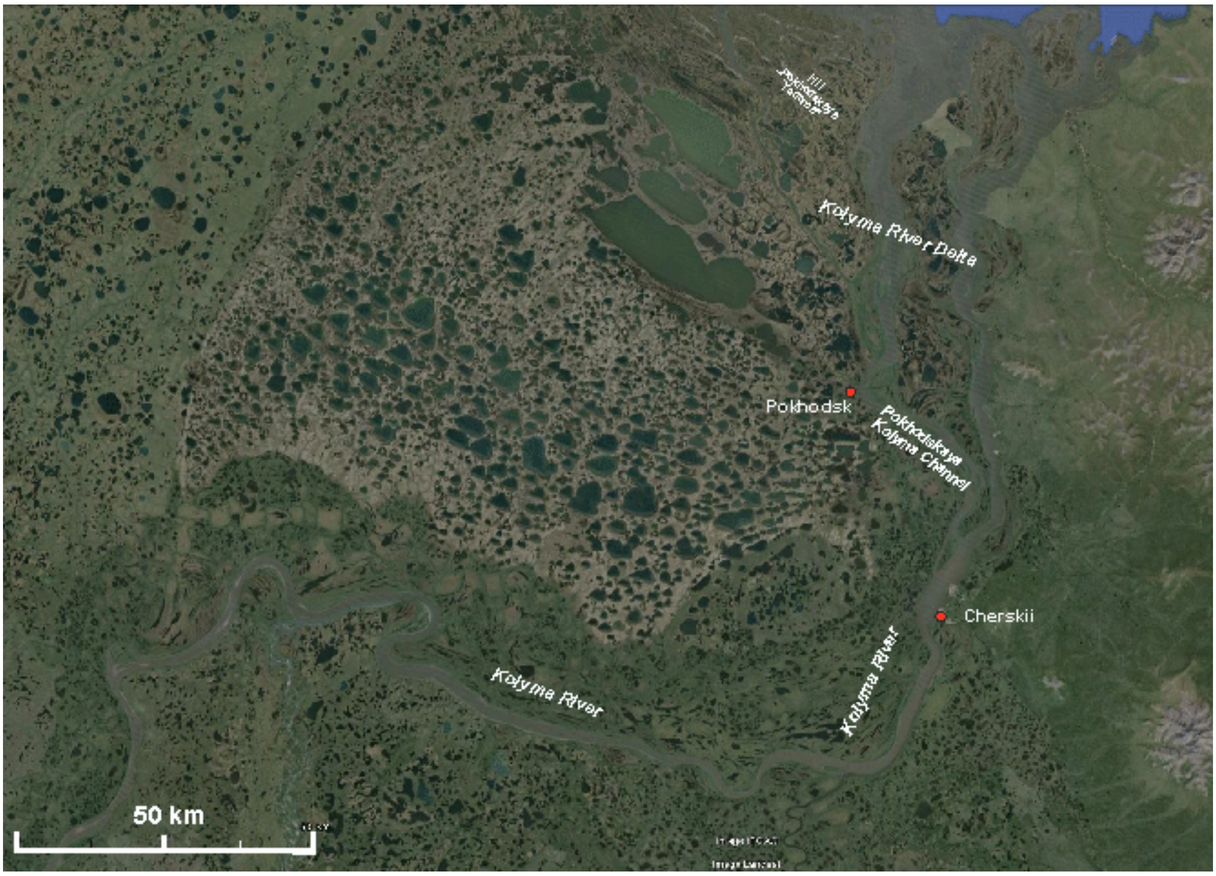

Fig. 2-1: The study region of the Kolyma Delta and the Lower Kolyma River (Google Earth).

According to the Circumpolar Arctic Vegetation Map (CAVM Team, 2003), the study areas in the Kolyma Delta near Pokhodsk and in the lower Kolyma flood plain are described as sedge, moss low-shrub wetland (W3 class) and low shrub tundra (S2 class). According to meteorological data (Cherskii, WMO station no. 25123) the climate conditions are characterized high annual temperature amplitudes and low precipitation (T_{July} +12°C, $T_{January}$ –33.3°C, T_{Mean} -11.6 °C, and p_{ann} 290 mm). The permafrost temperature in the region reaches -5 to –7 °C and the permafrost thickness is mapped to be between 100 to 300 m (Geocryological Map, 1991)

The study region consists of four major landscape units:

- the Kolyma River Delta
- the Kolyma River flood plain
- the flood plain of the Pokhodskaya Viska River (Pokhodsk area)
- the Khalerchinskaya Tundra west of the lower Kolyma R.
- the mountain foothills and floodplains East of the Kolyma R.

According to the State Geological Map of the Russian Federation 1:1,000,000 (map sheet Nizhnekolymsk, Pre-Quaternary Formations, Auslov et al., 1998), the study region is mostly underlain by Neogene soft deposits (e.g. sand, silt, clay, peat, gravels). Only in the Kolyma Delta some small hard rock outcrops are exposed, for example the Cretaceous granodiorit hill of the Pokhodsk Yedoma. The underground is crossed by several faults of NW-SE and ENE-WSW orientation. A major fault runs directly south of Pokhodsk.

The details of the Quaternary map (Fig. 2-2, Ivanenko, 1998) presents late Holocene marine-alluvial deposits (amIV$_2$) in the Kolyma Delta, Early Holocene marine-alluvial deposits (amIV$_1$) in the Pokhodsk area, late Holocene limnic-boggy deposits (lbIV$_2$) in the Khalerchinskaya Tundra, and alluvial deposits in the floodplains of the Kolyma and their tributaries like the Bol'shoy and the Maly Anyuy rivers. Late Pleistocene deposits are not mapped in the study area under consideration. South of Pokhodsk a dashed line marks the supposed extension of the Holocene marine transgression. This line also fits with a major fault line shown in the map of Pre-quaternary deposits.

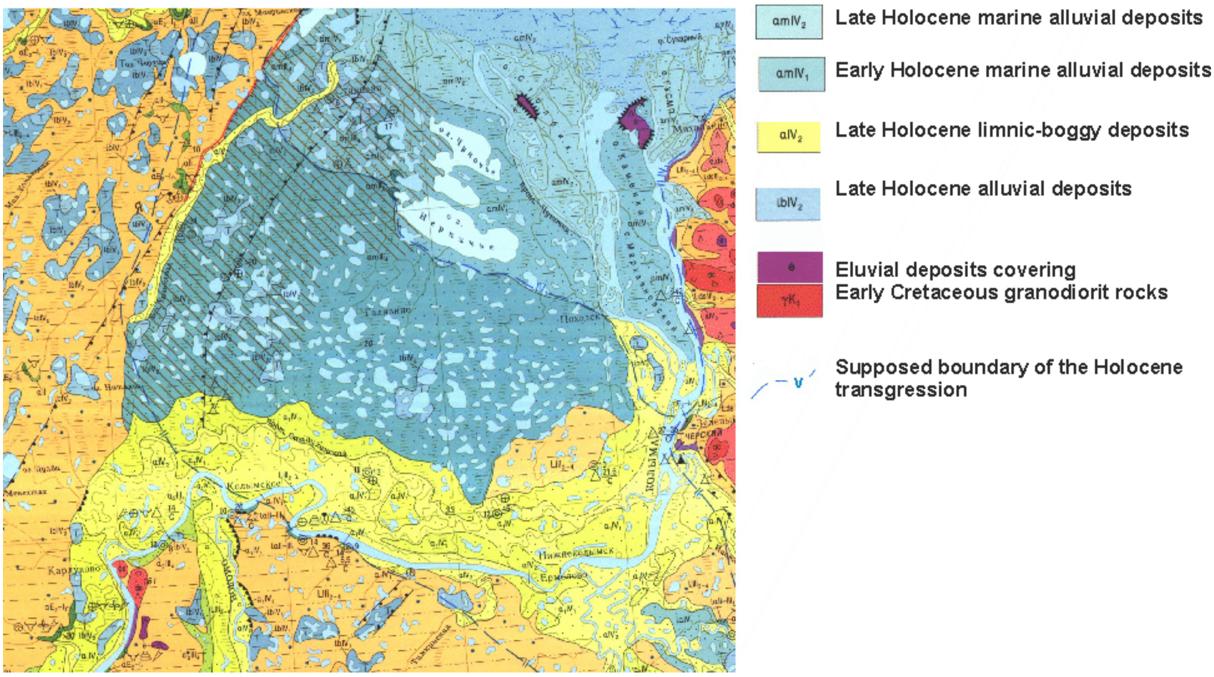

Fig. 2-2: Detail of the geological map of the study region (according to Ivanenko, 1998).

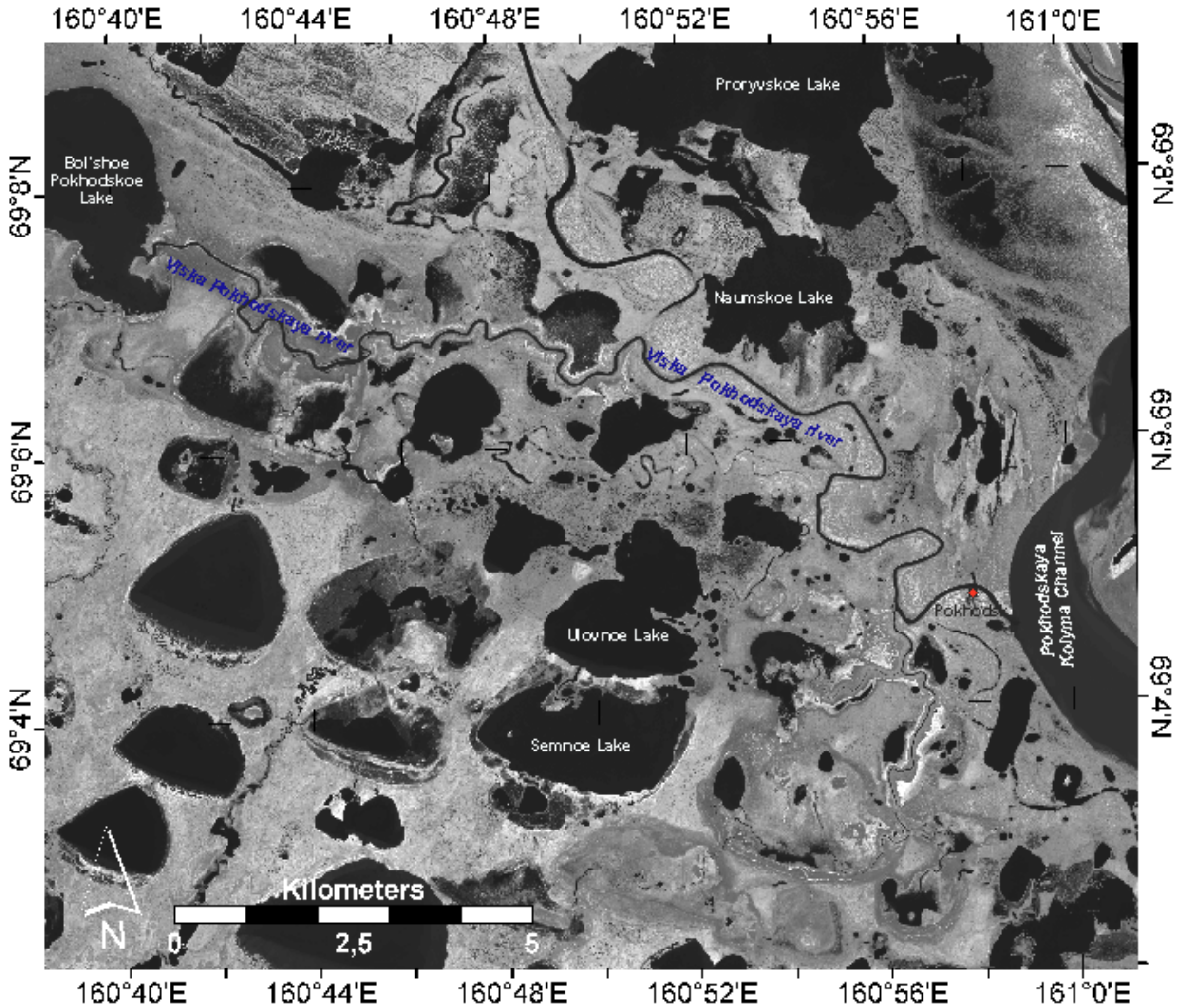

Fig. 2-3: The major study area around Pokhodsk (red dot), (WORLDVIEW image from 28.06.2009, 0.5 m/pixel resolution) Map compiled by Frank Günther and Mathias Ulrich.

In the major study area around Pokhodsk (Fig. 2-3), the monitoring program in one low-centered polygon was carried out (chapter 3) as well as the detailed botanical, active layer and surface survey of one model polygon (chapter 6) and the comprehensive botanical (chapter 10), ecological and limnological survey of polygon ponds (chapter 4) and thermokarst lakes (chapter 5). In addition, exemplary polygon sites were selected for pedological analyses (chapter 7) and permafrost exposures (chapter 8), pits and short permafrost cores (chapters 4) were studied here. The coordinates of each site are summarized in appendix 2. Each kind of study sites (e.g. ecological, limnological, pedological, drill points) have a specific signature, presented in Fig. 2-4. Because of the high concentration of study points, two sites, the so-called “Polygon site” and the “Pingo site” are additionally presented in zoom-in maps (Fig. 2-5 and 2-6).

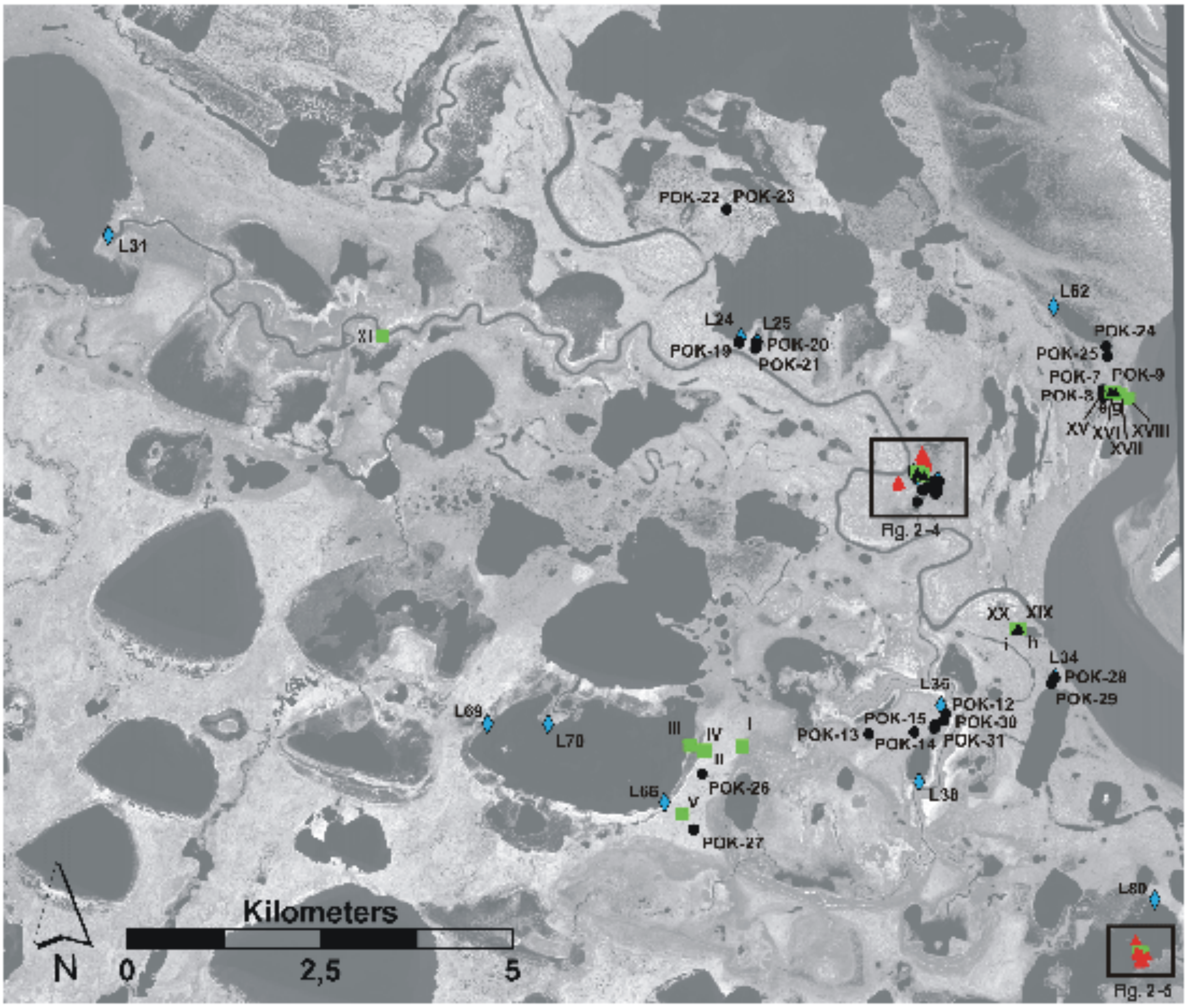

POK 1 to 31: Ecological study sites (Chapter 4)

L 4, L 6, L 8 ...: Limnological study sites (Chapter 5)

MNP (mnogo polok): Model polygon (Chapter 6)

P1 to P40; Pi01 to Pi14; 1, 2, 3 ...: Pedological study sites (Chapter 7, 8)

I to XXI: Drill holes and pits (Chapter 7, 9)
I: 12P-2007-1; II: 12P-2007-2; III: 12P-2007-3; IV: 112P-2007-4; V: 12P-1008; VI: 12P-1908-A; VII: 12P-2008-A; VIII: 12P-2008-1; IX: 12P-2208-1; X: 12P-2208-B, XI: 12P-2308-A, XII: 12P-1607-1 (POK1 W); XIII: 12P-1707-1 (POK1 C); XIV: 12P-1907-1 (POK3 W), 12P-1907-2 (POK3 C); XV: 12P-2107-1 (POK4 W), 12P-2107-2 (POK4 C); XVI: 12P-2707-1 (POK5); XVII: 12P-2707-2; XVIII: 12P-2707-3; XIX: 12P-3007-1 (POK7); XX: 12P-3007-2 (POK8); XXI: 12P-2507-1, 12P0708-1

Fig. 2-4: Overview of the study sites (map compiled by Mathias Ulrich). The legend is also valid for Figs. 2-5 and 2-6.

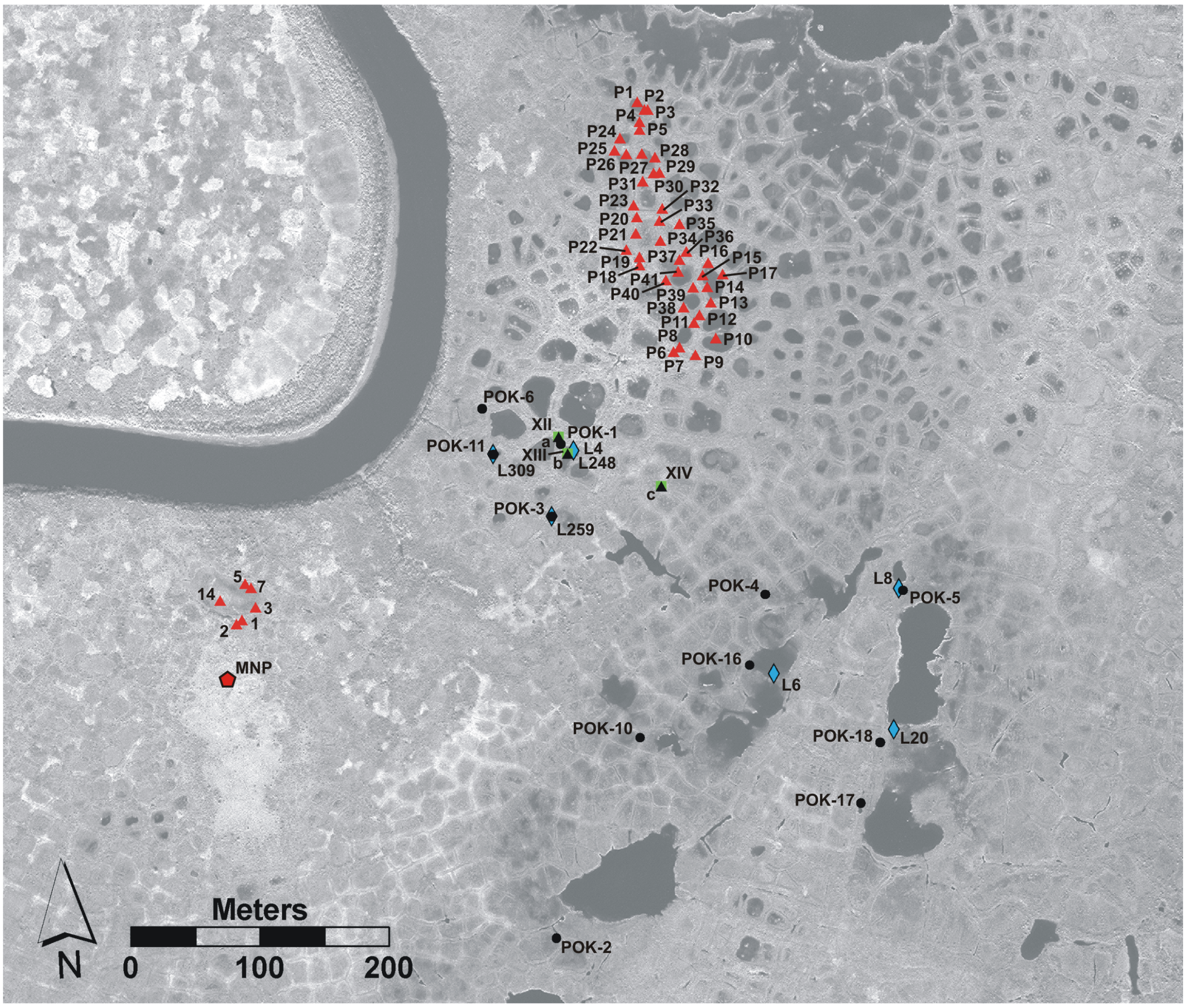

Fig. 2-5: Study area of the so-called "Polygon site" (see chapters 2, 4, 5, 7, 9, 10). For legend see Fig. 2-4.

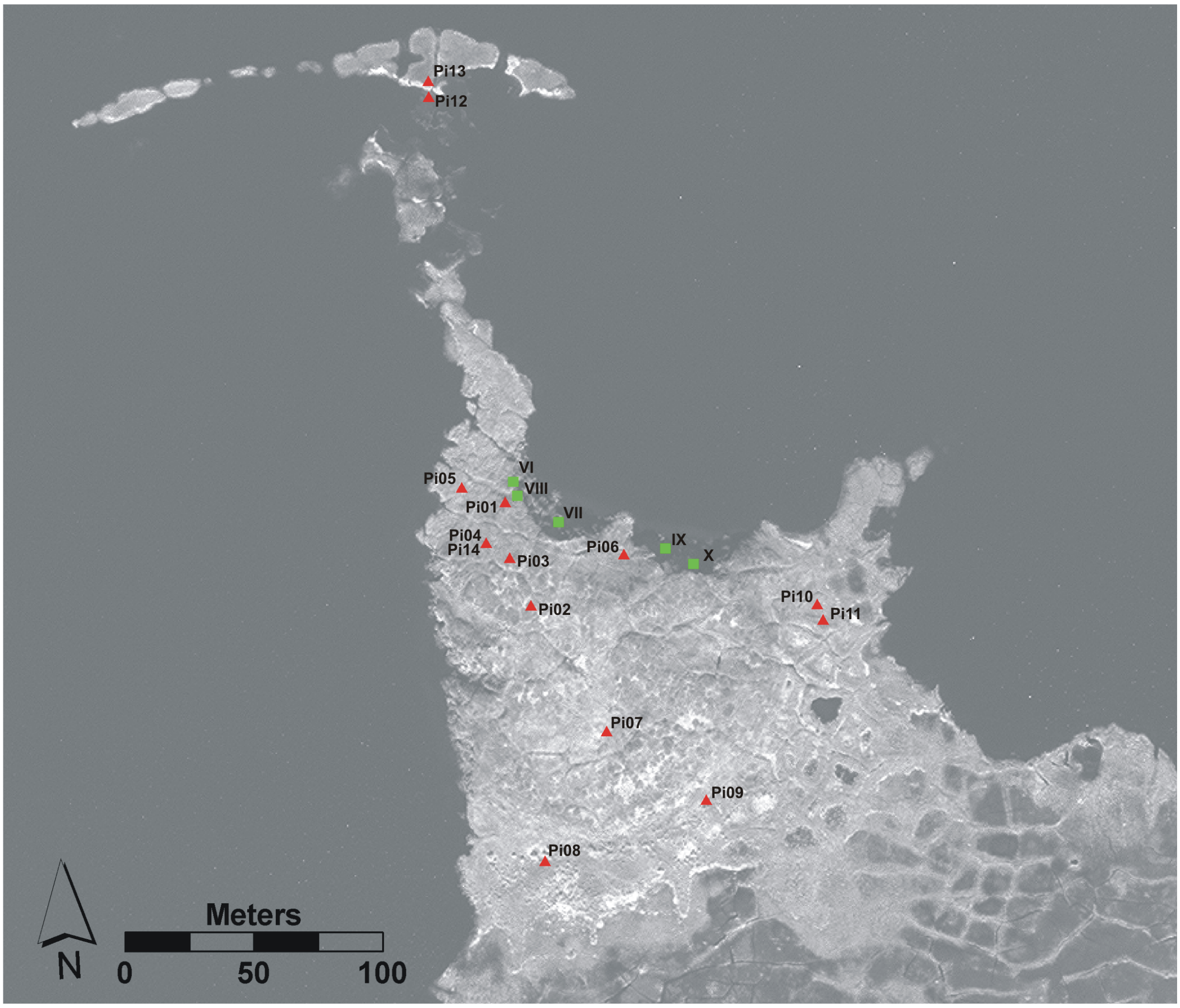

Fig. 2-6: Study area of the pingo called Shirokovsky Kholm (see chapter 8). For legend see Fig. 2-4.

3. MONITORING OF A POLYGON SITE (POK-01)

Andrea Schneider, Lutz Schirrmeister & Sebastian Wetterich

3.1 Site description and scheme

The monitoring site POK-01 (69.09510°N, 160.93877°E, Figs. 3-1, 3-2, 3-3) is located in the Viska floodplain and is part of a low-center polygon field. We selected a typical intrapolygon pond in order to investigate its present-day abiotic and biotic conditions. Hummocky polygon rims and frost cracks enclose the 20 x 17 m wide pond. The pond substrate is composed of fine dispersed organic mud with weakly decomposed plant material. The material floated, but was still submerged ca. 20 cm below the water table.

Fig. 3-1: Photograph of the monitored pond POK-01.

We visited the monitoring site every six to seven days to collect the following data and sample packages:

- Water and air temperature,
- Active layer depth,
- Water depth,
- Water samples for measurements of alkalinity, acidity, oxygen content, total water hardness, electrical conductivity, pH, cations, anions, isotopic composition and nutrients,
- Substrate sample,
- Ostracodes (approx. 100 individuals per sample),
- Macrozoobenthos,
- Phytoplankton and Zooplankton.

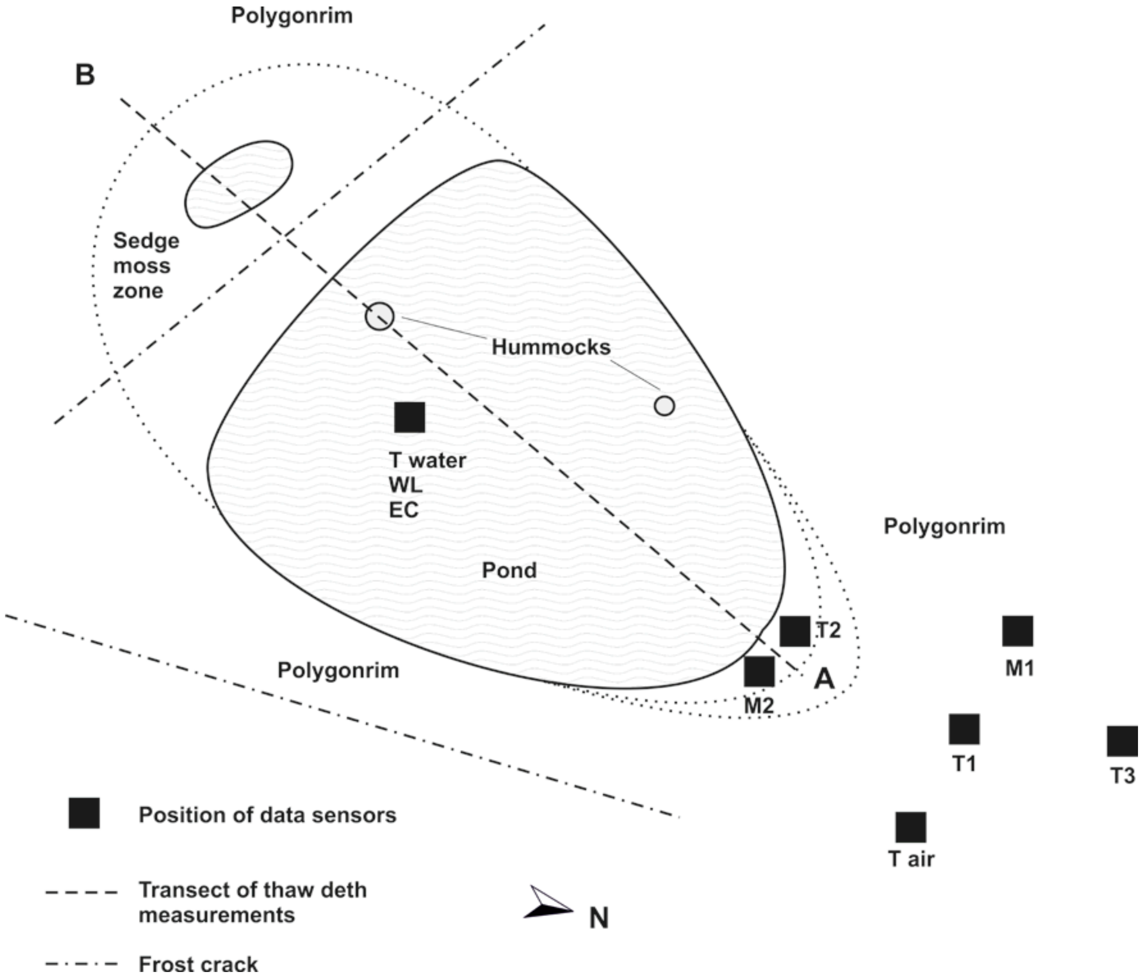

Fig. 3-2: Site scheme (top view) and location of all data sensors. The line AB marks the position of a ground surface, active layer and vegetation survey (see chapter 3.5).

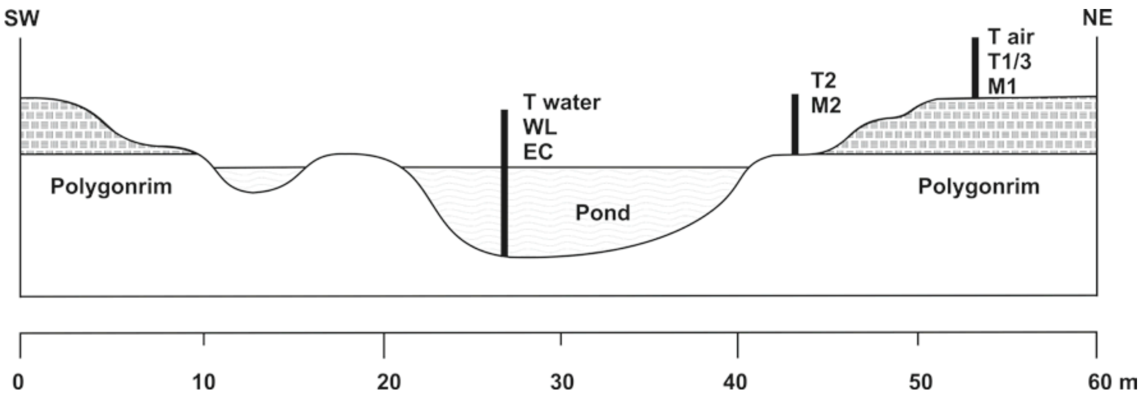

Fig. 3-3: Profile of the monitoring site with data logger markers.

Furthermore, data sensors were installed between 16 July and 25 August 2012 in order to receive continuous data-sets from ground, water and meteorological conditions (A 3-1, Fig. 3-2 to 3-6). We installed sensors for ground temperature (T1 - T3) and soil moisture conditions (M1 and M2). Sensors T1 and M1 were installed on the dry upper polygon rim, sensors T2 and M2 were installed on the lower polygon rim near the pond margin. This part of the rim was moist and vegetated predominantly with mosses. Sensor T3 is located in a permafrost drill hole of 95 cm depth (chapter 9). The borehole was refilled with its original (frozen) material after instrumentation. In the pond electrical conductivity (EC), water level (WL) and water temperature (Tw) were recorded. The EC and WL sensor included additional temperature sensors. Air temperature (Ta) was measured in 2 m height on the wall between both polygons.
All data loggers measured their specific value every 15 (air temperature, water temperature, EC) or 30 minutes (water level, ground temperature, soil moisture) to provide a daily resolution. Temperature sensors have been calibrated at AWI Potsdam by putting them into icy water for 24 hours.
To reduce disturbing influences from the logger boxes lying directly on the ground surface we set them up in little distance depending on the length of the cables and closed the pit carefully. According to the manufacturer the logger systems are said both waterproof and cold resistant from -30 to +50°C. But to prevent any kind of data loss due to technical problems both cables and connectors were wrapped in PE-bags and fixed with tape additionally.

3.2 Recorded meteorological, limnological and ground conditions

The recorded air and water temperatures (Fig. 3-4 a) behave parallel and show similar patterns during the monitored time period. The mean air temperature was 7.4°C, with a range of min. - 1.1°C and max. + 23.1°C. Diurnal fluctuations of the water column exceed 10°C in the upper 20 cm water depth. The water temperature in 60 cm water depth below the floated pond substrate is close to 0° in the beginning of the monitored time period and reaches 2-3°C at its end. Daily fluctuations are absent.
Both air and water temperatures seem to correspond to variations in EC of the shallow pond water body (Fig. 3-4 b). The EC ranges between 50 and 97 µS/cm and shows clear diurnal fluctuations. EC is high during warm and low at cooler days.
The pond water level was calculated from differences in air pressure and water pressure records. Air pressure records from Cherskii were available in three- to six-hour intervals (WMO 25123). The water depth increased quickly from about 200 mm to 300 mm at the end of July. In August, the water level was still rising, but much slower compared to the end of July.
Water depth and thaw depth in the pond centre behave contrary; while the water depth increased, the thaw depth decreased (Fig. 3-5). This might be related to the submerged floating pond substrate. The water depth relates to the water column above the floating substrate, thaw depth measurements represent the distance between the upper surface of the floating substrate and the permafrost table. Thus, the floating substrate changed its vertical position, mainly due to scientists stepping and working in the pond. The thaw depth in

the moist lower and dry upper polygon rim is similar over the summer season; but at the end of august the curves diverge slightly.

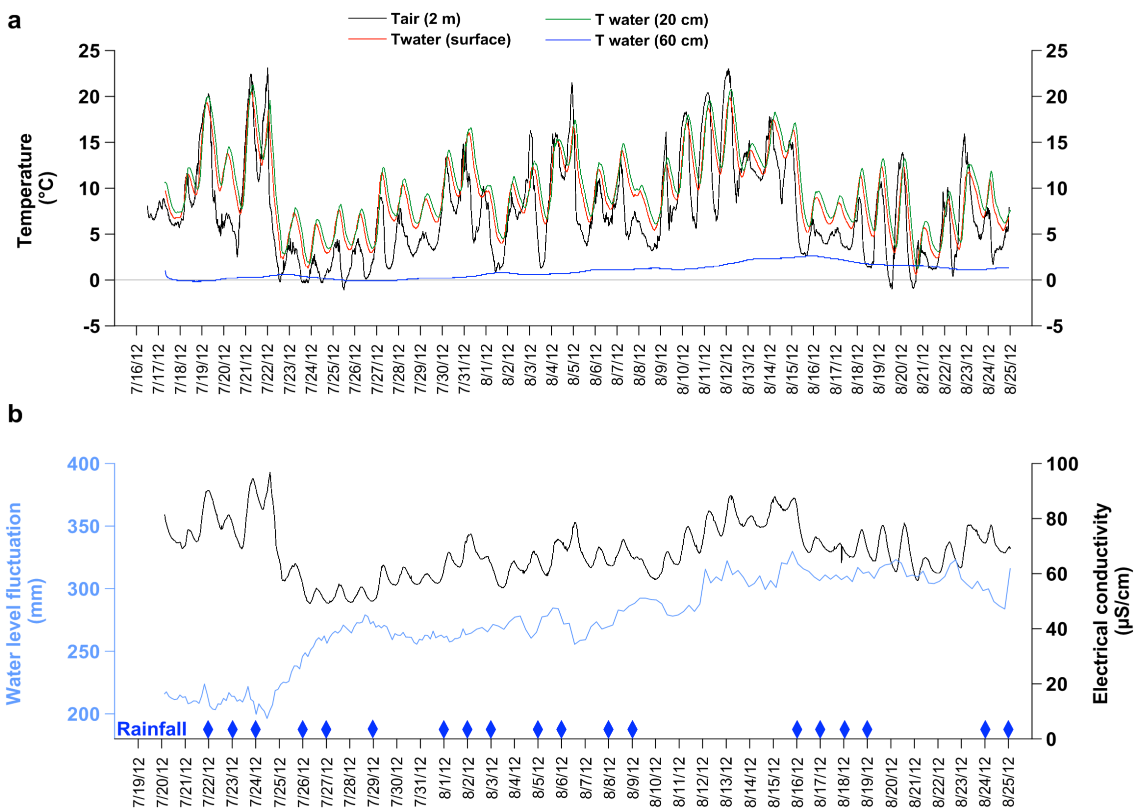

Fig. 3-4: **(a)** Air and water temperatures, **(b)** water level and EC at the monitoring site POK-01 from July 16 until August 25, 2012. Depth information for water temperatures are below water surface, for air temperature above the ground surface. Blue diamonds indicate rainfall days.

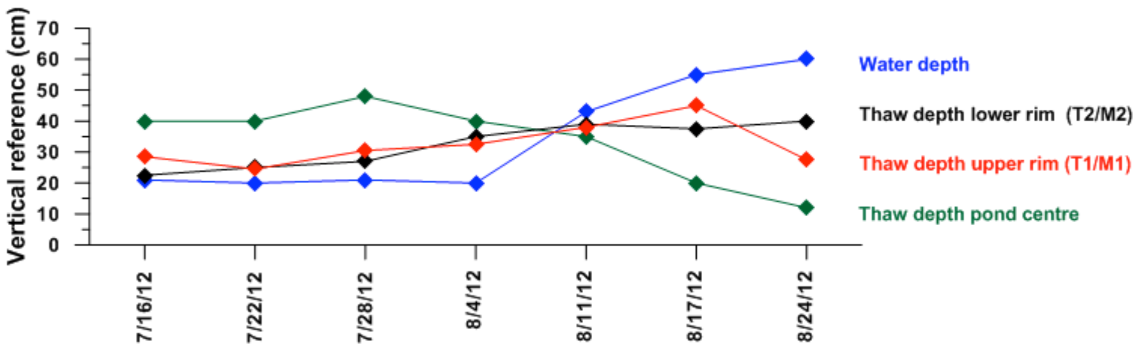

Fig. 3-5: Water and thaw depths at the monitoring site POK-01.

The data derived from the soil moisture sensors shown in figure 3-6 reflect the driest conditions in the uppermost soil layers of 2 – 5 cm depth, interrupted by some short-term events which point to abruptly increasing surface moisture (rainfall). Sensor M1 (Fig. 3-6), installed on the upper polygon rim, reflects largely constant largely constant moisture conditions in different soil horizons. The volumetric water content in the ground did not exceed 0.4 m³/m³. The maximum moisture content was observed in 14 cm depth. In deeper soil horizons, soil moisture content decreased and was lowest in the near-surface horizon.

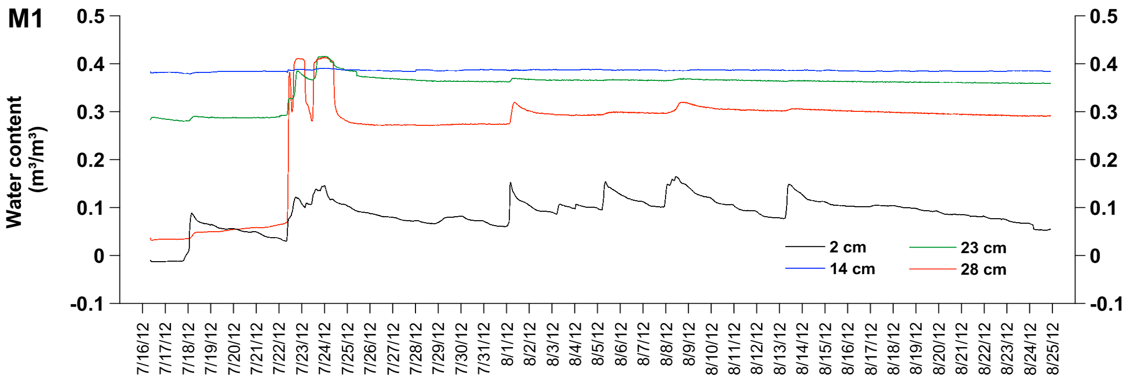

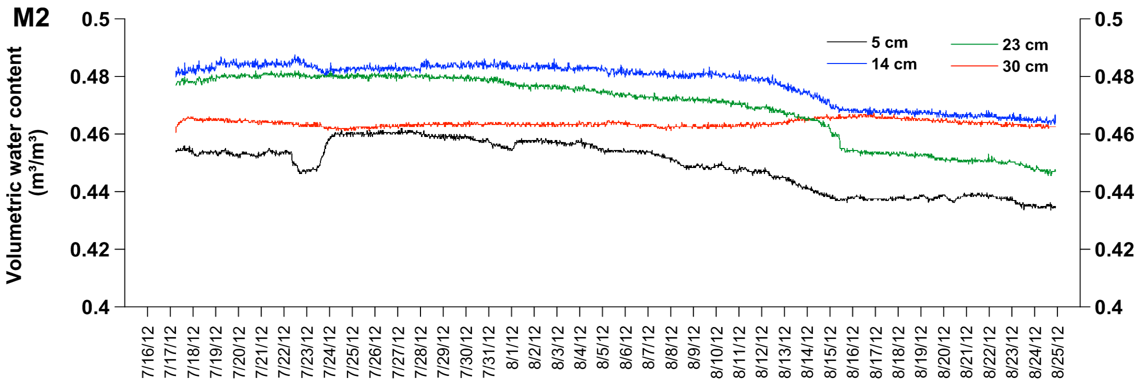

Fig. 3-6: Soil moisture conditions measured in the upper and lower polygon rim of POK-01 from July 17 until August 25, 2012.

Sensor M2 (Fig. 3-6), installed on the lower polygon rim near the pond margin, displayed also largely constant moisture conditions in the different soil horizons, but displays also small-scale variations that were absent in the record from M1. The volumetric water content in the ground was higher than in M1. As observed in M1, the driest conditions were present in the uppermost soil horizon (5 cm), while the highest soil moisture content occurred in 14 cm depth. Furthermore, a decrease in soil moisture was observed in mid August in all depths except in 30 cm, where the water content increased.

Ground temperature records appear to be in relation with the air temperature in the uppermost centimeters (Fig. 3-7, T1 and T2). Sensor T1, installed on the upper polygon rim, recorded ground temperatures in 5 cm depth that are close to the recorded air temperature. The ground temperature in 15 cm depth did not exceed 3.5°C (max: 3.2°C, mean: 1.3°C), shows little variability and weak diurnal fluctuations. In contrast, the lower most sensors in 23 and 31 cm depth recorded soil temperatures constantly close to 0°C (mean 23 cm: 0.16°C, mean 31 cm: -0.11°C). The thaw depth at July 17 was 15 – 30 cm.
Sensor T2 (Fig. 3-7), installed on the lower polygon rim near the pond margin, displays diurnal fluctuations in the uppermost 3 cm but with considerably smaller amplitudes than observed in T1. The ground temperature in 13 cm depth displays weak diurnal fluctuations and clearly reflects periods of warmer

and cooler air temperatures. Temperatures in 23 and 33 cm depth stay below 5°C and reflect periods of warmer and cooler air temperatures. The thaw depth at July 17 was 22 cm on the lower polygon rim.

Ground temperatures in the drill hole (Fig. 3-7, T3) are generally around 0°C for the entire monitored period. The data sensor installed in 25 cm depth reflects temperatures slightly above the freezing point (mean: 0.28°C) while all other sensors continuously recorded frozen ground conditions. The mean temperature in 50 cm depth was - 0.58°C, in 75 cm depth was -0.89°C, and in 95 cm depth was -1.24°C. Ground temperature in 25 cm depth is slightly above 0°C from August on, and reaches almost 1°C (0.88°C) on August 15. A gradational temperature drop as displayed in the first three days until July 22 is related to thermal disturbance of the ground after drilling.

T1

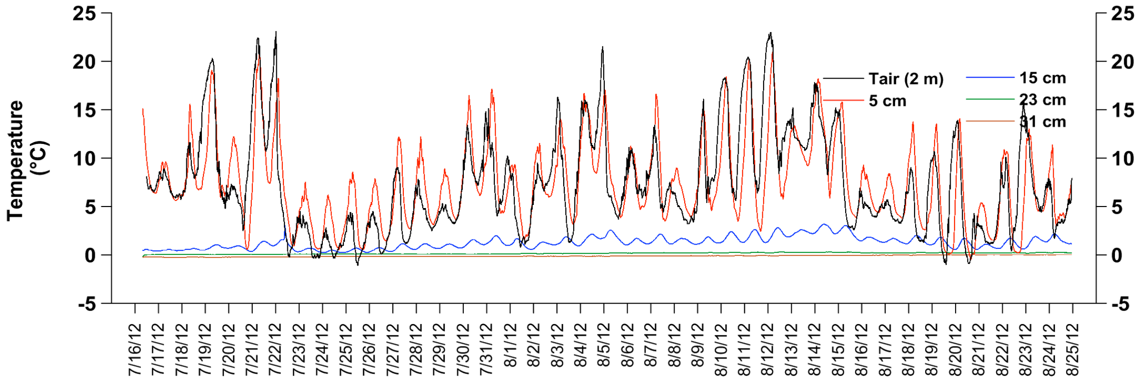

T2

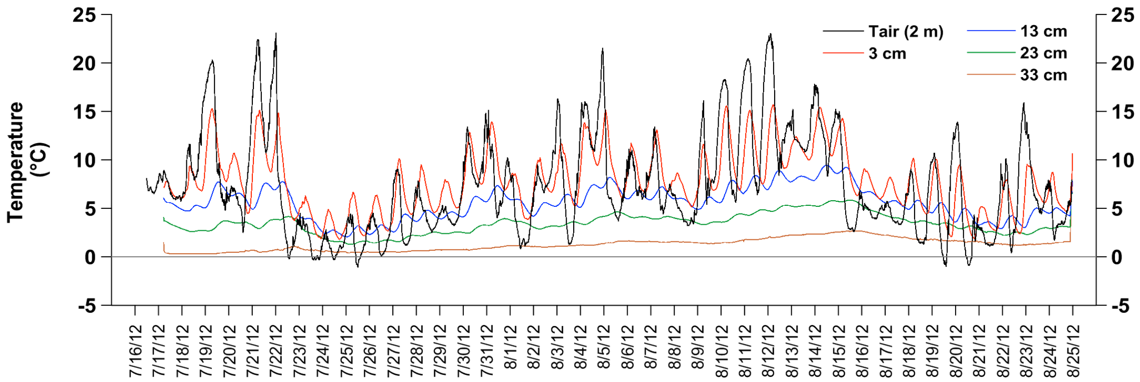

T3

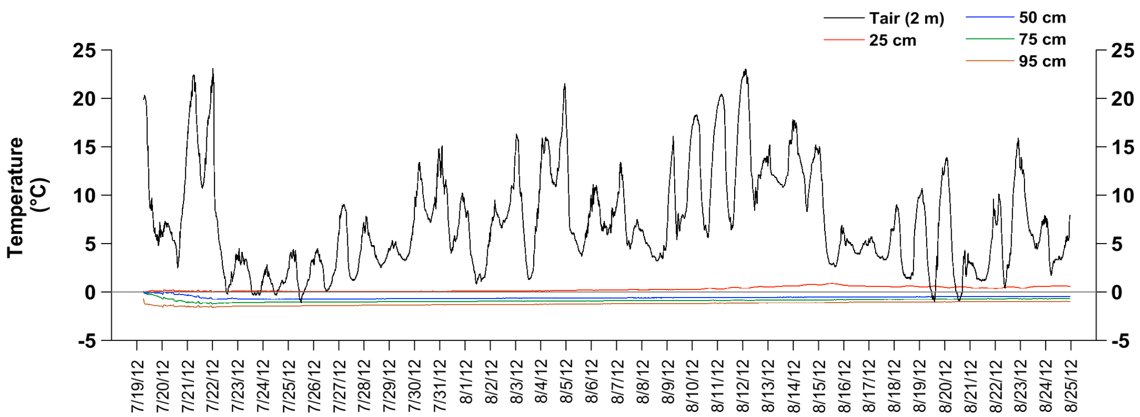

Fig. 3-7: Air and ground temperatures measured in the upper () and lower polygon rim of POK-01 from July 17 until August 25, 2012. Depth information for ground temperatures are below the ground surface, for air temperature above the ground surface.

3.3 Hydrobiology

Ostracods were caught from various zones in the pond: From the bottom, in the center and margin, from the water column, between plants and open water areas without vegetation. Approx. 100 animals were caught with a plankton net and exhauster system according to (Viehberg 2002), and preserved in alcohol. Further identification by soft body characteristics for species identification and isotopic analyses of the valve calcite will be undertaken.
We collected macrozoobenthos from different places, mainly from the substrate near the margin of the pond. We picked eye-visible specimens and preserved them in Whirl Packs with formalin.
Furthermore, we collected zooplankton and phytoplankton samples from the water column. We waved the plankton net for 10 times through the water column and obtained 100 ml sample volume. The samples were filled into Whirl Packs and preserved with formalin. The samples and corresponding measuring data are summarized in appendix A 3-2.

3.4 Hydrochemistry

We collected water samples for analyzing standard water parameters (alkalinity, acidity, electrical conductivity, pH, oxygen content, cations, anions, total hardness), isotopic composition and nutrients were taken ~15 cm below water table.
Most water parameters were measured in the station after our return from the field. Acidity, alkalinity, oxygen content, and total hardness were analyzed with titrimetric test kits (Viscolor). Electrical conductivity and pH were quantified by a WTW pocket meter additionally. We used a spectral photometer (Hach Lange DR 2800) for nutrient analyses (see chapter 7) such as NH_4^+, NO_3^- and PO_4^{3-}. Samples for kation (8ml), anion (15ml) and isotopic analyses (30ml) and residue samples were prepared in PE bottles or PE tubes for transport and stored in a cool place. Kation and anion samples were filtered by a cellulose-acetate filtration set (pore size 0.45 µm) prior to conservation. Kation samples were acidified with 200 µl HNO_3. Samples for anion analysis, isotope analyses and residue samples were preserved without any conservation. The composition of dissociated ionic compounds (cations and anions) in the pond water was determined with Inductively Coupled Plasma-Optical Emission Spectrometry (cations) and ion chromatography (anions) in the lab.
Samples and measuring data are summarized in appendices A 3-2 and A3-3. The major ion composition of the monitored pond POK-01 (Fig. 3-8) was dominated by Ca within the cations and HCO_3 within the anions. S was absent. Values of the 7 monitoring events form a clear cluster and do not show much variation.
The major ion composition of rain water, river water and ground ice is described in chapter 4.2.

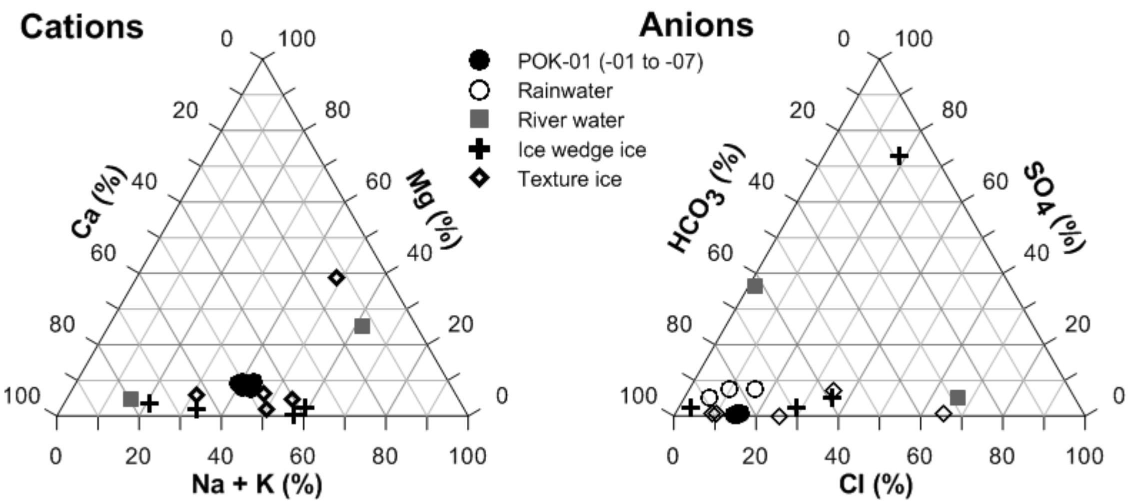

Fig. 3-8: Major ion composition of POK-01 (-01 to -07), rain water, river water and ground ice.

Obtained hydrochemical characteristics and physical properties are presented in figure 3-9: Both air and water temperature reflect a decreasing trend towards the end of the season and coalescent with the main trends measured by the temperature loggers (Fig. 3-4). The EC varies between 90 and 114 µS/cm. Values of NH_4^+ and NO_3^- were generally low. PO_4^{3-} values have been below detection limit. Total hardness of the pond water was 3.0 or 3.5°dH and pH values were measured around 7. The dissolved oxygen content of the pond water lies between 9 and 11 mg/l and was increasing throughout summer 2012.

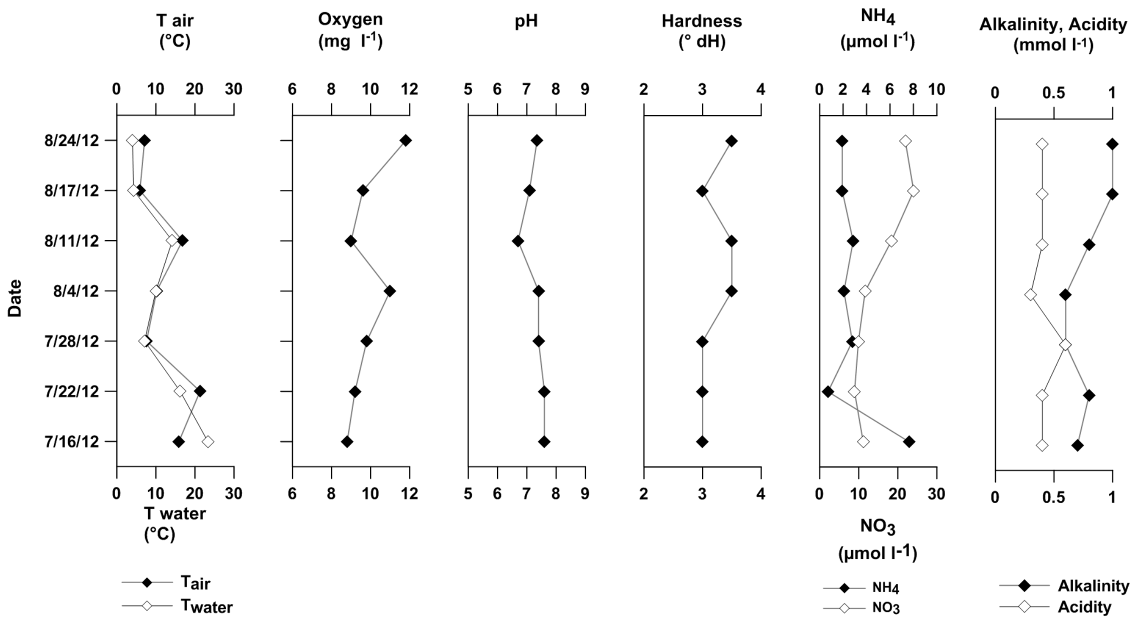

Fig. 3-9: Temperatures and hydrochemical properties of the monitoring site POK-01.

3.5 Surface transect and vegetation record

Along a 50 m long SW-NE transect AB (Fig. 3-2, Fig. 3-10) across the pond site we carried out surface microrelief measurements. From a string in a fixed height we undertook downward measurements of the ground surface elevation, the height of the water table, and the thaw depth in one-meter intervals.
The thaw depth follows closely variations in ground surface and is mainly around 50 cm underneath both the pond and dry areas. Sharp dips after 9 and 42 m (as indicated by arrows) might be related to frost cracks in the subsurface.

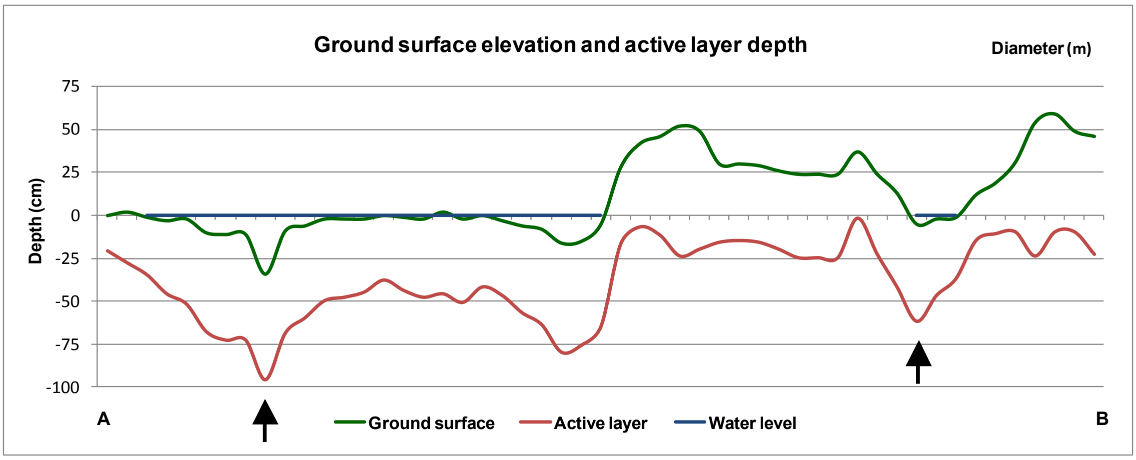

Fig. 3-10: Ground surface elevation and active layer depth of the monitoring site POK-01.

In the vegetation record (Fig. 3-11), we found 17 taxa of vascular plants, furthermore several mosses and lichens growing around POK-01. Around the pond, shrub tundra assemblages with *Alnaster fruticosa, Andromeda polifolia, Betula exilis, Chamaedaphne calyculata, Eriophorum vaginatum, Ledum decumbens, Vaccinium uliginosum, Sphagnum* spp. and brown mosses dominated. On hummocks and in areas near the water *Carex* spp., *Drephanocladus* cf. *revolvens, Potentilla palustris*, *Rubus chamaemorus, Vaccinium vitis-ideae* were common.

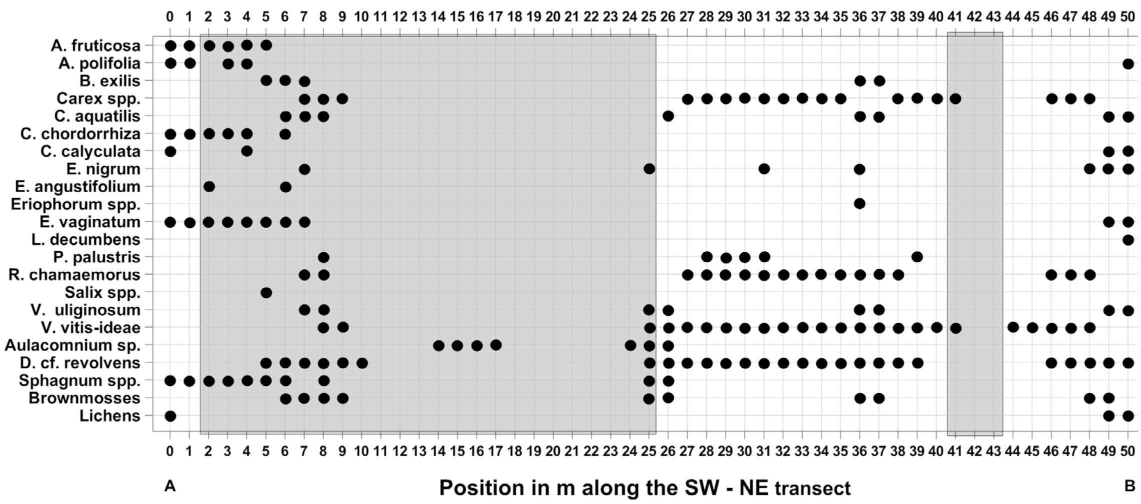

Fig. 3-11: Vegetation record along the NW – SE transect across POK-01. Each black dot indicates the presence of a certain taxa at a certain position (in m across transect). Areas highlighted in grey represent water areas.

3.6 Occasional amphibia findings near Pokhodsk

On a data logger box, we found a ca. 10 cm long smooth-skinned salamander with a light brown dorsal band, a laterally compressed tail and 4 toes (Fig. 3-12). We believe it was the Siberian Salamander (*Salamandrella keyserlingii,* Amphibia, Caudata, DYBOWSKI, 1870). *S. keyserlingii* inhabits the widest geographical range of any recent amphibian species. It is known from Russia, China, Korea, north of Kazakhstan, Mongolia, China, Korea, and Japan. The northern margin of the range extends to the Arctic part of the Urals, the south of Taimyr Peninsula, to the north of Yakutia Republic and Chukotka Peninsula (Fig. 3-13).

Fig. 3-12 The Siberian Salamander (*Salamandrella keyserlingii*) on a HOBO data logger box.

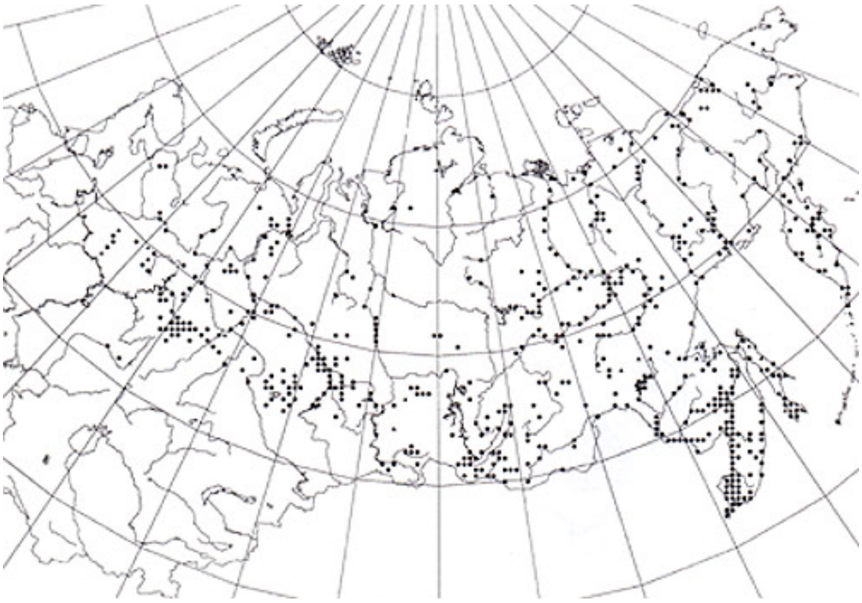

Fig. 3-13 Distribution areal of *Salamandrella keyserlingii.* From Kuzmin (1999).

Terrestrial adults of *S. keyserlingii* inhabit wet forests in the taiga zone and riparian groves in forest steppe and tundra landscapes. At the northern margins of its habitat range, the aquatic phase of the larvae tends to increase in duration. Thus, the existence of populations demands the presence of permanent pools such as polygon ponds.
S. keyserlingii is a unique amphibian in its freeze-tolerance during hibernation (Potapov 1993). Adults are able to survive freezing to -35 to -40°C and are mobile at +0.5 to +1.0°C. The spawn can survive short-term freezing. The total duration of overwintering in the northern distribution ranges of *S. keyserlingii* to about 75% of a year. The adult salamander is able to adapt to low temperatures and survive in a frozen state for a very long time by replacing the water in its blood and cells with a cryoprotective substance (glycerin or glycerol) thereby protecting its tissues from damage. Another example for freeze-tolerant amphibians is the North American wood frog (*Rana sylvatica,* LECONTE, 1825), which can tolerate temperatures as low as -8°C.

We thank Ewan Shilland (Environmental Change Research Centre, Department of Geography, University College London, UK) for the identification of *S. keyserlingii.*

4. ECOLOGICAL STUDIES OF POLYGON PONDS

Andrea Schneider, Lyudmila Pestryakova, Lutz Schirrmeister & Sebastian Wetterich

4.1 Polygon ponds on different landscapes

In the surroundings of Pokhodsk 30 (POK-02 to POK-31) small periglacial waters with polygonal origin were sampled. Different types of polygon ponds with respect to their degradation stage were chosen (Fig. 4-1); for example ponds in polygon depressions (intrapolygon ponds), above degrading ice wedges (interpolygon ponds), and thermokarst lakes have been studied. The data and sample packages were obtained as previously described in chapter 3 (see also appendix 4-1 to 4-3). All ponds were documented in a photo collection.

The sampling sites comprised the following locations (the number of ponds is given in brackets):

- Viska floodplain (10),
- Kolyma floodplain (5),
- Southern Kolyma floodplain near Pingo outcrop (2),
- Near Naumovskoje Osero (5),
- Hummocky tundra southwest of Pokhodsk (6),
- Khalerchinskaya Tundra (2).

In order to characterize the surrounding plant communities we record the main vegetation components for each study site. Here we concentrated on vascular plants (chapter 10) because mosses were not identified in the field. Bottom substrate samples and samples for testate amoebae analyses were taken from each site.

Fig. 4-1: Examples of sampled ponds in the surroundings of Pokhodsk.

4.2 Hydrochemical characteristics of the studied waters

In Fig. 4-2 air and water temperatures and selected hydrochemical variables are visualized. Water and air temperatures largely corresponded. Many of the deeper interpolygon ponds displayed a temperature gradient with depth. Water sampling for

hydrochemical analyses was conducted 10 - 30 cm below the water surface. Electrical conductivity varies between 23 and 132 µS/cm. The oxygen content was between 2.4 and 11.8 mg/l. The measured pH values range between 6 and 7 with the exception of ponds POK-26 (pH 4.8) and POK-27 (pH 4.7) which were located on the Khalerchinskaya Tundra. In those two ponds, no ostracods were found. Total water hardness was ranges from 2 to 6 °dH in the studied ponds. Acidity values varied between 0.2 and 4.0 mmol/l while alkalinity ranged up to 1.8 mmol/l.
Nutrients such as NH_4, NO_3 and PO_4^3 are present in low concentrations and which are partly below the detection limits of the used spectral photometer (Hach Lange DR 2800). Nitrogen compounds (NH_4, NO_3) and phosphate (PO_4^3) of the pond waters were measured in the field station with a portable spectral photometer (Hach Lange DR 2800) and test kits (Hach Lange: LCK 304 [Ammonium], LCK 339 [Nitrate], LCK 349 [Phosphate]). According to the manufacturer, the following limits for the detection of dissolved nutrient compounds are given: 0.015 - 2 mg/l (1.0 - 142.8 µmol/l) for NH_4, 0.23 - 13.5 mg/l (16.4 - 963.8 µmol/l) for NO_3 and 0.15 - 4.5 mg/l (4.8 - 145.3 µmol/l) for PO_4.

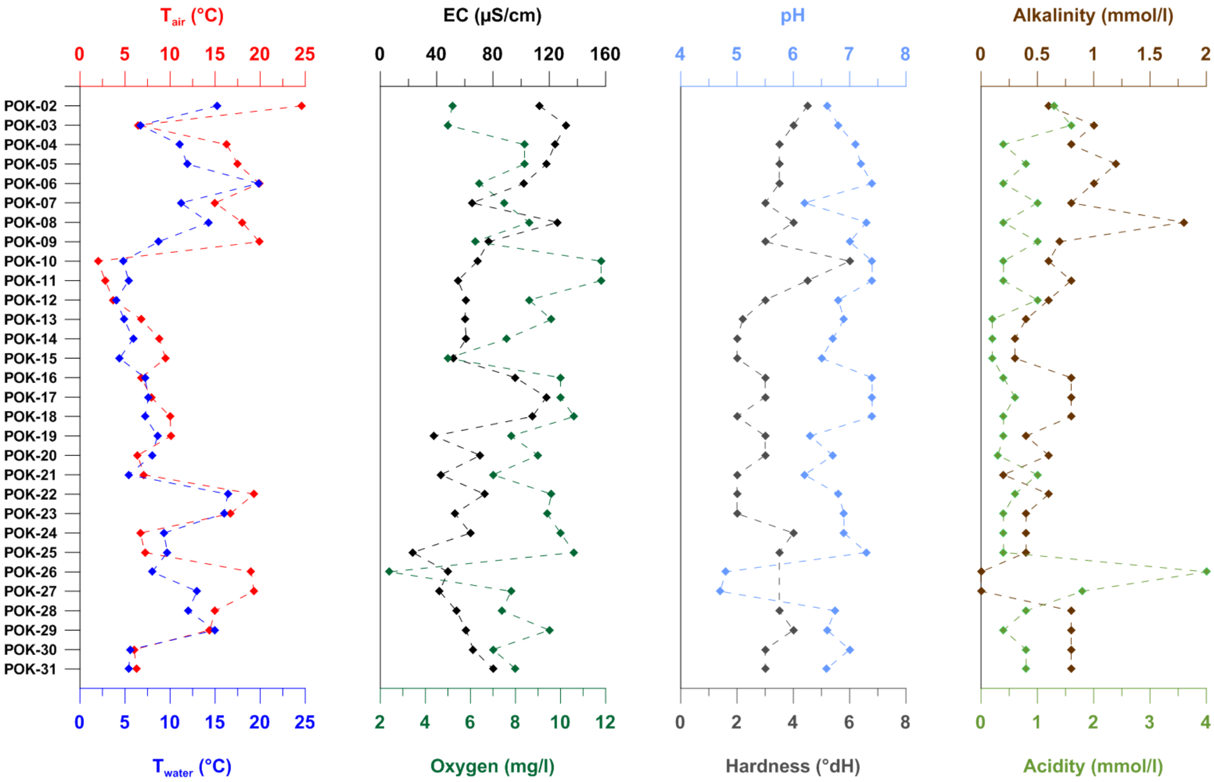

Fig. 4-2: Temperatures and hydrochemical properties in the studied ponds POK-02 to POK-31.

In total, 30 pond waters (POK-02 to POK-31), 3 rainwater samples, 2 river water samples and 9 ground ice samples (5 - texture ice, 4 - ice wedge ice) were analysed for their major ion composition (Fig. 4-3). The major ion composition of the 30 pond waters was dominated by Ca within the cations and HCO_3 within the anions. S was absent.

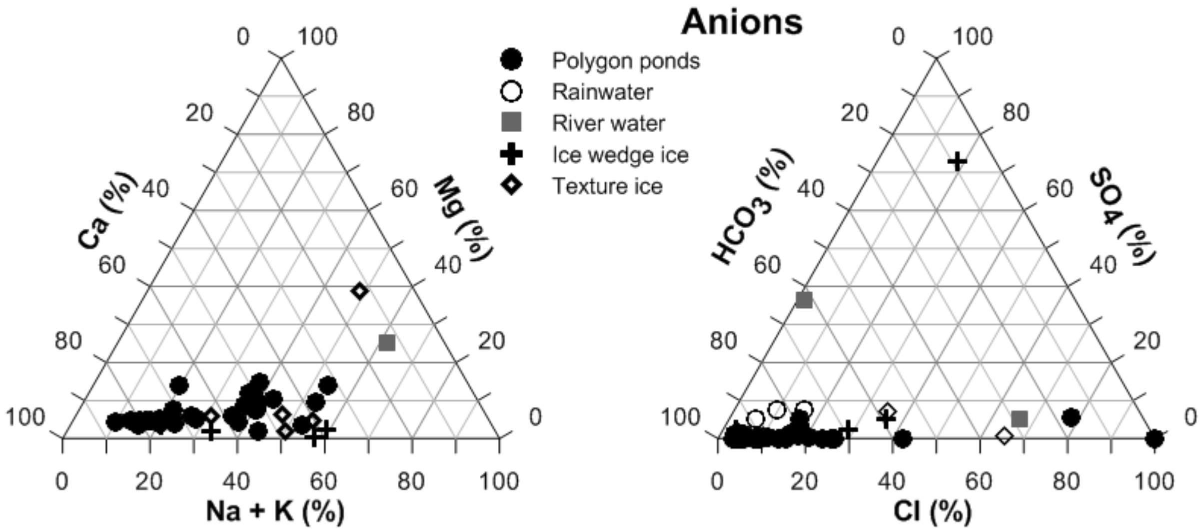

Fig. 4-3: Major ion composition of POK-02 to POK-31, rainwater, river water and ground ice.

Rain water, river water and different types of ground ice display larger variations in major ion content. With two exceptions, they are dominated by Ca and HCO_3, rich in Na and K, and low in Mg and Cl. Rainwater contained anions only; cations were at the detection limit and are therefore excluded from the diagram. The major ion composition of ground ice and river water was similar, but in 2 cases higher amounts of S were present.

Table 4-1: Samples used for the analyses of major ion composition in Fig. 4-3.

Sample code	Pond	Rain	River	Texture ice	Ice wedge ice
POK-02 to POK-31	x				
12-POK-Rainwater (15)		x			
12-POK-Rainwater (20)		x			
12-POK-Rainwater (28)		x			
12-P-Kanal-Pokhodsk			x		
12-P-2207-2			x		
12-P-2007-5-1				x	
12-P-3007-1-8				x	
12-P-1907-2-6-TH				x	
12-P-1907-2-9-TH				x	
12-P-2107-2-5-TH				x	
12-P-2507-1-7-H				x	
12-P-2507-1-12-H				x	
12P-1908-A-04-IW					x
12-P-2507-1-1-IWH					x

4.3 Pond characteristics

POK-02
Date: 15.07.2012 **Type:** Interpolygon pond
Coordinates: 69.09165 °N 160.93837°E
Area: Viska floodplain

Size of the water body: 8 x 1.4 m
Water depth: 50 - 64 cm

Substrate: organic mud with plant fragments

Vegetation
Menyanthes trifoliata, Betula nana, Carex aquatilis ssp. *stans, Eriophorum scheuchzeri, Vaccinium uligunosum, Salix* sp., *Alnus fruticosa, Utricularia intermedia, Utricularia vulgaris, Andromeda polifolia, Carex* sp., *Sphagnum* spp.

POK-03
Date: 18.07.2012 **Type:** Interpolygon pond
Coordinates: 69.09460°N 160.93855°E
Area: Viska floodplain

Size of the water body: 3 x 4 m
Water depth: 20 - 30 cm

Substrate: weakly decomposed plant material

Vegetation
Polygonrim: *Arctagrostis latifolia, Alnus fruticosa, Betula exilis, Ledum palustre, Vaccinium vitis-idea, Eriophorum vaginatum, Rubus chamaemorus, Empetrum nigrum, Vaccinium uligunosum, Polygonum tripterocarpa*
In pond: *Salix* sp., *Betula nana (submerged), Eriophorum vaginatum, V. uligunosum, Rubus chamaemorus, Ranunculus lapponicus*

Remarks
Yellow-brownish water colour

POK-04
Date: 19.07.2012 **Type:** Intrapolygon pond
Coordinates: 69.09401°N 160.94266°E
Area: Viska floodplain

Size of the water body: 17.3 x 16 m
Water depth: 70 cm

Substrate: brown organic mud

Vegetation
Polygonrim: *Alnus fruticosa, Betula exilis, Ledum palustre, Rubus chamaemorus, Vaccinium uliginosum*
At shore: *Menyanthes trifoliata, Eriophorum angustifolium, Eriophorum scheuchzerii, Carex aquatilis* ssp. *stans, Chamaedaphne calyculata, Salix* sp., *Potentilla palustre, Utricularia vulgaris*

Remarks
Steep shore, core available (S-08-1, 50 cm long, taken with Russian corer)

POK-05
Date: 19.07.2012 **Type:** Interpolygon pond
Coordinates: 69.09400°N 160.94534°E
Area: Viska floodplain

Size of the water body: 10 x 16 m
Water depth: > 1 m

Substrate: brown organic mud

Vegetation
Menyanthes trifoliata, Carex rotundata, Carex chodorrhizza, Calamagrostis cf. *neglecta, Utricularia vulgaris, Utricularia intermedia, Potentilla palustre, Carex aquatilis ssp. aquatilis, Carex aquatilis* ssp. *stans, Eriophorum russoleum, Eriophorum angustifolium, P. palustre, Hippuris vulgaris, Betula exilis, Sparganium hyperboreum*

Remarks
Degraded polygon walls, steep margins, fish living in the pond

POK-06
Date: 19.07.2012 **Type:** Intrapolygon pond
Coordinates: 69.09537°N 160.93726°E
Area: Viska floodplain

Size of the water body: 11.5 x 9 m
Water depth: 59 cm

Substrate: brown organic mud

Vegetation
Polygonrim: *Eriophorum vaginatum, Alnus fruticosa, Betula nana, Rubus chamaemorus, Vaccinium vitis-idea, Ledum palustre, Vaccinium uliginosum, Empetrum nigrum, Salix* sp.
At shore: *Eriophorum scheuchzeri, Carax rariflora, Carex aquatilis* ssp. *stans, Carex chodorrhizza, Carex rotundata, Eriophorum angustifolium, hummocks with Betula nana, Salix* sp., *Andromeda polifolia*

POK-07
Date: 21.07.2012 **Type:** Intrapolygon pond
Coordinates: 69.10400°N 160.99977°E
Area: Kolyma floodplain

Size of the water body: 17.10 x 6 m
Water depth: 80 cm

Substrate: brown organic mud and weakly decomposed plant detritus

Vegetation
Polygonrim: *Alnus fruticosa, Betula exilis, Salix cf. pulchra, Ledum palustre, Vaccinium uligunosum, Chamaedaphne calyculata, Carex aquatilis ssp. stans, Empetrum nigrum, Arctagrostis latifolia, Carex vaginata, Calamagrostis neglecta*
At shore: *Menyanthes trifoliata, Carex rostrata, Eriophorum angustifolium, Potentilla palustre*

POK-08
Date: 21.07.2012 **Type:** Intrapolygon pond
Coordinates: 69.10322°N 160.99983°E
Area: Kolyma floodplain

Size of the water body: 25.8 x 22.5 m
Water depth: 80 cm at the margin

Substrate: green-brownish fine organic mud

Vegetation
Polygonrim: *Alnus fruticosa, Betula exilis, Salix cf. pulchra, Ledum palustre, Vaccinium uligunosum, Chamaedaphne calyculata, Carex aquatilis* ssp. *stans, Empetrum nigrum, Arctagrostis latifolia, Carex vaginata, Calamagrostis neglecta*
At shore*: Carex rotundata, Betula exilis, C. calyculata, Carex chodorrhizza, M. trifoliata, Salix* cf. *pulchra, A. polifolia, Potentilla palustre, Salix cf. fruescens, Carex aquatilis* ssp*. stans, C* cf. *neglecta*
In pond: Menyanthes trifoliata, Potentilla palustre, Sparganium

POK-09
Date: 21.07.2012 **Type:** Interpolygon pond
Coordinates: 69.10347°N 161.00114°E
Area: Kolyma floodplain

Size of the water body: 9 x 7 x 11 m, 1.5 m wide
Water depth: 62 cm

Substrate: brown organic mud and weakly decomposed plant detritus, silty fine sand

Vegetation
Polygonrim: *Alnus fruticosa, Pyrola grandiflora, Vaccinium uliginosum, Vaccinium vitis-idea, Salix* cf. *glaucescens, Betula exilis, Ledum palustre, Empetrum nigrum, Polygonum tripterocarpum, Orthilia* sp.*, Poa* sp.*, Rubus chamaemorus, Arctagrostis latifolia, Stellaria longipes, Valeriana capitata, Parrya nudicaulis, Salix* cf. *pulchra, Carex aquatilis* spp. *stans, Potentilla palustre, Calamagrostis neglecta*
At shore*: Carex aquatilis ssp. stans, Potentilla palustre, Betula exilis (submerged), Vaccinium uligunosum, Eriophorum russeolum, Ledum palustre, Chamaedaphne calyculata*

Remarks
High and dry polygon rim

POK-10
Date: 25.07.2012 **Type:** Intrapolygon pond
Coordinates: 69.09303°N 160.94014
Area: Viska floodplain

Size of the water body: 11 x 10 m
Water depth: 7 cm

Substrate: brown organic mud and weakly decomposed plant detritus

Vegetation
Polygonrim: *Carex sp., Alnus fruticosa, Eriophorum vaginatum, Salix* cf. *pulchra, Chamaedaphne calyculata, Betula nana, Potentilla palustre, Ledum palustre, Eriophorum angustifolium*
In pond: *Carex aquatilis ssp. aquatilis, Carex sp., Carex chodorrhizza, Utricularia intermedia, Eriophorum scheuchzeri*

POK-11
Date: 25.07.2012 **Type:** Intrapolygon pond
Coordinates: 69.09504°N 160.93744°E
Area: Viska floodplain

Size of the water body: 4.3 m
Water depth: 21 cm

Substrate: reddish-brown organic mud

Vegetation
Alnaster fruticosa, Betula exilis, Carex aquatilis, Carex chordorrhiza, Chamaedaphne calyculata, Eriophorium angustifolium, Eriophorum vaginatum, Ledum decumbens, Potentilla palustris, Rubus chamaemorus, Salix spp.*, Sparganium hyperboreum, Utricularia minor, Vaccinium* spp.

Remarks
Low number of ostracods due to fish living in the pond

POK-12
Date: 26.07.2012 **Type:** Interpolygon pond
Coordinates: 69.06686°N 160.94519°E
Area: Hummocky tundra

Size of the water body: 10.2 x 5.1 m, width: 1 m
Water depth: 52 cm

Substrate: coarse brown plant material

Vegetation
Carex aquatilis ssp. *aquatilis, Carex aquatilis ssp. stans, Carex* sp.*, Salix* cf. *pulchra, Betula exilis, Alnus fruticosa, Ledum palustre, Vaccinium vitis-idea, Eriophorum angustifolium, Chamaedaphne calyculata, Utricularia vulgaris, Sphagnum* sp.

POK-13
Date: 27.07.2012 **Type:** Intrapolygon pond
Coordinates: 69.06633°N 160.93851°E
Area: Hummocky tundra

Size of the water body: 10.6 x 7.2 m
Water depth: 52 cm

Substrate: brown organic mud and weakly decomposed plant material

Vegetation
Polygonrim: *Chamaedaphne calyculata, Eriophorum vaginatum, Betula nana, Alnus fruticosa, Rubus chamaemorus, Carex* sp., *Ledum palustre*
In pond: *Eriophorum angustifolium, Sparganium, Potentilla palustre, Menyanthes trifoliata, Carex* sp.

Remarks
Many large ostracods

POK-14
Date: 27.07.2012 **Type:** Intrapolygon pond
Coordinates: 69.06490°N 160.93497°E
Area: Hummocky tundra

Size of the water body: 7.8 x 5.2 m
Water depth: 31 cm

Substrate: brown organic mud and weakly decomposed plant material

Vegetation
Polygonrim: *Salix* cf. *pulchra, Betula nana, Ledum palustre, Vaccinium uligunosum, Alnus fruticosa, Eriophorum vaginatum, Eriophorum angustifolium, Andromeda polifolia, Rubus chamaemorus*
In pond: *Carex aquatilis* ssp. *stans*

Remarks
No open water surface, many big ostracods

POK-15
Date: 27.07.2012 **Type:** Interpolygon pond
Coordinates: 69.06528°N 160.94135°E
Area: Hummocky tundra

Size of the water body: 7.8 x 3.5 m
Water depth: 49 cm

Substrate: brown organic mud

Vegetation
Eriophorum vaginatum, Potentilla palustris, Carex sp., *Carex aquatilis* ssp. *stans, Sphagnum, Ledum palustre, Betula nana, Alnus fruticosa, Chamaedaphne calyculata, Vaccinium vitis-idea*

Remarks
Carex hummocks in the ponds, many big ostracods except in the central deepest part of the pond

POK-16
Date: 30.07.2012 **Type:** Intrapolygon pond
Coordinates: 69.09351°N 160.94231°E
Area: Viska floodplain

Size of the water body: 24 x 18 m
Water depth: 210 cm in the centre, 31 cm at the margin

Substrate: brown organic mud

Vegetation
Polygonrim: *Betula nana, Salix* cf. *pulchra, Ledum palustre, A. fruticosa, Chamaedaphne calyculata, Carex aquatilis ssp. stans*
In pond: *Menyanthes trifoliata, Sparganium, Eriophorum scheuchzeri, Carex aquatilis* ssp. *stans, Carex chodorrhizza, Carex* sp.*, Utricularia intermedia, Carex rotundata*

Remarks
2 cores available (S-06-1, 30 cm long, S-06-2, 40 cm long, taken with Russian corer)

POK-17
Date: 30.07.2012 Type: Thermokarst lake
Coordinates: 69.09253°N 160.94440°E
Area: Viska floodplain

Size of the water body: 8 x 6,5 m
Water depth: 50 cm at the margin

Substrate: brown organic mud

Vegetation
Alnus fruticosa, *Betula nana*, *Salix* sp., *Ledum palustre*, *Vaccinium vitis-idea*, *Polygonum tripterocarpum*
At shore: *Carex chodorrhizza*, *Eriophorum scheuchzeri*, *Carex aquatilis* ssp. *stans*
In water: *Menyanthes trifoliata*, *U. vulgaris*

POK-18
Date: 30.07.2012 **Type:** Thermokarst lake
Coordinates: 69.09295°N 160.94479°E
Area: Viska floodplain

Size of the water body: 96 x 30.5 x 35.7 m
Water depth: centre: 240 cm, margin: 35 cm

Substrate: brown organic mud

Vegetation
Polygonrim: *Alnus fruticosa, Betula nana, Salix* sp.*, Ledum palustre, Vaccinium vitis-idea*
At shore*: Carex chodorrhizza, E. scheuchzeri, C. aquatilis* ssp. *stans, E. angustifolium*
In pond: *Menyanthes trifoliata, U. vulgaris, R. pallasii, H. vulgaris, Arctophila fulva*

Remarks
Core available (S-20-1, 50 cm long, taken with Russian corer)

POK-19
Date: 01.08.2012 **Type:** Intrapolygon pond
Coordinates: 69.11090°N 160.88188°E
Area: Naumovskoe ozero

Size of the water body: 14.5 x 10.9 m
Water depth: 17 - 25 cm

Substrate: brown organic mud and weakly decomposed plant material

Vegetation
Polygonrim: *Salix cf. pulchra, Alnus fruticosa, Betula nana, Ledum palustre, Rubus chamaemorus, Eriophorum vaginatum, Andromeda polifolia, Sphagnum* sp.
In pond: *Carex aquatilis* ssp. *stans, Carex chodorrhizza, Utricularia intermedia, Eriophorum russoleum*

Remarks
Low number of ostracods

POK-20
Date: 02.08.2012 **Type:** Thermokarst lake
Coordinates: 69.11073°N 160.88734°E
Area: Naumovskoje ozero

Size of the water body: 72.1 x 26.5 m
Water depth: 70 - 110 cm

Substrate: brown organic mud

Vegetation
Polygonrim: *Eriophorum vaginatum, Andromeda polifolia, E: nigrum, Salix* cf. *pulchra, B. nana, L. palustre, V. vitis-idea*
At shore: *Carex rotundata, E. angustifolium, E. scheuchzeri, Betula nana, Salix* cf. *pulchra, C. chodorrhizza, Andromeda polifolia, C. calyculata, Carex aquatilis* ssp. *aquatilis*
In pond: *Ranunculus pallasii, E. angustifolium*

Remarks
Viktors lake N0. 25-1, 2 cores available (both 28 cm long, taken with Russian corer). Samples from outside the core have codes 25-1A-1 until 25-1A-9. Samples from the inside the corer have codes 25-1B-1 until 25-1B-11.

POK-21
Date: 02.08.2012 **Type:** Interpolygon pond
Coordinates: 69.11008°N 160.88716°E
Area: Naumovskoe ozero

Size of the water body: 6.8 x 1.2 m
Water depth: 58 cm

Substrate: weakly decomposed brown organic material

Vegetation
Carex aquatilis ssp. *aquatilis, Alnus fruticosa, Betula nana, Salix* cf. *pulchra, Rubus chamaemorus, Chamaedaphne calyculata, Ledum palustre, Eriophorum vaginatum*

POK-22
Date: 05.08.2012 **Type:** Intrapolygon pond
Coordinates: 69.12644°N 160.87906°E
Area: Naumovskoe ozero

Size of the water body: 21 x 21 m
Water depth: 10 cm

Substrate: weakly decomposed brown organic material

Vegetation
Rubus chamaemorus, Ledum palustre, V. vitis-idea, Chamaedaphne calyculata, Eriophorum vaginatum, Carex aquatilis ssp. *stans, Sphagnum* sp., *C. chodorrhizza, Salix* cf. *pulchra, Betula nana, Alnus fruticosa*

POK-23
Date: 05.08.2012 **Type:** Intrapolygon pond
Coordinates: 69.12675°N 160.88002°E
Area: Naumovskoje ozero

Size of the water body: 14.5 x 6.5 m
Water depth: 21 cm

Substrate: weakly decomposed brown organic material

Vegetation
Betula nana, Ledum palustre, Carex sp., *Alnus fruticosa, Rubus chamaemorus, Salix* cf. *pulchra, Vaccinium vitis-idea, Eriophorum scheuchzeri*

POK-24
Date: 08.08.2012 **Type:** Intrapolygon pond
Coordinates: 69.10909°N 161.00142°E
Area: Kolyma floodplain

Size of the water body: 20 x 30 m
Water depth: center: > 1m, margin: 38 cm

Substrate: organic mud

Vegetation
Polygon rim: *Alnus fruticosa, Betula nana, Andomeda polifolia, Salix* cf. *pulchra, Carex aquatilis* ssp. *stans* ., *Chamaedaphne calyculata, Carex* sp., *Ledum palustre*
In pond: *Utricularia intermedia, Sparganium hyperboreum, Menyathes trifoliata*
At shore: *Carex chodorrhizza*

Remarks
Coalescent intrapolygon ponds

POK-25
Date: 08.08.2012 **Type:** Intrapolygon pond
Coordinates: 69.10789°N 161.00182°E
Area: Kolyma floodplain

Size of the water body: 6 x 7 m
Water depth: 15 cm

Substrate: fine disperse organic mud

Vegetation
Polygon rim: *Rubus chamaemorus, Betula nana, Salix* cf. *pulchra , Alnus fruticosa, Ledum palustre, Vaccinium vitis-idea, Empetrum nigrum, V. uligunosum*
In pond: *Carex sp.*
Hummocks: *Carex* sp., *C. calyculata, Betula nana, Sphagnum* ssp., *Ledum palustre*

Remarks
low-center polygon with high and broad rim, rim height above water level ca. 0.5m, hummocks with Carex and Betula in the pond, no ostracods present in the pond

POK-26
Date: 10.08.2012 **Type:** Interpolygon pond
Coordinates: 69.06082°N 160.86557°E
Area: Khalerchinskaya Tundra

Size of the water body: 7.4 x 1.0 m
Water depth: 30 cm

Substrate: weakly decomposed peat, mainly Eriophorum vaginatum and moss (Sphagnum)

Vegetation
Betula nana, Rubus chamaemorus, Ledum palustre, Eriophorum vaginatum, Sphagnum spp. (submerged)

Remarks
no ostracods present in the pond, no benthos

POK-27
Date: 10.08.2012 **Type:** Interpolygon pond
Coordinates: 69.05436°N 160.86235°E
Area: Khalerchinskaya Tundra

Size of the water body: 7 x 7 x 2.4 m
Water depth: 30 cm

Substrate: weakly decomposed peat

Vegetation
Betula nana, Rubus chamaemorus, Ledum palustre, Eriophorum vaginatum, Sphagnum spp. (submerged)

Remarks
no ostracods present in the pond, no benthos

POK-28
Date: 15.08.2012 **Type:** Interpolygon pond
Coordinates: 69.07072°N 160.98106°E
Area: southern Kolyma floodplain

Size of the water body: 32 x 2 m
Water depth: 75 cm

Substrate: coarse, low decomposed organic mud

Vegetation
In pond: *Eriphorum angustifolium, Caltha palustris, moss*
At shore: *Alnus* sp., *Betula* sp., *Ledum palustre, Sphagnum* spp.

Remarks
water above ice in the central part; 0.1 m a.l. at the water margin; 0.6 m a.l. on land

POK-29
Date: 15.08.2012 **Type:** Intrapolygon pond
Coordinates: 69.07005°N 160.97990°E
Area: southern Kolyma floodplain

Size of the water body: 25 x 14 m
Water depth: 1 cm

Substrate: organic mud, slightly silty

Vegetation
In pond: *Eriphorum angustifolium, Caltha palustris,Menyanthes trifoliota, moss*
At shore: *Alnus* sp., *Betula* sp., *Ledum palustre, Sphagnum* spp.

POK-30
Date: 26.08.2012 **Type:** Interpolygon pond
Coordinates: 69.06606°N 160.94453°E
Area: Hummocky tundra

Size of the water body: 9 x 32 m
Water depth: 55 cm

Substrate: coarse organic mud

Vegetation
Betula nana, Alnus sp., Ledum palustre, Eriophorum vaginatum, Potentilla palustris

Remarks
T-shape of the pond, many ostracods present

POK-31
Date: 26.08.2012 **Type:** Interpolygon pond
Coordinates: 69.06575°N 160.94202°E
Area: Hummocky tundra

Size of the water body: 2 x 9 m
Water depth: 70 cm

Substrate: fine disperse organic mud

Vegetation
Betula nana, Alnus sp., Ledum palustre, Eriophorum vaginatum, Potentilla palustris, Sphagnum spp., *Hippuris vulgaris*

5. LIMNOLOGICAL STUDIES

Viktor Sitalo, Lutz Schirrmeister & Dmitry Subetto

5.1 Polygonal ponds on the Kolyma river lowland near Pokhodsk

We described six ponds on different degradation level, located on the tree study areas. Four ponds located on the left side of Viska river floodplain (ID codes: 04, 06, 259, 309), one pond located on the left side of Rassokha river floodplain (ID code: 036), and one pond located near Naumovskoe Lake (ID code: 025). Most of them formed by integration of 2 to 3 ponds into one waterbody, which are characterized by good-visible polygon walls, medium depths of 60-70 cm and a thick bottom layer of decomposed organic material. For a general description were measured and recorded water temperature, depth and extension. Water samples were obtained for physico-chemical analyses (Appendix 5-1). Ponds were drilled to get a sediment samples from the unfrozen active layer (Appendix 5-2). The total number of cores from polygonal ponds is eight (Fig. 5-1).
The studied thermokarst lakes are located in different landscape types. Lakes on the floodplains of the Kolyma, Viska and Rassokha rivers have various genesis, size, shape form, depth and bottom surface (Fig. 5-1).

Fig. 5-1: Location of sampled polygonal ponds (left image) and thermokarst lakes (right image) in the study area.

Pond 4
Interpolygon pond with degraded walls, vegetation in water and tight layer of plant material on bottom.

Coordinates: 69°05.703' N, 60°56.341' E
Depth: 20-40 cm
Size:

T_{Air}:

T_{Water}: 14.2 °C
pH:
EC:
Alkalinity:
Acidity:
Total hardness:
Oxygen:

Short core: 11 cm long, **POK-258**
From upper layer to 5 cm – dark brown decomposed plant material. From 5 cm to 11 cm – light dust-coloured decomposed plant material with inclusion of fine sand.

Pond 6
Interpolygon pond formed by collapse of ice wedge. Process of genesis is clearly visible in the diagram (see right diagram).

Coordinates: 69°05.607' N, 160°56.567' E
Depth: 0.7 - 1.1 m
Size: 24 × 18 m

T_{Air}: 6.8 °C

T_{Water}: 7.2 °C
pH: 6.5
EC:
Alkalinity: 0.8 mmol/l
Acidity: 0.4 mmol/l
Total hardness: 3.0°dH
Oxygen:

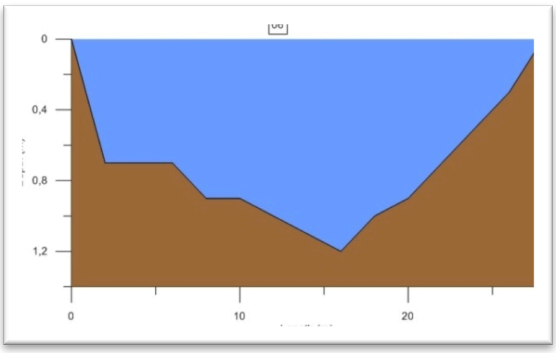

Short core: 40 cm long, **S-06-1**
From upper layer to 25 cm – dark greyish brown strong decomposed plant material.
From 25 cm to 40 cm – light brownish grey dry and compact strong decomposed plant material.

Pond 36
Polygonal pond is in the low-centred polygon. Walls are well-marked.

Coordinates: 69°04.073' N, 160°56.638' E
Depth: 1.1 m
Size: 17 × 8 m

T_{Air}: 6.6 °C
at 0 m / 1 m / 3 m water depth
T_{Water}: 6.4 / 6.2/ 5.8 °C
pH: 7.4 / 7.3 / 7.2
EC: 90 / 70 / 66 μS/cm
Alkalinity: 0.4 / 0.5/ 0.6 mmol/l
Acidity: 0.4 / 0.4 / 0.2 mmol/l
Total hardness: 4.2/ 1.5/ 2.5 °dH
Oxygen: 11.6 / 12 / 12 / mg/l

Short core: 9 cm long, **S-36-1**
From upper layer to 2 cm – brown decomposed plant material. From 2 cm to 3 cm – greyish brown decomposed plant material. From 3 cm to 9 cm – dark grey silty sand.

Pond 025
Polygonal pond located near Naumovskoe lake. Formed by collapse of two lakes walls.

Coordinates: 69°06.646' N, 160°53.275' E
Depth: 0.9 m
Size: 72.1 × 26.5 m

T_{Air}:
at 0.2 m water depth
T_{Water}: 9.6-11 °C
pH: 7.1
EC: 6.7 μS/cm
Alkalinity:
Acidity:
Total hardness:
Oxygen:

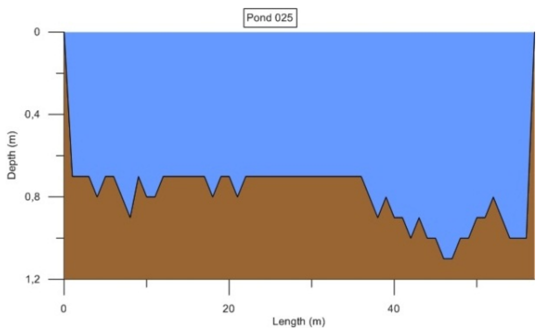

2 short cores: 28 cm long, **S-25-1A** and **S-25-1B**
From upper layer to 17 cm – light grey, light brown silty sand and fine sand. From 27 cm to 28 cm – light grey compact and dry sand material.

Pond 259
Pond located on the left side of Viska river floodplain. Walls are half-collapsed. Frost cracks are marked a shape of water body.

Coordinates: 69°09460' N, 160°93855' E
Depth: 0.4 m
Size: 18 x 16 m

T_{Air}: 5.9 °C

T_{Water}: 4.3-6.3 °C
pH:
EC:
Alkalinity:
Acidity:
Total hardness:
Oxygen:

Short core: 6 cm long, **POK-259**
From upper layer to 2 cm – dark grey not decomposed organic material. From 2 cm to 6 cm – dark greyish brown not decomposed organic material.

Pond 309
Pond located on the left side of Viska river floodplain. Water level is low. Water goes out by frost cracks around walls.

Coordinates: 69°09504' N, 160°93744' E
Depth: 0.2 m
Size: 25 x 17 m

T_{Air}: 6.0 °C

T_{Water}: 4.3-6.3 °C
pH:
EC:
Alkalinity:
Acidity:
Total hardness:
Oxygen:

Short core: 13.5 cm long, **POK-309**
From upper layer to 6 cm – Light brown little decomposed organic material. From 6 cm to 13.5 cm – Light brown fine decomposed organic material with slim and short roots particles.

Lake 038
Lake is close to meander Rassokha river. Located on the Rassokha floodplain. Maximal depth is 4.7m.

Coordinates: 69°03.545' N, 160°56.162' E
Depth: 3.9 - 4 m
Size: 25 x 17 m

T_{Air}: 6.6 °C
at 0 m / 1 m / 3.5 m water depth
T_{Water}: 7 / 7 / 7 °C
pH: 7.2 / 7.2 / 7.1
EC: 69 / 63 / 60 μS/cm
Alkalinity: 0.3 / 0.3 / 0.3 mmol/l
Acidity: 0.2 / 0.2 / 0.4 mmol/l
Total hardness: 0.4 / 0.4 / 0.3 °dH
Oxygen: 10.8 / 7.4 / 10.8 mg/l

2 short cores: 9 and 15cm long, **S-38-1**
Cores taken at 4 m water depth. The 9 cm long core characterised by grey wet silty material. At 6 cm depth decomposed plant fragments.

Lake 024 (Naumovskoe Lake)
Naumovskoe lake is a thermokarst lake with large water surface. Lake based on the bottom of lake which previously gone away. This evolution process is good visible on the satellite image. Probably Naumovskoe Lake changed his form two or three times in the past.

Coordinates: 69°06.682' N, 160°52.962' E
Depth: 2.5 – 3.2 m
Size:

T_{Air}: 10.2 °C
at 0 m / 2 m / 2.5 m water depth
T_{Water}: 7 / 7.2 / 6.9 °C
pH: 6.5 / 6.6 / 6.6
EC: 127 / 126 / 128 μS/cm
Alkalinity: 0.4 / 0.4 / 0.4 mmol/l
Acidity: 0.4 / 0.4 / 0.4 mmol/l
Total hardness: 2.0 / 2.0 / 2.0 °dH
Oxygen: 9.6 / 10 / 9.6 mg/l

3 short cores: 24, 28 and 10.5 cm long, **S-24-2**
Core contained 20 samples and has a 28 cm length. From upper layer to 10 cm – fine decomposed plants and little sandy material. From 10 cm to 20 cm – silty sand material, without any organic inclusions. From 20 to 28 cm – compact and dry brownish silty sand and plant material.

Lake 034
Large rectangular lake with a ninety degree angle sides. Lake located parallel to the Kolyma river meander. Maximal depth is 5 m.

Coordinates: 69°04.241' N, 160°58.876' E
Depth: 3.5 m
Size: 1310 × 428 m

T_{Air}: 12.1 °C
at 0.5 m / 3 m water depth
T_{Water}: 8 / 7.1 °C
pH: 6.8 / 6.7
EC: 80 / 57 μS/cm
Alkalinity: 0.6 / 0.2 mmol/l
Acidity: 0.3 / 0.3 mmol/l
Total hardness: 2.5 / 3.0 °dH
Oxygen: 9.0 / 6.2 mg/l

2 short cores: 20 and 30 cm long, S-55-1, S-56-1
From upper layer to 8 cm – light brown small decomposed plant material. From 8 cm to 22 cm – light greyish sandy silt with short slim roots inside. From 22 cm to 30 cm – grey-blue compact dry silty material

Lake 066
Large thermokarst lake (Setnoe Osero) on the Khallertchinskaya Tundra. Lake has an "old" shape borders, good visible on satellite images

Coordinates: 69°03.456' N, 160°51.191' E
Depth: 2.1m
Size: 1310 × 428 m

T_{Air}: 12.1 °C
at 0.5 m / 1 m / 3 m water depth
T_{Water}: 11.5 / 11.5 / 11.5 °C
pH: 7.3 / 7.5 / 6.5
EC: 48 / 47 / 48 μS/cm
Alkalinity: 0.4 / 0.4 / 0.4
Acidity: 0.4 / 0.4 / 0.4 mmol/l
Total hardness: 1.5 / 1.5 / 2 °dH
Oxygen: 9.0 / 9.0 / 4.0 mg/l

Short cores: 29.5 cm long, **S-66-1**
From upper layer to 10cm – black fine sand, plant fragments. From 10cm to 23cm – grey, light grey fine sand, compact, some aggregates 1×1.5cm.
From 23cm to 29.5 – light grey fine sand with small white particles (Ø1-2mm).

Lake 080
Thermokarst lake at the pingo site
Coordinates:
Depth:
Size:

T_{Air}:
at 0 m / 1 m / 2.4 m water depth
T_{Water}: °C
pH: 6.4 / 6.8 / 6.8
EC: 51 / 52 / 52 µS/cm
Alkalinity: 0.4 / 0.4 / 0.4 mmol/l
Acidity: 0.4 / 0.4 / 0.4 mmol/l
Total hardness: 2.5 / 1.5 / 2.5 °dH
Oxygen: 9.0 / 9.0 / 8.8 mg/l

3 short cores: cm long, S-80-1 (48 cm long), S-80-2 38 cm long), S-80-3 (32 cm long)

6. Records from the collapsed polygon complex MNP12 for actuo- and palaeoecological studies

Enrico Behrens, Pim de Klerk & Hans Joosten

6.1 Introduction

Polygon mires are highly complex and dynamic ecosystems that are widely distributed in the (sub)arctic. They show typical short-distance diversity in site conditions and vegetation and are characterized by a complex interplay of water, ice, vegetation and peat (Minke et al., 2007; Donner et al., 2012).
Climate change is particularly intense in the Arctic (McGuire et al., 2007) and might have substantial influence on arctic ecosystems, especially on polygon mires. However, it is hardly known to what extent polygon mire dynamics are controlled by climate change and to what extent they result from polygon internal feed-back processes. Recent high resolution studies indicate that - in contrast to previous ideas - ice wedge polygons may be highly dynamic as a result of climate triggers interfering with polygon internal self-organisation processes (Minke et al., 2009, De Klerk et al., 2011, Donner et al., 2012; Teltewskoi et al., in press). Over a period of a few years polygon structural elements may change from dry to wet and from wet to dry (by development of segregation ice) (De Klerk et al., 2011).
In order to better understand ice-wedge polygon dynamics and their dependence on weather and climate, we carried out fine-scale-mapping of vegetation and site conditions of a collapsed polygon complex. Identifying the spatial distribution and mutual relation of the causal factors will allow a better understanding of ecological indicators that are helpful for the interpretation of palaeo-data from (sub)recent and fossil ice-wedge polygons (Teltewskoi et al., 2012, in press). Furthermore we collected strategically situated peat profiles to reconstruct the past development of the polygon complex.

6.2 Study site

The study site MNP12 (69.093539° N and 160.932125° E; Fig. 6-1) is located in the Kolyma lowland at the Pokhodskaya Viska River, a tributary of the Kolyma River, approximately 2 km northwest of the village Pokhodsk (Figs. 2-4, 2-5). MNP12 seems to be a collapsed polygon complex. Currently it includes a large central depression of which the northeastern and southwestern sides are formed by relatively high polygon ridges. The polygonal structures around the depression indicate that the depression itself may have consisted of 6-8 single polygons. On the border between the depression and the ridges distinct ice-wedge trenches occur. In the centre of the depression there are only very slight indications of the former presence of polygon ridges: the relief is very even, and the vegetation seems at first sight to consist of homogenous sedge vegetation. Further to the west of MNP12 the polygon landscape gradually changes into an extensive sedge field with local vegetational traces of collapsed ice wedges and polygon ridges.

Fig. 6-1: The collapsed polygon complex MNP12 seen from the northeast.

6.3 Methods

We created with wooden sticks, strings and a water level tube an imaginary horizontal reference plane (Fig. 6-2) and constructed a regular grid over an area of 50 x 68m consisting of 3400 plots of each 1m² with coordinates A to BS (long axis) and 0 to 49 (short axis). The level of the imaginary reference plane was approximately 20 cm above the highest point of the polygon complex, and all height measurements were relative to this plane.

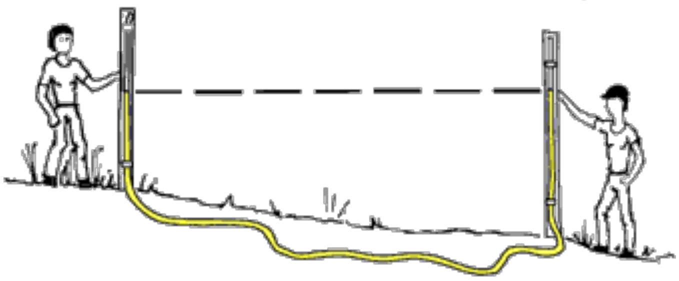

Fig. 6-2: Usage of a water level tube (source: http://www.boeingconsult.com/tafe/ss&so/survey1/Module4/equipment-s1.htm)

For every 1 m^2 plot we recorded the presence/absence of some 30 selected plant taxa (Appendix 6). Ground surface height and frost table height were measured in

the centre of each plot with a wooden rod. The active layer thickness is the difference between ground surface height and frost table height.
In addition, we took surface samples for palynological analysis in order to study the relation between recent vegetation and pollen distribution. This aids in a more accurate interpretation of palaeoecological profiles (De Klerk et al., 2009, 2011, 2014). Surface samples (volume about 50 cm³) were taken along transect Y by collecting mosses (or in their absence litter) from the centre of each plot and storing these in plastic bags.
Five strategically situated peat profiles of about 50 cm length were excavated using spade, saw and axe: one pair of profiles at the northeastern side of the depression, one pair on the southwestern side of the depression and a single section in the centre of the depression where the vegetation indicates a collapsed ridge. The profiles were adjusted by sawing to sods of 15 cm x 10 cm x individual length and stored in a wooden box for transportation (Fig. 6-3, Table 6-1). Using the Damocles-device (Joosten & De Klerk, 2007), these peat profiles will be cut in contiguous slices of 0.5 cm thickness for analyses of pollen, macrofossils, rhizopods, and geochemistry.

Fig. 6-3: Collection of the peat profiles: Left: Location AE-7 after removal of the profile, right top: manual removal of the cut-free profile AE-7; right bottom: storing the adjusted profile AX-29 in a wooden box.

Tab. 6-1: Peat profiles collected in MNP12 (Pokhodsk), 26.08.2012 (see Fig. 6-4).

Coordinates	Description	Weight
AE-3	Top of northeastern polygon ridge	7.34 kg
AE-7	Collapsed part of the northeastern ridge	5.30 kg
AN-34	Collapsed part of the southwestern ridge	(together)
AN-38	Top of the southwestern ridge	10.54 kg
AX-29	Central depression	6.01kg

Tab. 6-2: Data and sample numbers for studying MNP12

Data	Number of samples/records
Vegetation relevés	3400
Measurements of ground surface height and permafrost table height	3400
Surface samples for actuo-palynological research	50
Peat profiles for palaeoecological analysis	5

6.4 First results

A 3-dimensional model (Fig. 6-4) displays the contours of MNP12 consisting of a large oval central depression bordered by pronounced ridges. The size of the depression is approximately 60 m x 25 m.
The ground surface height corresponds well to the frost table height (Fig. 6-4). At the transition between the depression and the high ridges locally ice wedge hollows are present (see also Fig. 6-6). No clear height level differentiation indicative for former ridge structures is observable in the depression, except for small ridges around samples Y27-AB27 and AX24-AX10. Thaw depth (being the difference between ground surface and frost table height) was 34.65 cm in average with a maximum of 67 cm and a minimum of 2 cm (!) on a high ridge.

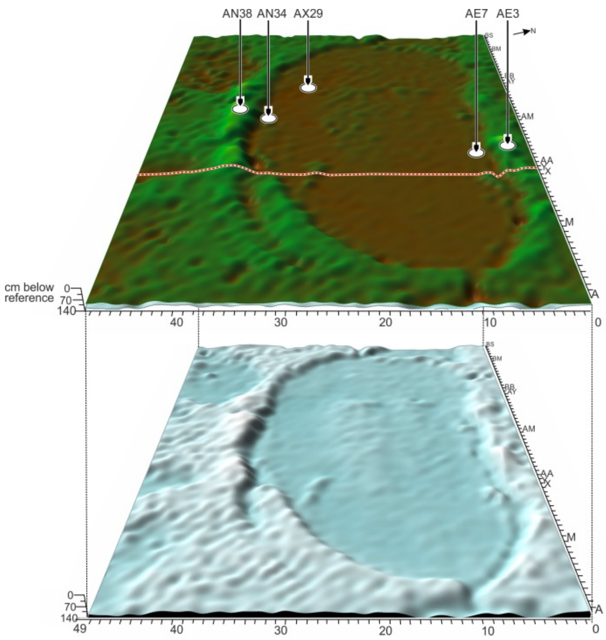

Fig. 6-4: 3D-model of MNP12 (prepared by Martin Schrön): ground surface height (top) and frost table height (bottom) during field research. Arrows indicate the location of the collected peat profiles, the red line marks the location of the surface sample transect Y. Note that rows Z, AZ, and BA do not exist.

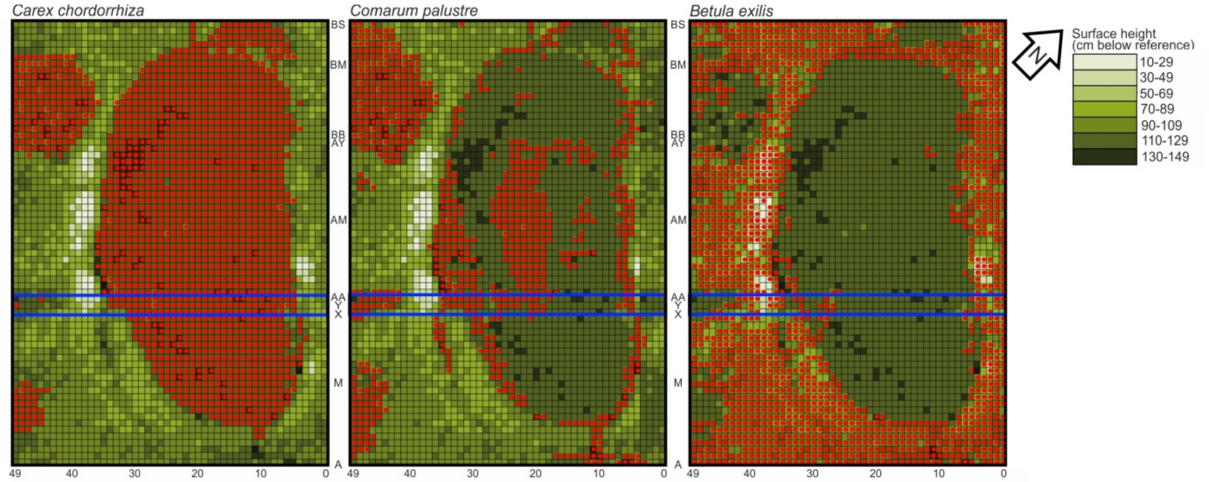

Fig. 6-5: Distribution (red dots) of *Carex chordorrhiza*, *Comarum palustre*, and *Betula exilis* relative to the polygon surface. Note that rows Z, AZ and BA do not exist. Blue frame: transects X, Y and AA (see Fig. 6-6).

Also the vegetation clearly reflects surface height (Fig. 6-5). *Carex chordorrhiza* only occurs in the wet low-lying parts of the polygon complex. A similar distribution is shown by *Comarum palustre*, but this species is less widely spread in the large central depression and occurs conspicuously along its margins. *Betula exilis* occurs (almost) exclusively on the higher dry sites.

The palynological surface samples display typical patterns of pollen deposition in relation to the vegetation of transect Y and the adjacent transects X and AA (Fig. 6-6). Whereas *Betula exilis* grows predominantly on the ridges and at the high reaches of the ridge-slopes, high values of BETULA pollen only occur at plots Y48, Y41-35, Y28-27, and Y0. A complete correspondence with birch presence does not exist due to differences in birch coverage, or by optimal flowering or pollen production being restricted to only some specimens. CYPERACEAE pollen shows high values in the southwestern depression and in the central depression between plots Y34-29. Although Cyperaceae taxa (including *Carex* and *Eriophorum*, cf. Appendix 6) occur widespread along transects X, Y and AA, maximum pollen deposition is also restricted to some plots. This illustrates the complex relationship between plants, flowers and flowering, pollen production, - dispersal and - deposition. Although absence or low values of pollen types do not necessarily indicate the absence of producing plants, high values of CYPERACEAE pollen are indicative for low areas, and high values of BETULA pollen indicate dry areas. Pollen fluctuations of these pollen types in peat profiles, thus, allow the inference of wet (depression) conditions and the formation and collapse of dry ridges at the sampled location (De Klerk et al., 2011), thus allowing a reconstruction of past ice-wedge polygon dynamics.

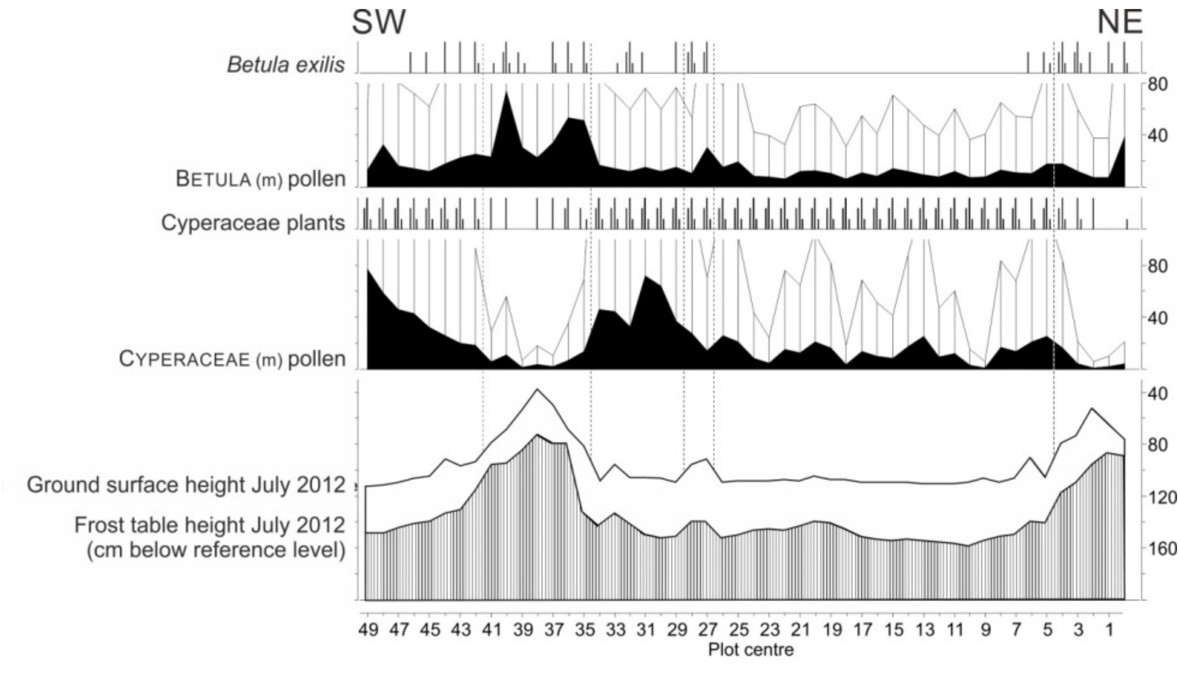

Fig. 6-6: Soil surface and top of the permafrost along transect Y; distribution of CYPERACEAE pollen and BETULA pollen (actual values in black curves, and a 5-time exaggeration in white curves with sample lines) in relation to Cyperaceae and *Betula exilis* occurrence along transect Y (long bars) and the adjacent transects X (mediate bars) and AA (short bars).

7. PEDOLOGICAL STUDIES OF VARIOUS POLYGON SITES

Fabian Beermann, Lilith Pogosyan, Nils Hanke, Lars Kutzbach

7.1 Introduction

Low-centered polygons are characteristics of poorly-drained lowland tundra ecosystems. The depressed polygon centers are characterized by high soil water contents because drainage is impeded by the underlying permafrost. The elevated ridges vary from a dry to a moderately moist water regime (French 2007; Meyer 2003). This small-scale variability causes a heterogeneous plant species composition: The wet polygon centers are mainly characterized by sedges and grasses. The lower soil water contents on the polygon ridges provide the conditions for the growth of lichens, mosses and dwarf shrubs (French 2007)

Substantial portions of the permafrost in arctic regions may thaw in the coming decades (Grosse et al. 2011; ACIA 2004). This would mobilize formerly bound resources like carbon and other nutrients (Kuhry et al. 2010). Plant growth in arctic ecosystems is mainly limited by low supply of nitrogen (Elser et al. 2007; Reich et al. 2006; Chapin III et al. 1995) where plant species composition (e.g. shrub encroachment) depends more on climatic conditions like the short growing season and low temperatures (Gurevitch et al. 2002; Blok et al. 2011)

The combination of higher temperatures and a deeper thawed active layer will provide enhanced nutrient supply and influence the plant species composition of arctic ecosystems (Sturm et al. 2005; ACIA 2004). An increase of nutrient availability in high latitudes can lead to a doubling of primary production but also net carbon losses from soils are possible (Mack et al. 2004). Changes of nutrient availability will indirectly control changes of the carbon balance of arctic ecosystems by controlling changes in the plant species composition (Weintraub & Schimel 2005). Thus, nutrient pools in the permanently frozen ground play a key role for the further progression of arctic ecosystems.

There is already evidence for nutrient release after permafrost degradation (Schuur et al. 2007; Bowden et al. 2012). Furthermore, Keuper et al. (2012) recently found increased amounts of plant-available nitrogen in the uppermost part of the permafrost in Swedish peatlands. Hence, initial evidence of mobilizable nitrogen stores in arctic permafrost soils has already been found.

There is also a high potential for mobilized carbon from thawing permafrost to be released to the atmosphere as carbon dioxide or methane due to microbial activity (Schuur et al. 2008). Billings et al. (1982) concluded, that under warming conditions aerobic respiration may exceed photosynthetic uptake of CO_2 in arctic tundra regions. These regions would then become carbon sources, especially under widespread water table height decrease. While total lake area in Siberia has decreased in the past years, continuous permafrost areas in Siberia show an increase in total lake area and amount of lakes (Smith et al. 2005). Though this might be a temporary phenomenon, it has a major impact on the fate of soil organic carbon.

Release of carbon from formerly frozen soil under anaerobic conditions, as on the ground of thermokarst lakes, may lead to emissions of methane and carbon dioxide. As decomposition rates under anaerobic conditions are much lower than under aerobic conditions the latter produces a higher warming feedback (Schuur et al. 2008).
It is still important to quantify anaerobic decomposition to predict exchanges between tundra soils and atmosphere under a warming climate and predict possible future emissions. Evaluating the potential of anaerobic decomposition and the associated feedback on global warming is difficult, as not all mechanisms in the anaerobic carbon cycle in cold climates are fully investigated. One of these processes is the inhibition of methanogenesis in the presence of iron reduction - a process that plays a major role in anaerobic sediments under warmer conditions (Lovley and Phillips 1986; Lovley 1991). During decomposition microorganism oxidize organic matter to gain energy. In the absence of oxygen, other substances need to be used as electron acceptors during oxidation. These electron acceptors mainly are nitrate, Mn(IV)-oxides, Fe(III)-oxides, sulfate and carbon dioxide, ordered from high energy gain to low energy gain (Ottow 2011). Microorganisms that use iron(III) as an electron acceptor during organic matter oxidation outcompete sulfate reducers and methanogens for electron donors. Similar to aerobic oxidation, which outcompetes all anaerobic processes. Additionally, iron reducing organisms have been shown to reduce electron donor concentrations below the threshold of sulfate reducers and methanogens (Lovley 1991). This process will be investigated at low temperatures on soil samples of the polygonal tundra.
Small polygonal lakes have a large heat capacity and thus a large biological potential during the summer season. Polygonal tundra is particularly sensitive to changes in climatic conditions and arctic microorganisms have a high indicative potential. Rhizopoda are a broad group of protozoan amoeboid organisms. Rhizopodes inhabit all elements of the polygonal structure and form very complex communities in the arctic tundra (Bobrov et al, 2003). The development of the rhizopode communites is driven by the specific environmental conditions of the habitat. Basic determinative factors for the composition of testacea amoebae community are water regime, nutrients and oxygen content, temperature, light, availability of food and building material for shells (Heal, 1964). Despite the long history of research in flora and fauna on the East Siberian Arctic, the data on the protozoan populations of this region are scarce (Bobrov, 2009).

2.2 Goals & Questions

The present study was conducted to gain insight into nutrient dynamics and the complex of rhizopode communities of polygonal tundra ecosystems. Also inhibition of methane production in the presence of reducable iron at low temperatures will be quantified. The small-scale variability of soils in the polygonal tundra will be analyzed by establishing a soil map of the study area.
The following questions are planned to be answered

A. *Soil mapping*
    a. *How does the soil distribution depend on micro-relief?*
B. *Nutrient distribution*
    a. *Is there a general difference of plant available nitrogen compounds between the active layer and the permanently frozen ground?*

C. *Rhizopod Analyses*
    a. *Which species can be found in the dominant rhizopod complexes?*
    b. *What are the differences of the complex of rhizopods between different polygonal tundra sites?*
D. *Inhibition of methane production in the presence of reducible iron*
    a. *Does reducible iron inhibit methane production in the polygonal tundra?*
    b. *In which amount inhibit reducible iron methane production at low temperatures?*

7.3 Fieldwork

A part of the study area (~ 11,000 m^2) was selected for a detailed soil mapping on a scale of 1:1000 (Fig. 5-1).
Seven profiles were selected in polygon centers, the others were selected on different polygon ridges. Characterization of the soil types were conducted following US Soil taxonomy (Soil Survey Staff, 2010) as well as the Russian soil classification (Shishov et al., 2004). A spectrozonal satellite image was used to create a soil map of the study area.
Rhizopode analyses will be conducted on samples from the soil mapping as well as on samples from the soil cores.
For nutrient analyses nine soil cores of 1 m depth have been drilled to investigate the depth distribution of nutrients in the polygonal tundra and the adjacent floodplains. For sampling of the soil cores a portable permafrost auger set was used. This set contained a small engine STIHL BT 121 (Andreas Stihl AG & Co KG) as well as a Snow-Ice-Permafrost-Research-Establishment (SIPRE) coring auger (Jon´s Machine Shop, Fairbanks, Alaska) (Zubrzycki, 2011). The maximum depth of the thawed soil has been measured at the end of August.
All soil cores were divided into subsamples of 5 cm which have been analyzed for their contents of extractable plant available ammonium and nitrate as well as for their water contents. The nutrients were extracted by shaking for one hour in a solution of 0.0125 M $CaCl_2$ (VDLUFA 1991). Within this extract, the amounts of nutrients have been measured photometrically with a portable photometer (Hach LANGE DR 2800) and rapid chemical analysis tests (Hach LANGE: LCK 304 (Ammonium), LCK 339 (Nitrate)). By determining the gravimetrical water contents, the results of the nutrient analyses could be calculated to the dry mass of the soils.
For the measurement of methane inhibition samples were taken from four different points inside a single ice-wedge polygon: Two in the polygon center and two on the polygon wall. Each spot consisted of three repetitive profiles. Samples were taken from each soil horizon. For all samples, pH has been determined using a portable measuring device (WTW pH/Cond 340i).

7.4 Labwork

Inhibition of methane production will be evaluated by anaerobic incubation at 4°C. Headspace methane and carbon dioxide concentrations will be determined using gas chromatography. Iron(II) and iron(III) concentrations in solution will be determined photometrically using the ferrozine method (Stookey 1970; Viollier et al. 2000). Carbon dioxide and methane production rates will then be compared to iron reduction rates. Additionally bulk values for carbon, nitrogen and iron will be determined to test for correlations to methane production and reduction rates.

7.5 Preliminary results
7.5.1 Site description (Tab. 7-1)

POKF1: A typical ice-wedge polygon with dry and elevated ridges and a depressed center consisting of a small pond. The soil of the polygon ridge was a Typic Haploturbel, the soil of the polygon center was a Typic Fibristel.

POKF3: This site was located near the polygon POKF1. It was located in a very flat and wet area which was characterized by either remnants of ice-wedge polygons or newly developing ice-wedges. The soil of this polygon center was a Fluvaquentic Sapristel. The soil of the polygon ridge directly above the ice-wedge was characterized as a Glacic Histoturbel.

Tab. 7-1: Description of all collected soil cores

Core number	Site	Latitude	Longitude	Soil Type	Vegetation	Thawing depth (cm)
POKF1 W	Polygon ridge	69.05709	160.5632	Typic Haploturbel	B. Nana / A. glutinosa	47
POKF1 C	Polygon center			Typic Fibristel	Pond	61
POKF3 W	Polygon ridge	69.05687	160.56442	Glacic Histoturbel	C.aquatilis / E. angustifolium	46
POKF3 C	Polygon center			Fluvaquentic Sapristel	C.aquatilis / E. angustifolium	53
POKF4 W	Polygon ridge	69.06225	161.00145	Fluvaquentic Historthel	B. Nana / A. glutinosa	35
POKF4 C	Polygon center			Fluvaquentic Sapristel	C.aquatilis / E. angustifolium	53
POKF5	Floodplain	69.06224	161.00234	Fluvaquentic Aquorthel	C.aquatilis / E. angustifolium	59
POKF7	Floodplain	69.04594	160.58222	Fluvaquentic Aquorthel	Equisetum fluviatile	61
POKF8	Shrub tundra	69.04589	160.58158	Fluvaquentic Fibristel	Arctagrostis latifolia	33

POKF4: This low-center polygon was characterized by comparatively high rims. Due to the adjacent Kolyma River, there were high amounts of mineral soil material within the soil profiles. Frequent flooding due to the Kolyma River is also reflected in the soil classification results: The soils of the polygon ridge and the polygon center were classified as Fluvaguentic Historthel and Fluvaquentic Sapristel, respectively.

POKF5: This site was located on the Kolyma River floodplains near to the site POKF4. Due to the nearby river, no ice-wedge polygons were developed. One soil core was drilled at this site. The soil was characterized by high amounts fluvial sediments and iron oxides down to a depth of ~70 cm. This soil has been classified as a Fluvaquentic Aquorthel.

POKF7: This site was located on the floodplain of a small lake with connection to the Kolyma River. Again, this soil was characterized as a Fluvaquentic Aquorthel.

POKF8: This site was located on a very dry spot approximately 3 m above the water level of the Kolyma River. One soil core was drilled which was characterized as a Fluvaquentic Fibristel.

7.5.2 Pedodiversity

The spectrozonal satellite image revealed three main positions in the micro-relief which were related to different soil groups (Fig. 7-1). There were elevated dry spots, polygon ridges and polygon centers. The soils of the elevated dry spots belonged in most cases to the suborder “Turbels”. At the highest point of the polygonal micro-relief the soil at a single hummock of dried peaty material was characterized as Typic Folistel.

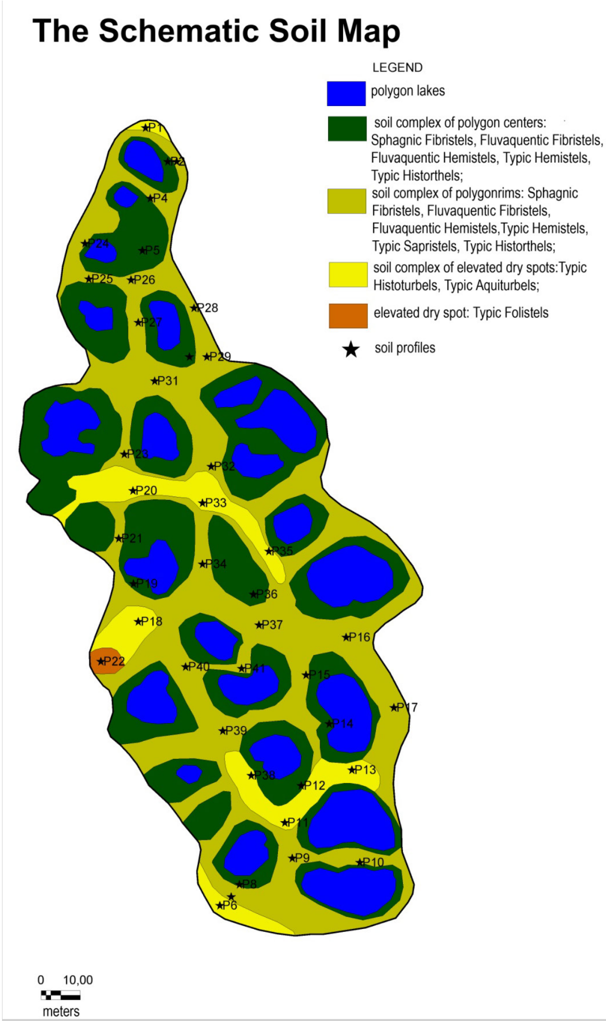

Fig. 7-1: Basic soil map of the investigation area

The polygon ridges are characterized by a soil complex of Sphagnic Fibristels, Fluvaquentic Fibristels, Fluvaquentic Hemistels, Typic Hemistels, Typic Sapristels, Typic Historthels. The polygon centers consist of a soil complex of the same composition except Typic Sapristels

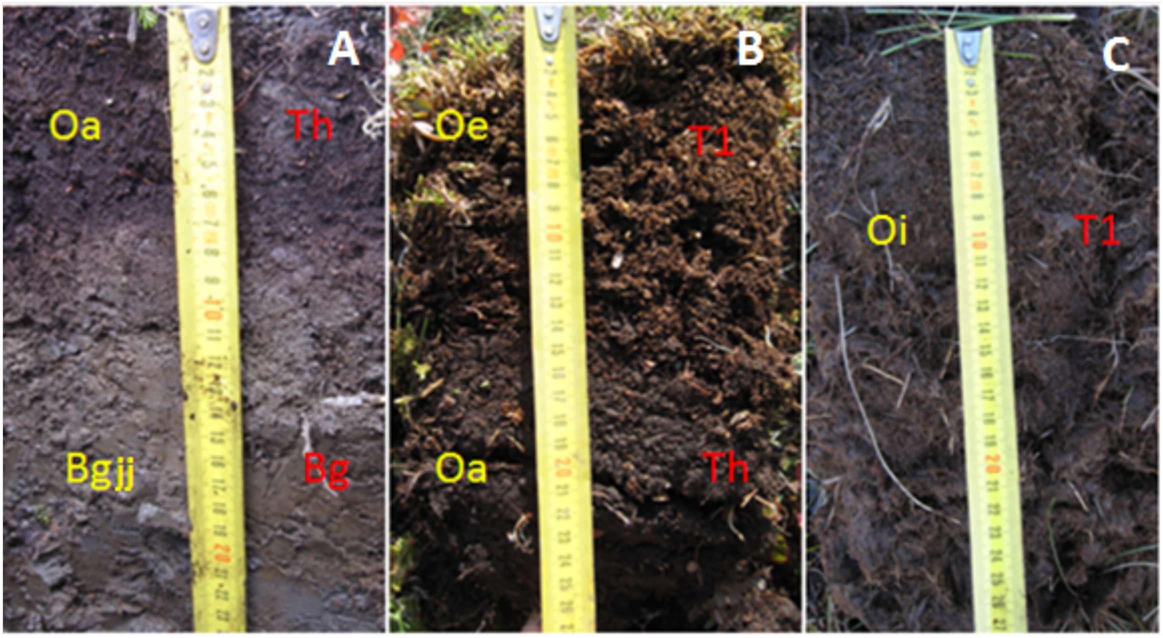

Fig. 7-2: Three typical soil profiles of the study site. Horizon symbols after the US Soil Taxonomy in yellow, after the Russian classification in red (A): Soil Profile 6 (elevated dry spot) – Typic Aquiturbel and Peat Cryozem gley, respectively) (B): Soil Profile 32 (polygon ridge) –Typic Sapristel and Peat Eutrothic typic, respectively (C): Soil profile 30 (polygon center) – Typic Fibristel and Peat Eutrothic typic, respectively

Three typical soil profiles of the different soil units are shown in Fig. 7-2. The elevated dry spots (Fig. 7-2A) were characterized by high amounts of mineral soil showing properties of cryoturbation (Bgjj horizon. Therefore, these soils were characterized as Turbels after US soil classification (Soil Survey Staff 2010). The polygon centers as well as the polygon ridges were mainly characterized by high amounts of organic material. Most soils belonged to the suborder “Histel”. Sapristels, with more decomposed organic material were only found in the polygon rims (Fig.7-2B). In the polygon centers, most of the organic material were only initially decomposed (Fibristel, Fig.7-2C). Following the Russian soil classification (Shishov et al., 2004) there are no differences between Sapristels and Fibristels: Both soils are characterized as Peat Eutrophic typic

Differences between the soil units are also reflected in the thawing depths: The range of the maximum thaw depth was bigger at the polygon ridges than at the polygon centers. But on average, maximum thaw depth was highest at the polygon centers (Fig. 7-3).

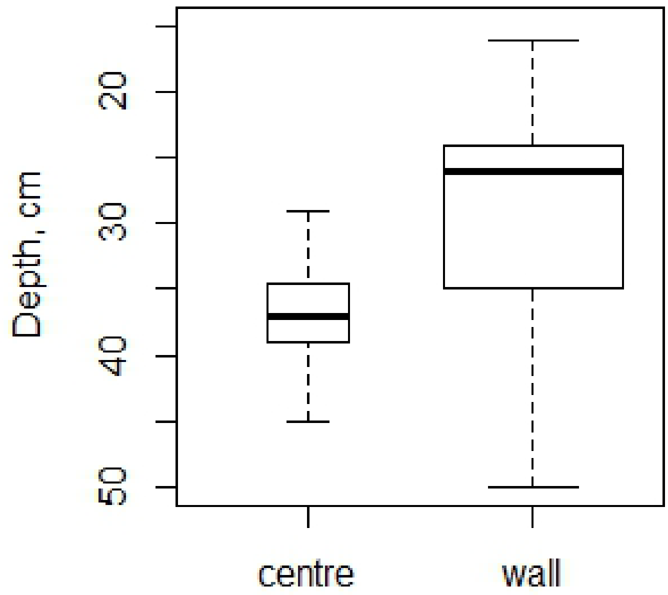

Fig. 7-3: Depth of thawing between 05.08.2012 and 15.08.2012

7.5.3 Lab results

In all investigated soil cores we found an increase in the concentration of plant available ammonium in the permanently frozen ground (Fig. 7-4). The start of the ammonium accumulation started on average approximately 10 cm below the late season active layer of 2012 (see also Tab.5-1). High amounts of ammonium were also found in the active layer of the core POKF1 C, which was drilled at the bottom of a small polygonal pond.

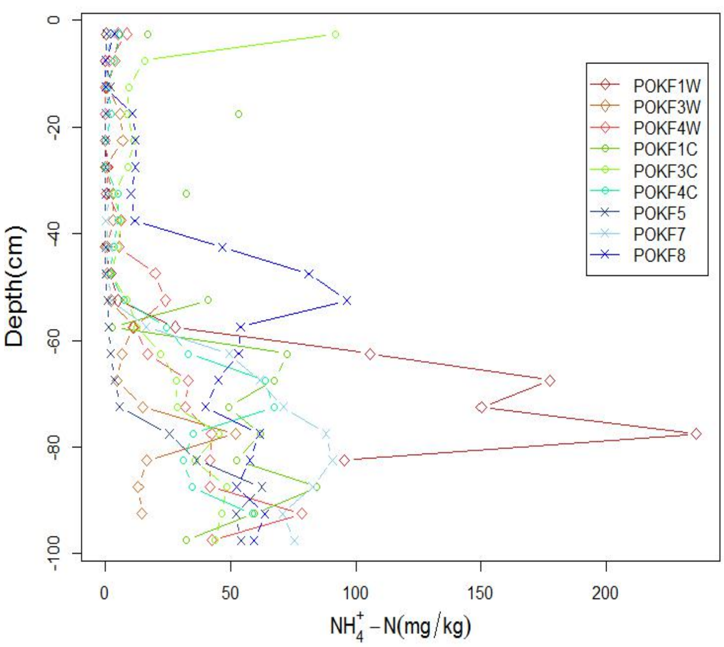

Fig.7- 4: Concentration of plant available ammonium in relation to the dry mass of the soils in ten soil cores to a depth of 100 cm. Polygon rims are represented by diamonds, polygon centers are represented by circles, crosses indicate floodplains.

On average, the concentration of plant available ammonium in relation to the dry mass of the soil was seven times higher in the permanently frozen ground than in the active layer. The concentration of plant available nitrate in relation to the dry mass of the soil was lower than the concentration of plant available ammonium. There were no significant differences between the concentrations of plant available nitrate in the active layer and the frozen ground. (Fig.7-5)

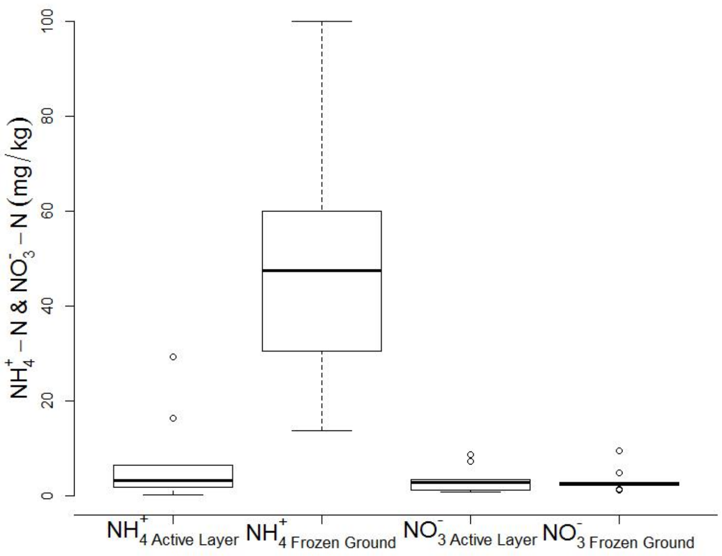

Fig. 7-5: Differences of plant available ammonium and nitrate in the first 100 cm of the investigated soil cores. NH_4^+: $Mean_{Active\ Layer}$ = 6,6 mg/kg, $Mean_{Frozen\ ground}$ = 48,7 mg/kg, p=<0.0005; NO_3^-: $Mean_{Active\ Layer}$ = 3.2 mg/kg, $Mean_{Frozen\ Ground}$ = 3.2 mg/kg, p=>0.25

7.6 Discussion

7.6.1 Pedodiversity

After The Russian Classification (Shishov et al. 2004) soils with mineral horizon have been classified as “Peat Cryozems” with the suffixes “homogeneous” and “gley”, respectively. Soils that consisted only of organic horizons were classified as “Peat Eutrophic” with the suffix “typic”.

Soils of the suborder Turbels (Soil Survey Staff, 2010), which are characterized by cryoturbated mineral material, develop on the elevated dry spots. These elevated dry spots possibly could be developing due to palsa dynamics on the polygon rims (French, 2007). Soils in wet conditions in the polygon centers contain more organic material in different stages of decomposition. Also there is a difference between the depth of thawing at the polygon ridges and the polygon centers. This can be explained by differences in thermal conductivity (Bobrov et al. 2013). Soils on higher positions on the micro relief have less stable temperature and water conditions, which makes them vulnerable to turbation.

7.6.2 Chemistry

All soil cores contained high amounts of organic material. The adjacent Kolyma River and its flooding events are also indicated in the soil classification by the prefix “Fluvaquentic” in six of the nine investigated soils cores.
In all soil cores, there was a significant accumulation of ammonium in the permanently frozen ground compared to the active layer. In contrast, there were no differences in the concentration of nitrate between the active layer and the permanently frozen ground.
Biological activity in permafrost-affected soils is mainly limited to the active layer. The pace of biochemical reactions depends on temperatures and water availability (Madigan & Martinko 2006). But the underlying permanently frozen ground is not a static system. Also in frozen soils, liquid water exists which is the basis for microbial activity (Ershov 1998). Despite of the harsh conditions, microbial communities are active in the permanently frozen ground, even down to temperatures of -10 °C and lower (Wagner et al. 2007).
Commonly, high water contents of tundra soils provide an anoxic regime which allows only anaerobic decomposition of the organic material (Gebauer et al. 1996). Our results support the thesis that there is accumulation of ammonium due to microbial decomposition in the anoxic and frozen milieu below the active layer. Though decomposition rates may be slow at temperatures below 0 °C (Mikan et al. 2002; Wagner 2008), decomposition over long time scales could lead to this accumulation. As the frozen ground builds a physical barrier for plant root growth (Gurevitch et al. 2002), there is lower consumption of these reservoirs at recent temperatures. Due to anoxic conditions, the mineralized ammonium cannot get oxidized further to nitrite and nitrate (Madigan & Martinko 2006).
If there are generally high amounts of plant available ammonium stored in the permanently frozen part of tundra soils, this has great implications on the further progression of arctic tundra. It is projected that climate change will be most pronounced in high latitudes, a phenomena known as polar amplification (IPCC 2007) which may lead to a significant increase in active layer thickness (Grosse et al. 2011). An increase in active layer thickness would allow plants to access these large accumulated ammonium stores. As the arctic tundra has been reported to respond most strongly to nitrogen addition in comparison to other sites (Elser et al. 2007), major changes in plant species composition could follow.
Elevated nitrogen supply could enhance the carbon sink function of arctic tundra (Reich et al. 2006) which could compensate – at least partly – higher carbon emissions from arctic tundra (Mack et al. 2004) which are projected in the course of climate change. Also a shift of the shrub line would be supported by higher nitrogen availability which would have major impacts on arctic tundra like, e.g., altered snow-holding capacities, changes in hydrology and changes in surface albedo (Sturm et al. 2005).

7.6.3 Rhizopodes

The list of rhizopode species in Arctic regions includes about 291 species, varieties and forms (Beyens and Chardez, 1995). This inventory is based on more than 1000 samples representing typical soil and aquatic habitats in arctic tundra landscapes, published in studies since the beginning of the 20th century including regions of the North American Arctic.

Based on literature we can conclude that arctic testate amoebae communities include several biogeographic fractions: (1) endemic arctic species; (2) sphagnobiontic species of the tundra and taiga zones; (3) holarctic species of the forest zone; (4) non-holarctic species of the pan-tropical and circum-australian zones; (5) eurybiontic cosmopolitan species (Bobrov et al, 2012).
The biggest testacean population density and variety will possibly be present in the uppermost horizons of the profiles (Vincke et al., 2006).

7.7. Outlook

After detecting significant stores of plant available Ammonium in the permanently frozen ground we have to evaluate the importance of these amounts in comparison to other studies and sites. For this approach the results have to be recalculated to pools to be comparable to the results from the POLYGON expedition in 2011 (Beermann & Kokhanova 2012) and to soils from the Lena river delta.

8. THE PINGO EXPOSURE 'SHIROKOVSKY KHOLM' AND ITS SURROUNDING

Sebastian Wetterich, Lutz Schirrmeister, Viktor Sitalo, Lilith Pogosyan & Evgenya Zhukova

8.1 Scientific rationale

In course of the POLYGON expedition in 2012 to the Kolyma Delta different features of periglacial landscapes have been studied including a prominent pingo (*bulgunyakh* in Russian) exposure near the settlement Pokhodsk on the right bank of the Kolyma River (Figs. 2-4 and 2-6; 69.03836 °N, 161.00642 °E).

Hydrostatic pingos like the studied one form in drained thermokarst lake basins when pressurised water in the refreezing zone (talik) under the former lake migrates towards a common freezing front and accumulates in a growing ice core (Mackay, 1985). Due to the development of this massive ground ice body the terrain surface and above-lying frozen deposits dome up and form conical, perennial frost mounds which are covered with soil and vegetation. Characteristic are the elliptical to circular planar shape reaching diameters of up to several hundred meters and heights of up to several dozen meters if largest (van Everdingen, 1998). The formation and presence of pingos is closely linked to past and present local climatological, geological, and hydrological conditions.

Pingos represent common features in circum-arctic lowlands with continuous permafrost which are rather well studied in the North-American Arctic in terms of formation (e.g. Mackay, 1962), structure (e.g. Yoshikawa et al., 2006), distribution (e.g. Jones et al., 2012). Pingo growth and decay rates, pingo age, and past distribution of pingos have been used for the reconstruction of past periglacial landscape conditions (e.g. Flemal, 1976; Mackay, 1986; Walker et al., 1996; Grosse et al., 2007). Pingo inventories were furthermore employed in palaeoenvironmental reconstructions (Hyvärinen and Ritchie, 1975; Wetterich et al., 2012). Grosse and Jones (2011) recently provided a detailed spatial geodatabase of more than 6000 pingo locations in a 3.5 x 10^6 km^2 region of Eurasia, and linked the pingo distribution with climate and permafrost.

The pingo 'Shirokovsky Kholm' revealed access to the exposed ice core because a fire in summer 2003 burnt overlying peaty soils (personal communication by Natalya Ivanovna Arbatskaya, Pokhodsk) and caused extensive melting of the massive ice, thaw subsidence, slumping and slope erosion since then (Fig. 8-1). This exceptional anthropogenic impact let to the onset of rapid pingo destruction. In order to characterise the pingo as example for the typical landscape feature of the Kolyma Delta and to uncover its formation detailed sampling of the exposed massive ice, its surrounding frozen deposits and overlying soils have been undertaken. Additionally, short cores from the thermokarst lake basin (see chapter 5) have been taken to highlight the interaction between Holocene thermokarst and pingo formation, exemplarily for vast areas of the Kolyma Delta.

8.2 The pingo exposure 'Shirokovsky Kholm'

The pingo remnant is present by about three quarters of its former extent. The maximal height of the pingo remnant is about 12 m above lake level (m a.l.l.). The largest diameter of the pingo remnant extends to about 120 m (Fig. 2-6). The ice core was exposed in the north-facing part of the pingo in different steep exposures of core ice and frozen sediment (Fig. 8-1). Sediment and ice samples have been taken between August 19 and 22, 2012 by axe and hammer. Still in the field, pH and electrical conductivity (EC) measurements have been performed on thawed material using a WTW340i pocket meter equipped with a Tetracon 925 conductivity cell for EC (reference temperature: 25 °C) and Sentix 43-1 electrode for pH measurements (Appendices 8-1, 8-2). For further sample processing, massive and texture ice samples for element analyses (15 ml) were acidified with 50 µl 65% HNO_3, whereas samples for anion analysis and residue samples were cool stored. Before conservation, samples for element (cation) and anion analyses were filtered by a cellulose-acetate filtration set (pore size 0.45 µm). Additionally, samples for $\delta^{18}O$ and δD isotope analyses (30 ml) were preserved without any conservation.

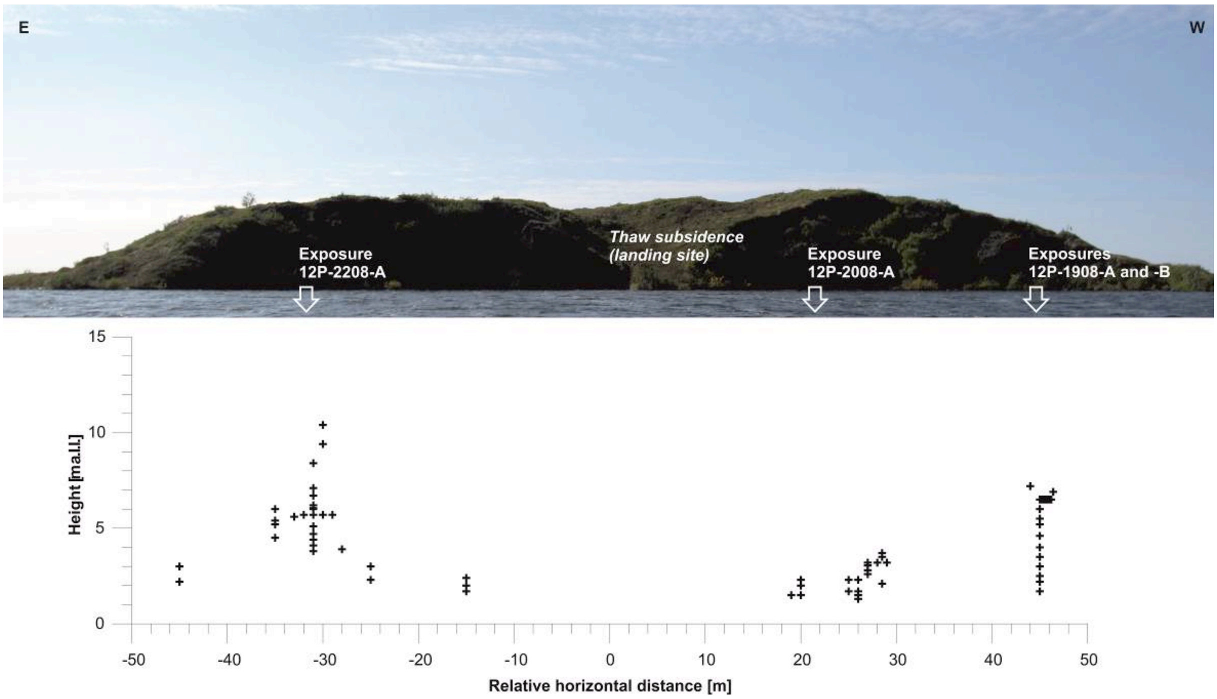

Figure 8-1: Overview sketch of the sampled outcrops from the landing site at the pingo exposure 'Shirokovsky Kholm'. Note that the photograph is not to scale. Details are given in Figures 8-2 to 8-6.

8.2.1 Exposures 12P-1908-A (site VI in Fig. 2-6) and 12P-1908-B

The exposures 12P-1908-A and 12P-1908-B are located at the western edge of the study site (Fig. 8-1). The 12P-1908-A profile comprises a 6-m-deep sequence of frozen fine-grained sediments, peat and ice belts as well as an ice wedge on top (Fig. 8-2; Appendix 8-1).

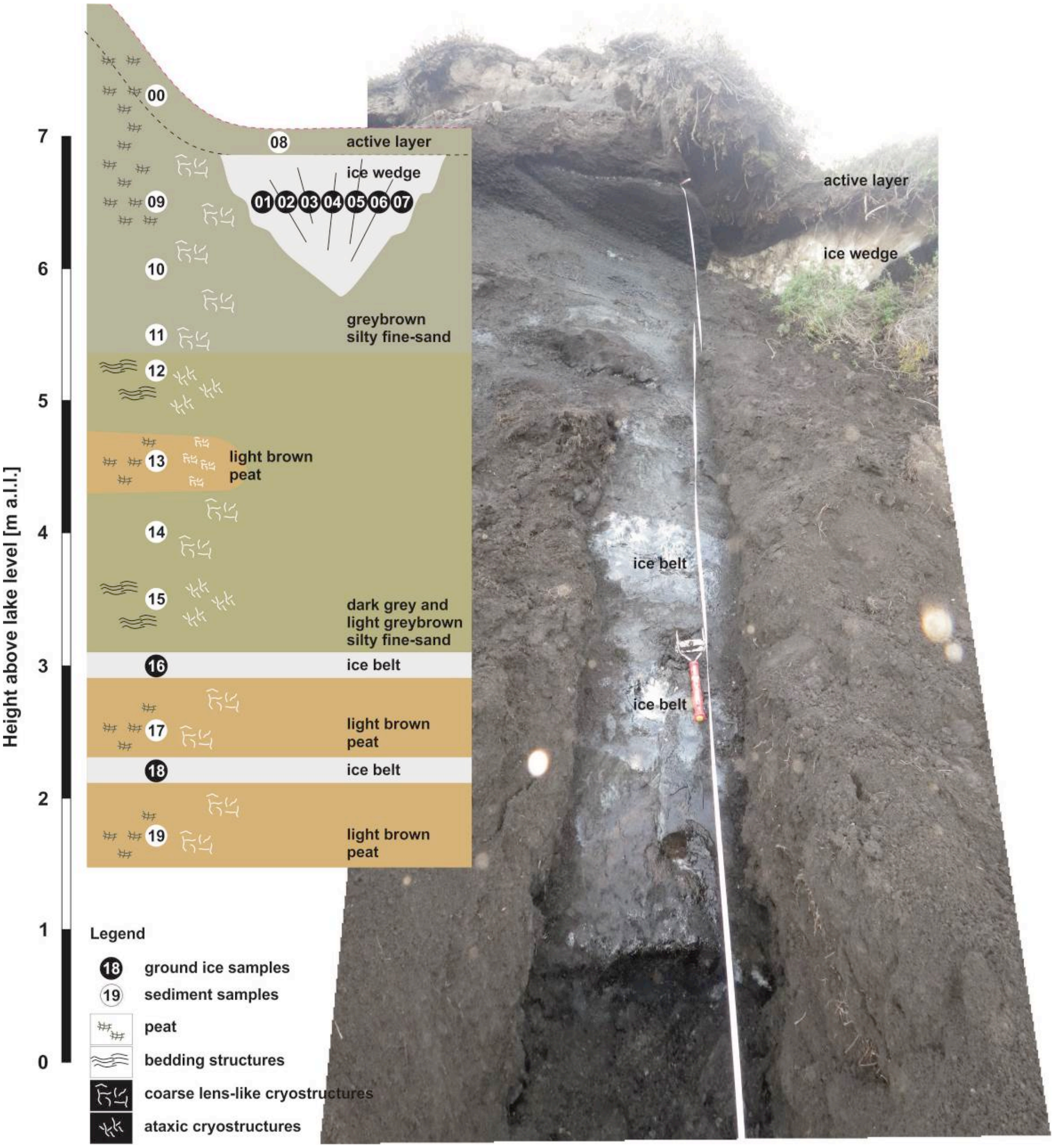

Figure 8-2: Merged photographs and sampling scheme of the exposure 12P1908-A.

The lowermost light brown moss peat is interrupted by two ice belts up to several decametres thick until about 3 m a.l.l. and shows signs of cryoturbations and coarse lens-like cryostructures. The peat is overlain by bedded grey silty fine-sand of lacustrine origin with coarse lens-like and ataxic cryostructures until about 5.2 m a.l.l. The uppermost grey-brown silty fine-grained sands exhibit peaty inclusions and coarse lens-like cryostructures. The syngenetic ice wedge within the uppermost unit is 1.8 m in visible width and 1.2 m in visible length is composed of milky white ice with irregular vertical elongated and rounded air bubbles of 1 mm in diameter. The EC of the ice wedge ice is rather low with 66 µS cm^{-1} and the pH acidic with pH 5.7 (Appendix 8-2).

The exposure 12P-1908-B has not been sampled, but represents the lowermost light brown moss peat of 12P-1908-A with clear ice belts (20 to 30 cm thick) (Fig. 8-3) and signs of cryoturbation and is located a few metres east of exposure 12P-1908-A.

Figure 8-3: Photograph of the exposure 12P1908-B (not sampled; site VIII in Fig. 2-6).

8.2.2 Exposure 12P-2008-A (site VII in Fig. 2-6)

The exposure 12P-2008-A between about 1 to 3 m a.l.l. represents the massive ice of the pingo core which has been sampled in different parts over a lateral distance of about 10 m (Fig. 8-1). Additionally, samples of overlying and enclosed sediments have also been taken (Appendix 8-1).

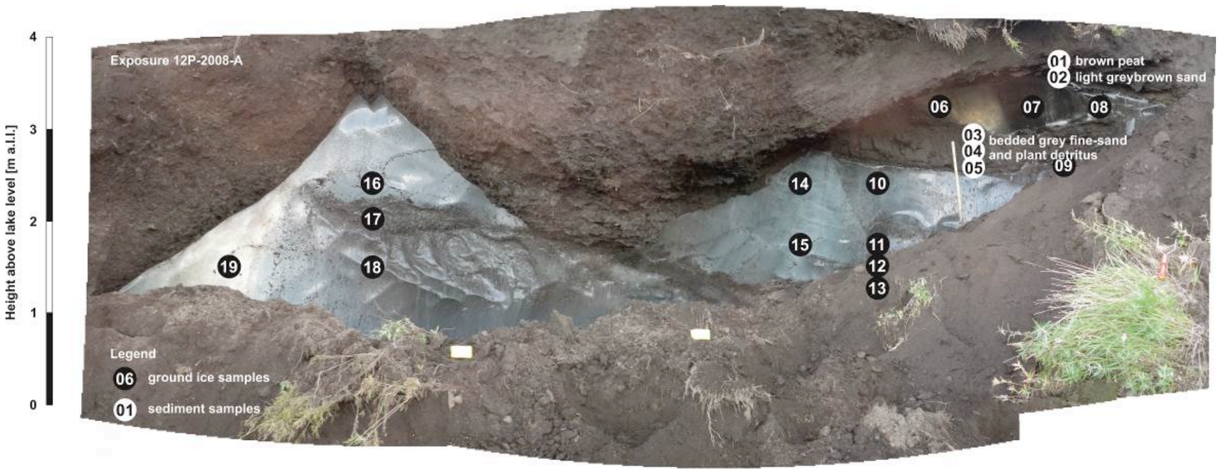

Figure 8-4: Merged photographs of the exposure 12P-2008-A.

The latter are bedded alternations of grey fine-sand and brownish plant detritus with peat inclusions and diagonal ice veins. The massive ice itself differs in colour and air bubble content. Approximate sampling positions are given in Figure 8-4. The EC of the clear pingo ice varies between 32 and 203 µS cm^{-1}, but reaches high values of up to 2020 µS cm^{-1} if the ice is in close contact to sediment. The pH is mainly neutral with values around 7 (Appendix 8-1).

8.2.3 Exposure 12P-2208-A (sites IX and X in Fig. 2-6)

The exposure 12P-2208-A exhibits the massive ice of the pingo ice core and its overlying sediments in the eastern part of the outcrop between about 4 and 10 m a.l.l. over a lateral distance of about 30 m (Figs. 8-1, 8-5 and 8-6). The main sample amount (12P-2208-A-01 to -23) was collected in vertical and horizontal profiles (Fig. 8-5). The deposits covering the massive ice are greybrown and light brown (silty) fine-sands (Appendix 8-1) with single wood, root and peaty inclusion. The cryostructures are mainly ataxic. The massive ice itself differs in colour and air bubble content. Approximate sampling positions are given in Figure 8-5.

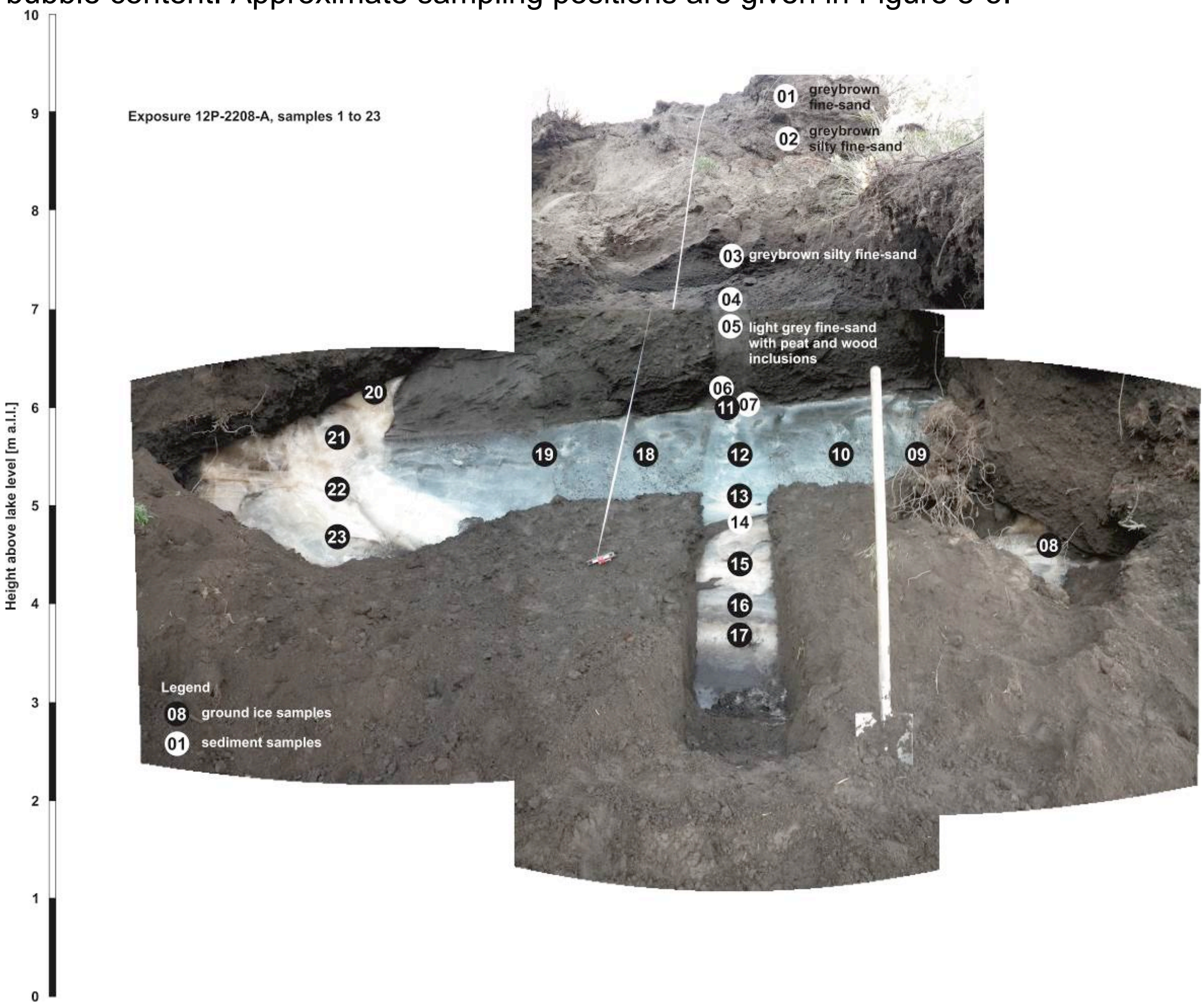

Figure 8-5: Merged photographs of the exposure 12P-2208-A (samples 12P-2208-A-01 to -23).

Additionally, massive ice was sampled in three 'windows' between 1.5 and 3 m a.l.l. to complete the lowermost exposed ice record (Fig. 8-6). The EC of the clear pingo ice varies between 32 and 116 µS cm^{-1}, but reaches values of 251 µS cm^{-1} if the ice is in close contact to sediment. The pH is mainly slightly acidic to neutral with values between pH 6.5 and pH 7.2 (Appendix 8-2).

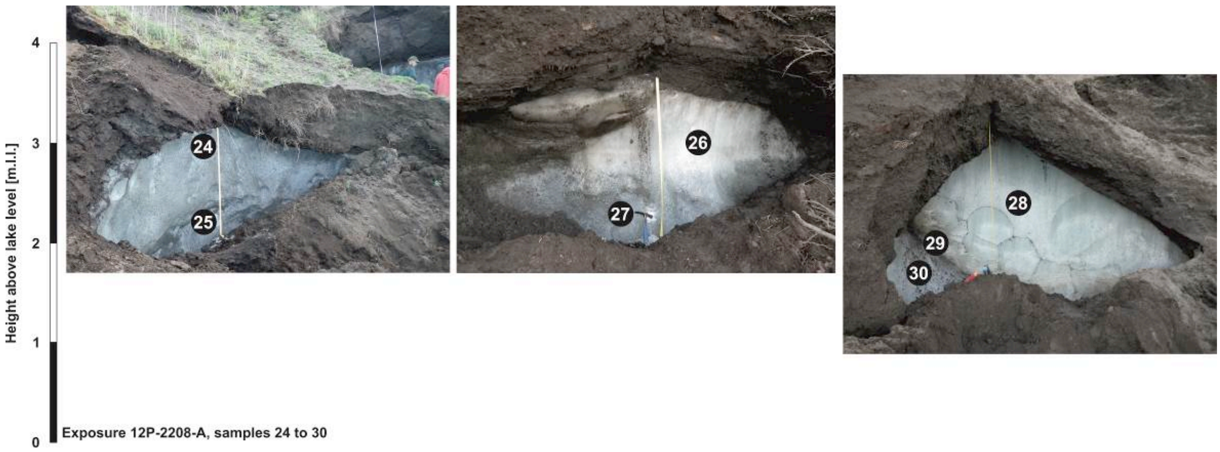

Figure 8-6: Photographs of the exposure 12P-2208-A (samples 12P-2208-A-24 to -30).

8.3 The soil and vegetation cover of the pingo 'Shorokovsky Kholm'

In order to detect soil type distribution on top of the pingo and in its surroundings soil pits within the active layer have been described and sampled following the North-American (Soil Survey Stuff, 2010) and Russian (Shishov et al., 2004) classifications of soils (Appendix 8-3). Sampling positions are given in Figures 2-6 and 8-7.

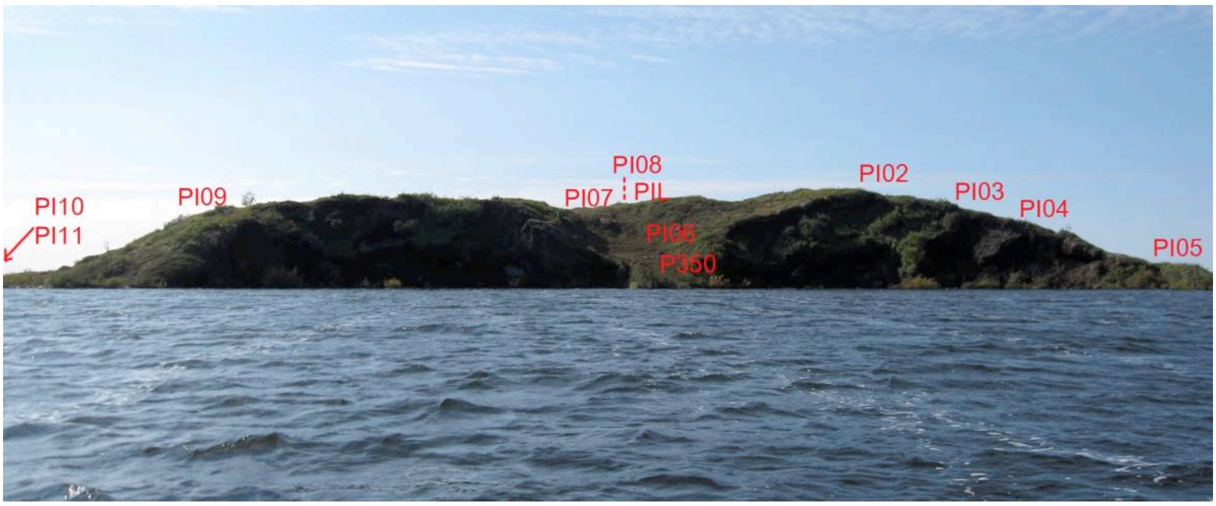

Figure 8-7: Sampling sites of soil pits.

The vegetation cover is dominated by *Salix* shrubs, mosses and grass while in wind-protected areas also *Betula nana* occurs.

The northern part of the pingo is characterised by active erosion and denudation. On a small area with undisturbed soil cover a Typic Historthel has been found (site PI06; Fig. 2-6). Starting on the western flank of the flat pingo top downslope, a soil catena (sites PI02 to PI05) has been studied (Fig. 8-7).

On pingo top Typic Historthels (site PI02) were found while Typic Sapristels (PI03) and Typic Historthels (site PI04) occurred in different steep parts of the slope, and the slope base was characterised by Typic Hemistels under the subhorizontal surface (site PI05).

In the center of the flat pingo top a small water-filled depression (10 to 15 cm water depth) takes place which is underlain by Typic Historthels (site PIL).
On the southern part of the flat pingo top a bowl-like basin is vegetated by *Sphagnum sp.*, *Rubus chamaemous*, *Vaccinium vitis-idaea* and *Ledum decumbens*, and the soil belongs to Sphagnic Fibristels (PI07).
The steep southern slope is almost completely covered by *Betula nana* shrubs up to 60 cm high. Meanwhile *Duschekia fruticosa* (up to 3 m high), *Sphagnum* sp., *Rubus chamaemous*, *Ledum decumbens* and *Veratrum lobelianum.* cover the slope base. The soil belongs to Sphagnic Fibristels (site PI08; Fig. 8-8).

Figure 8-8: Sphagnic Fibristel from site PI08 on the southern slope base of the pingo

The eastern slope is not completely vegetated; here *Chamerion angustifolium* occurs. The soil profile of site PI09 reaches a depth of 75 cm below surface (b.s.) while the wavy border of the organic horizon occurs at about 12 cm b.s. The mineralic part is represented by fine- and middle-grained sands and includes coal particles (up to 2 cm in diameter) likely originated by the fire mentioned in section 8-1. The soil is classified as Typic Psammorthel (site PI09).
On the north-eastern base of the pingo poorly-developed ice-wedge polygons take place. The shallow wall of such polygons represent Typic Historthels (site PI10), and the center Typic Hemistels (site PI11).
North-west of the pingo poorly developed polygon structures have been found on small islands. Mineralic soils have not been found. The polygon walls are

characterized by Typic Hemistels (site PI12), and the centers by Typic Fibristels (site PI13).
Each described and sampled soil horizon has been analysed for pH of soil suspension using WTW340i pocket meter equipped with a Sentix 43-1 electrode (Appendix 8-3). In almost all profiles the pH increases from the soils surface towards the lower border of the mineralic horizon. The pH in general varies between 4 and 6.

9. DRILL HOLES AND PITS AROUND POKHODSK

Vladimir Tumskoy, Evgenya Zhukova, Lutz Schirrmeister & Sebastian Wetterich

9.1 Scientific background, objectives and methods

In order to study the structure and composition of the active layer as well the near-surface frozen ground eighteen short-cores up to 130 cm depth below surface were drilled and six pits were dug into the polygonal tundra landscape around Pokhodsk (Figs. 2-4/5, Tabs.9-1/2). The material will further be used for paleoenvironmental studies of the Holocene landscape dynamics as well as for permafrost organic matter characteristics. At eight sites, cores were drilled parallel, were the second core labelled as POK1 to POK8 is used for pedological and nutrient studies (see chapter 7).

For drilling we used a “Snow-Ice-Permafrost-Research-Establishment” (SIPRE) Coring Auger Set (Ø 70 mm) with a one meter long extension according to Zubrzycki, S. (2012). Pits were dug with spades or cut by chain saw and cleaned by hacks.

Sediment and ice structures were described, sketched and photographed. Frozen deposits of exemplary profiles were sampled for further multidisciplinary studies (sedimentology, hydrochemistry, paleoecology, geochronology, organic geochemistry) using hammers and small axes (appendix 9). The thawed sediment samples were stored in plastic bags. Already during expedition gravimetric ice contents were measured according to van Everdingen (1998). Therefore, frozen samples were taken in aluminium boxes, weighted, dried, and weighted again. In addition, from selected core segments V. Tumskoy measured the volumetric ice content by estimating the volume and weight of a core segment and measuring the loss of weight of a smaller so-called average subsample.

In addition, ice wedges were described and sampled for hydrochemistry and stable isotope studies (appendix 9). Thawed samples of ice wedges and segregation ice were measured for electrical conductivity (EC) and pH using the WTW pocket meter in the field lab. Similar to pond water samples the exemplary melt water samples were prepared for cation and anion analyses by filtering through a cellulose-acetate filtration set (pore size 0.45 µm). Melt water samples for cation analyses (15 ml) were acidified with 200 µl HNO_3, whereas samples for anion analyses and residue samples were only cool stored. The samples for $\delta^{18}O$ and δD isotope analyses (30 ml) were preserved without any conservation.

Tab. 9-1: List of permafrost cores with coordinates (W – polygon wall, C – polygon centre).

Labels in Figs. 2-4, 2-5	Core label	Site description	Coordinates	Core number	Remarks
XII	12P-1607-1 (POK1 W)	Viska flood plain, wall of the monitoring site	N 69.095150° E 160.938733°	2	0.5 m distance
XIII	12P-1707-1 (POK1 C)	Viska flood plain, low-centred polygon	N 69.095033 E 160.938900	1	
XIV	12P-1907-1 (POK 3W)	Viska flood plain, near the monitoring site, rim without walls	N 69.094783 E 160.940700	2	0.7m distance
XIV	12P-1907-2 (POK3 C)	Viska flood plain, polygon centre,	8 m distance from 12P-1907-1	2	
XV	12P-2107-1 (POK4 W)	Kolyma flood plain, Pokhodskaya Channel, wall	N 69.103750 E 161.002417	2	0.2 m distance
XV	12P-2107-2 (POK4 C)	Kolyma flood plain, Pokhodskaya Channel, centre	8 m distance from 12P-2107-1	2	0.5 m distance
XVI	12P-2707-1 (POK5)	Kolyma flood plain, Pokhodskaya Channel, highest part of the low floodplain	N 69.103733 E 161.003900	1	
XVII	12P-2707-2 (POK6)	Kolyma flood plain, Pokhodskaya Channel middle part of the low floodplain	N 69.103483 E 161.005517	1	
XVIII	12P-2707-3	Kolyma flood plain, Pokhodskaya Channel, lowermost level	N 69.102917 E 161.008283	1	6 m distance from the shore
XIX	12P-3007-1 (POK7)	Lake flood plain near Pokhodsk	N 69.076583 E 160.970367	2	
XX	12P-3007-2 (POK8)	Lake terrace near Pokhodsk	N 69.076483 E 160.969300	1	
V	12P-1008	Khalerchinskaya Tundra	N 69.05617 E 160.85904	1	

Tab. 9-2: List of pits and exposures with coordinates.

Labels in Fig. 2-4, 2-5	Site label	Site description	Coordinates
I	12P-2007-1	Khalerchinskaya Tundra, mud boil	N 69.063860 E 160.878890
II	12P-2007-2	Khalerchinskaya Tundra	N 69.063550 E 160.866040
III	12P-2007-3	Khalerchinskaya Tundra, mud boil	N 69,064070 E 160.861890
IV	12P-2007-4	Khalerchinskaya Tundra, mud boil	N 69.063500 E 160.866700
XXI	12P-2507-1 12P-0708-1	Ice wedge pit, near the monitoring site	N 69.09503292 E 160.937147
XI	12P-2308	Viska flood plain, exposure	N 69.11288 E 160.76570

9.2 Core description

12P-1607-1 (POK1-W), drill core at the monitoring site

Centre of the wall, 2 cores in 0.5 m distance,
Modern vegetation: moss, lichens, dwarf birch up to 30 cm high, alder shrubs of 0.5-1 m height, a.l. depth 40, 25, 43, 41 cm

0-5 cm, vegetation cover

5-20(30) cm, peat, medium decomposed, brown, cryoturbated, peat thickness and a.l. depth are almost similar.

20(30)-54 cm, silty fine-sand, brownish grey, in contact to the overlain peat weakly reddish-brown, patchy, a.l. 40 cm, lower part frozen, cryotexture: massive up to 44 cm depth , 44-49 cm horizontal lens-like, (thickness 0.1-1.5 mm, distance 1-3 mm, 49-54 cm diagonal, ice veins (1mm thick, up to 1 cm long), 54-57 cm ice-rich peat inclusion.

54-76(81) cm, peaty silty fine-sand, with small roots (0.5 mm diameter), dark to light-brown, 54-58 cm dark-brown peat sublayer, deeper 64 cm alternation of sublayers with stronger (3 cm) and weaker (2 cm) peaty composition; variable cryotexture: up to 58 cm massive, at about 48 cm vertical ice veins (0.2-0.3 mm thick), at 55 cm, 1 mm thick ice lens, 58-76 cm horizontal netlike (ice veins 0.2-0.5 mm thick, in 1-2 mm distance), at 63 cm 2 mm thick ice lens; at 64 cm transit to belt-like(5-10 mm thick) in 1-1.5 cm distance; separate ice inclusions (ca. 5 mm) in the strong peaty silt; at 65 cm 5 mm thick ice lens with vertical air bubbles.

76(81)-120 cm, grey silty fine sand, weakly peaty, with horizontal peat sublayers (3 mm thick) up to 96 cm, at 79 cm depth 6-7 mm thick ice lens with vertical air bubbles; cryotexture: horizontal lattice-like (thickness 1-2 mm, blocks 1-2 x 5-10 mm), partly ataxitic.

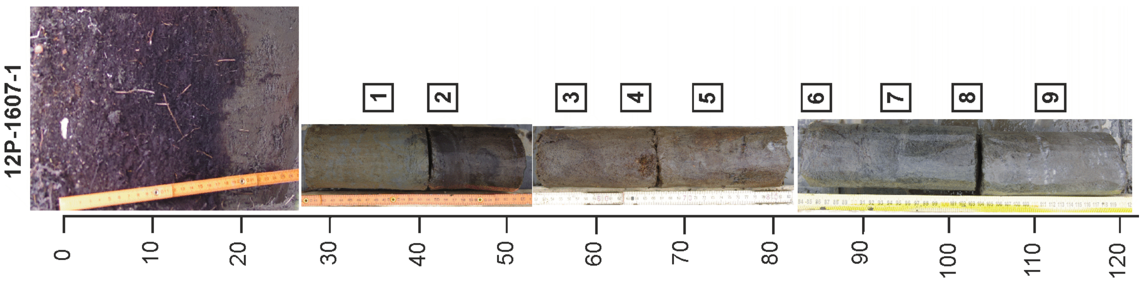

Fig. 9-1: Core 12P-1607-1 with sample positions

12P-1707-1

Pond in a low-centered polygon, water depth 8 cm; a.l. depth 45-46 cm, depth measured from the water surface.

1st core (POK1 C):

8-53 cm, peat, water- saturated, brown

53-125 cm, peat, weakly to medium decomposed, weakly condensed, with inclusions of peaty silt, dominated by roots (up to 3 mm in diameter); peat content decreased with the depth; cryotexture: up to 75 cm depth horizontal lens-like (ice veins 0.2-0.3 mm thick, 5-10 mm long), single 2 mm thick vertical ice veins; deeper of 75 cm occurred thicker (up to 3 mm) ice veins and ice inclusions of 1 cm size (coarse porphyric). In the interval 81.5-84 cm a 4 cm thick ice lens occurred, composed of two similar sublayers, transparent ice with vertical needle-like air bubbles (0.5 mm diameter); at 109 cm 7-8 mm thick ice lens. In the interval 118 to 125 cm a transparent layer of ice occurred with peaty silt inclusions.

2nd core (12P-1707-1)

54-61 cm, strong peaty silty fine-sand; cryotexture: horizontal net-like, horizontal ice lenses (0.5 mm thick, 5-10 mm long), vertical lenses 1-1.5 mm thick

61-137 cm, strong peaty silty fine-sand; cryotexture: lens-like.

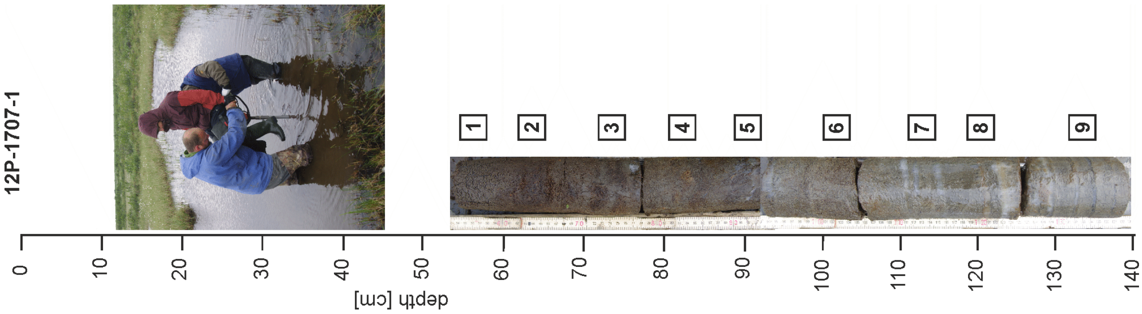

Fig. 9-2: Core 12P-1707-1 with sample positions

12P-1907-1

Near the monitoring site, without polygon walls, a.l. depth: 26, 30, 29, 35 cm, grass and water in between

1st core (POK3 W)

22-40 cm, silty fine-sand, grey, with peaty patches; cryotexture: at 22-26 cm depth, lattice-like (ice veins 0.5-1 mm thick, blocks 5 x 10 mm, vertical ice veins of 1-2 mm thickness down to 35 cm depth, at 26-40 cm depth massive cryotexture with vertical ice veins.

40-54 cm, silty fine-sand, peaty, brownish-grey; cryotexture: lattice like (ice veins 1 mm thick, blocks 1 x 1,1.5 cm); at 40-48 cm depth vertical ice veins (1 mm thick) in 1-2 cm distance. 54-82(88) cm; silty fine-sand weakly peaty, brownish-grey; cryotexture: net-like (ice veins 0.2-0.5 mm thick, blocks 2-5cm), at 54-64 cm depth single diagonal bended ice veins (1 mm thick); at 64-88 cm depth horizontal structured ice, at 64-70 cm depth with plant inclusions and sediment laminae, vertical air bubbles (0.5 mm wide, 2-10 mm long), at 70-75 cm depth ice with dark horizontal layers (ca. 5 mm thick) with small circular air bubbles (1 mm); at 75-82(88) cm depth cryotexture similar to 64-70 cm depth with very small air bubbles (1-2 mm).

82-85 cm; fine-sand, grey.

2nd core (12P-1907-1)

In 0.7 m distance, near the frost crack,

28-32 cm, frozen peat, base of the modern active layer, roots up to 3 mm diameter.

32-43 cm, silty fine-sand, brownish-grey, cryotexture: lattice-like.

43-57 cm, peaty silty fine-sand, patchy, brownish-grey, cryotexture: layered, lattice-like (ice veins 3-4 mm).

57-94 cm, ice wedge.

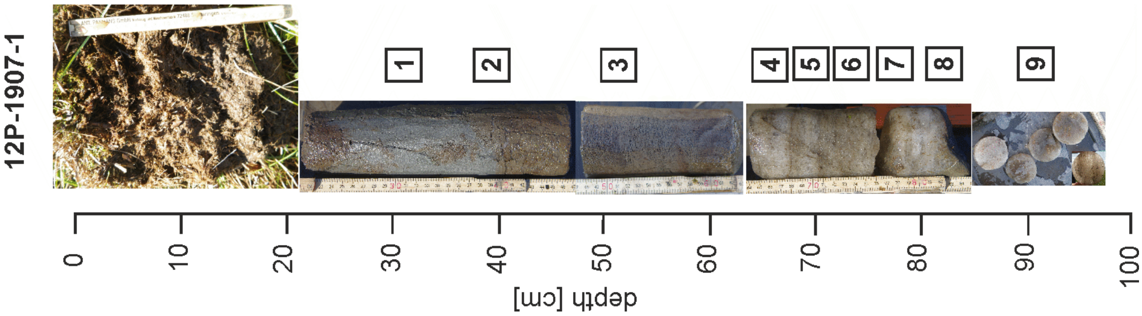

Fig. 9-3: Core 12P-1907-1 with sample positions

12P-1907-2

Polygon centre, 8 m distance from core 12P-1907-1 and 2 m from a 2nd generation frost crack, a.l. thickness: 30, 37, 38, 34, 31 cm

1st core (POK3 C)

37-83 cm, peat with sediments, dark brown; at 47-48 cm depth with roots or twigs up to 8 mm in diameter, at 69 cm depth twig of 5 mm diameter; cryotexture: massive, seldom lens-like, “pseudoataxaitic”.

83-100 cm, peaty silty fine-sand, grey-brown.

110-115 cm, silty fine-sand, transition of strong to medium peaty at 109 and 110 cm depth; cryotexture: layered-reticulated, (ice veins up to 0.5 mm thick), single ice inclusion of 2 mm size, vertical ice veins (0.5 mm thick), at 113-114 cm depth thick ice vein with vertical needle-like air bubbles.

2nd core (12P-1907-2)

Polygon centre, 5 m distance to a 2nd generation frost crack, a.l. 41 cm.

33-41 cm, thawed peat.

41-87 cm, peat, cryotexture: pseudoataxitic, well-preserved roots

87-120 cm, Silty fine-sand, weakly peaty, grey, cryotexture: lenses of horizontal layered ice (1-1.5 cm thick), vertical air bubbles (5 to 30-40 mm long, 0.5 mm diameter), lenses occur at 92-105 and 108-113 cm depths, with vertical thin grass roots.

120-132 cm, weakly peaty silty fine-sand; croyotexture: reticulated (ice veins 1-1.5 mm thick, blocks between vertical ice veins 1 x 0.5 at 126-132 cm depth. At 125 cm occurs an ice layer of 5-6 mm thickness.

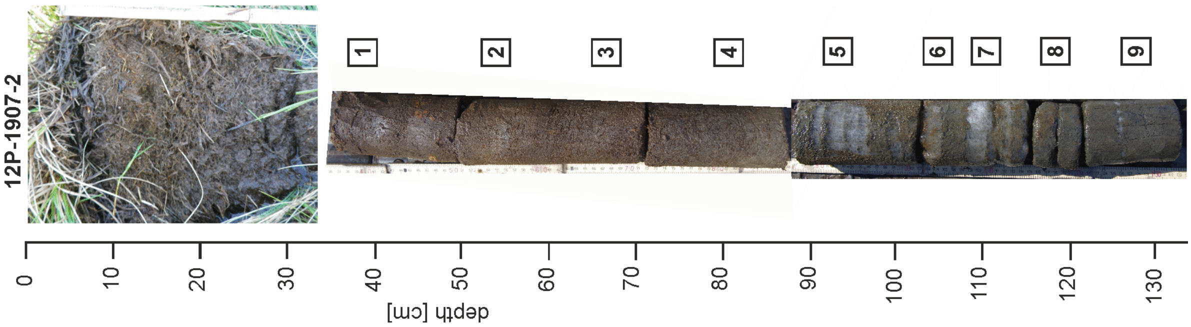

Fig. 9-4: Core 12P-1907-2 with sample positions

12P-21-07-01 (Kolyma flood plain, Pokhodsk Channel)

1s t core (POK4 W), Polygon wall a.l. 20 cm +4-0 cm, modern vegetation cover
0-6 cm, peat not compacted, weakly decomposed, grey-brown.
6-10 cm, peat, brown
10-23 cm, silty fine sand
26-26 cm, peat with sediment content, cryotexture: massive
26-30 cm, peaty sand, light-brown
30-48 cm, silty fine-sand, alternation of strong (1-1.5 cm) and weakly (0.5 cm) peaty layers, grey and brown, weakly inclined layered, vertical roots up to 5 mm diameter; cryotexture: reticulated (ice veins 0.5-1 mm, sediment blocks 1 x 3-4 mm) in thicker zones (ice veins 0.2 mm thick, 0.5-2 cm long, distance 2-3 mm), ice lenses (5 x 5 mm) below roots and twig fragments.
48-118 cm, peat with sediment content, at 58 cm depth silty sand lens (2 cm thick), rots 3 mm in diameter; cryotexture: massive, in silty parts occurred weakly inclined ice veins of 8 mm thickness, deeper of 66 cm; cryotexture: pseudoataxitic and porphyric, between 76-99 cm diagonal oriented grey silt lenses with ataxitic cryotexture and ice lenses, at 76-83 cm depth sediment blocks of 0.5 x 1 cm to 1 x 2 cm size; transparent ice veins with vertical air bubbles and silt stripes; at 83-99 cm transparent horizontal layered ice; circular (0.5 mm) air bubbles vertical oriented; at the interval 99-118 cm peat similar to the interval 66-76 cm depth.

2nd core (12P-21-07-1), 20 cm distance from the 1st core, a.l. depth 25 cm
25-29 cm, peat, lower part of the active layer; cryotexture: massive
29-34 cm, peaty silt; cryotexture: net-like, ice veins to 1 mm thick, block 2x 10 mm, further up the net is destroyed and broken (frozen from below)
34-54 cm, peat with vertical (1 cm thick, 4-5 cm long) and horizontal (1 cm thick) oriented silty sand patches, twig 2 mm in diameter; cryotexture in peat: pseudoataxitic, single ice lenses of 3 mm thickness and 1 cm length; cryotexture in silt: horizontal net-like, ice veins to 1 mm thick, sediment blocks 1-2 x 10 mm.
54-94 cm, peat, brown, silty, twig up to 1 cm in diameter, cryotexture: pseudoataxitic, in silty inclusion lens-like, lenses 0.2-0.3 mm, in the interval of 77-94 cm subvertical inclusions of silty sand and ice, ice is horizontal layered with vertical air bubbles (8mm long, 0.5 mm wide).

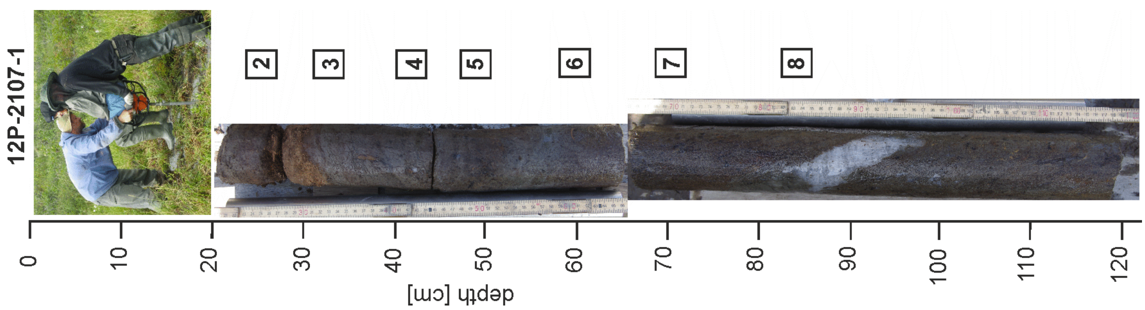

Fig. 9-5: Core 12P-2107-1 with sample positions

12P-2107-2 (Kolyma flood plain, Pokhodsk channel),
Polygon center, Equisetum, hummocks, grass 40-50 cm, water between the hummocks, a.l. depth 40 cm

1st core (POK4 C), 8m from the core 12P-21-07
0-45 cm, peat weakly decomposed, at 40 cm depth frozen; cryotexture: massive
45-59 cm, silty peat, brownish grey, weakly decomposed, root up to 5 mm in diameter; cryotexture: massive, ice crusts (around roots fragments ?)
59-83 cm, peat brown, weakly decomposed, cryotexture: massive, porphyric, ice inclusion of 0.5 x 1 cm, at 81 cm depth horizontal ice lens (3 mm thick, 1-1.5 cm long)
83-94 cm, silty peat, dark-brownish grey, cryotexture: pseudoataxitic, porphyric inclusions 0.5 cm large

2nd core (2P-2107-2) 0.5 m from the 1st core)
0-45 cm, peat like in the 3rd core, a.l. 41 cm
45-58 cm, silty peat, brownish grey
58-64 cm, peat, brown; cryotexture: massive
64-75 cm, silty peat, brownish grey, pseudoataxitic, porphyric, ice inclusions of 1 x 2 cm size
75-112 cm, peat with silty lenses; cryotexture: massive, porphyric, between 88-109 cm depth lenses of peaty silty fine-sand, the largest ice lenses (5-7 cm long) were found in 89-93 cm, 97-98 cm and 100-103 cm depth, transparent ice, horizontal layered with vertical air bubbles (0.5 mm).

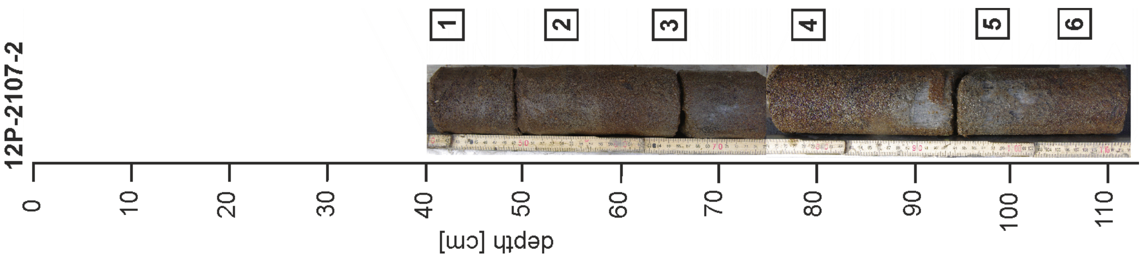

Fig. 9-6: Core 12P-2107-2 with sample positions

12P-2707-1 (POK5)
Highest part of the low floodplain, cotton grass meadow, a.l. depth 45 cm

43-56 cm, gray silty fine-sand with iron oxid patches, peaty, pophyric cryotexture, single vertical to subvertical ice veins (1 mm thick).
56-73 cm, peat layer at 56-58 cm, deeper interbedded gray loam, peaty loam, brownish-gray and reddish-gray sandy loam, horizontally lying ferruginized wood fragment (rounded), cryotexture: horizontally-layered, ice veins <0.5-2 mm parallel to the bedding, distinct vertical and oblique branched ice veins of 1 mm thickness.
73-108 cm, alternate bedding of gray clayish silt and plant detritus layers of 2 to 6 cm thickness; upper boundary not clearly expressed; detritus layers consist of large numbers of horizontally lying isolated roots, between 87-90 cm peat layers are bent. The lower boundary of detritus layers is usually more accurate, though not always, slightly inclined; cryotexture in

silty interlayers (1.5-2 cm thick): between 94-99 cm depth micro-streaky (up to 5 mm long) to complex horizontal-netlike with diagonal branching ice veins (1-5 mm thick); in 90-92 cm an ice-soil lens occurred, clear ice with vertical air bubbles; cryotexture in detritus interlayers: massive, rare lenses, porphyric, ice crusts, ice veins marked deformation structures auf the detritus layers.

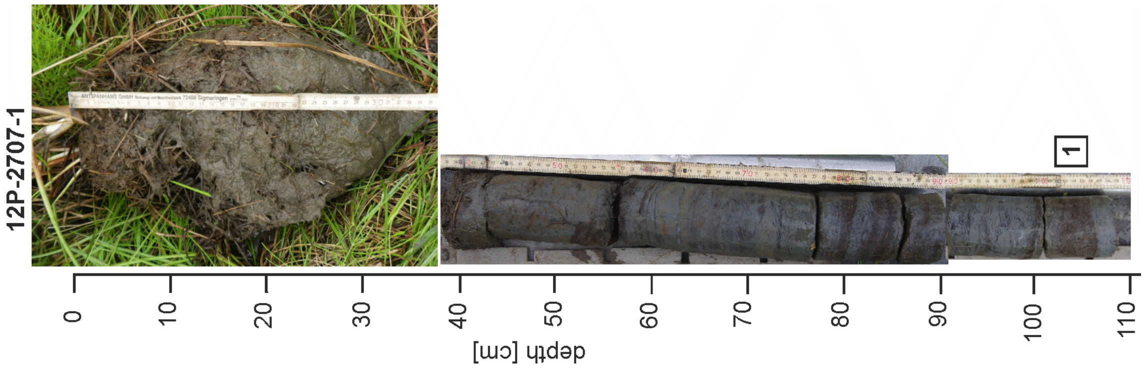

Fig. 9-7: Core 12P-2707-1 with sample positions

12P-2707-2 (POK6)

Middle part of the low floodplain area, covered by cotton grass, closer to the rear border. The drilling point was 3 m far from a modern frost crack; a.l. depth 43 cm

43-53.5 cm, horizontal interbedded layers of plant detritus and clayish silty fine-sand, peaty, small peaty layers 1.5-2 mm; plant detritus dominated, cryotexture: massive; in the upper part dens micro lens-like cryotexture; at 50-52 cm separate ice lenses 1-1.5 cm long and 1 mm thick.

53.5-58 cm, interbedding loam more or less peaty, inclined bedding, at 53.5 cm depth cross-bedding abruptly cut off the horizontal layering; cryotexture: massive, well-developed vertical streaks with a thickness of 1 mm, starting at a depth of 54 cm and reaching further down.

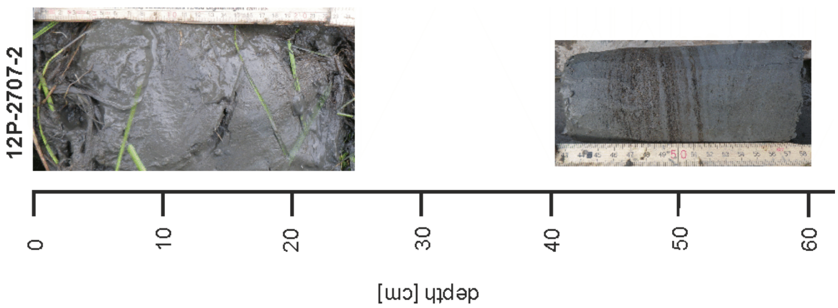

Fig. 9-8: Core 12P-2707-2

12P-2707-3

Lowermost part of the floodplain was overgrown by cotton grass, 6 m from the shore near the boat. A small area of dense sedge *Carex stans* between cotton grass; grass height 30-40 cm; a.l. 70 cm

70-86 cm, sandy silt, gray, laminated, peaty lenses above 60 cm - modern turf (core 47-92 cm), cryotexture: horizontal micro-streaks at 82 cm vertical ice streaks: 0.1-0.2 mm wide, 1mm wide ferruginizated zone at the edges.

86-92 cm, interbedded sands and sandy silt, fine-grained sands dark ocher, sandy silt light ocher, interlayers 0.5-1 cm thick, unclear boundary at 86 cm.

12P-3007-1

Lake at the lower floodplain south of Pokhodsk. The lake is connected to the Viska-Channel so that during the flood, it is flooded; the surface is about 0.5 m above the lake level (average water level); lake floodplain width 6-10 m high lake floodplain level about 1.7 m above; vegetation - a thick Equisetum cover (40 cm high) on the lower flood plain with some cotton grass, surround back stitch dense bush on the higher flood plain (1-2 m high).

1st core (POK7), a.l. depth 45 cm

45-72 cm, peaty silty sand (loam), brown, at 54-63 cm - peat, interlayer dark brown to black, cryotexture: massive, separate ice inclusions up to 1 mm.

72-110 cm, gray loam, with coarse (5 x 1 cm) black and light-brown plant residues; peat inclusion at 92-95 cm; cryotexture: horizontal lenticular; the sizes of ice lenses varies with the depth: at 72-75 cm 0.5-2 mm, at 80-88 cm 0.5-1.5 cm and deeper 0.3-0.5 cm; size of sediment blocks in between 0.5-1 cm blocks; 2 mm thick diagonal ice streaks occur at 90-99 cm near the peat inclusion.

2nd core (12P-3007-1)

30 cm distance to the 1st core with 80 degree inclination. Similar stratigraphy and structure are to the first well, except the lowermost segment:

104-112 cm, silty sand (loam), as described above; at the lower boundary, the horizon ends with thick ice streaks.

112-137 cm, silty sand (loam), as described above. cryotexture: horizontal lenticular, thickness 1-2 mm, the distance between ice veins 0.5-2 cm, micro lens-like.

12P-3007-2 *(POK8)*

3rd core at a high level lake floodplain, clearing of bushes, a.l. depth 33 cm

33-38 cm, dark brown peat, weakly decomposed.

38-70 cm peat brown, cryotexture: pseudoataxitic; at 38-40 cm loamy turf, at 60-63 cm icy interlayer with peat inclusions (base of the active layer?)

70-87 cm, peat brownish-gray, at 72-78 cm grayish-brown loamy, at 83-87 cm dark brown to black peat; cryotexture: pseudoataxitic, ice barks.

87-100 cm, strongly mineralized peat, brownish-gray, cryotexture: pseudo-ataxitic.

100-140 cm, peat, below 120 cm more loamy, cryotexture: wavy-lenticular, mostly conformal of the peat structure.

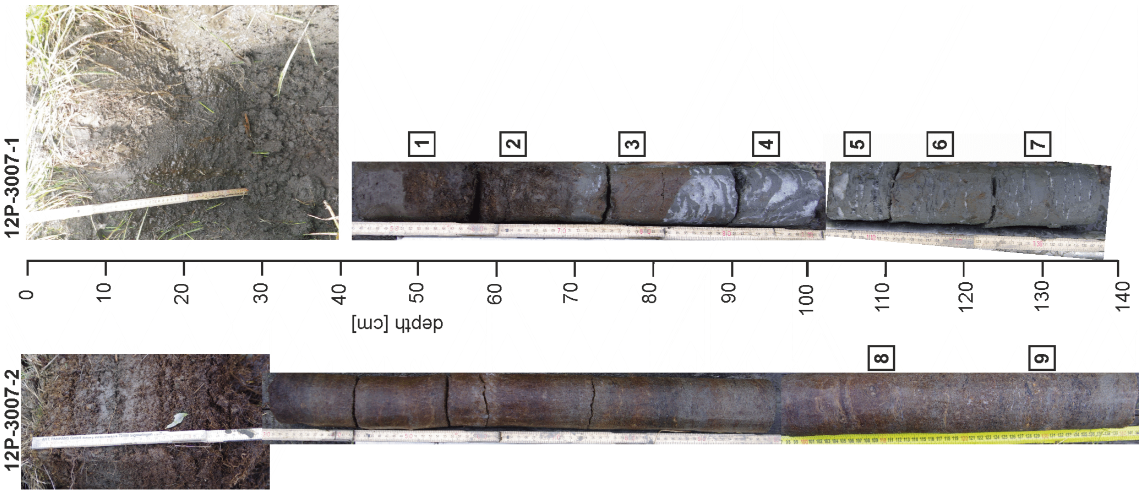

Fig. 9-9: Cores 12P-3007-1 and 12P-3007-2 with sample positions

12P-1008-1

Khalerchinskaya Tundra, ca. 250 m east of the Lake Semnoe, a.l. depth 50 cm

0-8 cm, surface vegetation (lichens, *Carex* cf. *stans*, Salix, cranberries, blueberries, dwarf birch.

0-50 cm, soil horizon (typic psamoturbel).

50-69 cm, grey-brown, fine sand, not bedded, single iron oxide patches, cryotexture massive.

69-99 cm, grey-brown, fine sand, weakly bedded, cryotexture: massive.

99-110 cm, grey-brown, fine sand, alternate bedded, reddish coloured patches.

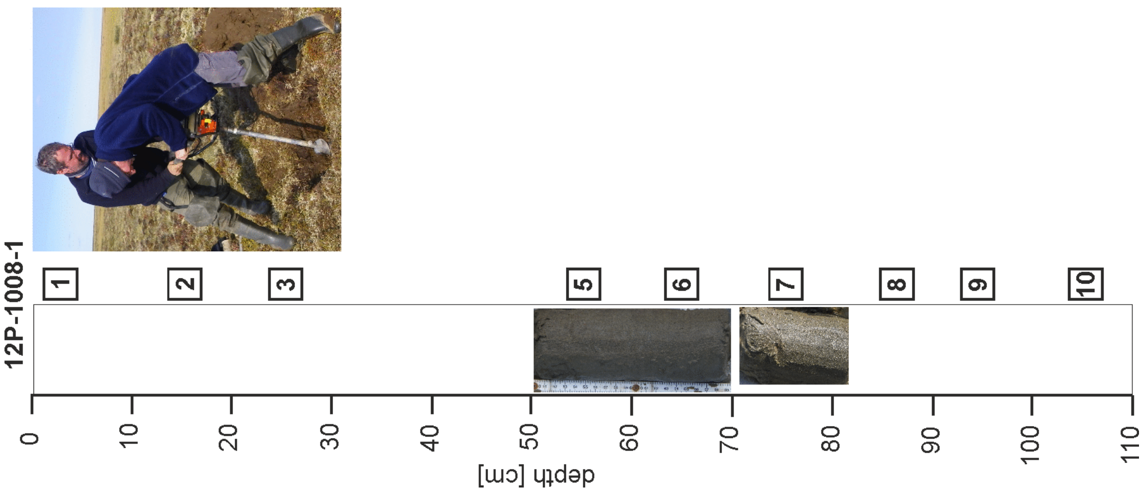

Fig. 9-10: Cores 12P-1008-1 with sample positions

9.3 Pit and exposure description

12P-2007-1

Khalertchinskaya Tundra, mud boil, surface sample, peaty sand, unfrozen

Fig. 9-11: Sample site 12P-2007-1 mud boil

12P-2007-2

Khalertchinskaya Tundra, pit, a.l. depth 40 cm

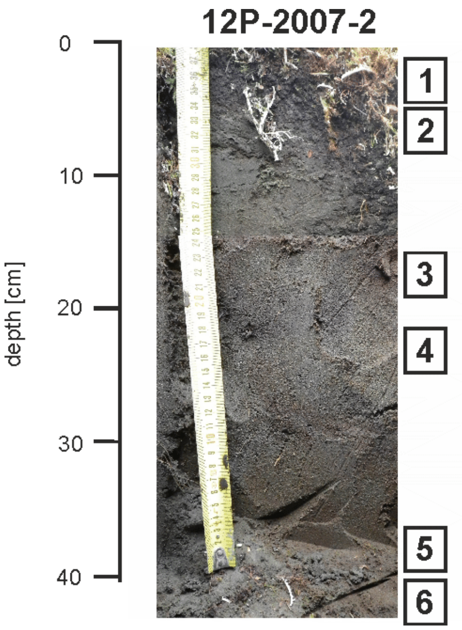

0-6 cm, surface vegetation (mapping F. Kienast): *Betula exilis, Carex artisibirica*, *Salix* sp, *Vaccinium vitis-idea, V. uligunosum, Arctous alpine, Pedicularis* sp., *Polygonum tripterocarpum, Hierochloe alpine, Luzula confuse)*.

6-11 cm, dark-brown peat, strongly decomposed.

11-40 cm, grayish/reddish brown fine-sand with roots.

Fig. 9-12: Pit 12P-2007-2 with sample sites

12P-2507-1/12P0708-1 (a.l. 15-17 cm)
An ice wedge cross cut was done near the monitoring site by chain saw at 25.07.2012 (Fig. 9-13) in order to study the lower part of the still peaty frozen active layer below an ice wedge. The pit was again visited and studied at 07.08. 2014.

Fig. 9-13: Pit 12P-2507 with the studied walls A-B and C-D (left) and the same pit at August 7th

From two walls (A-B and C-D) frozen block were cut (Fig. 9-14), described and sampled, while the transect C-D was again studied in August 7th.
The exposed ice wedge was milky-white colored and composed of numerous ice veins mostly parallel oriented, about 1 to 2.5 cm wide. The ice wedge contains numerous irregular gas bubbles (< 1 mm). Some ice veins were marked by small dark sediment spots. The major stripes structure was diagonal crossed by single ice veins reflecting other frost crack orientation. The ice wedge was sampled horizontally in a lateral distance of 10 to 15 cm at the side A-B (12P-2507-1-1 to 1-6) and in a longer transect again at the side C-D (12P-0708-1-01 to14). In the boundary zone between the ice wedge and frozen active layer an ice layer existed that was composed of elongated and vertical oriented ice needles (12P-2507-1-11).
The ice wedge was covered by a 5 to 10 cm thick layer of cryoturbated greyish-brown silt and weakly decomposed peat that contains separate peat lenses of 10 to 15 cm in diameter 12P-2507-1-9, 1-10). The cryotexture was coarse lens-like reticulated. From the frozen part of the active layer special ice samples were taken from a 3 cm wide elementary ice vein (12P-2507-1-13).
The frozen part was covered by 10 cm of moss peat and a 10 cm thick plant cover that contain numerous dark-brown moss roots.

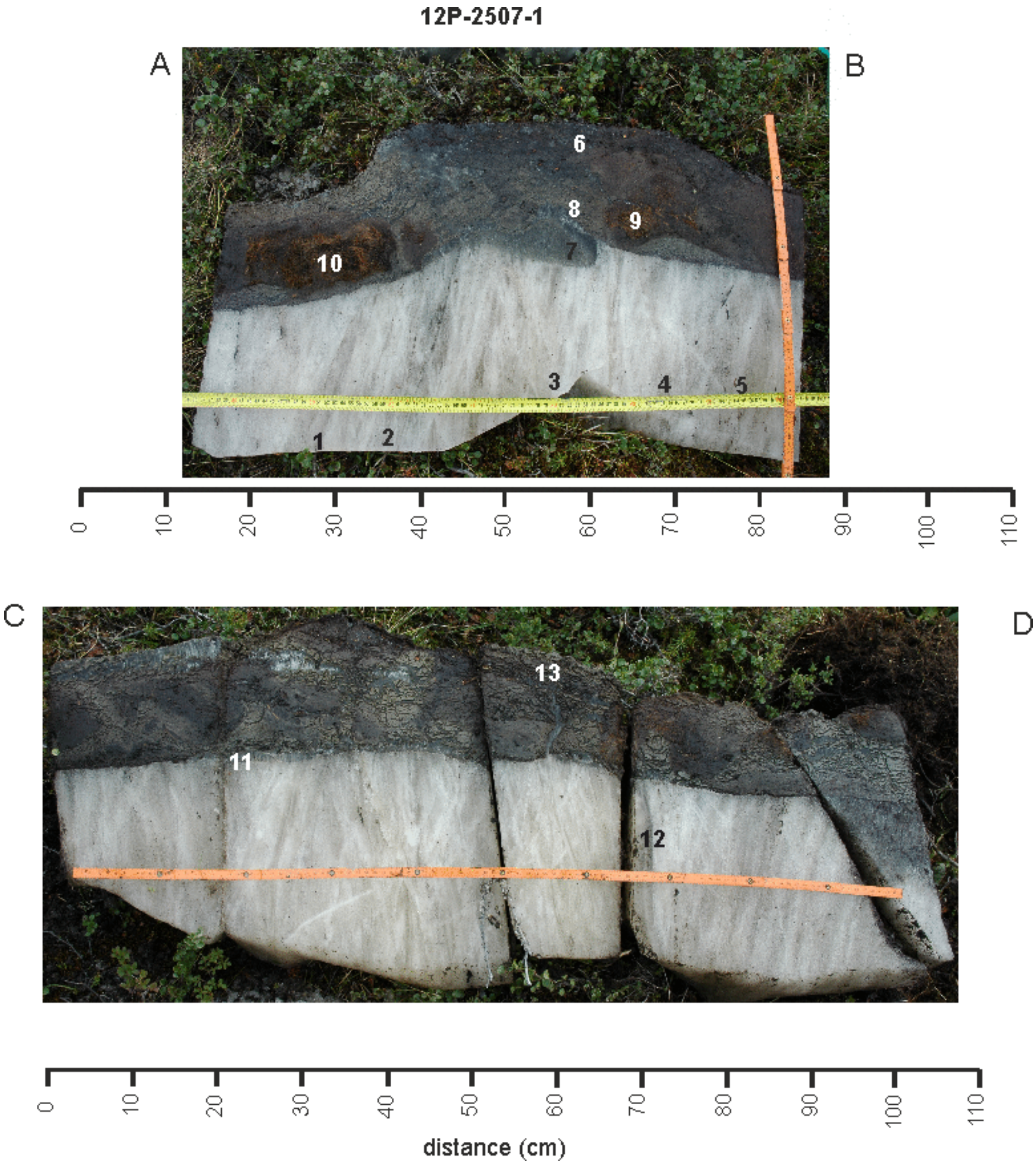

Fig. 9-14: The blocks A-B and B-C cut from the pit 12P-2507 with sample sites

12P-2308-A/B

The flood plain exposure at the southern bank of the Viska Channel was studied as a reference for modern alluvial deposits (a.l. depth 45 cm).

The cleaned wall of the first exposure 12P2308-A (Fig. 9-15 right) was about 1.5 m high above the water level and 1 m wide. The lowermost part consists of greyish-brown silty fine-sand with numerous reddish-brown patches (1-3 cm long, 1 cm wide). The cryotexture was horizontal micro-lens-like with <1 mm thick and 1-2 mm long ice lenses. Further up a 3 to 5 cm thick dark bent silty layer with micro lens-like follows. The upper part consists of alternate-bedded silty fine-sand with dark grey-brown silt layers (1-3 mm thick) and light grey-brown sand layers (5-7 mm). Numerous black 1-2 cm long patches of decomposed r fragments and more diffuse light-brown patches of iron oxide impregnation were irregularly distributed in this section.

The unfrozen part of the profile was sample only 4 m further east (Fig. 9-15 left) and presents a non-regular layered brownish-grey silty fine-sand that contain plant detritus and modern shrub and grass roots.

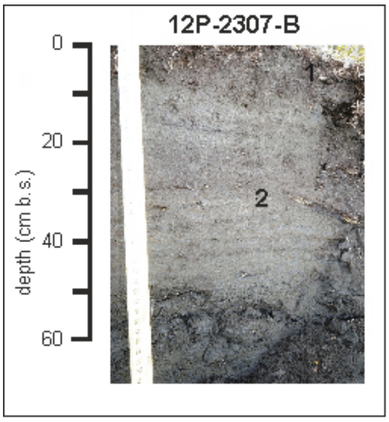

Fig. 9-15: The floodplain exposures 12P-2308-A/B with sample sites

10. STUDIES OF MODERN VEGETATION AND SAMPLING OF PERMAFROST DEPOSITS FOR PALAEOBOTANICAL STUDIES AT THE LOWER KOLYMA

Frank Kienast

10.1 Scientific background and objectives

The lower Kolyma is a key region for understanding the mechanisms underlying the biotic impoverishment in northern latitudes during the late Quaternary, when numerous large-bodied mammals disappeared and the thitherto prevailing diverse grassland vegetation (tundra steppe or mammoth steppe) degraded to modern monotonous wetland tundra. The rapid demise of the Pleistocene megafauna in Eurasia and North America coincided with human dispersal and also with abrupt climatic changes at the Pleistocene – Holocene transition (Guthrie, 2006; Nikolskiy et al., 2011). Thus, both the arrival of hunting modern humans in formerly uninhabitated areas and climatic and associated vegetational changes are considered possible extinction drivers (Campos et al., 2010, MacDonald et al., 2012; Prescott et al., 2012). E.g. in the Arctic, rising temperature and increased humidity triggered the transformation of the Pleistocene nutritious grassland vegetation into birch shrubland, coniferous forest tundra and finally into low-diverse tundra wetlands (Binney et al., 2009; Kienast, 2013), which are an inappropriate habitat for most large herbivores. Correspondingly, the demise of mainland mammoth populations coincided with the expansion of coniferous forests and the formation of extensive northern peatlands (MacDonald et al., 2012).

Herbivore - vegetation interactions in the now-extinct tundra steppe biome are so far hardly considered in this concept. Megaherbivores significantly affect the structure, composition, diversity, and dynamics of plant communities (Johnson, 2009; Owen-Smith, 1988). Openness of vegetation, the existence of mosaics of different structural types of vegetation, a high proportion of productive grasses, and high habitat and species diversity as recorded in NE Siberian plant macrofossil assemblages (Kienast et al., 2005, 2008a, 2011) might be the result of megafaunal activities (Johnson, 2009). Grazing and trampling of megaherbivores generally suppresses mosses and woody vegetation (trees, shrubs, and dwarf shrubs) and supports plants adapted to withstand frequent disturbances, such as grasses. Grasses can achieve a high rate of transpiration and might be able to shift precipitation minus evapotranspiration toward a negative (arid) rate when brought to dominance by grazing (Zimov, 2005, Zimov et al., 2012). Lacking grazing pressure after the loss of key megafaunal components might have resulted in a shift from diverse grassland vegetation to more dense and uniform formations: wet tundra along the coasts and coniferous forests more inland. Accordingly, it might be possible to regenerate the former grassland ecosystem through reintroducing large herbivores in sufficiently high densities (Zimov, 2005; Zimov et al., 2012). The long term project ‘Pleistocene Park’, conducted by the Northeast Science Station Chersky, aims to reconstitute a mammoth steppe like ecosystem experimentally in a 160 km^2 area at the lower course of the Kolyma River. For this purpose, large herbivores such as Yakutian horses, reindeer, moose, Altai-wapiti, musk ox, and bison were placed into the station, where they are kept in a fenced area to achieve high mammal densities. The ‘Pleistocene Park’ project is now progressing for more than 20 years. The impact of permanent disturbances on vegetation by the introduced herbivores and by man via bulldozers and fire has, however, not yet been investigated from a vegetation ecology perspective. It remains hence unclear how structural, functional and species diversity as well as composition of plant communities within the ‘Pleistocene Park’ have changed in response to the intense disturbances. The assumption that permanent disturbances resulted in an altered structure and composition of vegetation resembling the Pleistocene tundra steppe (Zimov, 2005) requires verification.

The field work in 2012 was supported by the DFG (KI 849/3-1) as pre-project in preparation of another intended research proposal that was applied for in 2013. In the frame of the proposed project, we intend to investigate the ecological interactions of Quaternary vegetation and large herbivores in the terrestrial Arctic by combining the analysis of reconstructed Late Pleistocene palaeovegetation, as recorded in the Duvanny Yar permafrost type sequence, with studies of modern plant communities at variously disturbed sites within the ‘Pleistocene Park’ in comparison to largely ungrazed vegetation along the climate gradient in the taiga/ tundra transition zone at the lower Kolyma River.

In the first reconnaissance 2012, it was planned to carry out preliminary comparative botanical investigations in different vegetation zones within the lower Kolyma region (Fig. 10-1) such as tundra, northern taiga, extrazonal relict steppes, and disturbed areas of the Pleistocene Park and to collect modern reference material for palaeobotanical studies. In addition, sediment material from the late Quaternary permafrost section Duvanny Yar was sampled for palaeobotanical analyses. Another aim of the stay was it to undertake personal consultations with cooperation partners at the Northeast Science Station and to evaluate the existing logistical infrastructure in Chersky in terms of the feasibility of the intended project.

The field work in 2012, especially the studies of modern vegetation in the tundra zone around Pokhodsk, was furthermore a contribution to the POLYGON project, where the author is cooperation partner. The conducted works might be of interest for following subprojects within POLYGON (see contents of these reports):

- Ecological studies of polygonal ponds
- Records from a model polygon for modern and palaeoecological studies
- Pedological studies of various polygon sites
- Dendrochronological and ecological studies in the tree line zone

The field work was divided into three parts:

- 1- vegetation studies in various subarctic tundra habitats in the vicinity of **Pokhodsk** in close collaboration with POLYGON partners
- 2- vegetation studies in the boreal zone: relict steppe habitats, natural and disturbed forest tundra and taiga habitats at the **NE Science Station Chersky** and the **Pleistocene Park**
- 3- visit and sampling of the late Pleistocene permafrost sediment section **Duvanny Yar**

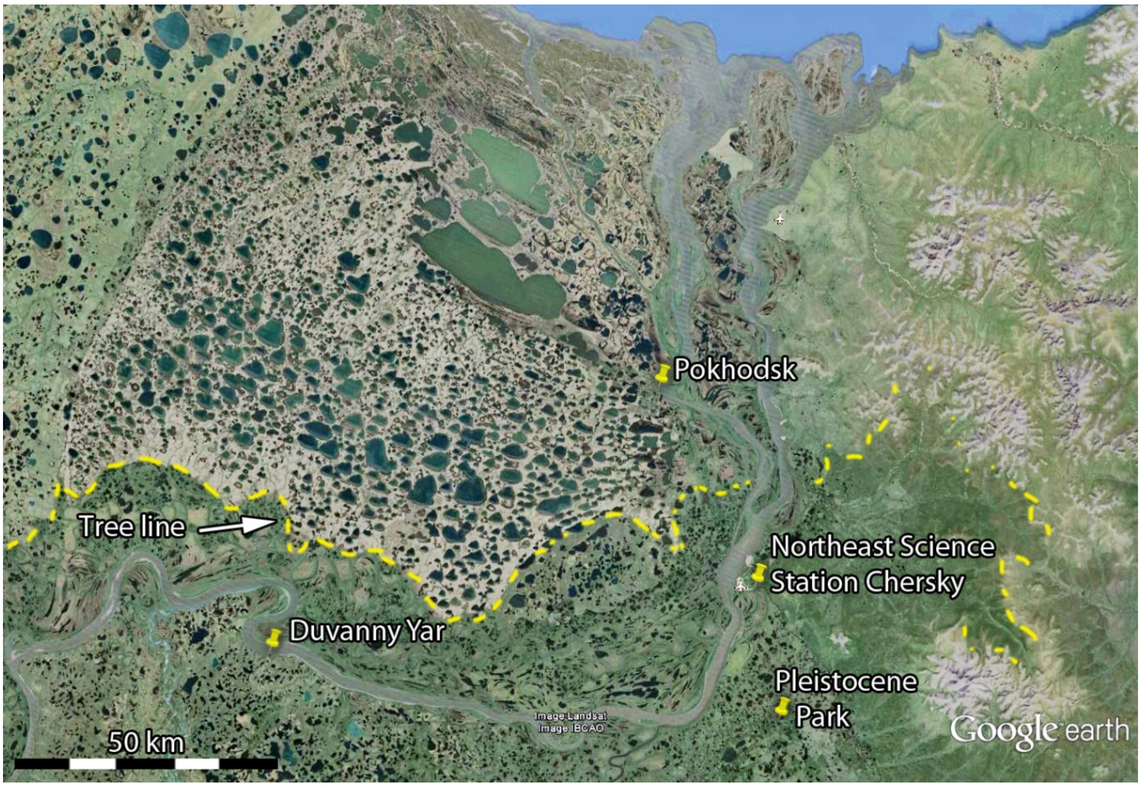

Fig. 10-1: Sites along the lower course of the Kolyma River where fieldwork was done in summer 2012. The northern tree line is illustrated by a yellow dashed line. Satellite picture processed from Google earth.

10.2 Study area

The Kolyma lowland can be regarded as model region for the investigation of the late Quaternary environmental restructuring. The 'Pleistocene Park' grazing experiment takes place in close proximity to Duvanny Yar (Fig. 10-1) - one of the most important Pleistocene key sections in the former subcontinent Beringia (Giterman et al., 1982) with fossils of megaherbivores outcropped in large abundances. The region around Chersky at the lower course of the Kolyma River is also a transitional area, covering an E-W continentality gradient and a N-S gradient in terms of summer temperature and vegetation (taiga, tundra) illustrated by the polar tree line (Fig. 10-1). Temperature during the growing season is the main factor controlling modern vegetation characteristics. Studies of modern vegetation along the N-S transect can be carried out with reasonable logistic effort (e.g. watercraft). The region is also known for the presence of extrazonal relict steppe patches considered as potential analogues of Pleistocene vegetation (Yurtsev, 1982) - another advantage for the comparison of reconstructed fossil and extant vegetation. In the lower Kolyma region, steppe patches are still present though being restricted to specific sites in southern exposures and to coarsely clastic substrate.

10.3 Vegetation records

To record the vegetation on each plot, all identified vascular plant species were listed in relevés (Fig. 10-2) following Braun-Blanquet (1964). Critical taxa were collected for subsequent identification in the Senckenberg Research Station of Quaternary Palaeontology Weimar. Other specimens were picked for the Herbarium Senckenbergianum Weimar as reference for future identification of fossil plant parts. In addition, cryptogams were collected exemplarily at characteristic sites for offsite determination in the Senckenberg Museum of Natural History Görlitz. They were later identified by Volker Otte. Plots were selected according to homogeneity in terms of plant composition, vegetation structure, coverage, and habitat characteristics (moisture, disturbances, shadowing, substrate, exposition etc.) and described accordingly. GPS data, when specified, were generated using the integrated GPS sensor of a Nokia 5800 cell phone or were later reconstructed with Google earth. Plot sizes were geared to the minimal area (Minimalareal) as defined in Sedlag & Weinert (1987). They thus depended on the character of vegetation. E.g. forest plots were much larger than steppe or ruderal plots. The coverage/abundance scale of Braun-Blanquet for the recorded individual species was adapted as follows (Tab 10-1):

Indication	Coverage
+	< 5 %
1	5-15 %
2	15-30 %
3	30-50 %
4	50-80 %
5	> 80 %

Tab. 10-1: Adapted cover scale

Fig. 10-2: Recording vegetation in the field. Collected specimens were stored in zip bags and, using a mounted polyester bag, transported to the base camp - the Pokhodsk Elementary School or, later, the Northeast Science Station, where plants then were pressed and dried. Photo: A. Schneider.

In total, 110 relevés were listed recording 163 vascular plant taxa and 22 cryptogam taxa. For some genera such as *Salix*, a detailed identification was omitted due to the lack of adequate identification keys (e.g. Flora of Siberia and Flora of the Russian Arctic are both deficient) and lacking existing reference material. Even more crucially, because of the confusing and poorly conceived taxonomical status of most of the subarctic species in *Salix* or also in *Draba,* their determination is regarded nearly impossible for the time being. Within these genera, many cryptic (sibling) species formed obviously due to numerous hybridisation events in their evolutionary history resulting in a high level of allopolyploidy and intraspecific polymorphism. E.g. the Flora of the Russian Arctic lists 43 *Salix* species with more or less distinct characteristics. Since most subarctic *Salix* species have broad ecological amplitude, their value in bioindication, which was the main task in the conducted vegetation studies, is negligible. Nonetheless, numerous herbarium sheets of indetermined *Salix* species were collected and are now available in the Herbarium Senckenbergianum Weimar e.g. for future taxonomical studies and subsequent identification.

10.4 Vegetation studies in the subarctic tundra adjacent to Pokhodsk

The first part of expedition in summer 2012 was dedicated to vegetation studies in the subarctic tundra in the vicinity of the settlement Pokhodsk, which was the base camp of the field work (Fig. 10-3). The study area is characterized over large distances by polygonal tundra shaped as result of the formation of below-ground ice wedge systems. Site conditions and vegetation alter here over short distances in consequence of variable moisture (Fig. 10-10).

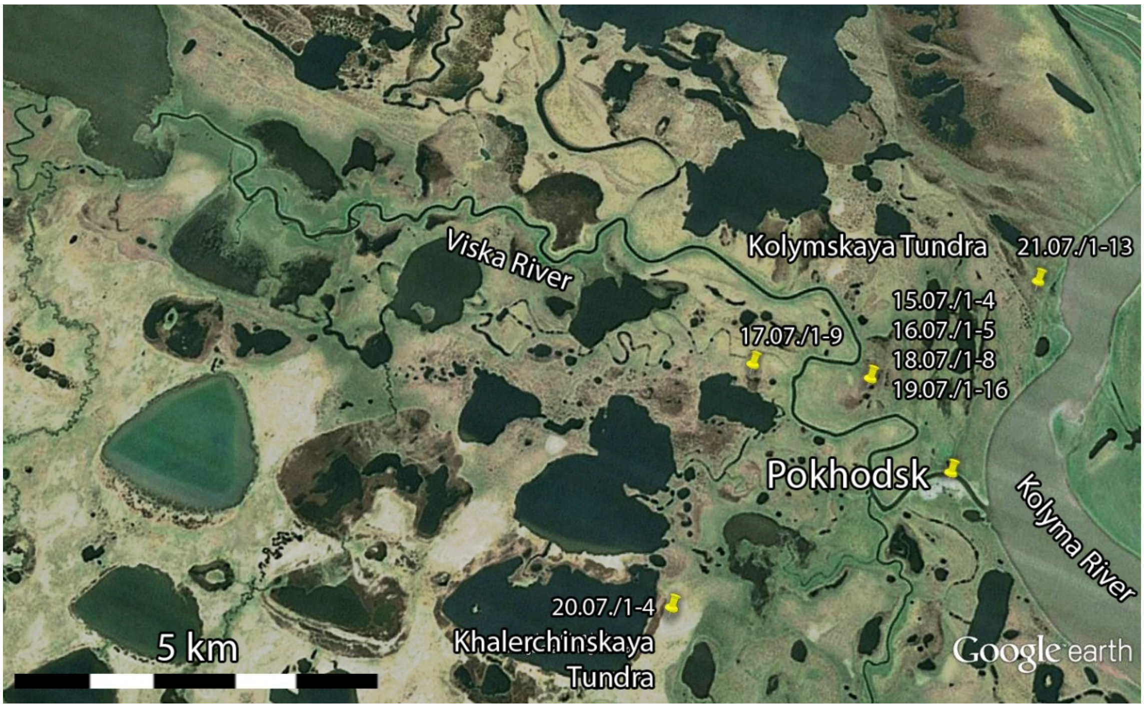

Fig. 10-3: Location of vegetation records in the subarctic tundra around Pokhodsk performed in the course of the first part of the summer 2012 fieldworks. Satellite picture processed from Google earth.

The vegetation of following landscape units was studied in detail:

- Polygonal tundra
- Ponds and lake shores
- Upland tundra
- Pingos

Most vegetation records (15.07./1-4, 16.07./1-5, 18.07./1-8, 19.07./1-16) were performed close to the monitoring sites of the POLYGON project partners NW of Pokhodsk (Fig. 10-3). This area was regarded characteristic for the Kolymskaya Tundra. At first, a transect from the shore of a small lake to the adjacent polygonal tundra was studied. In contrast to lake shore vegetation in the Yakutian high arctic tundra (Kienast, 2008b), the high percentage of boreal aquatics such as *Menyanthes trifoliata, Comarum palustre* and several *Utricularia* species was notable (Fig. 10-4). Also the occurrence of several boreal shrub and dwarf shrub species including *Duschekia fruticosa, Chamaedaphne calyculata, Vaccinium* spp. and even of scattered larches at drier upland sites was a clear indication of the proximity of the northern tree line.

Fig. 10-4: Shore of a small lake, where vegetation was recorded in striking distance to POLYGON monitoring sites (vegetation transect 15.07./1-2). All photos, if not otherwise declared, taken by F. Kienast.

Following, relevés with site descriptions are presented in tables, where is also listed whether field photos are available and if herbarium or carpological material was collected. The first two days were dedicated to vegetation records along transects fom lakes into the surrounding tundra highlighting vegetation changes from wet (Fig. 10-4) to dry (Fig. 10-5) sites following the polygonal microrelief close to POLYGON monitoring sites.

Vegetation transect Nr. 15.07./1-2

Site:	Shore of a small lake in Kolymskaya Tundra, lake shore vegetation in subarctic tundra about 1.8 km linear distance NW from Pokhodsk		
Latitude:	69° 5'29.02"N	**Longitude:**	160°56'18.19"E
Elevation:	planar	**Inclination:**	flat
Date:	15.07.2013	**Exposition:**	none
Substrate:	peat	**Lighting conditions:**	100%
Soil type:	histosol	**Soil heating:**	poor
Soil reaction:		**Soil moisture:**	submerged, emerged
Humus form:	peat	**Groundwater table:**	above ground
Disturbances:		**Human impact:**	none

Vegetation record Nr. 15.07./1

Lake shore vegetation in subarctic tundra

Taxon	Coverage	Photo Nr.	Specimen collected	Seeds collected
Hippuris vulgaris	1			
Menyanthes trifoliata	4	5771-5782	x	
Utricularia vulgaris	1		x	
Comarum palustre	+			
Utricularia intermedia	+		x	
Carex rostrata	+			

Vegetation record Nr. 15.07./2

Site description like 15.07./1
riparian sedge/ cotton grass community further landwards

Taxon	Coverage	Photo Nr.	Specimen collected	Seeds collected
Carex aquatilis ssp. stans	2		x	x
Carex chodorrhiza	3		x	x
Eriophorum russeolum	2		x	x
Carex rotundata	1		x	
Carex rostrata	+		x	
Hippuris vulgaris	+			
Menyanthes trifoliata	+			
Utricularia intermedia	1			
Utricularia vulgaris	+			
Ranunculus pallasii	1			
Cryptogams				
Hamatocaulis lapponicus (Norrl.) Hedenäs			x	
Meesia triquetra (Richt.) Ångstr.			x	

Vegetation transect Nr. 15.07./3-4

Site:	Site close to 15.07./1; small mound (polygonal ridge?) in subarctic tundra		
Latitude:	69° 5'29.02"N	**Longitude:**	160°56'18.19"E
Elevation:	planar	**Inclination:**	flat
Date:	15.07.2013	**Exposition:**	none
Substrate:	peat	**Lighting conditions:**	100%
Soil type:	histosol	**Soil heating:**	mediate
Soil reaction:		**Soil moisture:**	mesic to dry
Humus form:	peat	**Groundwater table:**	about 30 cm
Disturbances:		**Human impact:**	none

Vegetation record Nr. 15.07./3

small mound in subarctic tundra

Taxon	Coverage	Photo Nr.	Specimen collected	Seeds collected
Betula nana ssp. exilis ssp. exilis	4			
Chamaedaphne calyculata	2		x	
Salix cf. pulchra	1			
Vaccinium uliginosum	+			
Carex chodorrhiza	+			
Andromeda polifolia	+			
Carex aquatilis	1			

Vegetation record Nr. 15.07./4

Top of the mound in subarctic tundra; thick moss layer, driest place in the area

Taxon	Coverage	Photo Nr.	Specimen collected	Seeds collected
Betula nana ssp. exilis ssp. exilis	2			
Duschekia fruticosa	2			
Vaccinium uliginosum	3			
Ledum palustre	2			
Chamaedaphne calyculata	1	5783-5784		
Salix cf. pulchra	+			
Vaccinium vitis-idaea	1			
Carex vaginata	+		+	
Rubus chamaemorus	1			
Polygonum tripterocarpum	+		+	

Vegetation record Nr. 16.07./1

Site description like 15.07./1
other riparian site of the same lake with steeper bank

Taxon	Coverage	Photo Nr.	Specimen collected	Seeds collected
Comarum palustre	1			
Carex aquatilis	3		+	
Menyanthes trifoliata	1			
Carex chodorrhiza	+			
Chamaedaphne calyculata	+			
Betula nana ssp. exilis ssp. exilis	+			
Salix cf. fuscescens	+		x	
Calamagrostis cf. neglecta	+			

Vegetation record Nr. 16.07./2

Polygonal ridge at the lake shore

Taxon	Coverage	Photo Nr.	Specimen collected	Seeds collected
Comarum palustre	3			
Salix cf. fuscescens	1			
Betula nana ssp. exilis ssp. exilis	1			
Carex aquatilis	1			
Calamagrostis cf. neglecta	+		x	
Chamaedaphne calyculata	1			
Andromeda polifolia	+			
Duschekia fruticosa	+			
Sphagnum sp.	+			

Vegetation record Nr. 16.07./3

Polygonal depression near the lake

Taxon	Coverage	Photo Nr.	Specimen collected	Seeds collected
Eriophorum russeolum	+			
Carex aquatilis	5			
Carex chodorrhiza	3			
Salix cf. pulchra	1			
Chamaedaphne calyculata	1		x	
Andromeda polifolia	+			
Betula nana ssp. exilis	+			
Duschekia fruticosa	+			
Comarum palustre	+			
Vaccinium uliginosum	+			

Vegetation record Nr. 16.07./4

Polygonal ridge, relatively dry				
Taxon	**Coverage**	**Photo Nr.**	**Specimen collected**	**Seeds collected**
Duschekia fruticosa	4		x	
Betula nana ssp. exilis	3			
Eriophorum russeolum	+			
Rubus chamaemorus	2			
Ledum palustre	3			
Chamaedaphne calyculata	1			
Calamagrostis cf. neglecta	+			
Vaccinium uliginosum	1			
Vaccinium vitis-idaea	1			x
Salix cf. pulchra	+			

Fig. 10-5: *Artemisia tilesii* (left) and *Polygonum tripterocarpum*, found in vegetation record 16.07./5, are characteristic of relatively dry, at least well drained sites in tundra.

Vegetation record Nr. 16.07./5

Top of a flat, well drained, densely vegetated hill in the Kolymskaya tundra				
Taxon	**Coverage**	**Photo Nr.**	**Specimen collected**	**Seeds collected**
Betula nana ssp. exilis	3			
Ledum palustre	3			
Polygonum tripterocarpum	2	5815-5816	x	x
Artemisia tilesii	+	5814	x	
Empetrum nigrum	2			
Vaccinium vitis-idaea	2			
Arctous alpina	2	5817-5818		
Luzula confusa	+		x	
Lichens				
Bryoria nitidula (Th. Fr.) Brodo & D. Hawksw.			x	
Cetraria islandica (L.) Ach.			x	
Cladonia arbuscula (Wallr.) Flot.			x	
Cladonia rangiferina (L.) F. H. Wigg.			x	
Flavocetraria cucullata (Bellardi) Kärnef. & A. Thell			x	

On July 17th, a pingo was visited in expectance to encounter extrazonal xeric vegetation (Figs. 10-6, 10-7). For location of the pingo - see Fig. 10-3 (17.07./1-9). The trip was made together with botanists from Yakutsk: Elena Troeva, Michael Telyatnikov and Sergey Pristyazhnuk.
In contrast to our expectations, genuine xerophytes were not found.

Vegetation transect Nr. 17.07./1-5

Site:	Pingo in Kolymskaya tundra about 1.6 km W of site 15.07./1 estimated about 10m above surrounding tundra (coordinates reconstructed using Google Earth) expected to display more or less dry conditions in the study area		
Latitude:	69° 5'35.14"N	**Longitude:**	160°53'49.16"E
Elevation:	ca 20 m a.s.l.	**Inclination:**	steep
Date:	17.07.2013	**Exposition:**	various
Substrate:	organic	**Lighting conditions:**	100%
Soil type:		**Soil heating:**	poor
Soil reaction:		**Soil moisture:**	mesic to dry
Humus form:	peat	**Groundwater table:**	

Fig. 10-6: View from the top of the studied Pingo into the surrounding tundra.

Vegetation record Nr. 17.07./1

Top of the Pingo

Taxon	Coverage	Photo Nr.	Specimen collected	Seeds collected
Arctagrostis latifolia	3		x	
Artemisia tilesii	2			
Descurainia sophioides	+			
Calamagrostis neglecta	2		x	
Stellaria longipes	+		x	
Salix cf. pulchra	2			
Betula nana ssp. exilis	2			
Chamaenerion angustifolium	+			
Stellaria longifolia	2		x	
Taraxacum cf. sibiricum	+		x	

Vegetation record Nr. 17.07./2

upper slope of the pingo

Taxon	Coverage	Photo Nr.	Specimen collected	Seeds collected
Betula nana ssp. exilis	3			
Ledum palustre	4			
Vaccinium vitis-idaea	1			
Empetrum nigrum	+			
Arctagrostis latifolia	1			
Salix cf. pulchra	2			
Arctous alpina	2		x	
Pyrola grandiflora	+			

Vegetation record Nr. 17.07./3

south exposed slope of the pingo

Taxon	Coverage	Photo Nr.	Specimen collected	Seeds collected
Calamagrostis neglecta	1			
Salix cf. pulchra	1			
Ledum palustre	4			
Betula nana ssp. exilis	4			
Vaccinium vitis-idaea	3			
Empetrum nigrum	1			
Arctagrostis latifolia	1			
Arctous alpina	1			
Eriophorum vaginatum	+			

Vegetation record Nr. 17.07./4

lower slope at the base of the pingo

Taxon	Coverage	Photo Nr.	Specimen collected	Seeds collected
Arctagrostis latifolia	2			
Arctous alpina	2			
Petasites frigida	1			
Rubus chamaemorus	1			
Ledum palustre	2			
Betula nana ssp. exilis	2			
Eriophorum vaginatum	2			
Vaccinium vitis-idaea	1			
Empetrum nigrum	1			

Fig. 10-7: The diversity of vegetation on the pingo is distinctly higher than in the surrounding wetland. Sedges, cotton grass and mosses are there replaced by dwarf shrubs, forbs and Gramineae.

For comparison reasons, the zonal subarctic wetland tundra surrounding the pingo was thereafter recorded as following.

Vegetation record Nr. 17.07./5

Tussock tundra in the surrounding of the pingo

Taxon	Coverage	Photo Nr.	Specimen collected	Seeds collected
Eriophorum vaginatum	4			
Carex bigelowii ssp. lugens	4		x	
Salix cf. pulchra				
Ledum palustre				
Betula nana ssp. exilis				
Duschekia fruticosa				
Chamaedaphne calyculata				
Empetrum nigrum				
Vaccinium vitis-idaea				
Carex aquatilis ssp. stans				
Eriophorum russeolum				
Vaccinium uliginosum				

Vegetation record Nr. 17.07./6

Low ridge in the tussock tundra surrounding the pingo
Peaty substrate, dry at the surface, moist in a few cm depth

Taxon	Coverage	Photo Nr.	Specimen collected	Seeds collected
Duschekia fruticosa	2			
Betula nana ssp. exilis	2			
Eriophorum vaginatum	1			
Ledum palustre	2			
Salix cf. pulchra	1			
Vaccinium uliginosum	1			
Chamaedaphne calyculata	1			
Vaccinium vitis-idaea	1			
Carex minuta	+		x	x

Vegetation record Nr. 17.07./7

lower, moister place at the ridge in the tussock tundra surrounding the pingo

Taxon	Coverage	Photo Nr.	Specimen collected	Seeds collected
Betula nana ssp. exilis	1			
Chamaedaphne calyculata	1			
Salix cf. pulchra	1			
Eriophorum polystachion	+			
Carex minuta	2			
Duschekia fruticosa	+			
Vaccinium uliginosum	1			
Comarum palustre	1			
Carex aquatilis ssp. stans	1			
Eriophorum vaginatum	1			
Ledum palustre	+			

Vegetation record Nr. 17.07./8

wet place in the tussock tundra surrounding the pingo

Taxon	Coverage	Photo Nr.	Specimen collected	Seeds collected
Eriophorum russeolum	2			
Carex aquatilis ssp. stans	4	5926		
Carex chodorrhiza	3			
Chamaedaphne calyculata	1			
Betula nana ssp. exilis	1			
Vaccinium uliginosum	1			
Salix pulchra	+			
Carex bigelowii ssp. lugens	1		x	
Comarum palustre	+			

Vegetation record Nr. 17.07./9

depression with standing water and emersed sedges

Taxon	Coverage	Photo Nr.	Specimen collected	Seeds collected
Carex chodorrhiza	2			
Carex aquatilis ssp. stans	1			

Cryptogams

Campylium polygamum (Schimp.) Lange			x	
Rhizomnium punctatum (Hedw.) Kop.			x	

The following two days were used to specify the vegetation close to POLYGON monitoring sites more in detail (locality: compare 15.07/1-4, Fig. 10-3). Vegetation was studied again along transects from ponds (Figs. 10-8 to 10-10) and lakes (Fig. 10-11) into the surrounding tundra.

Vegetation transect Nr. 18.07./1-8, proceeded next day: 19.07./1-16

Site:	Monitoring site of the POLYGON Project, Polygonal tundra with low shrubs incl. *Duschekia fruticosa* and ponds with water depths of 10 cm above a floating organic cover (with scattered *Carex stans*) about 60 cm of mud on the pond bottom, down to the permafrost table		
Elevation:	planar	**Inclination:**	flat
Date:	18.07.2013	**Exposition:**	none
Substrate:	Organic: gyttja in ponds, otherwise peat	**Lighting conditions:**	100%
Soil type:	Histosol	**Soil heating:**	various
Soil reaction:		**Soil moisture:**	Submerged to mesic
Humus form:	peat	**Groundwater table:**	50 cm to above ground

18.07./1 Tussock emerging in a pond

Taxon	Coverage	Photo Nr.	Specimen collected	Seeds collected
Carex chodorrhiza	5			
Carex aquatilis ssp. stans	1			
Eriophorum polystachion	+			
Carex vaginata	+			
Chamaedaphne calyculata	+			
Andromeda polifolia	+			
Carex williamsii	+			

Vegetation record Nr. 18.07./2

shallow riparian site at the pond

Taxon	Coverage	Photo Nr.	Specimen collected	Seeds collected
Carex chodorrhiza	4			
Carex rotundata	+			
Eriophorum russeolum	+			
Betula nana ssp. exilis	1			

Vegetation record Nr. 18.07./3

Tussock at the pond margin				
Taxon	**Coverage**	**Photo Nr.**	**Specimen collected**	**Seeds collected**
Salix cf. pulchra	1			
Betula nana ssp. exilis	1			
Andromeda polifolia	2			
Carex williamsii	2			
Carex chodorrhiza	+			

Vegetation record Nr. 18.07./4

elevated riparian site at the pond margin (10 cm moss layer)				
Taxon	**Coverage**	**Photo Nr.**	**Specimen collected**	**Seeds collected**
Ledum palustre	1			
Rubus chamaemorus	1			
Empetrum nigrum	1			
Vaccinium uliginosum	1			
Vaccinium vitis-idaea	1			
Betula nana ssp. exilis	+			
Andromeda polifolia	+			
Carex bigelowii ssp. stans	+			

Vegetation record Nr. 18.07./5

polygonal ridge, more or less dry				
Taxon	**Coverage**	**Photo Nr.**	**Specimen collected**	**Seeds collected**
Ledum palustre	3			
Betula nana ssp. exilis	2			
Duschekia fruticosa	1			
Rubus chamaemorus	2			
Vaccinium vitis-idaea	1			
Polygonum tripterocarpum	+			
Vaccinium uliginosum	2			
Arctagrostis latifolia	+			
Arctous alpina	1			
Eriophorum vaginatum	1			
Valeriana capitata	+			
Salix sp.	+			

Vegetation record Nr. 18.07./6

Tussocks at the edge of the next polygonal pond				
Taxon	**Coverage**	**Photo Nr.**	**Specimen collected**	**Seeds collected**
Carex bigelowii ssp. stans	3			
Betula nana ssp. exilis	1			
Chamaedaphne calyculata	1			
Andromeda polifolia	+			
Comarum palustre	+			
Carex williamsii	1			
Ledum palustre	+			

Vegetation record Nr. 18.07./7

aquatic vegetation of the next polygonal pond				
Taxon	**Coverage**	**Photo Nr.**	**Specimen collected**	**Seeds collected**
Menyanthes trifoliata	3			
Carex rotundata	2			

Vegetation record Nr. 18.07./8

shallow riparian site at the edge of the pond				
Taxon	**Coverage**	**Photo Nr.**	**Specimen collected**	**Seeds collected**
Eriophorum polystachion	1			
Carex bigelowii ssp. stans	3			
Carex chodorrhiza	1			
Menyanthes trifoliata	1			
Carex rotundata	+			

Vegetation record Nr. 19.07./1

other polygonal pond next to the POLYGON Monitoring site, 10 cm water column above rubiginous Gyttja, scattered sedges emerged in the water				
Taxon	**Coverage**	**Photo Nr.**	**Specimen collected**	**Seeds collected**
Carex chodorrhiza	1	6122-6123		

Fig. 10-8: A polygonal tundra pond with characteristic rubiginous gyttja (record 19.07./1).

Vegetation record Nr. 19.07./2

shallow riparian site at the pond margin

Taxon	Coverage	Photo Nr.	Specimen collected	Seeds collected
Carex bigelowii ssp. stans	3			
Carex rotundata	1		x	x
Carex chodorrhiza	2			x
Chamaedaphne calyculata	+			

Vegetation record Nr. 19.07./3

polygonal ridge at the pond margin

Taxon	Coverage	Photo Nr.	Specimen collected	Seeds collected
Carex bigelowii ssp. stans	1			
Ledum palustre	2			
Vaccinium vitis-idaea	1			
Betula nana ssp. exilis	1			
Vaccinium uliginosum	1			
Salix cf. pulchra	+			
Duschekia fruticosa	+			
Chamaedaphne calyculata	1			
Andromeda polifolia	1			
Carex chodorrhiza	+			
Rubus chamaemorus	+			

Vegetation record Nr. 19.07./4

dry top of polygonal ridge, 0,5 - 1 m above water level

Taxon	Coverage	Photo Nr.	Specimen collected	Seeds collected
Arctagrostis latifolia	1			
Duschekia fruticosa	1			
Betula nana ssp. exilis	2			
Rubus chamaemorus	2			
Vaccinium vitis-idaea	3			
Vaccinium uliginosum	1			
Ledum palustre	3			
Poa filiculmis	+		x	
Eriophorum vaginatum	1	6140		
Carex vaginata	+			x


Fig. 10-9: *Eriophorum vaginatum* (left photo) is in the wetland tundra rather typical of elevated places such as polygonal ridges (record 19.07./4). *Utricularia intermedia* (right) is one of three bladderwort species in the area (record 19.07./5).

Vegetation record Nr. 19.07./5

another polygonal pond
10 cm water column above ca 50 cm rubiginous Gyttja down to the permafrost table

Taxon	Coverage	Photo Nr.	Specimen collected	Seeds collected
Eriophorum russeolum	3			
Utricularia intermedia	2	6138-6139, 6141-6144		
Carex chodorrhiza	+			

Vegetation record Nr. 19.07./6

shallow riparian site at the pond margin, water level above the ground

Taxon	Coverage	Photo Nr.	Specimen collected	Seeds collected
Carex rotundata	3			
Eriophorum russeolum	1			
Carex chodorrhiza	1			
Utricularia intermedia	+			
Carex bigelowii ssp. stans	+			

Vegetation record Nr. 19.07./7

19.07./7 as 19.7./6 but higher, water below the ground

Taxon	Coverage	Photo Nr.	Specimen collected	Seeds collected
Eriophorum russeolum	2			
Eriophorum polystachion	1			
Betula exilis	+			
Carex rotundata	1			
Vaccinium uliginosum	+			

Vegetation record Nr. 19.07./8

close to 19.7./7 on top of tussocks

Taxon	Coverage	Photo Nr.	Specimen collected	Seeds collected
Carex vaginata	+			
Andromeda polifolia	+			
Betula exilis	1			
Carex chodorrhiza	2			
Carex rotundata	1			
Carex bigelowii ssp. stans	+			
Salix cf. pulchra	+			
Chamaedaphne calyculata	+			

Vegetation record Nr. 19.07./9

between the tussocks

Taxon	Coverage	Photo Nr.	Specimen collected	Seeds collected
Eriophorum russeolum	1			
Eriophorum polystachion	1			
Carex rotundata	+			
Carex bigelowii ssp. stans	+			
Betula nana ssp. exilis	+			
Salix cf. pulchra	+			

Vegetation record Nr. 19.07./10

Polygonal ridge				
Taxon	**Coverage**	**Photo Nr.**	**Specimen collected**	**Seeds collected**
Rubus chamaemorus	1			
Vaccinium uliginosum	1			
Ledum palustre	2			
Betula nana ssp. exilis	2			
Duschekia fruticosa	1			
Andromeda polifolia	+			
Eriophorum vaginatum	1			
Vaccinium vitis-idaea	2			
Empetrum nigrum	+			
Polygonum tripterocarpum	+			
Carex vaginata	+			
Chamaedaphne calyculata	+			
Arctagrostis latifolia	+			
Carex bigelowii ssp. stans	1			
Pedicularis sp.	+			

Fig. 10-10: Moisture conditions determine the differentiation of polygonal tundra vegetation depending on the distance to the groundwater-damming permafrost table. Lower photo: A. Schneider.

Vegetation record Nr. 19.07./11

POLYGON site POK 5: deep pond in ice wedge cast with very steep flanks
emerged and submerged plants

Taxon	Coverage	Photo Nr.	Specimen collected	Seeds collected
Menyanthes trifoliata	3			
Hippuris vulgaris	+			
Comarum palustre	1			
Utricularia vulgaris	3			
Utricularia intermedia	+			
Carex aquatilis	+		x	
Betula nana ssp. exilis	+			

Vegetation record Nr. 19.07./12

POLYGON site POK 5: adjacent sedge-cotton grass mire
Water table above ground

Taxon	Coverage	Photo Nr.	Specimen collected	Seeds collected
Menyanthes trifoliata	+			
Comarum palustre	+			
Eriophorum russeolum	2	6188		
Eriophorum polystachion	1			
Salix cf. pulchra	+			
Carex bigelowii ssp. stans	2			
Carex chodorrhiza	4			
Betula nana ssp. exilis	+			
Carex rotundata	1			
Calamagrostis neglecta	+			
Utricularia intermedia	+			

Vegetation record Nr. 19.07./13

POLYGON site POK 5: adjacent sedge-cotton grass mire
deeper water

Taxon	Coverage	Photo Nr.	Specimen collected	Seeds collected
Menyanthes trifoliata	+			
Utricularia vulgaris	+			
Utricularia intermedia	+			
Carex bigelowii ssp. stans	+			

Vegetation record Nr. 19.07./14

POLYGON site POK 5: moist polygonal ridge above water lavel

Taxon	Coverage	Photo Nr.	Specimen collected	Seeds collected
Betula nana ssp. exilis	4			
Vaccinium uliginosum	1			
Carex bigelowii ssp. stans	+			
Duschekia fruticosa	+			
Comarum palustre	+			
Chamaedaphne calyculata	+			
Salix cf. pulchra	+			

Vegetation record Nr. 19.07./15

dry polygonal ridge with 1.5 m high *Duschekia* shrubs
ground covered by dead branches

Taxon	Coverage	Photo Nr.	Specimen collected	Seeds collected
Duschekia fruticosa	2			
Vaccinium uliginosum	3			
Betula nana ssp. exilis	1			
Salix cf. pulchra	+			
Carex bigelowii ssp. stans	+			

Fig. 10-11: Aquatic plants in record 19.07./16: *Sparganium hyperboreum* with floating leaves and the white flowering *Ranunculus pallasii.*

Vegetation record Nr. 19.07./16

Lake shore, (submerged and emerged) aquatic vegetation

Taxon	Coverage	Photo Nr.	Specimen collected	Seeds collected
Carex aquatilis	4	6174	x	
Hippuris vulgaris	+	6174		
Ranunculus pallasii	+	6165-6173, 6181-	x	
Utricularia vulgaris	+			
Sparganium hyperboreum	1	6157-6158, 6177-		
Menyanthes trifoliata	1	6154-6158		
Utricularia intermedia	+			
Ranunculus gmelinii	+	6175-6176	x	

To get a broader picture on various aspects of the zonal vegetation in the study area, a survey excursion was undertaken into the Khalerchinskaya Tundra, which differs from the Kolymskaya Tundra in the underlying sandier, more acidic substrate and dryer soil conditions. The location is illustrated in Fig. 10-3 (20.07./1-4). After a long day roaming the plateau, a small transect presenting vegetation changes from a dry plateau down to an adjacent lake terrace was recorded (Fig. 10-12).

Vegetation record Nr. 20.07./1

Site:	Khalerchinskaya tundra (coordinates reconstructed using Google Earth) slope at the brim of a lake terrace Thick layer of moss and lichen above sand		
Latitude:	69° 3'47.19"N	**Longitude:**	160°52'4.12"E
Elevation:	planar	**Inclination:**	moderate
Date:	20.07.2013	**Exposition:**	W
Substrate:	moss & lichens on sand	**Lighting conditions:**	100%
Soil type:	regosol?	**Soil heating:**	moderate
Soil reaction:	acidic?	**Soil moisture:**	dry
Humus form:		**Groundwater table:**	

Fig. 10-12: On the well-drained, sandy plateau of the Khalerchinskaya Tundra, vascular plants recede in favour of lichens, which cover high percentages of the ground. The transect 20.07./1-4 from the plateau to the lake terrace is pictured.

Vegetation record Nr. 20.07./1

dry, upper slope

Taxon	Coverage	Photo Nr.	Specimen collected	Seeds collected
Ledum palustre	1			
Rubus chamaemorus	2			
Carex bigelowii ssp. lugens	1		x	
Pedicularis labradorica	+			
Vaccinium vitis-idaea	+			
Duschekia fruticosa	+			
Pinguicola algida	+			

Vegetation record Nr. 20.07./2

lower slope

Taxon	Coverage	Photo Nr.	Specimen collected	Seeds collected
Ledum palustre	2			
Carex bigelowii ssp. arctisibirica	+		x	
Rubus chamaemorus	+			
Betula nana ssp. exilis	2			
Vaccinium vitis-idaea	+			
Polygonum tripterocarpum	+			
Salix cf. glaucescens	+			
Arnica iljinii	+		x	
Salix cf. lanata	+			

Vegetation record Nr. 20.07./3

dry plateau on Khalerchinskaya tundra

Taxon	Coverage	Photo Nr.	Specimen collected	Seeds collected
Ledum palustre	2			
Betula nana ssp. exilis	2			
Vaccinium vitis-idaea	+			
Vaccinium uliginosum	+			
Salix cf. pulchra	+			
Pedicularis labradorica	+			
Arctous alpina	2			
Polygonum tripterocarpum	+			
Hierochloe alpina	+		x	
Luzula confusa	+			
Carex bigelowii ssp. arctisibirica	+			

Vegetation record Nr. 20.07./4

Lichen-dominated plateau on Khalerchinskaya tundra				
Taxon	**Coverage**	**Photo Nr.**	**Specimen collected**	**Seeds collected**
Carex bigelowii ssp. arctisibirica	1			
Vaccinium uliginosum	1			
Vaccinium vitis-idaea	+			
Ledum palustre	1			
Salix cf. pulchra	+			
Betula nana ssp. exilis	+			
Lichens				
Alectoria ochroleuca (Hoffm.) A. Massal.			x	
Bryocaulon divergens (Ach.) Kärnefelt			x	
Cetraria islandica (L.) Ach.			x	
Dactylina arctica (Hoff. f.) Nyl.			x	
Flavocetraria cucullata (Bellardi) Kärnefelt & A. Thell			x	
Stereocaulon paschale (L.) Hoffm.			x	

The last tundra vegetation surveys during the first part of the fieldworks were realised in a polygonal tundra landscape situated in the floodplain of the Pokhodsk Channel of the Kolyma River (locality: see Fig. 10-3: 21.07./1-13). Polygonal depressions are covered by sedges and cotton grass or, when permanently inundated by boreal aquatics (Fig. 10-13, 10-16). The vegetation merges here gradually into forest tundra, as is indicated by scattered larches, up to 4 m tall, growing in distances of several 100 m from each other (Fig. 10-13). Also, abundant and relatively large-growing erect birch and alder shrubs and their parasites (Fig. 10-14), occur here together with dwarf shrubs (Fig. 10-15) at drier places such as polygonal ridges, indicating progressively increasing boreal conditions, which result possibly from the thermal transfer in the vicinity of the Kolyma River.

Vegetation transect Nr. 21.07./1-13

Site:	Kolymskaya tundra, POLYGON site POK 7: polygonal tundra near the floodplain of the Kolyma River, in polygonal depressions: sedge-cotton grass mire, along the ridges: low shrubs, scattered larches (up to 4m tall) in distances of several hundred m of each other		
Latitude:	69°06'14" N	**Longitude:**	160°59'58" E
Elevation:	planar	**Inclination:**	flat
Date:	21.07.2013	**Exposition:**	none
Substrate:	decomposed moss peat	**Lighting conditions:**	100%
Soil type:	Histosol	**Soil heating:**	moderate
Soil reaction:	acidic?	**Soil moisture:**	depending on micro relief

Vegetation record Nr. 21.07./1

more or less dry peaty hill with larch

Taxon	Coverage	Photo Nr.	Specimen collected	Seeds collected
Larix gmelinii	1	021-023, 026-034		
Betula nana ssp. exilis	2			
Vaccinium vitis-idaea	2			
Empetrum nigrum	2			
Ledum palustre	+			
Duschekia fruticosa	+			
Poa sp.	+			
Calamagrostis sp.	+			
cf. Agrostis sp.	+			


Fig. 10-13: Vegetation transect 21.07./1-13: erect shrubs and scattered larches at drier places, aquatics, such as *Menyanthes trifoliata*, and cotton grass in wet or, respectively, inundated depressions.

Vegetation record Nr. 21.07./2

adjacent to 21.07./1, lower, moister

Taxon	Coverage	Photo Nr.	Specimen collected	Seeds collected
Duschekia fruticosa	3			
Betula nana ssp. exilis	2			
Vaccinium uliginosum	1			
Ledum palustre	2			
Vaccinium vitis-idaea	1			
Stellaria longifolia	+		x	
Andromeda polifolia	1			
Empetrum nigrum	+			
Eriophorum vaginatum	+			
Carex bigelowii ssp. stans	+			
Pedicularis sp.	+			
Boschniakia rossica	+	037-039, 041-043	x	

Fig. 10-14: The shrub alder (*Duschekia fruticosa*) is the most important host plant of *Boschniakia rossica*.

Vegetation record Nr. 21.07./3

adjacent to 21.07./2 polygonal depression, on the tussocks

Taxon	Coverage	Photo Nr.	Specimen collected	Seeds collected
Betula nana ssp. exilis	1			
Duschekia fruticosa	+			
Larix gmelinii	+			
Andromeda polifolia	1			
Carex chodorrhiza	2			
Carex bigelowii ssp. stans	2			
Eriophorum russeolum	+		x	x
Salix sp.	+			
Carex rariflora	1		x	x

Vegetation record Nr. 21.07./4

adjacent to 21.07./2 polygonal depression, between the tussocks

Taxon	Coverage	Photo Nr.	Specimen collected	Seeds collected
Comarum palustre	+			
Carex bigelowii ssp. stans	+			
Carex chodorrhiza	+			

Vegetation record Nr. 21.07./5

adjacent polygon ridge

Taxon	Coverage	Photo Nr.	Specimen collected	Seeds collected
Duschekia fruticosa	2			
Betula nana ssp. exilis	2			
Salix cf. pulchra	1			
Ledum palustre	+	046		
Vaccinium uliginosum	1			
Chamaedaphne calyculata	+			
Carex bigelowii ssp. stans	+			
Arctagrostis latifolia	+			
Empetrum nigrum	+			
Carex vaginata	+	044-045		
Calamagrostis neglecta	+			


Fig. 10-15: Detail of dwarf shrub vegetation on polygonal ridges with *Ledum palustre, Betula nana ssp. exilis* and *Vaccinium vitis-idaea* (left photo). *Carex vaginata* is growing at the edge of polygonal ponds (right).

Vegetation record Nr. 21.07./6

adjacent polygonal depression (POK 7), water depth 60 cm, emerged vegetation

Taxon	Coverage	Photo Nr.	Specimen collected	Seeds collected
Menyanthes trifoliata	3	039-040		
Carex rostrata	1	039-040		
Eriophorum polystachion	+	039-040		
Comarum palustre	1			

Vegetation record Nr. 21.07./7

pond in adjacent polygonal depression (POK 8), water depth 200 cm, rubiginous Gyttya, aquatic on the pond margin

Taxon	Coverage	Photo Nr.	Specimen collected	Seeds collected
Sparganium hyperboreum	2			
Menyanthes trifoliata	3			
Comarum palustre	1			

Fig. 10-16: *Sparganium hyperboreum*, the northernmost bur-reed species (left photo) occurs abundantly in the Kolymskaya tundra. *Utricularia minor* (on the right) was described in the study area for the first time.

Vegetation record Nr. 21.07./8

large tussocks within *Menyanthes* population of POK 8, tussocks isolated

Taxon	Coverage	Photo Nr.	Specimen collected	Seeds collected
Sparganium hyperboreum	2			
Carex chodorrhiza	2			
Comarum palustre	+			
Saxifraga cernua	+			
Betula nana ssp. exilis	+			
Carex bigelowii ssp. stans	+			
Epilobium palustre	+		x	
Menyanthes trifoliata	+			
Salix cf. pulchra	+			
cf. Calamagrostis sp.	+			

Vegetation record Nr. 21.07./9

tussocks at the margin of POK 8

Taxon	Coverage	Photo Nr.	Specimen collected	Seeds collected
Carex rotundata	+			
Betula nana ssp. exilis	+			
Chamaedaphne calyculata	2			
Carex chodorrhiza	2			
Menyanthes trifoliata	+			
Salix cf. pulchra	+			
Andromeda polifolia	+			
Comarum palustre	+			
Salix cf. fuscescens	+			
Carex bigelowii ssp. stans	+			
Calamagrostis neglecta	+			

Vegetation record Nr. 21.07./10

high, more or less dry polygon ridge at the margin of POK 9, which is a T-shaped, deep pond between polygon walls directly above ice wedges, substrate: moss peat

Taxon	Coverage	Photo Nr.	Specimen collected	Seeds collected
Ledum palustre	4			
Empetrum nigrum	+			
Polygonum tripterocarpum	+			
Vaccinium vitis-idaea	1			
Salix cf. glaucescens	1			
Betula nana ssp. exilis	1			
Orthilia obtusata	+			
Poa sp.	+			
Duschekia fruticosa	1			
Calamagrostis sp.	+			

Vegetation record Nr. 21.07./11

pond POK 9, ankle-deep zone

Taxon	Coverage	Photo Nr.	Specimen collected	Seeds collected
Carex bigelowii ssp. stans	1			
Comarum palustre	+			
Betula nana ssp. exilis	+			
Vaccinium uliginosum	+			
Eriophorum russeolum	+			
Ledum palustre	+			
Chamaedaphne calyculata	+			

Vegetation record Nr. 21.07./12

other bank of pond POK 9, base of polygon ridge

Taxon	Coverage	Photo Nr.	Specimen collected	Seeds collected
Carex bigelowii ssp. stans	1			
Betula nana ssp. exilis	+			
Chamaedaphne calyculata	+			
Ledum palustre	+			
Duschekia fruticosa	+			
Rubus chamaemorus	+			
Vaccinium uliginosum	+			
Vaccinium vitis-idaea	+			
Comarum palustre	+			

Vegetation record Nr. 21.07./13

bank of pond POK 9, top of polygon ridge

Taxon	Coverage	Photo Nr.	Specimen collected	Seeds collected
Ledum palustre	3			
Rubus chamaemorus	1			
Vaccinium uliginosum	1			
Vaccinium vitis-idaea	1			
Pyrola grandiflora	+			
Duschekia fruticosa	1			
Arctagrostis latifolia	+			
Stellaria longipes	+			
Orthilia obtusata	+			
Salix cf. pulchra	+			
Valeriana capitata	+			
Parrya nudicaulis	+			

10.5 Vegetation studies in the boreal zone: relict steppe and disturbed taiga habitats at the NE Science Station Chersky and the Pleistocene Park

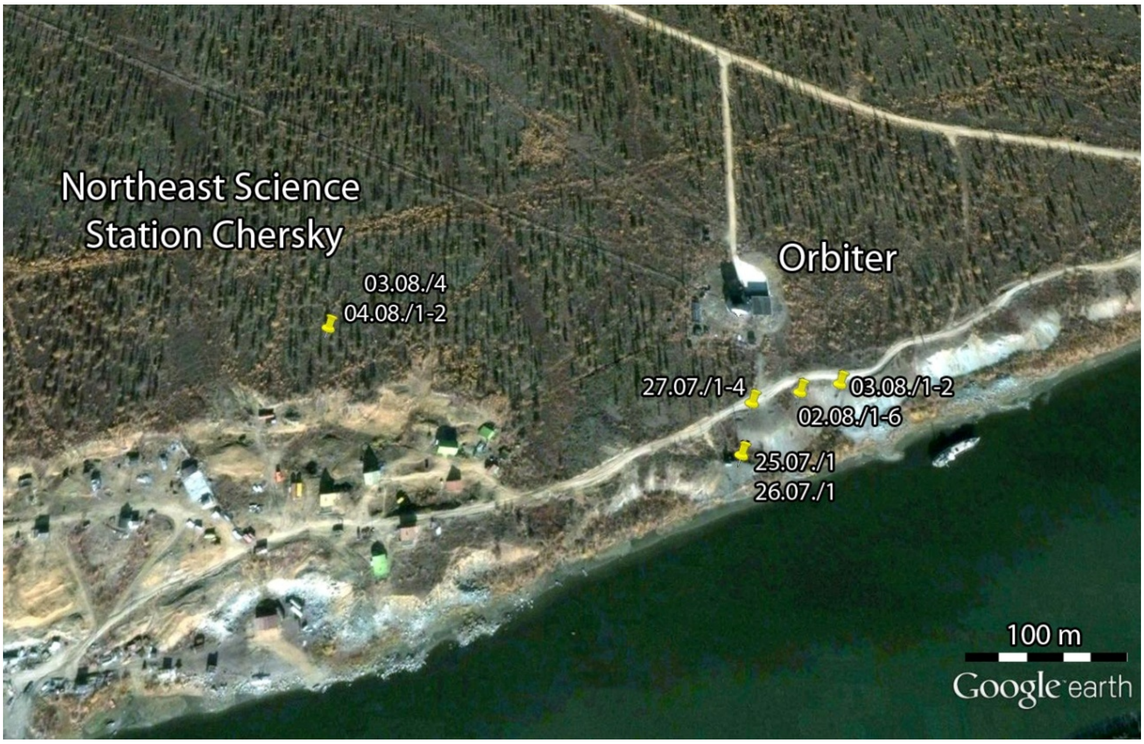

Fig. 10-17: Location of vegetation records at the Northeast Science Station Chersky. Satellite picture processed from Google earth.

Whereas the first part of the expedition was devoted to the present situation of modern tundra in the study area, the second part was intended to approach to Pleistocene vegetation conditions in either steppe relicts or plant communities permanently disturbed by large mammals and human impact.

The Northeast Science Station Chersky (Fig. 10-17) was the base of the fieldwork during that section of the expedition. In the adjacencies of the station, there was an extensive occurrence of extrazonal steppe vegetation, which was studied in very detail (Fig. 10-18). Such steppe patches within the northern taiga or even tundra zones, too far away from other steppe occurrences to enable gene flow between them, are considered to be relicts and, respectively, analogues of the Pleistocene tundra steppe (or mammoth steppe). Although this vegetation is a quite low-diverse, floristically degraded descendant of northern steppes, the species diversity there is many times higher than in the zonal tundra or taiga within the study region. Likewise isolated as their hosting steppe vegetation, even consumers of the ancient mammoth-steppe ecosystem, viz. the arctic ground squirrel (*Urocitellus parryii,* Fig. 10-19), survived here in high abundances. Their fossil remains can be found frequently in Pleistocene permafrost deposits e.g. of Duvanny Yar just like their extinct counterparts mammoth, steppe bison and woolly rhino.

In addition, the Pleistocene Park was visited in the frame of a short trip to study northern taiga vegetation under different regimes of long term disturbances by introduced large herbivores.

Fig. 10-18: Steppe relict vegetation on steep slopes in southern exposition at the Northeast Science Station Chersky.

Fig. 10-19: The northern pika (*Ochotona hyperborea*, on the left) and the Arctic ground squirrel (*Urocitellus parryii*, right) in the area of the Northeast Science Station Chersky. Both small mammals are restricted to dry ground, where they can burrow their dens. The active layer in zonal habitats of the lower Kolyma region (tundra or taiga) is mostly very wet or even saturated, preventing the construction of subterranean burrows. Especially ground squirrels are, thus, dryness indicators just like the plants in the steppe patches where they occur.

A floristically rich relevé was recorded on a steep slope directly at the station (Figs. 10-20 & 21), representing a mixture of widespread Eurasian steppe plants like *Androsace septentrionalis, Veronica incana, Carex pediformis*, *Thymus serpyllum* and xerophytes restricted to northeastern Siberia such as *Dracocephalum palmatum* and *Eremogone tschuktschorum* (Fig. 10-21).

Vegetation record Nr. 25.07./1

Site:	Northeast Science Station Chersky, steep slope over coarsely clastic scree material, very dry, well drained, southern exposition, frequent disturbances, aside from the cliff: open larch-birch woodland		
Latitude:	68°44'19.51"N	**Longitude:**	161°23'57.36"E
Elevation:	40 m a.r.l.	**Inclination:**	very steep
Date:	25.07.2013	**Exposition:**	S
Substrate:	coarsely clastic scree	**Lighting conditions:**	100%
Soil type:	rendzina	**Soil heating:**	high
Soil reaction:	basic	**Soil moisture:**	dry, well drained
Humus form:	mull	**Groundwater table:**	


Fig. 10-20: Detail of steppe vegetation in the area of the Northeast Science Station Chersky. Rendzina with a thin humus layer on coarsely clastic scree material is the characteristic soil type in the area (left picture with *Phedimus aizoon*). *Dianthus repens* and *Veronica incana* occur in high abundance here (on the right).

Vegetation record Nr. 25.07./1

upper slope highly disturbed through trampling, denudation and grazing by ground squirrels and hares

Taxon	Coverage	Photo Nr.	Specimen collected	Seeds collected
Festuca kolymensis	2		x	
Veronica incana	+			
Potentilla arenosa	+			
Dianthus repens	+	6703-6704	x	
Pulsatilla multifida	1		x	
Thymus serpyllum s.l.	1	6709-6710	x	
Eremogone tschuktschorum	1	6712	x	
Dracocephalum palmatum	+	6705-6708	x	
Androsace septentrionalis	+		x	
Vicia cracca	+		x	
Galium verum	+			
Galium boreale	+		x	
Pedicularis alopecuroides	+			

Lychnis sibirica	1		x	
Carex pediformis	1			
Vaccinium vitis-idaea	+			
Trisetum sibiricum	1			
Rosa acicularis	+			
Erysium hieraciifolium	+		x	
Allium strictum	+		x	
Poa botryoides	1		x	
Poa cf. kolymensis	+		x	
Pinus pumila	+			
Draba sp.	+		x	
Phedimus aizoon	+	6635-6636	x	
Artemisia arctica	+		x	
Chamaenerion angustifolium	+			
Carex rupestris	1		x	x
Arnica frigida	+		x	x
Phlox sibirica	1		x	x
Comastoma tenellum	+		x	
Thalictrum foetidum ssp. acutilobum	1			

Fig. 10-21: *Eremogone tschuktschorum* (left photo) and *Dracocephalum palmatum* (on the right) might be regarded northern contributors to the floristic spectrum of Pleistocene tundra steppe vegetation. Fossil seeds of *E. tschuktschorum* were found in Pleistocene permafrost deposits in arctic lowlands of Yakutia (Kienast et al., 2005).

Vegetation record Nr. 26.07./1

shrubbery adjacent to 25.07./1, more or less undisturbed

Taxon	**Coverage**	**Photo Nr.**	**Specimen collected**	**Seeds collected**
Betula divaricata	3			
Larix gmelinii	2		x	
Empetrum nigrum	2			
Vaccinium vitis-idaea	2			

Duschekia fruticosa	3			
Ledum palustre	1			
Vaccinium uliginosum	1			
Galium boreale	+			
Tanacetum boreale	+			
Chamaenerion angustifolium	+			
Salix cf. glauca	+			
Ribes triste	1		x	x
*Salix cf. udensis (*2.5 m tall*)*	1		x	

Fig. 10-22: *Potentilla stipularis* (left) and *Stellaria longifolia* (right) recorded in relevé 27.07./1.

Vegetation record Nr. 27.07./1

pioneer vegetation at the Northeast Science Station track, further uphill,
next escarp a few dozen m E of 25.07/1, highly disturbed by crossing cars and trampling

Taxon	Coverage	Photo Nr.	Specimen collected	Seeds collected
Festuca kolymensis	2			
Poa botryoides	2			
Elymus repens	1			
Hordeum jubatum	+	6779-6781		
Potentilla stipularis	+	6735-6737	x	
Stellaria longifolia	1	6740	x	
Thymus serpyllum s.l.	1			
Arnica intermedia	+			
Potentilla arenosa	+			x
Tanacetum boreale	+		x	
Galium verum	+			
Pedicularis cf. alopecuroides	+		x	x

Vegetation record Nr. 27.07./2

more steppic vegetation further downhill

Taxon	Coverage	Photo Nr.	Specimen collected	Seeds collected
Eremogone tschuktschorum	1	6790		
Dianthus repens	1	6789		
Potentilla stipularis	1			x
Galium verum	2			
Phlox sibirica	2			
Thymus serpyllum s.l.	1			
Stellaria longifolia	+		x	
Arnica intermedia	+			
Androsace septentrionalis	+			
Festuca kolymensis	1			
Poa botryoides	+			
Potentilla arenosa	+	6789	x	x
Veronica incana	+	6789		
Pulsatilla multifida	+			
Artemisia arctica	+			
Vaccinium vitis-idaea	+			
Erigeron acris	+		x	
Potentilla tanacetifolia	x	6782-6783	x	x

Fig. 10-23: *Potentilla tanacetifolia* (record 27.07./2) is a plant typical of the zonal steppes in Mongolia and Buryatia.

Vegetation record Nr. 27.07./3

steppe vegetation further downhill, less disturbed

Taxon	Coverage	Photo Nr.	Specimen collected	Seeds collected
Pulsatilla multifida	1			
Carex rupestris	4		x	
Galium verum	+			
Pedicularis cf. alopecuroides	+			
Trisetum agrostideum	1		x	
Lychnis sibirica	+		x	
Potentilla arenosa	+			
Thymus serpyllum s.l.	1			
Androsace septentrionalis	+			
Phlox sibirica	1			
Veronica incana	+			
Dracocephalum palmatum	+			
Carex pediformis	1			

Vegetation record Nr. 27.07./4

steep rock slope a few m further East, highly disturbed by denudation and grazing, ground squirrel burrow, Coverage 40-50 %

Taxon	Coverage	Photo Nr.	Specimen collected	Seeds collected
Festuca kolymensis	2			
Thalictrum foetidum ssp. acutilobum	2	6743-6746		
Phedimus aizoon	+	6766-6767		
Eremogone tschuktschorum	+	6741-6742		
Pulsatilla multifida	1			
Dracocephalum palmatum	1	6769		
Androsace septentrionalis	+			
Dianthus repens	+			
Potentilla arenosa	+			
Veronica incana	+			
Thymus serpyllum s.l.	+			
Carex pediformis	2			
Phlox sibirica	+			
Lychnis sibirica	+			
Pinus pumila	+			
cf. Ranunculus affinis	+			
Artemisia dracunculus	+		x	

Vegetation surveys in the Pleistocene Park

Studying the response of vegetation to permanent disturbances like grazing or trampling by large mammals might be a key for solving the problem whether the extinction of megaherbivores at the end of the Pleistocene was the cause or the consequence of vegetation restructuring in high latitudes. Vegetation surveys in the Pleistocene Park were therefore an important aspect of the fieldwork in 2012. The Pleistocene Park is situated about 25 km south of Chersky (Fig. 10-1) in poorly-drained, permafrost-affected, wet lowland, originally covered with northern taiga and numerous lakes. The park is divided into a small inner part, densely populated and intensely grazed by large mammals (Fig. 10-24) and a wide, extensively pastured outer part. Most records were done in the small inner range with massive disturbances. In this area, numerous horses, a few muskoxen and a single wisent (*Bison bonasus*) were observed during the stay (Fig. 10-24). Many logs and charred trunks indicated human efforts to repress the natural woody vegetation in the area. As result of human and animal actions, large areas are exempt from woods and, instead, covered with open grassland, mostly composed of sedges and *Arctagrostis latifolia*. Even in the less disturbed, larger-fenced area (outer range), larch forests seem to be replaced by tall *Salix* shrubs (Fig. 10-25). The first record describes woody vegetation in the outer, extensive range.

Fig. 10-24: Wisent, muskox and Yakutian horses in the intensely disturbed part of Pleistocene Park.

Vegetation record Nr. 28.07./1

Site:	Pleistocene Park, upland vegetation around the Eddy Tower outside the floodplain range (not inundated in spring) Northern taiga or forest tundra respectively, dense shrubbery with scattered larches, solid, relatively dry ground, charred trunks point to past fire events, moderate grazing		
Latitude:	68°30'54"N	**Longitude:**	161°31'40"E
Elevation:	10 m a.r.l.	**Inclination:**	flat
Date:	28.07.2013	**Exposition:**	none
Substrate:		**Lighting conditions:**	40 %
Soil type:		**Soil heating:**	
Soil reaction:	Acidic?	**Soil moisture:**	mesic
Humus form:	Raw humus	**Groundwater table:**	

Vegetation record Nr. 28.07./1

Northern taiga forest around Eddy Tower in the Pleistocene Park

Taxon	Coverage	Photo Nr.	Specimen collected	Seeds collected

Larix gmelinii	1	6141, 6748	x
Salix sp.	1		
Salix sp.	1	6855	
Betula divaricata	2		
Salix sp.	2		
Rosa acicularis	+		
Salix cf. fuscescens	+		
Arctous erythrocarpa	2		
Betula nana ssp. exilis	+		
Ledum palustre	1		
Vaccinium vitis-idaea	+		
Vaccinium uliginosum	+		
Empetrum nigrum	+		
Parnassia palustris	+		
Equisetum arvense	1		
Calamagrostis neglecta	1		
Valeriana capitata	+		
Chamaenerion angustifolium	+		
Pyrola grandiflora	+		
Erigeron acris	+		

Fig. 10-25: Overview (left photo made from the Eddy tower) and detail of open, extensively disturbed, boreal wood vegetation in the outer range of the park, dominated by *Salix* shrubs, as described in vegetation record 28.07./1.

The problems with *Salix*-identification, described in chapter 10.3, hampered recording vegetation, since many different willow shrub species existed here. The floristic composition in that part of the park didn't change very much over large distances. Structural diversity in the inner, more disturbed range was obviously distinctly higher. So, vegetation within the smaller fenced area was studied in detail the next two days, spanning aquatic vegetation in small ponds (Fig. 10-26) to heavily grazed meadows and shrubberies (Figs. 10-27 to 29).

Vegetation transect 29.07./1-11

Site:	Pond in the most heavily disturbed fenced part of the Pleistocene park, aquatic vegetation		
Latitude:	68°30'44,92"N	**Longitude:**	161°29'4788"E
Elevation:	3 m a.r.l.	**Inclination:**	flat
Date:	29.07.2013	**Exposition:**	none
Substrate:		**Lighting conditions:**	80 %
Soil type:	mud	**Soil heating:**	
Soil reaction:		**Soil moisture:**	Submerse, emerse
Humus form:		**Groundwater table:**	above ground

Vegetation record Nr. 29.07./1

Aquatic vegetation in a pond in the most heavily disturbed fenced part of the Pleistocene Park

Taxon	Coverage	Photo Nr.	Specimen collected	Seeds collected
Hippuris vulgaris	3			
Ranunculus gmelinii	4			
Sparganium hyperboreum	3			
Arctophila fulva	2			
Thacla natans	1			
Comarum palustre	+			
Utricularia vulgaris	+			

Vegetation record Nr. 29.07./2

Pond in the most heavily disturbed, fenced part of the Pleistocene park, riparian vegetation

Taxon	Coverage	Photo Nr.	Specimen collected	Seeds collected
Arctagrostis latifolia	5			
Rorippa palustris	+			
Ranunculus repens	+			
Caltha palustris	+			
Rubus arcticus	+			
Epilobium palustre	+			
Carex lapponica	1		x	
Salix sp.	+			

Vegetation record Nr. 29.07./3

adjacent to the pond margin, wet, muddy heavily disturbed ground, tussocks

Taxon	Coverage	Photo Nr.	Specimen collected	notes
Arctagrostis latifolia	5			> 1 m tall
Carex lapponica	1		x	
Ranunculus gmelinii	+			between tussocks
Rorippa palustris	+			between tussocks

Vegetation record Nr. 29.07./4

wet depression with standing water, heavily grazed

Taxon	Coverage	Photo Nr.	Specimen collected	Seeds collected
Arctagrostis latifolia, (grazed)	5			
Carex juncella, (large tussocks)	2		x	
Ranunculus gmelinii	4		x	x
Rorippa palustris	+		x	
Comarum palustre	+			
Thacla natans	1		x	
Hippuris vulgaris	+			

Vegetation record Nr. 29.07./5

heavily disturbed shrub vegetation, many sedge tussocks (*C. juncella, C. minuta*), grazed and trampled by large herbivores (wool of musk ox in the shrubs), solid ground, no water above ground, shrubs ca. 2.5 m high, much charred wood, tussocks burned too

Taxon	Coverage	Photo Nr.	Specimen collected	Seeds collected
Salix cf. lanata (large)	3		x	
Duschekia fruticosa	1			
Betula divaricata	1			
Salix cf. glauca	+		x	
Betula nana ssp. exilis	3			
Vaccinium uliginosum	3			
Rubus arcticus	+			
Calamagrostis neglecta	1		x	
Arctagrostis latifolia	1		x	
Carex juncella/ appendiculata	4 (differentiation in the field impossible)		x	x
Carex minuta			x	x
Equisetum arvense	+			

Vegetation record Nr. 29.07./6

open wetland vegetation, only scattered shrubs, standing water above ground, Tussocks standing in water, heavily grazed

Taxon	Coverage	Photo Nr.	Specimen collected	Seeds collected
Arctagrostis latifolia	1			
Comarum palustre	+			
Equisetum arvense	+			
Rubus arcticus	1			
Salix cf. lanata (large)	+			

Vaccinium uliginosum	+			
Thacla natans	+			
Carex juncella/ appendiculata	4 (differentiation in the field impossible since inflorescences mostly eaten)			
Carex lapponica			x	x
Carex minuta			x	x

Vegetation record Nr. 29.07./7

open wetland vegetation, no shrubs, only scattered tussocks, standing water above ground

Taxon	Coverage	Photo Nr.	Specimen collected	Seeds collected
Carex minuta	2			
Eriophorum polystachion	3			
Comarum palustre	1			
Hippuris vulgaris	+			
Ranunculus gmelinii	+			
Caltha palustris	+			
Arctagrostis latifolia	1			

Vegetation record Nr. 29.07./8

Shrubbery in the disturbed, fenced part of the Pleistocene park, solid ground, no standing water above ground

Taxon	Coverage	Photo Nr.	Specimen collected	Seeds collected
Salix cf. lanata (large)	2			
Betula nana ssp. exilis	2			
Vaccinium uliginosum	4			
Arctagrostis latifolia	1			
Betula divaricata	1			
Duschekia fruticosa	1			
Eriophorum polystachion	+			
Carex minuta	+			
Rubus arcticus	+			

Vegetation record Nr. 29.07./9

heavily grazed upland vegetation, grassland, only one larch left standing

Taxon	Coverage	Photo Nr.	Specimen collected	Seeds collected
Larix gmelinii	+			
Salix cf. lanata (large)	+			
Arctagrostis latifolia	5			
Rubus arcticus	+			
Galium aparine	+			
Rumex cf. arcticus	+			
Ranunculus repens	+			

Vegetation record Nr. 29.07./10

heavily grazed wetland vegetation, no mosses, only sedges, muddy, wet ground (standing water above ground)

Taxon	Coverage	Photo Nr.	Specimen collected	Seeds collected
Equisetum variegetum	+		x	
Equisetum scirpoides	+		x	
Carex aquatilis	2			
Carex juncella	1		x	
Arctagrostis latifolia	2			
Caltha palustris	+			
Alopecurus alpinus	+			
Salix cf. glauca	+			
Ranunculus repens	+			
Callitriche palustris	+			
Arctophila fulva	+			
Eriophorum russeolum	+			
Rumex arcticus	+			
Ranunculus gmelinii	+			
Equisetum arvense	2			

Vegetation record Nr. 29.07./11

grazed riparian vegetation at a pond margin

Taxon	Coverage	Photo Nr.	Specimen collected	Seeds collected
Ranunculus gmelinii	1			
Eriophorum polystachion	1			
Carex rostrata	2			
Petasites frigidus	+			
Comarum palustre	+			
Carex aquatilis	1			
Carex juncella	1			
Salix cf. lanata	+			
Arctagrostis latifolia	1			
Equisetum scirpoides	+			
Ranunculus repens	+			
Rorippa palustris	+			
Rubus arcticus	+			
Pedicularis cf. sudetica	+			
Caltha palustris	+			
Vaccinium uliginosum	+			

Vegetation record Nr. 30.07./1

deep pond in the Pleistocene park, eutrophic, zoogenous impact, aquatic vegetation

Taxon	Coverage	Photo Nr.	Specimen collected	Seeds collected
Potamogeton alpinus ssp. tenuifolius	2		x	
Utricularia vulgaris	3			
Myriophyllum verticillatum	2		x	
Sparganium minimum	3	6907-6909	x	x
Equisetum limosum	1	6907-6909	x	

Vegetation record Nr. 30.07./2

deep pond in the Pleistocene park, eutrophic, zoogenous impact, riparian vegetation, tussocks standing in water

Taxon	Coverage	Photo Nr.	Specimen collected	Seeds collected
Carex aquatilis	4			
Ranunculus gmelinii	+			
Comarum palustre	+			
Equisetum limosum	+			
Rorippa palustris	+			
Epilobium palustre	+		x	
Galium trifidum	+		x	

Fig. 10-26: Aquatic and riparian vegetation (30.07./1-3) in a small pond in the inner range of the Pleistocene Park.

Vegetation record Nr. 30.07./3

deep pond in the Pleistocene park, eutrophic, zoogenous impact, more distant, no direct contact with pond margin

Taxon	Coverage	Photo Nr.	Specimen collected	Seeds collected
Arctagrostis latifolia	3			
Carex aquatilis	3			
Comarum palustre	1			
Caltha palustris	+			
Galium trifidum	+			

Vegetation record Nr. 30.07./4

grazed cotton grass meadow close to the pond described

Taxon	Coverage	Photo Nr.	Specimen collected	Seeds collected
Eriophorum polystachion	4			
Comarum palustre	+			
Arctagrostis latifolia	1			
Carex juncella	1			

Fig. 10-27: Grazed cotton grass and *Arctagrostis* meadow after removal of boreal woods (records 30.07./4-5) in the inner range of the park.

Vegetation record Nr. 30.07./5

open vegetation between pond and adjacent shrubbery

Taxon	Coverage	Photo Nr.	Specimen collected	Seeds collected
Arctagrostis latifolia	2	6910		
Rubus arcticus	1		x	
Pedicularis sp. (no inflorescence)	+		x	
Comarum palustre	1			
Salix cf. lanata (juvenile)	+			
Carex bigelowii ssp. stans	1			

Vegetation record Nr. 30.07./6

open shrub vegetation disturbed by past fires and large herbivores

Taxon	Coverage	Photo Nr.	Specimen collected	Seeds collected
Salix cf. lanata	3		x	
Duschekia fruticosa	1			
Rubus arcticus	+			
Vaccinium uliginosum	1			
Pedicularis sp. (no inflorescence)	+			
Moehringia laterifolia	+		x	
Arctagrostis latifolia	3			
Carex minuta	2		x	x
Calamagrostis sp.	2			

Fig. 10-28: Open shrub vegetation disturbed by past fires and large herbivores (record 30.07./6).

Vegetation record Nr. 30.07./7

open larch woodland disturbed by past fires and large herbivores, high percentage of grasses, brushwood absent, abundant cervid droppings, musk ox wool

Taxon	**Coverage**	**Photo Nr.**	**Specimen collected**	**Seeds collected**
Larix gmelinii	3	6912-6913		
Salix cf. lanata	1	6912-6913		
Duschekia fruticosa	+			
Ledum palustre	2	6912-6913		
Vaccinium uliginosum	+			
Rubus chamaemorus	1	6912-6913		
Rubus arcticus	+			
Vaccinium vitis-idaea	2	6912-6913		
Arctagrostis latifolia	4	6912-6913		
Pyrola grandiflora	+			
Carex sp.	+			
Chamaenerion angustifolium	+			
Caltha palustris	+			
Valeriana capitata	+			

Vegetation record Nr. 30.07./8

relatively dry open larch woodland disturbed by large herbivores, grasses non abundant, many tracks of large herbivores

Taxon	Coverage	Photo Nr.	Specimen collected	Seeds collected
Larix gmelinii	2			
Salix cf. lanata	2			
Salix cf. glauca	+		x	
Rosa acicularis	1			
Ledum palustre	2			
Vaccinium uliginosum	+			
Rubus arcticus	2			
Vaccinium vitis-idaea	+			
Pyrola grandiflora	1		x	
Orthilia obtusata	+		x	
Chamaenerion angustifolium	+			
Equisetum arvense	+			
Arctagrostis latifolia	1			
Valeriana capitata	+			

Vegetation record Nr. 30.07./9

open, heavily disturbed upland vegetation, many dead, charred, tree, shrub and tussock remains, grassland with few large and juvenile scattered willow shrubs

Taxon	Coverage	Photo Nr.	Specimen collected	Seeds collected
Salix cf. lanata	+			
Salix sp.	+			
Salix cf. glauca	1			
Equisetum arvense	1			
Valeriana capitata	+			
Arctagrostis latifolia	5			
Vaccinium vitis-idaea	1			
Rubus arcticus	1			
Petasites frigidus	1			
Ledum palustre	+			
Chamaenerion angustifolium	+			
Pyrola grandiflora	+			
Vaccinium uliginosum	+			


Fig. 10-29: Open, heavily disturbed upland vegetation with few scattered, large and juvenile, willow shrubs and cotton grass tussocks (left photo). Many willow twigs bear wool fluff from moulting of muskoxes. Detail photo on the right: *Ledum palustre* growing on a charred cotton grass tussock.

Vegetation record Nr. 30.07./10

open, heavily disturbed upland vegetation resembling 30.07./9, but with very abundant cotton grass tussocks (*E. vaginatum*)

Taxon	Coverage	Photo Nr.	Specimen collected	Seeds collected
Salix sp.	+			
Salix cf. lanata	+			
Salix cf. glauca	1			
Eriophorum vaginatum (tussocks charred but still vital)	5			

Ledum palustre	+			
Arctagrostis latifolia	1			x
Carex minuta	2		x	x
Vaccinium vitis-idaea	+			
Rubus arcticus	+			

Vegetation record Nr. 30.07./11

outer range of the Pleistocene Park, upland outside floodplain, almost undisturbed taiga, thick needle litter, herb layer nearly absent

Taxon	Coverage	Photo Nr.	Specimen collected	Seeds collected
Larix gmelinii (5-10 m)	3			
Salix cf. glauca	2			
Arctous erythrocarpa	1		x	
Pedicularis sp.	+			
Vaccinium uliginosum	+			
Salix sp.	+			
Ledum palustre	+			
Equisetum arvense	+			
Arnica sp. (vegetative)	+			

Vegetation record Nr. 30.07./12

outer range of the Pleistocene Park, upland outside floodplain, taiga slightly disturbed by fire and large mammals, thin needle litter

Taxon	Coverage	Photo Nr.	Specimen collected	Seeds collected
Larix gmelinii	2			
Salix cf. glauca	1			
Salix sp.	1			
Vaccinium uliginosum	2			
Equisetum arvense	1			
Rubus arcticus	+			x
Arctous erythrocarpa	2			x
Pyrola grandiflora	1			
Empetrum nigrum	+			
Vaccinium vitis-idaea	+			
Valeriana capitata	+			
Ledum palustre	+			
Poa sp.	+			

Vegetation record Nr. 30.07./13

Muddy paddle, frequently disturbed by large mammals, finding of *Potentilla stipularis* in untypical habitat, plants directly in the water:

Taxon	Coverage	Photo Nr.	Specimen collected	Seeds collected
Ranunculus gmelinii	2			
Equisetum sp.	1			
Tephroseris palustris	+			
Androsace filiformis	+			
Hippuris vulgaris	+			

Vegetation record Nr. 30.07./14

Muddy paddle, frequently disturbed by large mammals, finding of *Potentilla stipularis* in untypical habitat, plants at the paddle margin outside the water:

Taxon	Coverage	Photo Nr.	Specimen collected	Seeds collected
Arctagrostis latifolia	+			
Equisetum sp.	+			
Betula nana ssp. exilis	+			
Tephroseris palustris	+			
Potentilla stipularis	+		x	x
Epilobium palustre	+			
Rorippa palustris	+			
Salix sp.	+			

Vegetation record Nr. 30.07./15

Muddy paddle, frequently disturbed by large mammals, finding of *Potentilla stipularis* in untypical habitat, plants growing more elevated near a stub

Taxon	Coverage	Photo Nr.	Specimen collected	Seeds collected
Ledum palustre	1			
Equisetum arvense	2			
Potentilla stipularis	+	6926	x	x
Rubus arcticus	+			
Vaccinium vitis-idaea	1			
Valeriana capitata	+			
Luzula wahlenbergii	+		x	x
Arctagrostis latifolia	+			
Betula nana ssp. exilis	+			

Vegetation record Nr. 30.07./16

finding of *Potentilla stipularis* in untypical habitat, plants growing more elevated near a stub, adjacent shrubbery

Taxon	Coverage	Photo Nr.	Specimen collected	Seeds collected
Salix cf. lanata	2			
Betula nana ssp. exilis	3			

Betula divaricata	1
Arctagrostis latifolia	+
Ledum palustre	1
Equisetum arvense	+

As first result of the vegetation surveys in the Pleistocene Park, it can be concluded that boreal woods were reduced due to heavy disturbances in support of open vegetation such as wet meadows and marshes. A shift towards dry vegetation, steppes in particular, could however not be detected, e.g. by steppe indicator plants. *Potentilla stipularis* was the only unusual species, which has, however, unclear habitat preferences. Potentially increased transpiration of the created grasslands, thus, didn’t bring dry conditions as presumed by Zimov (2012) despite regional low precipitation of only about 300 mm. The situation of the Pleistocene Park in wet lowland or the relatively small area of the park together with a still low level of disturbances over large parts of the park might be reasons for this result. As consequence of this conclusion, we decided for the subsequently proposed project to include vegetation studies in livestock-pastured areas within the more continental (and even less humid) region around Batagay in the Yana Highlands, where expansive steppe vegetation is still present. We hope to get then a broader picture for the assessment of zoogenous disturbances on northern vegetation under different climatic constellations within Beringia.

Back to the Northeast Science Station Chersky

After return to the Northeast Science Station, the focus was on completing the record of extrazonal steppe vegetation (Figs. 10-30 to 10-33, 10-36), especially when it was combined with high latitude xerophytes such as *Dryas punctata* or *Artemisia arctica*. Both species do not occur in zonal habitats in Arctic lowlands today but are restricted to dry places in mountains or on well drained ground. They could be proven for the Northeast Science Station (record 02.08/2, Fig. 10-30) representing a tundra steppe like species combination under cold and dry climate.

Beside shrub and ruderal vegetation adjacent to steppes (Figs. 10-31 to 10-34), also forest vegetation near the station was recorded as reference for potentially natural vegetation in the area outside the range of the south-exposed bluff (records 03.08./4 -04.08/2, Fig. 10-35).

Finally, vegetation records from Duvanny Yar are listed here, taken during a short trip when sediments from the permafrost section were sampled.

Vegetation record Nr. 02.08./1

Site:	Northeast Science Station, steep slope, loamy over coarsely clastic scree material, well drained, southern exposition, frequent disturbances, vegetation around the small plateau on top of the cliff		
Latitude:	68°44'19"N	**Longitude:**	161°23'57" E
Elevation:	40 m a.r.l.	**Inclination:**	very steep
Date:	02.08.2012	**Exposition:**	SSE
Substrate:	Loam on coarsely clastic scree	**Lighting conditions:**	100%
Soil type:	rendzina	**Soil heating:**	high
Soil reaction:	basic	**Soil moisture:**	dry, well drained
Humus form:	mull	**Groundwater table:**	

Vegetation record Nr. 02.08./01

oblique plateau on the cliff, slightly shaded by a single larch

Taxon	Coverage	Photo Nr.	Specimen collected	Seeds collected
Larix gmelinii	1 tree			
Empetrum nigrum	2			
Vaccinium vitis-idaea	1			
Arnica frigida	1		x	x
Pulsatilla multifida	+			
Artemisia arctica	+			
Thymus serpyllum s.l.	+			
Eremogone tschuktschorum	+			
Festuca kolymensis	1			
cf. Hierochloe alpina	+			
Arctous alpina	1			

Vegetation record Nr. 02.08./02

oblique plateau on the cliff, unshaded by larch, finding of *Dryas punctata*

Taxon	Coverage	Photo Nr.	Specimen collected	Seeds collected
Dryas punctata	1		x	x
Artemisia arctica	+			
Arnica iljinii	+			
Pulsatilla multifida	+			
Phlox sibirica	1			
Vaccinium vitis-idaea	1			
Pedicularis venustus	+			
Festuca kolymensis	2		x	
Eremogone tschuktschorum	1			
Thymus serpyllum s.l.	2			
Dianthus repens	+			
Androsace septentrionalis	+			
Carex rupestris	1		x	
Galium verum	+			
Veronica incana	+			
Poa cf. botryoides	1		x	
cf. Hierochloe alpina	+			
Potentilla arenosa	+			
Erigeron acris	+			


Fig. 10-30: *Artemisia arctica* and *Dryas punctata* on top of the cliff at the Northeast Science Station Chersky (left photo). Right: Detail of the *Dryas* stand.

Vegetation record Nr. 02.08./03

oblique plateau on the cliff, adjacent denser and taller vegetation with single shrubs				
Taxon	**Coverage**	**Photo Nr.**	**Specimen collected**	**Seeds collected**
Erigeron acris	+			
Tanacetum boreale	+			
Vaccinium vitis-idaea	+			
Ribes triste	+			
Veronica incana	+			
Dianthus repens	+			
Festuca kolymensis	4			
Eremogone tschuktschorum	+			
Thymus serpyllum s.l.	+			
Artemisia dracunculus	+		x	
Rosa acicularis	+			
Galium verum	+			
Poa cf. botryoides	*1*			
Pulsatilla multifida	+			
Stellaria longifolia	+			
Carex pediformis	+			

Fig. 10-31: Record 02.08./3: steppe vegetation with large stand of *Veronica incana* interspersedwith *Rosa acicularis* shrubs and adjacent to a *Betula divaricata* shrubbery.

Vegetation record Nr. 02.08./04

adjacent open shrub vegetation

Taxon	Coverage	Photo Nr.	Specimen collected	Seeds collected
Betula divaricata	3		x	
Artemisia dracunculus	+			
Empetrum nigrum	4			
Vaccinium vitis-idaea	+			
Vaccinium uliginosum	2			
Lactuca sibirica	+			
Poa cf. botryoides	1			
Eremogone tschuktschorum	+			
Dianthus repens	+			
Ledum palustre	+			
Salix sp.	+			
Chamaenerion angustifolium	+			
Galium verum	+			

Vegetation record Nr. 02.08./05

adjacent wood stand farther to the East

Taxon	Coverage	Photo Nr.	Specimen collected	Seeds collected
Ledum palustre	+		x	
Larix gmelinii	3			
Pinus pumila	1			
Salix cf. lanata	2			
Salix sp	1			
Rosa acicularis	1			
Betula divaricata	1			
Vaccinium uliginosum	1			
Vaccinium vitis-idaea	1			
Empetrum nigrum	3			
Equisetum arvense	+			
Eremogone tschuktschorum	+			
Chamaenerion angustifolium	+			
Artemisia arctica	+			
Poa sp.	+			
cf. Calamagrostis	+			

On top of the steppe cliff, ruderal vegetation with an eye-catching population of *Hordeum jubatum* along an unmade road, occasionally overrun by cars, was studied (Fig. 10-32). Its floristic composition is listed following.

Fig. 10-32: Pioneer vegetation with dominating *Hordeum jubatum* affected by motor vehicles.

Vegetation record Nr. 02.08./06

disturbed vegetation close to 02.08./2 adjacent to the track

Taxon	Coverage	Photo Nr.	Specimen collected	Seeds collected
Artemisia dracunculus	+		x	
Poa sp.	1			
Erigeron acris	+			
Hordeum jubatum	3			
Elytrigia repens	3			
Arnica frigida	+			
Thymus serpyllum s.l.	+			
Tanacetum boreale	+			
Festuca kolymensis	+			
Agrostis trinii	+		x	x

Farther to the East along the cliff (see Fig. 10-17), *Antennaria friesiana* was found in an open, mixed shrub/dwarf shrub/steppe vegetation mosaic (record 03.08./01, Fig. 10-33).

Fig. 10-33: *Antennaria friesiana* (grayish plants on the left photo) together with the subarctic dwarf shrub *Arctous alpina* (green leaves in front) growing in a steppe / shrub mosaic together with *Tanacetum boreale, Pinus pumila, Thymus serpyllum* and *Ribes triste* (right photo).

Vegetation record Nr. 03.08./01

Northeast Science Station further E than the day before, steep slope, loamy scree material

Taxon	Coverage	Photo Nr.	Specimen collected	Seeds collected
Vaccinium uliginosum	2			
Tanacetum boreale	+			
Thymus serpyllum s.l.	1			
Antennaria friesiana	1		x	x
Eremogone tschuktschorum	1			
Carex pediformis	+		x	
Galium verum	1			
Pulsatilla multifida	1			
Rosa acicularis	+			
Artemisia arctica	+			
Arctous alpina	1			
Phlox sibirica	+			
Comastoma tenellum	+		x	
Pinus pumila	+			
Salix sp.	+			
Poa sp.	+			
Vaccinium vitis idaea	+			
Empetrum nigrum	+			
Ribes triste	+			
Betula divaricata	+			
Galium boreale	+			
Vicia cracca	+			
Polygonum viviparum	+			
Rubus idaeus	+			
Androsace septentrionalis	+			
Draba sp.	+			
Dianthus repens	+			
Dracocephalum palmatum	+			

Vegetation record Nr. 03.08./02

ravine between cliff sections, less wind exposed, dense, waist-high shrubbery, upper slope

Taxon	Coverage	Photo Nr.	Specimen collected	Seeds collected
Vaccinium uliginosum	3			
Betula divaricata	4			
Duschekia fruticosa	1			
Empetrum nigrum	1			
Rosa acicularis	+			
Vicia cracca	+			
Salix cf. lanata	+			
Equisetum arvense	+			
Vaccinium vitis-idaea	1			
Pinus pumila	+			
Salix cf. glauca	+			
Ledum palustre	+			

Vegetation record Nr. 03.08./03

ravine between cliff sections, less wind exposed, dense, waist-high shrub vegetation, lower slope with dominating, up to 4 m tall *Duschekia* ‘trees’

Taxon	Coverage	Photo Nr.	Specimen collected	Seeds collected
Duschekia fruticosa	4			
Ribes triste	3			
Rosa acicularis	2			
Chamaenerion angustifolium	+			
Equisetum arvense	+			
Tanacetum boreale	+			
Vaccinium uliginosum	+			
Galium boreale	+			
Potentilla stipularis	+			
cf. Agrostis sp.	1			
Lactuca sibirica	+			

Fig. 10-34: Detail of *Ribes triste* from record Nr. 03.08./03.

As reference for potentially natural plant cover, forest vegetation around the Northeast Science Station was recorded (records 03.08./04–04.08./2, Fig. 10-35). Stumps indicated that the openness of the forest was partially the result of anthropogenic influence. In contrast to the Pleistocene Park, soil conditions were drier due to coarse rock debris, which resulted in better drainage.

Vegetation transect Nr. 03.08./04 – 04.08./2

Site:	area adjacent to the Northeast Science Station Chersky, further away from the cliff above the station, open, disturbed northern taiga, dry on coarse rock debris (palaeogene), well drained, southern exposition, little inclination, many hare droppings, approximation to zonal vegetation		
Latitude:	68°44'22.57"N	**Longitude:**	161°23'32.02"E
Elevation:	45 m a.r.l.	**Inclination:**	low
Date:	03.08.2012	**Exposition:**	SSE
Substrate:	Loam on coarsely clastic scree	**Lighting conditions:**	100%
Soil type:	rendzina	**Soil heating:**	
Soil reaction:	basic	**Soil moisture:**	dry, well drained
Humus form:	mull	**Groundwater table:**	

Fig. 10-35: Forest vegetation around the Northeast Science Station Chersky on reddish Palaeogene rock debris. The 'Orbiter' as a landmark is visible in the background (compare Fig. 10-17).

Vegetation record Nr. 03.08./04

disturbed open larch forest

Taxon	Coverage	Photo Nr.	Specimen collected	Seeds collected
Larix gmelinii	1			
Betula divaricata	3			
Vaccinium uliginosum	3			
Vaccinium vitis-idaea	2			
Empetrum nigrum	3			
Arnica frigida	+			
Salix cf. glauca	+			
Ledum palustre	+			
Pinus pumila	+			
Arctous alpina	+			
Artemisia arctica	+			
Salix cf. lanata	+			
Calamagrostis sp.	+			

Cryptogams	
Flavocetraria cucullata (Bellardi) Kärnefelt & A. Thell	x
Peltigera aphthosa (L.) Willd.	x
Aulacomnium turgidum (Wahlenb.) Schwägr.	x
Ptilidium ciliare (L.) Hampe	x
Tomentypnum nitens Loeske	x
Dicranum spec.	x

Vegetation record Nr. 04.08./01

close to the record 03.08./4, open larch forest, rich in lichens, stumps point to anthropogenic disturbances, larches of different ages, oldest trees possess scorch marks

Taxon	Coverage	Photo Nr.	Specimen collected	Seeds collected
Larix gmelinii	2			
Betula divaricata	4			
Salix cf. glauca	2			
Salix cf. lanata	+			
Vaccinium uliginosum	3			
Arctous erythrocarpa	+			
Ledum palustre	+			
Vaccinium vitis-idaea	3			
Empetrum nigrum	1			
Arnica frigida	+			
Artemisia arctica	+			
Pinus pumila	+			
Orthilia obtusata	+			
Cryptogams				
Bryoria simplicior (Vain.) Brodo & D. Hawksw. (an Larix)			x	
Cetraria laevigata Rass.			x	
Cladonia rangiferina (L.) F. H. Wigg.			x	
Flavocetraria cucullata (Bellardi) Kärnef. & A. Thell			x	
Peltigera aphthosa (L.) Willd.			x	
Peltigera frippii Holt.-Hartw.			x	
Aulacomnium turgidum (Wahlenb.) Schwägr.			x	
Dicranum spec.			x	
indet. liverwort			x	

Vegetation record Nr. 04.08./02

close to the record 04.08./1, denser stands of young larches with few "Überhälter", more or less open areas with low shrubs, *Betula* decreases where larches dominate

Taxon	Coverage	Photo Nr.	Specimen collected	Seeds collected
Larix gmelinii	3			
Betula divaricata	4			
Salix cf. glauca	1			
Salix cf. lanata	1			
Vaccinium uliginosum	2			
Vaccinium vitis-idaea	2			
Arctous erythrocarpa	+			
Empetrum nigrum	1			
Equisetum arvense	+			
Petasites frigida	+			

Vegetation record Nr. 04.08./03

Site:	steep slope, about 10 km SE of the Northeast Science Station, exposed bedrock, Carbonate rock		
Latitude:	68°43'025"N	**Longitude:**	161°29'049"E
Elevation:	30 m a.r.l.	**Inclination:**	moderate to steep
Date:	04.08.2012	**Exposition:**	SW
Substrate:	Loamy coarsely clastic scree		
Soil type:	rendzina	**Lighting conditions:**	100%
Soil reaction:	basic	**Soil moisture:**	dry, well drained
Humus form:	mull	**Groundwater table:**	

Fig. 10-36: Vegetation record 04.08./03 represents another steppe plant occurrence.

Vegetation record Nr. 04.08./03

Steep steppe slope

Taxon	Coverage	Photo Nr.	Specimen collected	Seeds collected
Pulsatilla multifida				
Eremogone tschuktschorum				
Galium boreale				
Carex pediformis			x	x
Calamagrostis purpurascens				
Bromopsis pumpelliana			x	
cf. Festuca altaica				
Rosa acicularis				
Chamaenerion angustifolium				
cf. Peucedanum sp.				
Lychnis sibirica			x	
Vicia cracca				
Sedum aizon				
Artemisia dracunculus				
Veronica incana				
Myosotis asiatica			x	
Thymus serpyllum				
Potentilla arenosa				
Allium strictum				
cf. Phlojodicarpus villosus				
Potentilla tanacetifolia			x	x
Anemone ochotensis			x	

Well accessible parts of the cliff are popular camping destinations for the local population since they allow a panoramic view over the landscape. At such places, ruderal plants are mixed among the xeric vegetation (Fig. 10-37 & 10-38) such as in record 05.08./1.

Vegetation record Nr. 05.08./01

Site:	Camping site close to Northeast Science Station, thin Rendzina, above Carbonate rock, GPS-data reconstructed using Google Earth		
Latitude:	68°44'24.70"N	**Longitude:**	161°24'28.82"E
Elevation:	40 m a.r.l.	**Inclination:**	moderate to steep
Date:	05.08.2012	**Exposition:**	SW
Substrate:	Loam on coarsely clastic scree	**Lighting conditions:**	100%
Soil type:	rendzina	**Soil heating:**	
Soil reaction:	basic	**Soil moisture:**	dry, well drained
Humus form:	mull	**Groundwater table:**	

Fig. 10-37: *Linaria acutiloba* at disturbed sites close to a ground squirrel burrow near a camping site.

Vegetation record Nr. 05.08./01

ruderal and disturbed steppe vegetation

Taxon	Coverage	Photo Nr.	Specimen collected	Seeds collected
Festuca kolymensis	3			
Carex cf. duriuscula	2			
Veronica incana	1			
Galium verum	1			
Dianthus versicolor	+			
Taraxacum officinale	+			
Phlox sibirica	+			
Tanacetum boreale	+			
Thymus serpyllum	1			
Pulsatilla multifida	+			
Potentilla nivea	+	x	x	
Hordeum jubatum	+		x	
Linaria acutiloba	+	x	x	
Eremogone tschuktschorum	+			
Androsace septentrionalis	+			
Erysium hieraciifolium	+			
Chamaenerion angustifolium	+			
Elytrigia repens	1			
Poa sp.	1			
Rosa acicularis	+			

Fig. 10-38: *Potentilla nivea* in record 05.08./1. Resembling *Dryas punctata* and *Artemisia arctica,* this cinquefoil is an arctic/ alpine xerophyte.

Vegetation at Duvanny Yar

With the aim to sample permafrost sediments for tentative plant macrofossil analyses in preparation of the intended research project (see scientific background and objectives), the Quaternary palaeobotanical (and palaeozoological) key section Duvanny Yar (Fig. 10-39) was visited for a short trip (see chapter 10.6). As a reference for comparison of modern plant cover at Duvanny Yar with palaeorecords, the vegetation on the fossil bearing ice-rich permafrost (Yedoma) section was recorded along a transect (records 08.08./1-5) from top of the Yedoma down to a small lake at the back side of the outcrop.

Vegetation transect Nr. 08.08./01 to 08.08./5

Site:	Duvanny Yar, zonal vegetation, open larch forest on top of the Yedoma, high gradient towards the outcrop and also towards the other site, which ends in a thaw lake		
Latitude:	68°37'45.72"N	**Longitude:**	159° 8'38.96"E
Elevation:	30 m a.r.l.	**Inclination:**	moderate to steep
Date:	08.08.2012	**Exposition:**	N
Substrate:	sandy silt	**Lighting conditions:**	
Soil type:		**Soil heating:**	
Soil reaction:		**Soil moisture:**	Moist to wet
Humus form:		**Groundwater table:**	

Vegetation record Nr. 08.08./01

open larch forest on Yedoma

Taxon	Coverage	Photo Nr.	Specimen collected	Seeds collected
Larix gmelinii	2			
Ledum palustre	4			
Salix sp.	1			
Salix sp.	+			
Vaccinium vitis-idaea	+			
Arctagrostis latifolia	1		x	x
Betula exilis	+			
Vaccinium uliginosum	+			

Vegetation record Nr. 08.08./02

further downslope towards the lake, tree coverage denser

Taxon	Coverage	Photo Nr.	Specimen collected	Seeds collected
Larix gmelinii	3			
Ledum palustre	3			
Vaccinium uliginosum	1			
Salix sp.	2			
Arctagrostis latifolia	2			
Salix sp.	1			
Pyrola grandiflora	+			
Vaccinium vitis-idaea	1			
Empetrum nigrum	+			
Rosa acicularis	+			

lower slope: successive increase of willows and Arctagrostis latifolia

Vegetation record Nr. 08.08./03

forest vegetation close by the lake

Taxon	Coverage	Photo Nr.	Specimen collected	Seeds collected
Larix gmelinii	1			
Betula exilis	3			
Salix sp.	2			
Arctagrostis latifolia	3			
Ledum palustre	1			
Vaccinium vitis-idaea	2			
Vaccinium uliginosum	+			
Pyrola grandiflora	+			
Ribes triste	+			
Rubus arcticus	+			

Fig. 10-39: The permafrost section Duvanny Yar at low water conditions. Northern taiga vegetation has formed on top of the Yedoma. The camping site is located on a small island in the Kolyma River, visible left in the photo.

Vegetation record Nr. 08.08./04

aquatic vegetation at the shore of the lake with clear water, large depth of visibility

Taxon	Coverage	Photo Nr.	Specimen collected	Seeds collected
Epilobium palustre	+			
Eriophorum russeolum	+			
Hippuris vulgaris	+			
Utricularia vulgaris	+			
Utricularia intermedia	+			
Comarum palustre	3			
Menyanthes trifoliata	3			x
Equisetum limosum	3			

Vegetation record Nr. 08.08./05

open forest vegetation on top of the Duvanny Yar Yedoma, farther to the west than 08.08./1, more open, only few larches, willows absent, but more dwarf birches, much more lichens

Taxon	Coverage	Photo Nr.	Specimen collected	Seeds collected
Larix gmelinii	1			
Betula exilis	4			
Ledum palustre	3			
Vaccinium vitis-idaea	1			
Arctagrostis latifolia	1			
Vaccinium uliginosum	+			
Equisetum arvense	+			
Salix sp.	+			
Betula divaricata	+			

10.6 Survey of the Pleistocene permafrost sediment section Duvanny Yar and sampling for palaeobotanical studies

In the frame of the subsequently proposed research project, it is intended to investigate the ecological interactions of Quaternary vegetation and large herbivores in the terrestrial Arctic by combining studies of modern plant communities, as described above, with Late Pleistocene palaeovegetation as recorded in the Duvanny Yar permafrost type sequence. Structure, composition and dynamics of late Quaternary vegetation in the study area are to be reconstructed using macroscopic plant remains preserved in ice-rich syngenetic permafrost (Ice Complex) deposits of Duvanny Yar (Fig. 10-40), which accumulated during the last cold stage (Marine Isotope Stages [MIS] 2-3 and likely 4) until about 10 ka BP (Strauss, 2010). At the outcrop, permafrost deposits are exposed over a length of about 12 km along the right bank of the Kolyma River and are hence accessible for sampling. This exposure is regarded stratotype in the Beringian late Quaternary stratigraphy (Hopkins, 1982) and key section of the Late Pleistocene Ice Complex (Yedoma Suite) in Northeast Siberia (Kaplina et al., 1978; Giterman et al., 1982). Duvanny Yar, located about 100 km to the west of the Northeast Science Station Chersky (Fig. 10-1), was therefore among the most important destinations during the expedition. Numerous organism remains such as fossil insect and plant parts, sometimes enclosed in fossil rodent burrows, as well as mammal bones are preserved partly in excellent condition in the sediment sequence (Sher & Kuzmina, 2007; Zanina et al., 2011, Zimov et al., 2012). Further details on the study area are described in Schirrmeister & Wetterich (2009).

Fig. 10-40: Ice rich permafrost (Ice Complex, Yedoma) with numerous large syngenetic ice wedges, which formed during MIS 4-2, is accessible at Duvanny Yar.

Owing to difficult weather conditions, Duvanny Yar was reachable only a few days before the end of the fieldwork (departure from Chersky back to Germany was August 13th), so that the stay was restricted to only two days from August 8th to 10th. After vegetation surveys done at August 8th (see chapter 10.5), the section was inspected in a first reconnaissance using a motorboat to get a general overview of the outcrop and to select suitable sampling sites. Beside accessible Ice Complex sections, particular emphasis was placed on deposits of the last interglacial or even older sediments to obtain an as long as possible record.

A few hundred m upstream an island, which served as camping site, a contact zone of Late Pleistocene Ice Complex deposits and taberites of assumedly older age was observed (Fig. 10-41). It was remarkable that Yedoma ice wedges didn't penetrate these slopingly subjacent low-ice deposits. The taberites didn't show any visible ground ice structures, but contained numerous ice wedge casts with woody remains, which might have formed by thermal degradation events during the last interglacial (Kazantsevo).

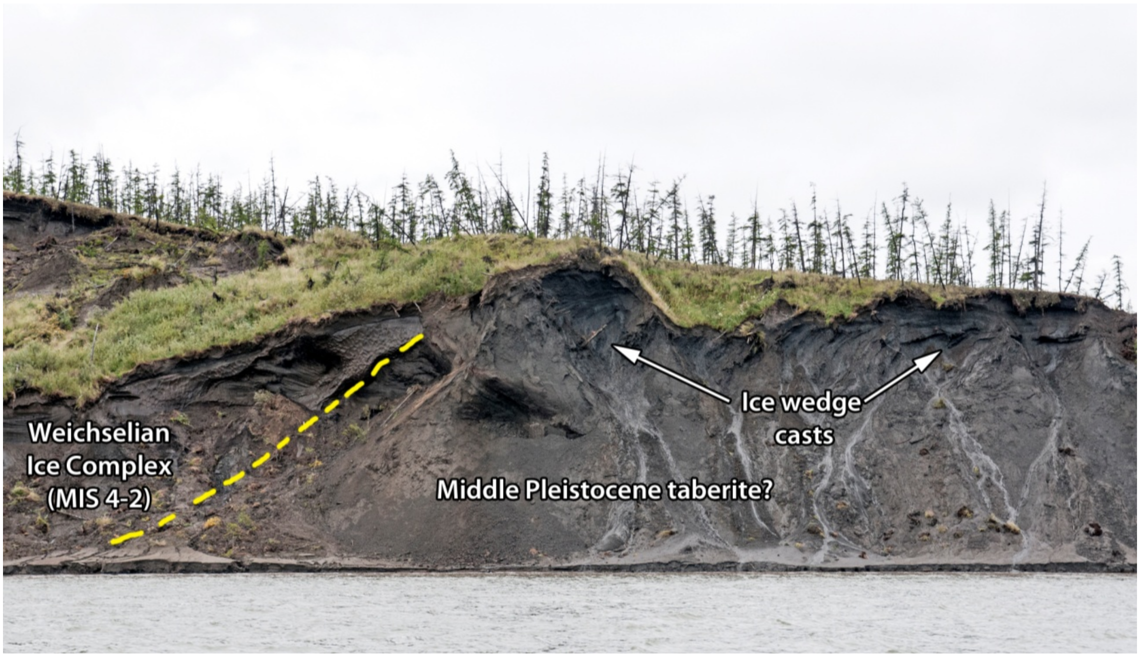

Fig. 10-41: Weichselian Ice Complex deposits marginally overlay older taberites - compacted permafrost sediments with low ice content and numerous ice wedge casts. These deposits don't contain any visible ground ice structures and are not penetrated epigenetically by Late Pleistocene ice wedges. The yellow dashed line illustrates the boundary of both sedimentological units.

From this taberite unit, a well accessible exposure was selected for sampling a composite profile consisting of two staggered subprofiles over a total height of 270 cm (Du 12/ 9.8.; Figs. 10-42 & 43). According to the GPS sensor of a Nokia 5800 cell phone, coordinates were as follows: 68°38'17,52'' N, 159°03'43,31'' E.

Fig. 10-42: In a steep, about 20m high bluff, a sequence of samples was taken from the pre-Weichselian taberite material (compare Fig. 10-43) for palaeobotanical studies.

The scarp was first cleaned using a hack. The light gray deposits consisted of bedded silt with low sand content (in beige ribbon structures), without visible plant remains except for few scattered woody remains. In 30 cm distances, sediment samples each of about 3 kg were taken in unfrozen state after removing the outermost about 5 cm of sediment from the steep scarp. The uppermost sample fom subprofile I corresponds in height position to the lowermost sample of subprofile II (Tab. in appendices). Height correlation was estimated using an 1m ruler and a tagged spade (Fig. 10-43). The sediment samples were packed in plastic bags for transport to the Northeast Science Station but remained otherwise untreated.

Fig. 10-43: Sample setting for the composite taberite section Du 12/ 9.8.

Fig. 10-44: Sampled thermokarst mound (section Du 12/ 10.8.)

Opposite to the camping island, the Weichselian Ice Complex section was accessible for sampling in a thermocirque. A thermokarst mound (baidzherakh) was sampled here over a total height of 6 m in sampling distances of about 50 cm (section Du 12/ 10.8.; Fig. 10-44). The baidzherakh almost continuously consisted of bedded, grey, organic-rich sandy silt and included large amounts of well preserved plant remains. In a height of 410 to 450 cm, the sequence contained a beige-brownish layer of silty sand, represented in sample Du 12/10.08/10 (Tab. in appendices). Above this sand layer, the sequence of organic rich sandy silt recurred up to a height of 550 cm. Another sand layer existed above this height until the top of the baidzherakh.

Sampling was overall conducted in the same way as in section Du 12/ 9.8. After return to the Northeast Science Station, the obtained samples were processed in the lab (Fig. 10-45). The sediment material was splitted into two portions per sample. The larger part was wet-sieved using 250 µm mesh size to remove most of the mineral part. The retention was then dried and packed for transport. The other part of the respective sample was dried without any further treatment to preserve material as reference for possible future investigations.

Fig. 10-45: Sediment lab available in the Northeast Science Station Chersky.

Acknowledgements

The reported fieldwork was supported by the German Science Fundation (DFG-Project KI 849/3-1). Many thanks to the colleagues of the Alfred Wegener Institute for Polar and Marine Research for the opportunity to join the POLYGON Expedition 'Pokhodsk-Kytalik' and for logistical support and excellent cooperation. Also the Northeastern Federal University 'M.K. Amossov' provided logistical support of the fieldwork. I would like to thank the Northeast Science Station Chersky for fruitful collaboration and for providing transport logistics (boats and cars), scientific equipment (lab) and accommodations. Special thanks to Sergey Davidoff for pleasant conversation and interesting discussions. Many thanks to Volker Otte, who brought his expertise in identification of cryptogams collected during the expedition.

11. Dendrochronological and ecological studies in the treeline zone

Mareike Wieczorek, Inga Jacobsen, Stefan Kruse, Alexei Kolmogorov, Anatoly Nikolaev

11.1. Introduction and Objectives

Global position of treelines is mainly controlled by climate (Holtmeier and Broll 2005) and climate warming, which is suggested to be pronounced in the Arctic regions, might lead to a northward expansion of treeline position (ACIA, 2004). Positive feedbacks between climate and vegetation due to e.g. reduced albedo (Bonan, 2008) could then result in even more elevated temperatures than recent projections suggest. However, treelines all over the world do not react consistently to climate warming and show a diverse pattern of northward movement, no change or even retreat (Harsch et al., 2009). The Russian treeline, which is exclusively formed by different *Larix* species, follows approximately today's 12 °C July isotherm (MacDonald et al. 2008). Some studies on treeline changes have been conducted in Russia (e.g. MacDonald et al. 1998; Shiyatov and Mazepa 2011, see also the review of Harsch et al. 2009), but data especially from the remote area of the lower Kolyma are scarce. With the help of dendrochronological and ecological studies, we want to detect past changes in tree growth and treeline position and find out, under which conditions *Larix cajanderi* Mayr is able to grow. Furthermore, with the help of genetic analyses, we want to find out more about the reproductive success of single individuals or genetic lineages.

Fig. 11-1 Locations of 2012 study sites
★ 12-KO-01 ✚ 12-KO-02 ◆ 12-KO-03
● 12-KO-04 ▲ 12-KO-05

11.2. Materials and Methods

Between July and August 2012, five sites on a transect along the Kolyma River were sampled (Fig. 11-1). They were primarily chosen by satellite pictures such that they spanned the transition range from forest tundra to the upper treeline with only sparse tree growth. However, conditions in the field were somewhat different than expected (appendix 11-1/2), as a large fraction of trees between the sites 12-KO-03 and 12-KO-04 was deforested, either by felling during gulag times (personal communication with local people) or by fire (Alexander et al. 2012), and the stands now depict rather a successional state than result of climatic influence.

Several different studies have been conducted at the study sites, to give a detailed overview on vegetation characteristics.

Vegetation Mapping for Pollen Analysis

To get modern pollen analogues of lake sediment pollen data, circles with 10 m radius were set up. Vegetation density was then estimated in 0.5 m steps on the first 6 m and in 1 m steps for the rest (Fig. 11-2). From the plot centre, surface layer samples were taken to analyse the pollen amount depending on the surrounding vegetation. These data can later be used to estimate former vegetation densities from lake sediment pollen data.

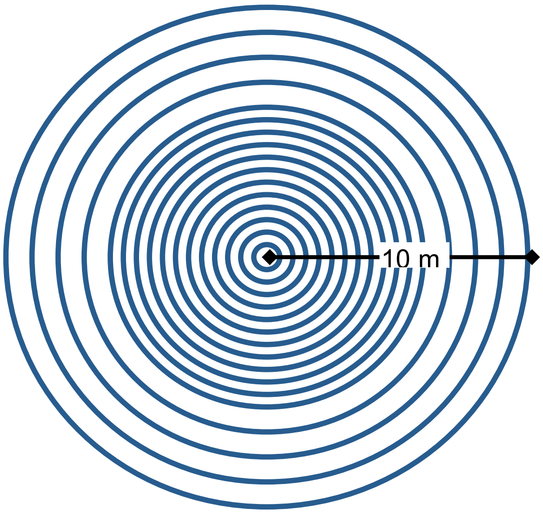

Fig.11-2 Scheme for vegetation mapping

Forest Ecology and Genetics

To analyse recent stand structure, plots of at least 250 m² in size were set up. Within these plots, individual properties of each tree were recorded, which comprise height, basal diameter, diameter at breast height, amount of cones (0, <10, <50 or >50), crown diameter and position in plot. Furthermore, we collected material (needles if accessible, otherwise bark and twigs) for further DNA analysis and cones of some trees to count the number of seeds per cone (appendix 11-4). Individuals were divided into three size classes, namely trees (≥ 200 cm), saplings (40-200 cm) and seedlings (≤ 40 cm). Of each size class we collected at least 10 cores or discs from basal and (if available) also from breast height. Moreover, each plot was divided in to 2x2 m² subplots in which vegetation density of understorey vegetation was estimated and active layer depth measured.

In 6-7 of these random subplots, a 50x50 cm² levelled out grid was installed in which a detailed analysis on establishment success of *Larix* seedlings was conducted. For each of these subplots, more general information were gathered, such as densities of trees, shrubs, lichens, mosses, litter and dead wood material and the distance to the next larch tree. In order to capture the micro-relief, surface coverage (i.e. grass, moss, lichen, litter, water), distances between grid to surface layer and mineral soil were determined in 10 cm steps at the nodes and active layer depth at the corners and in the centre of the grid was measured. Additionally, grid soil depth measurements for the whole grid were carried out 14 times. For each seedling, its position, distance to the nearest tree, estimated age (one of the following classes: establishment this year/‘at least last year but still young’/old), height above surface layer and number of living and dead needles were recorded and then sampled for genetic analysis.

Dendrochronology

With the help of cores taken from living and dead trees at each site (appendix 11-3), growth curves and a tree-ring chronology for the region will be created. An overview on the work done at each site is presented in Tab. 11-1.

Tab. 11-1 Overview on investigations and samples of the different sites

	12-KO-01	12-KO-02/I	12-KO-02/II	12-KO-03/I	12-KO-03/II	12-KO-04/I	12-KO-04/II	12-KO-05
Size forest plot		20x20 m²	14x20m²	16x20m²	16x16m²	20x26m²	20x20m²	0.9 km²
Establishment success (No. of grids)		✓(6)	✓(7)	✓(7)	✓(6)	✓(7)	✓(7)	
Discs/Cores (No. of trees/saplings)			✓(10/9)	✓(16/12)		✓(10/10)	✓(11/10)	✓(12/0)
Circle (r=10 m)	✓				✓			
Dendrochronology	✓	✓	✓	✓	✓	✓	✓	✓
Material for DNA analyses			✓	✓	✓	✓	✓	✓

11.3. 12-KO-01 (68.30° N, 161.24° E; 18th July 2012)

At this site, we stayed for one and a half day and conducted vegetation mapping for pollen analysis in one 10 m circle and collected cores of some trees for dendrochronological analyses.

12-KO-01 is situated near the confluence of the rivers Viska Osetrovka and Maly Anyuy and surrounded by three small lakes. It lies on a hilltop within a small forest patch with lots of offspring. Crown cover is rather light. It was disturbed, containing a high amount of dead wood and signs of fire. In the shrub vegetation we found only *Salix* spp. No bare soil was visible, as everything was covered by vegetation and needles.

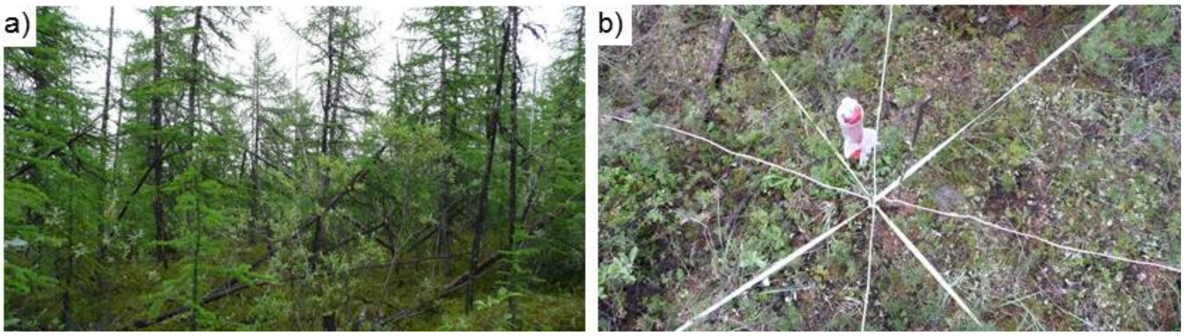

Fig.11-3 Study site 12-KO-01, visited at July 18, 2012 with (a) view of forest and dead wood, (b) ground cover with lines for the circle

Main ground cover consists of different species of moss and lichens, common dwarf shrubs are e.g. *Ledum palustre* L., *Vaccinium vitis-idaea* L. and *Arctous sp.*, the herbaceous vegetation consists of Poaceae and *Pyrola rotundifolia* L. Trees are only represented by *Larix cajanderi* Mayr. Active layer depth in the circle centre was 56 cm.

11.4. 12-KO-02 (68.39° N, 161.47° E; 20th-24th July 2012)

At the second site we had a stay for five full days and wanted to record two full forest plots plus an additional 50x50 m² plot for a detailed sampling of genetic material. Due to the visit of a bear with cub on the other river side and a cold snap with snow, we finished only one and a half forest plot. Furthermore, dendrochronological sampling was conducted on selected trees.

Site **12-KO-02/I** (Fig. 11-4) is situated near a brim of the river Protoka Malchikovskaja. It is surrounded by dense *Alnus fruticosa* Rupr. and *Salix* spp. patches. The plot area was flat, with only a slight gradient with north-northeast aspect. The site seemed to be disturbed, with many bended trees. The forest was rather dense, with only few offspring (13 saplings, 79 seedlings). The forest patch was young with maximum age of about 60 years. Mean tree height is 7.70 m.

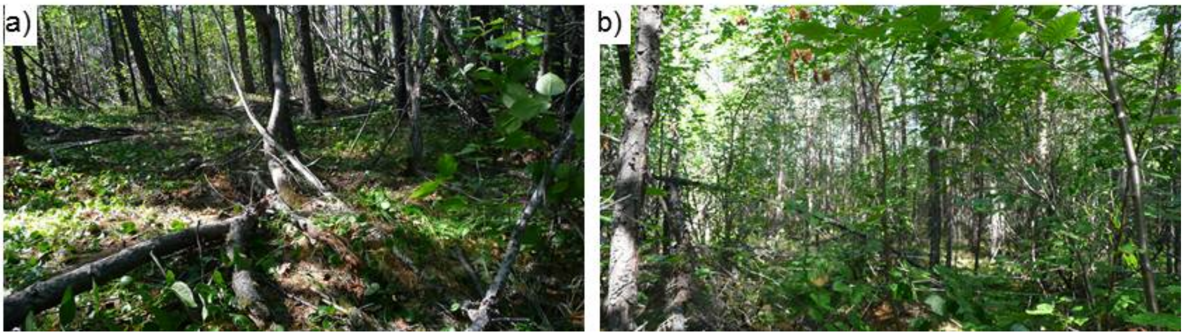

Fig. 11-4 Study site 12-KO-02/I, visited at July 20/21, 2012 with (a) ground cover, (b) view of forest patch

Understorey vegetation is dominated by *Alnus fruticosa* Rupr., up to 6 m high, while ground is mainly covered by needles, with only few mosses and lichens. We found only few dwarf shrubs (e.g. *Vaccinium uliginosum* L.), herbaceous vegetation consists mainly of *Pyrola rotundifolia* L. The ground had almost no relief and seemed to be very cold.

To study stand structure of *L. cajanderi*, a 20x20 m² plot divided into 100 subplots was established in which we recorded every tree and sapling, estimated vegetation density and measured active layer depth. As seedling search is rather time consuming, we searched them only in half of the area. Furthermore, six 50x50 cm² grids for research of establishment success were installed (see Tab. 11-1).

Site **12-KO-02/II** (Fig. 11-5) is situated on the opposite site of the river. It was established on a hilltop with slight eastern aspect. In contrast to site 12-KO-02/I, this one was quite dry, with a pronounced micro-relief. The forest patch has a light crown cover and slightly more offspring (63 saplings and 67 seedlings) than 12-KO-02/I. Mean tree height is 5.50 m. Ground cover was dominated by different species of lichens with only few mosses. The shrub layer had only very few individuals of *Salix* spp., dwarf shrub community consisted of e.g. *Ledum palustre* L., *Betula nana* L., *Empetrum nigrum* L. and *Vaccinium uliginosum* L., while in the herbaceous layer species like *Equisetum* spp., *Eriophorum* spp. and *Stellaria* spp. were present.

Due to rain and snowfall, we were only able to study stand structure on a 14x20 m² plot, searched for seedlings on 10x20 m² and made seven 50x50 cm² grids. We sampled material for genetic analyses of every individual in the plot and collected discs/cores and if available cones of 10 trees and 9 saplings (see Tab. 11-1).

11.5. 12-KO-03 (68.39° N, 161.46° E; 26th-30th July 2012)

At the third site we had our next stay for 5 full days and we recorded two forest plots, one circle for vegetation mapping and conducted dendrochronological sampling on selected trees. In this area, complete forests from big to small trees were cleared about 60 years ago. Thus, the actual vegetation represents the succession of *L. cajanderi* in the treeline ecotone without intraspecific competition in the first years. Both sites are situated between a second river named Viska Osetrovka, too, and an unnamed creek.

Fig. 11-5 Study site 12-KO-02/II, visited at July 22-24, 2012 with (a) view of ground cover and *L. cajanderi* seedlings, (b) view of forest, (c) ground cover with snow and grid

Site **12-KO-03/I** (Fig. 11-6) is situated on a hilltop with light northern aspect. The forest is very dense, with thin, fast growing trees with a mean height of 6.10 m. We found 29 saplings and 104 seedlings. Understorey vegetation includes *Salix* spp. up to 5 m, on the ground we found and lots of needles and mosses. Beside these, only little vegetation cover was present, consisting of e.g. *Empetrum nigrum* L., *Ledum palustre* L., *Vaccinium vitis-idaea* L., *Pyrola rotundifolia* L., Poaceae and *Chamaenerion angustifolium* (L.) Schur.

Due to the high amount of trees and saplings (up to 20 individuals on 4 m²) we were only able to finish a 16x20 m² plot. We searched for seedlings on 10x20 m² and made seven 50x50 cm² grids. We sampled material for genetic analyses of every individual in the plot and collected discs/cores and if available cones of 16 trees and 12 saplings (see Tab. 11-1).

Site **12-KO-03/II** (Fig. 11-7) is very similar to 12-KO-03/I and is situated on a hilltop with light northern aspect. It is surrounded by patches of dense *Salix* spp. cover. The forest is dense, with thin, fast growing trees (mean height 6.00 m) and we found 15 saplings and 68 seedlings. Understorey vegetation consists of *Salix* spp. up to 5 m, and lots of needles and mosses on the ground. Beside these, only little vegetation cover was present, consisting of e.g. *Empetrum nigrum* L., *Ledum palustre* L., *Vaccinium vitis-idaea* L., *Pyrola rotundifolia* L. and Poaceae.

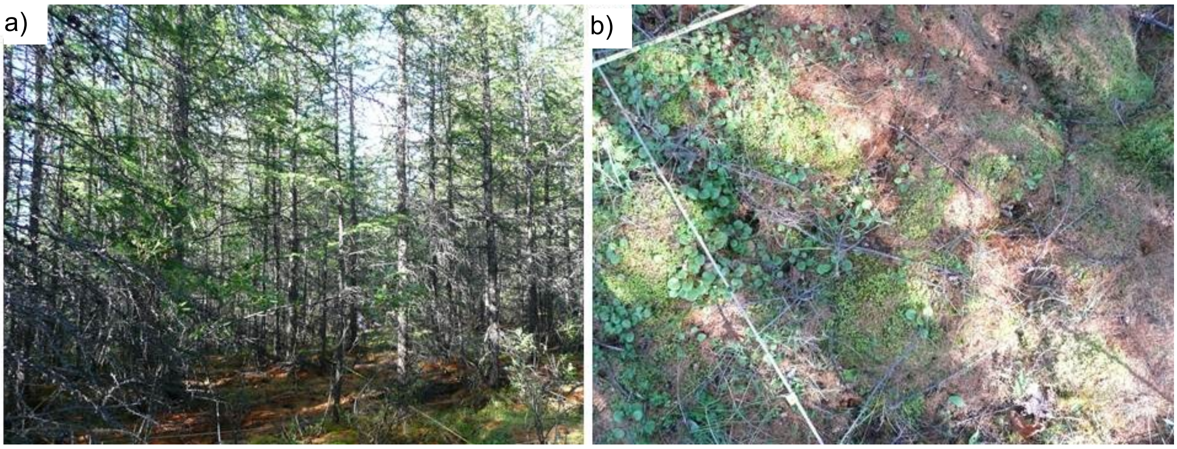

Fig.11-6 Study site 12-KO-03/I, visited at July 26-28, 2012 with (a) view of forest, (b) ground cover

Here we only installed a 16x16 m² plot for analysis of stand structure, due to the high amount of *L. cajanderi* individuals and searched seedlings on 8x16 m². Six 50x50 cm² grids for research of establishment success were installed. We sampled material for genetic analyses of every individual in the plot and collected discs and if available cones of 16 trees and 12 saplings. Furthermore, a circle for vegetation mapping with 10 m radius was installed, with both plots having the same centre.

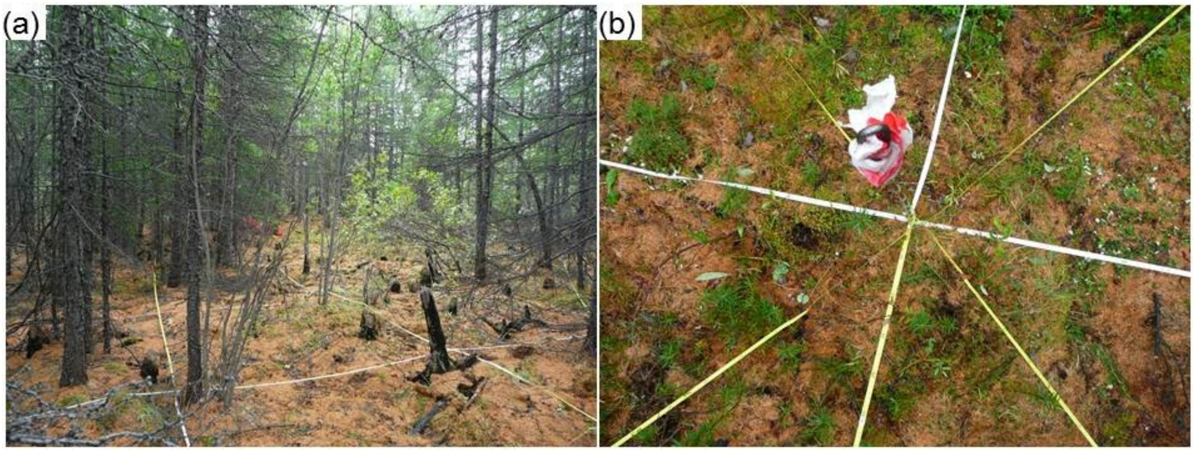

Fig. 11-7 Study site 12-KO-03/II, visited at July 29/30, 2012 with (a) view of forest with tree stumps, (b) ground cover with circle lines

11.6. 12-KO-04 (69.05° N, 161.23° E; 4th-10th August 2012)

At the fourth site, to which we made day trips from Pokhodsk, we recorded two full forest plots and took dendrochronological samples of selected trees. Both plots were situated on a floodplain between two arms of the Kolyma River (Pokhodskaya Kolyma and Kamennaya Kolyma). Also here we found signs of wood cutting; yet some trees seem to be older than 60 years.

Site **12-KO-4/I** (Fig. 11-8) was a wet plot with trees growing only on drier places. Trees looked much healthier than those on the previous sites; however they were smaller (mean tree height 3.37 m) and had less very small offspring (67 saplings and 33 seedlings). Understorey vegetation is dominated by mosses, *Carex* spp. and *Ledum palustre* L. We furthermore found species like *Alnus fruticosa* L., *Vaccinium vitis-idaea* L. and *Eriophorum* spp.

At this site we recorded all size classes of *L. cajanderi* on 20x26 m² but estimated vegetation densities only on 20x20 m². Seven 50x50 cm² grids were installed. We sampled material for genetic analyses of every individual in the plot and collected discs/cores and if available cones of 10 trees and 10 saplings (see Tab. 11-1).

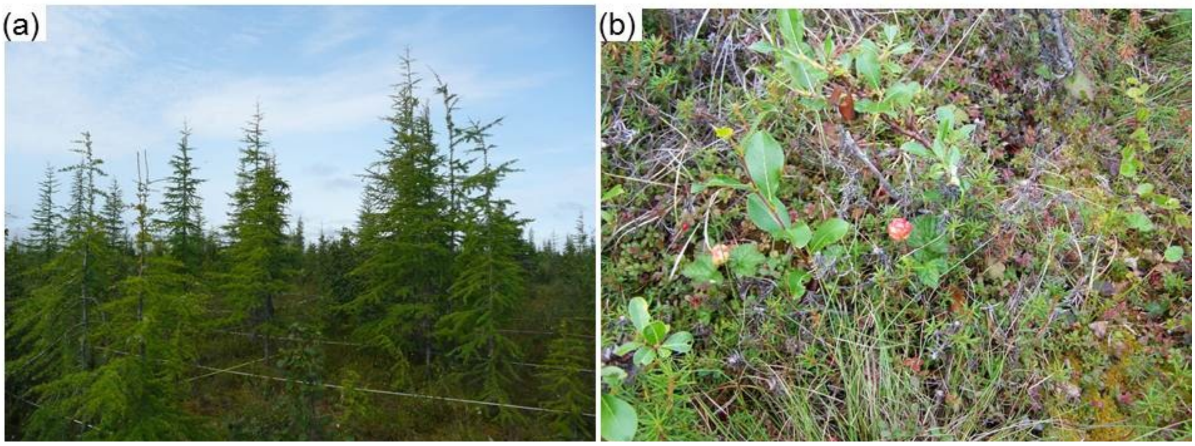

Fig.11-8 Study site 12-KO-04/I, visited at August 4/6, 2012 with (a) view of forest, (b) ground cover

Site **12-KO-04/II** (Fig. 11-9) was slightly more north and had even less trees (with mean height 3.59 m) and less offspring (28 saplings, 9 seedlings). On dead stumps we found signs of fire, but not on living trees. Understorey vegetation is similar to that of 12-KO-04/I, but the site seemed to be a little wetter.

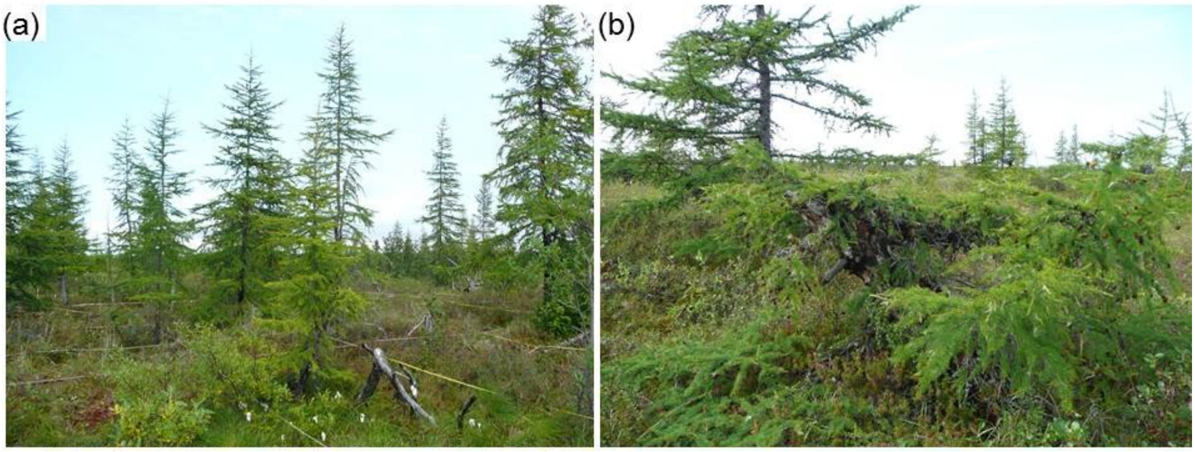

Fig. 11-9 Study site 12-KO-04/II, visited at August 7-10, 2012 with (a) view of forest patch, (b) re-sprouted stump

We recorded all size classes of *L. cajanderi* on 20x20 m² and made seven 50x50 cm² grids. We sampled material for genetic analyses of every individual in the plot and collected discs/cores and if available cones of 11 trees and 10 saplings (see Tab. 11-1). As we did not have many individuals in the plot, we extended the area for sampling material for genetic analyses to approximately 100x80 m² in which we measured and sampled all individuals we found.

11.7. 12-KO-05 (69.12° N, 161.02° E)

We used one full day to record *L. cajanderi* at our last site. 12-KO-05 (Fig. 11-10) is situated near the Pokhodskaya Kolyma. It is a polygon field with *L. cajanderi* growing on the rims. Trees grow very sparse, with only scattered individuals. All in all we found only 47 individuals. Offspring is only found in the near surrounding of older individuals. Apical meristem of $^1/_3$ of all trees is dead, so that their growth is crippled. Vegetation consists of e.g. *Alnus fruticosa* Rupr., *Salix* spp., *Vaccinium uliginosum* L., *Betula nana* L., *Ledum palustre* L., *Carex* spp., *Potentilla palustris (*L.) Scop., *Eriophorum* spp. and of course different species of mosses.

As tree growth is very sparse in this region, we did no set up any plot, but searched about 0.9 km² for trees and measured each individual we found. Vegetation density and active layer depth were measured in 2x2 m² around each individual and furthermore in two squares without *L. cajanderi* near the trees. We took discs/cores from basal and breast height of 12 trees and cones if available and sampled material for genetic analyses of each individual (see Tab. 11-1).

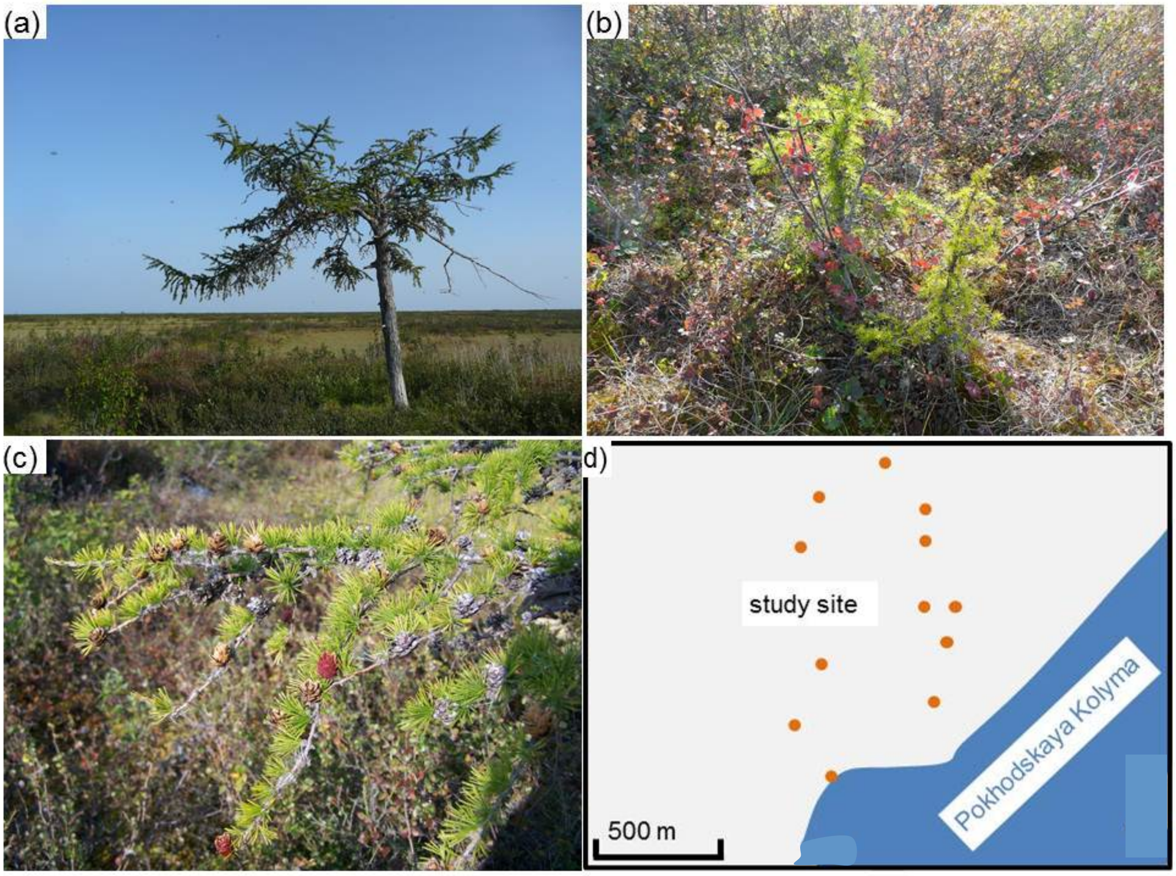

Fig. 11-10 Study site 12-KO-05, visited at August 11, 2012 with (a) view of tree at study site, (b) *Larix* offspring, (c) branch with cones, (d) map of study site near the Kolyma river, dots mark positions of *L. cajanderi* groups or individuals

12. OBSERVATIONS FROM KYTALYK AND ACHCHAGYI ALAIKHA

Lutz Schirrmeister, Andrea Schneider & Vladimir Tumskoy

12.1 Overwinter soil temperature record in a dry polygon

In summer 2011, soil temperature sensors were installed in different depths in the rim (T1) and the center (T2) of a dry low centred polygon in Kytalyk (Schneider and Schirrmeister 2011, Tab. 12-1). Soil temperatures were obtained in 30-minute-intervals in four different depths for both, T1 and T2.

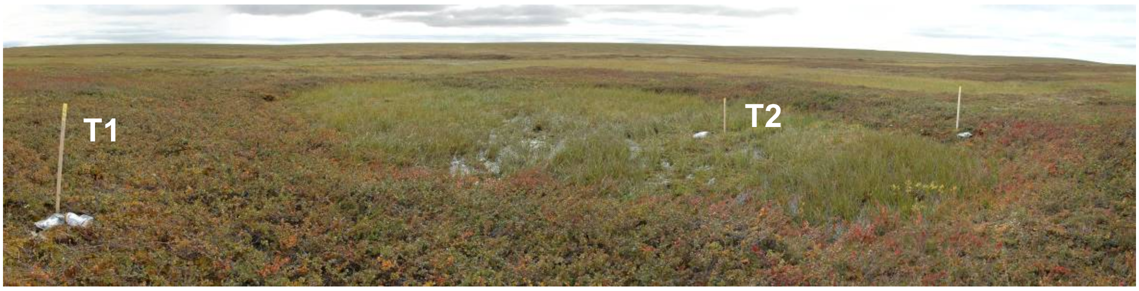

Fig. 12-1: Photographs of the studied low center polygon with the positions of the data loggers.

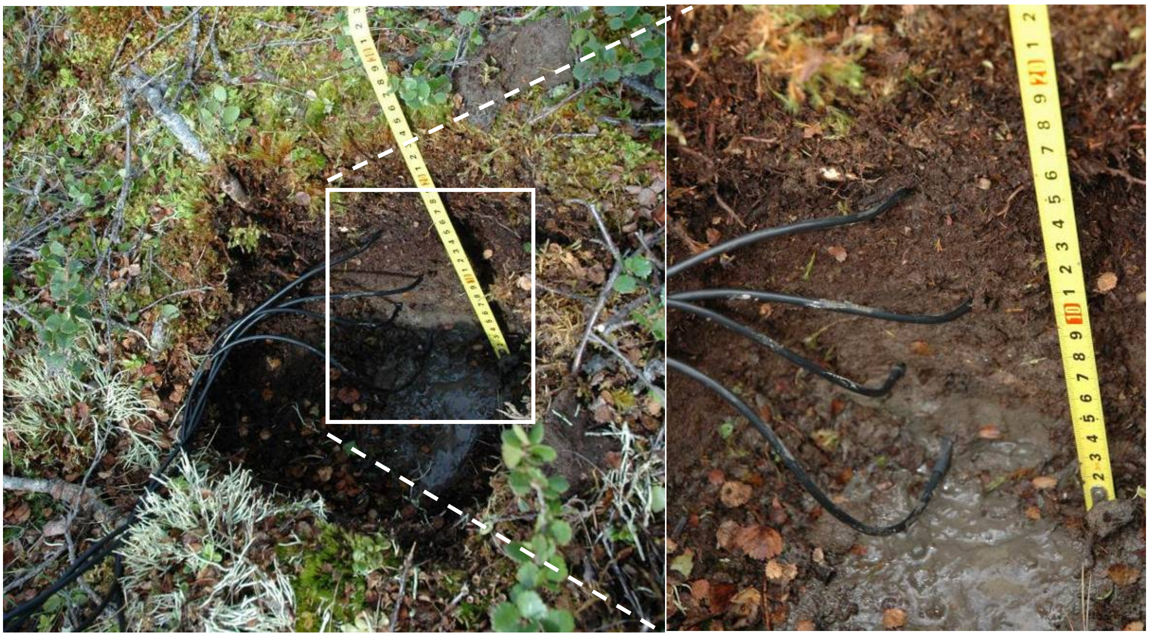

Fig. 12-2: Installation of the ground temperature data sensors in the polygon rim in summer 2011. The sensors were installed shifted against one other with approx. 5 cm height distance between each sensor. We installed the lowest one directly above the permafrost table on 19 July 2011.

Tab. 12-1: Overview about location, logger type and time period of the installed data loggers.

Name	**Location**	**Logger type**	**Measuring period**
Data loggers installed at the dry low-centered polygon:			
Ground temperature (T1)	polygon wall, depth: 5; 10; 15; 20 cm	HOBO Micro Station; HOBO 12-Bit Temperature Smart Sensor	19/07/ 2011 – 04/07/2012
Ground temperature (T2)	polygon centre, depth: 10; 15, 20; 30 cm	HOBO Micro Station, HOBO 12-Bit Temperature Smart Sensor	19/07/ 2011 – 04/07/2012

The data derived from the soil temperature sensors shown in Fig. 12-3 demonstrate that freezing of the soil in both the polygon wall and the depression occurred in late September and October. The polygon rim was freezing earlier than the depression. Freezing of the ground occurred several days after air temperatures went well below 0°C.

Soil temperatures in the polygon rim were about 5 °C lower than in the polygon depression. The minimum temperature in the polygon rim was -26°C and -22°C in the polygon depression. Even in winter the soil temperatures follow variations in air temperature despite being frozen solid. In April and May air temperatures reached 0°C and positive values. The ground started thawing in May. The thawing process was faster than the freezing process and the polygon rim and depression thawed in the same period of time.

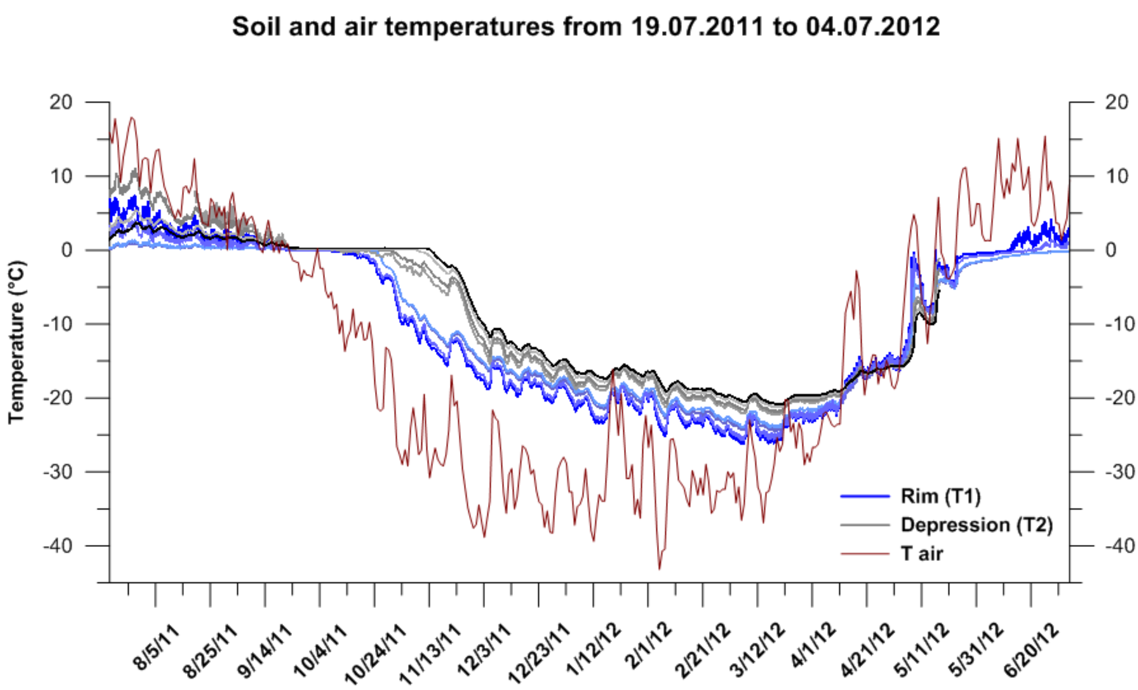

Fig. 12-3: Soil temperature record from the polygon rim and depression from 19 July 2011 until 04 July 2012. Air temperature data are daily means provided by the online climate data base from NCDC/NOAA (http://www.ncdc.noaa.gov/cdo-web/, assessed 13 February 2014).

12.2 Sampling of freshwater ostracods from the monitoring site Kyt-01

Repeated sampling of freshwater ostracods as well as water for hydrochemical analyses from the monitoring site Kyt-01 (Schneider and Schirrmeister 2011, Tab. 12-1) was performed in early July 2012. The ostracod sampling revealed the presence of abundant juvenile Candoninae, 3 – 10 female and 9 male specimens of adult *Fabaeformiscandona pedata*, and 3 – 10 specimens of *Candona muelleri-jakutica*.

Tab. 12-2: Physical properties of the ponds, taxa and number of ostracods caught in Kyt-01 in July 2012.

	Date / Weather	T air °C	T water °C	EC µS/cm	pH	O_2 mg/l	Alkalinity mmol/l	Acidity mmol/l
KYT-1-12-1	04/07/2012 cloudy	11.5	13.1		6.0	11.0	0.4	0.25
KYT-1-12-2	08/07/2012 cloudy	7.9	9.5		6.5	9.6	0.4	0.2

	Water hardness	Water depth cm	Thaw depth pond centre cm	*juv. Candoninae*	*F. pedata* ♀	*F. pedata* ♂	*C. muelleri-jakutica*
KYT-1-12-1	2.5°dH 0.4 mmol/l	30	25	157	10	-	10
KYT-1-12-2	3°dH 0.4 mmol/l	31	28-29	196	3	9	3

12.3 Drill cores around Kytalyk

In early July 2012 five surface drillings (Fig. 12-4, Table 12-3) were performed in Kytalyk with the aim to describe sediment and cryotexture in the active layer and below the frost table. Fours cores were drilled in a drained Alas depression while one drill site (12-KYT-0807-2) was located on the Yedoma in the west of the Kytalyk field station.

Tab. 12-3: List of Permafrost cores in the Kytalyk area with coordinates

Core label	Site description	Coordinates
12-KYT-0507-1	Upper alas level, near the station, no polygon pattern	70.829367° N; 147.483233° E
12-KYT-0607-1	Upper alas level, near the station, no polygon pattern	70.829483°N; 147.48305°E
12-KYT-0607-2	Monitoring Site, dry polygon center	70.83121°N; 147.48299°E
12-KYT-0807-1	Low center polygon with a small pond	70.830783°N; 147.48365°E
12-KYT-0807-2	Surface of the western Yedoma ridge, no polygon pattern	70.826233°N; 147.480483°E

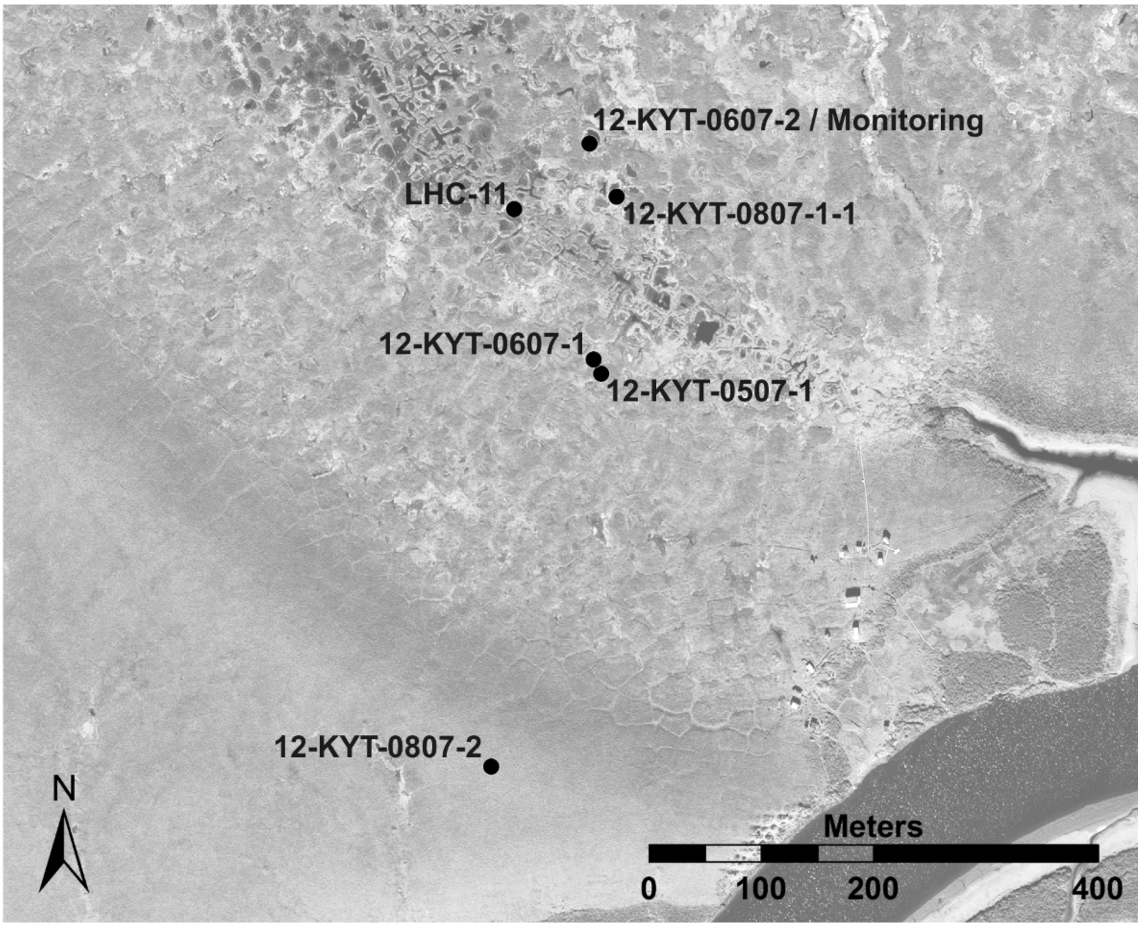

Fig. 12-4: Location of the drill cores around Kytalyk. Map compiled by Mathias Ulrich (Universität Leipzig).

12-KYT-0507-1

Nonpolygonal surface of the upper alas level near the station; covered by moss and some dwarf birch shrubs, a.l.: 15-19 cm.

0-6 cm, peaty loamy silt with near-surface ice lens under the moss; cryotexture: wavy bedded, lens-like, lenses < 1 mm thick.

6-40 cm, bluish and ocher-brown mottled loamy silt with some fine plant detritus and roots of 1 mm in diameter; cryotexture: massive to horizontal lens-like 1-2 mm lenses, at 10-15 cm depth an ice belt of 1-2 cm thickness was composed of vertical 1-2 mm thick ice needles.

40-60 cm, gray loamy silt, without iron oxide spots; cryotexture: predominantly lens-like reticulated, ice lenses 1-3 mm thick, thick ice layer of 1 cm; subvertical ice needles often inclined.

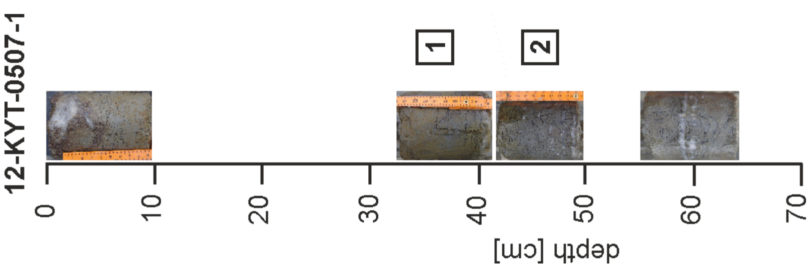

Fig. 12-5: Core 12-KYT-0507-1 with sample positions.

12-KYT-0607-1

16 m northwest of 12-Kyt-0507; a.l.: 28, 31, 28 cm, water between tussocks, vegetation cover - sphagnum and grass, and dwarf birch on little higher elevations.

0-14 cm, modern living sphagnum moss.

14-32 cm, peat moss, brown, melted to a depth of 30 cm.

32-41 cm, gray silty fine-sand, peat inclusions and peaty fragments, thin roots, cryotexture: horizontal micro lens-like, to 35-36 cm depth subvertical ice veins, 0.2-0.2 mm thick.

41-48 cm, dark-brown peat moss, similar to the above, cryotexture: massive

48-67 cm, homogeneous gray silty fine-sand, cryotexture: reticulated: long vertical ice lenses of 1-2 mm thickness, horizontal lenses 1 to 2 mm thick, concave bent, bottom ice lens of 5 mm thickness

67-72 cm, peat moss layer with massive cryotexture and rare ice lenses.

72-98 cm, gray silty fine-sand with brownish peat inclusions, cryotexture: horizontal ice belts of about 1 cm thickness at 74-75 cm, 82-83 cm, 89 cm, 91 cm, and 96.5-98 cm depth, transparent ice belts contain numerous vertical needle-like air bubbles. cryotexture between the belts: net-like, vertical and subvertical ice lenses of 1-2 mm thickness, horizontal lenses about 1 mm thick, sediment blocks horizontally elongated, size: 1 to 1, 0.5 to 1 cm.

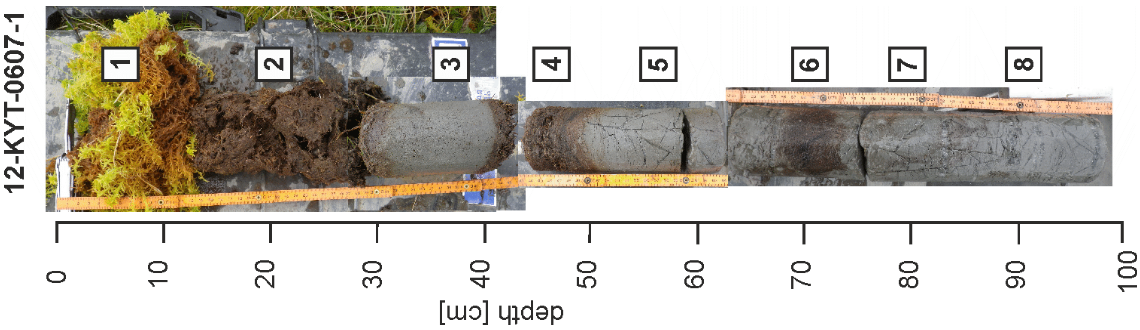

Fig. 12-6: Core 12-KYT-0607-1 with sample positions.

12-KYT-0607-2

Upper alas level, boggy low-center polygon at the monitoring site (Fig. 12-1); a.l.: 25 cm

0-20 cm, modern moss cover.

20-35 cm, moss peat, brown, weakly decomposed, to 27 cm depth thawed, cryotexture: layered, ice lenses 2-3 mm thick, rarely porphyritic inclusion of 1 mm size.

35-61 cm, silty loam, brownish-gray, cryotexture: reticulated, with 2 mm thick vertical and subvertical ice lenses and 1-2 mm thick horizontal lenses, which become a little bit thinner downwards.

61-73 cm, peat brown, with birch roots of 2-5 mm diameter, cryotexture: diagonal lens-like, ice lenses 0.5 mm thick, up to 1 mm ice crusts around the roots.

73-112 cm, irregular alternating silty fine-sand with gray streaks and inclusions of peat, roots, cryotexture up to 82 cm depth: oblique and horizontal lens-like, average thickness to 1 mm; individual 5 to 25 mm thick lenses of with transparent ice, containing vertical needle-like air bubbles, massive cryotexture in peat inclusions; below 85 cm depth diagonal net-like cryotexture with subvertical ice veins of up to 3 mm thickness and 1-2 mm thick horizontal veins, and sediment blocks in between from 1-2 to 5-20 mm; at 97-100 and 105-108 cm depth clear ice bands exist containing vertical needle-like air bubbles 0.5-1 mm diameter.

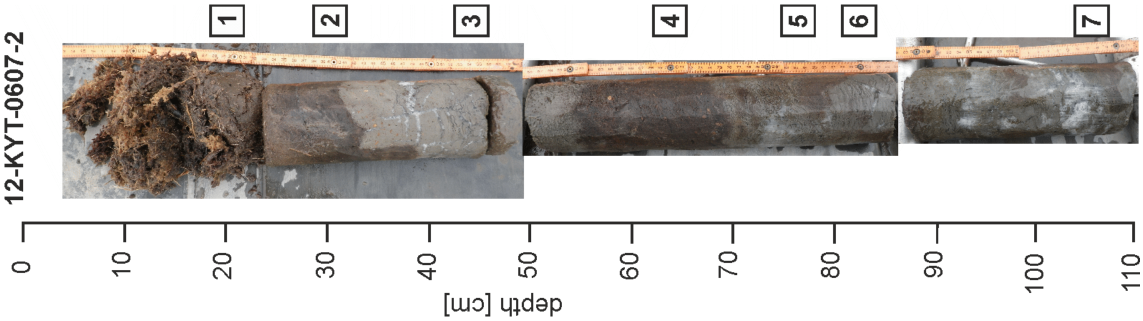

Fig. 12-7: Core 12-KYT-0607-2 with sample positions.

12-KYT-0807-1

Upper alas level, near the monitoring site, low-center polygon, 15-20 m in diameter, with a small grass-covered pond (20-25 cm deep) in the center, free water area 6-7 m; a.l.: 27-30 cm.

0-34 cm, aquatic vegetation and peat, frozen at 31 cm depth.

34-56 cm, homogeneous gray sandy silt, at 39 cm depth shrub roots of 5 mm in diameter, peat inclusion of about 10 cm size in the middle part, cryotexture: gently sloping ice lenses of 2-3 mm thickness in dark peat at 32-33 cm depth, down to 40-43 cm depth lattice-like cryotexture of inclined 2 mm thick ice veins, at 47 cm depth appears thin (0.5 mm) horizontal, slightly concave ice lenses, they gradually are larger and more frequently and have a thickness of 1-2 mm at 52 cm depth.

56-68 cm, gray silty sand with plant inclusions, at 56t-56.8 cm, 59 cm, 63-65 cm, and 67-67.5 depth 3 mm thick ice veins with needle-like air bubbles.

68-95 cm, inclined (30°) dark brown peat layers with gray silt lenses, thick silt interlayer at 85-90 cm depth, plant roots of 2-5 mm in diameter at 70-71 cm depth, cryotexture in peat lenticular-inclined, about 0.5 mm thick ice lenses, ice crusts surrounding the inclusion of twigs, at 87.5 to 89 cm depth a horizontal ice lens of transparent ice with needle-like air bubbles and vertical blades of grass.

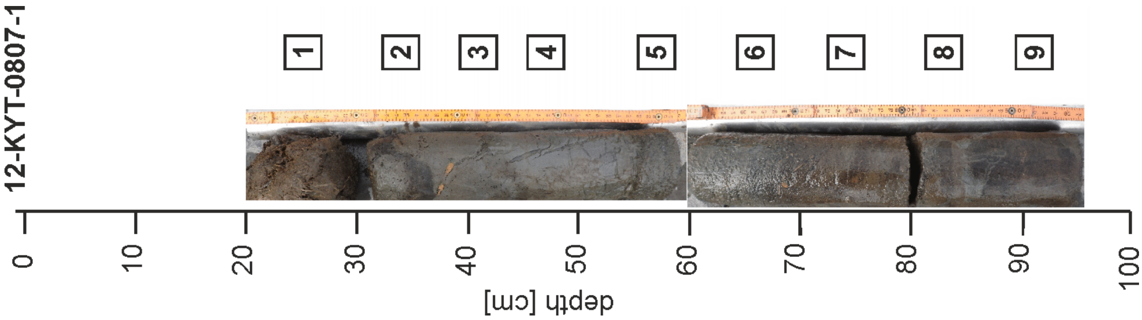

Fig. 12-8: Core 12-KYT-0807-1 with sample positions

12-KYT-0807-2

Hummocky surface of the western Yedoma Ridge near the Kytalyk field station, a.l.: 20 cm on hummocks, 15 cm between.

0-19 cm, modern moss cover with grass and birch shrubs.

19-30 cm, brown peaty silty fine sand. Cryotexture: massive and micro lens-like. at 19 to 25 cm depth inclusions of surface ice, under which extends a gradually narrowing, zigzag-shaped ice vein down to 35 cm depth.

30-41 cm, gray spotty sandy silt with patches of iron oxide, massive cryotexture.

41-49 cm, dark brown peaty silt, cryotexture: diagonal net-like, up to 0.5 mm thick ice veins.

49-66 cm, peaty silt, cryotexture: to 52 cm depth - horizontal net-like, ice veins to 1-3 mm thick, blocks of 2-3 mm thickness in between, from 52 cm depth 1 mm thick vertical ice veins and horizontal ice veins of 0.5 mm thickness each 3 to 5 mm.

66-80 (85) cm, gray loam, cryotexture: horizontal net-like, thickness of ice veins < 0.2 mm, size of sediment blocks 1-2 mm.

80-110 cm, gray silty fine-sand, with a few peat inclusions, cryotexture: horizontal net-like, almost ataxitic, ice veins of 3-8 mm thickness, sediment blocks in between 2-5 mm high.

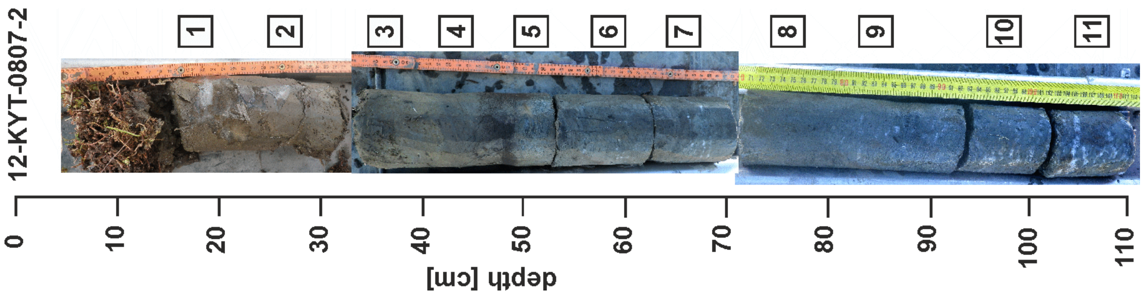

Fig. 12-9: Core 12-KYT-0807-2 with sample positions.

12.4 Achchagyi Allaikha (70.560633°N, 147.44015°E)

Permafrost exposures along the Achchagyi Alleikha River are well known since the sixties of the last century (Lavrushin, 1963, Kaplina et al., 1980). The exposures are considered as a stratigraphic key site for the late Quaternary of the Indigirka lowland und could be used as a reference site for similar stratigraphic profiles studied by the AWI at the lower Kolyma River and on the Bol'shoy Lyakhovsky Island.

The studied outcrop is located at the left bank of the Achchagyi-Allaikha River, a contributory of the Indigirka River about 20 km southwest of the settlement Chokurdakh (Fig. 12-10). The one day field trip at July 10th 2012 was carried out by motorboat from Chokurdakh. The objective was to visit, and to sample characteristic horizon of this Pleistocene key location.

Fig. 12-10: Location of the studied permafrost exposure at the Achchagyi-Allaikha River (google earth map).

According to the recent publication of Nikolskyi et al. (2010) studying mammoth bones along the Achchagyi-Allaikha bank and the cryolithological description of Kaplina et al. (1980), the general stratigrafic profile consists of three, middle to late Pleistocene units overlain by slope deposits. The lower unit (Allaikhovskaya Suite, observed thickness 20-22 m) consist of horizontal and ripple-bedded silty and fine-sand with peaty interlayers of paleosols. The Allaikhovskaya Suite is penetrated by large ice wedge casts composed of fine-grained laminated lacustrine sediments that reaching deeper below the river water level. The sediments in these ice wedge casts (up to 15 m thick) belong to the Achchagyskaya Suite that contains shells of fresh-water mollusc. This unit could be considered perhaps as Eemian (Krest Yuryask Suite) lake deposits. The Achchagyskaya Suite is overlain by the Ice Complex of the Yedoma Suite, which is composed of ice-rich silty fine sand and characterized by large syngenetic ice wedges and ice belts in between. The Yedoma unit contains the mammoth bones studied by Nikolskyi et al. (2010).

Because of difficult outcrop conditions (Fig. 12-11), only the lower part of the exposure 12-AA-1007 up to about 12 m above the river level (a.r.l) was accessible and could be studied and sampled in detail (Appendix xxx). In the lower part that belongs to the Allaikhovskaya Suite a 2-3 m wide ice wedge was exposed and sampled (Fig. 12-12). This ice wedge consists of 4 to 5 mm wide vertical ice veins containing numerous circular gas bubbles of 0.2 mm size and contains several small vertical sediment stripes. The wide ice wedge was penetrated by a smaller ice wedge coming from above.

Fig. 12-11: Overview of the studied exposure 12-AA-1007.

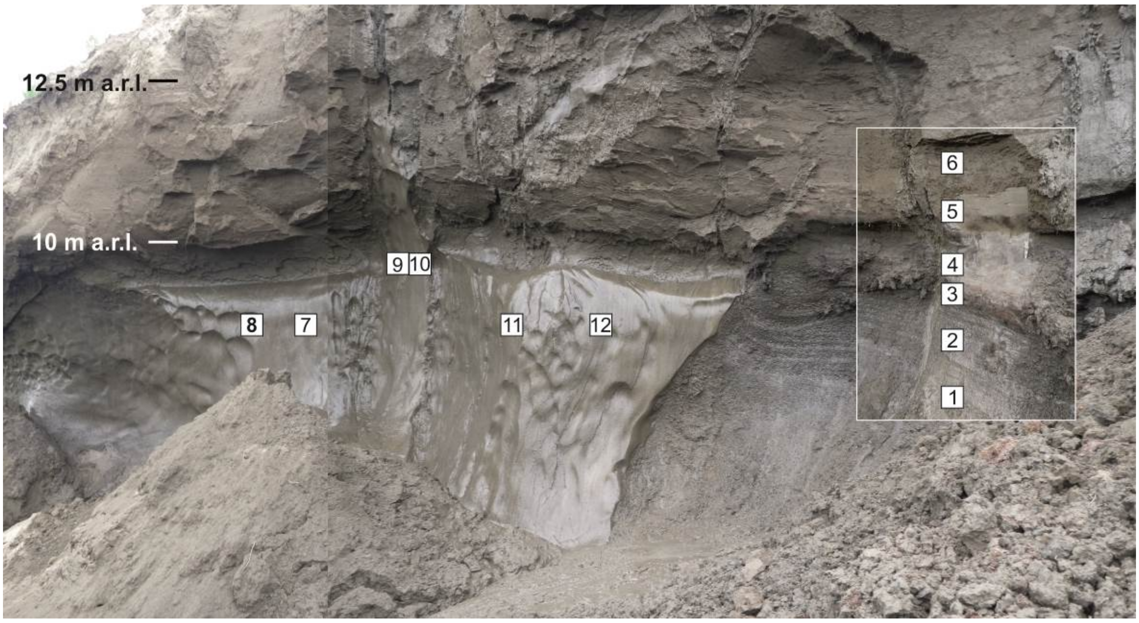

Fig. 12-12: Lowe part of the exposure 12-AA-1007 with sample positions - boundary between Allaikhovskaya Suite and Achchagyskaya Suite.

Between the ice wedges ice-rich columns of brownish-grey silty fine-sand (loam) were observed. In addition, 5 to 8 cm thick ice belts occurred in a distance of 20 to 30 cm that bent upwards to the ice wedge. The cryotexture was dominantly net-like or ataxitic.

A short sediment profile that covers the transition from the Allaikhovskaya Suite to the Achchagyskaya Suite was sampled between 8 and 10.7 m a.r.l (Fig. 12-12). The boundary between both suites is probably represented by a buried paleo active layer, which ice traceable at about 10 m a.r.l. along the river bank.

Profile description (Fig. 12-12, right):

8-8.5 m a.r.l., silty clayish fine-sand (loam), ocher and gray, contact zone to the ice wedge left of the sampled profile. Cryotexture: net-like, ice veins 1 mm thick, sediment blocks 1×1 to 1×2 cm.

8.5-9.6 m a.r.l., silty loam, brownish-gray, peat inclusions up to 5 × 10 cm. not modified by the ice wedge contact, cryotexture: horizontal layered, distance between ice bands 5-8 cm, transition to ataxitic cryotexture.

9.6 - 10.4 m. buried paleo active layer, subdivided in 4sublayer:

- 9.6-9.8 a.r.l., numerous peat, inclusions (5-10 cm) suspended in brownish-grey loam, cryotexture: massive in peat, net-like in loam -, ice veins 1-2 mm thick, sediment blocks 0.5-1 cm, high ice content in the loamy part.
- 9.8-10.0 m a.r.l., ocher-brown silty loam, peaty, cryotexture: horizontal layered sometimes net-like, ice veins 1-2 mm, distance between ice veins- < 5 mm.
- 10.0-10.15 m. a.r.l., brown peaty loam, cryotexture: horizontal fine lens-like.
- 10.15-10.4 m a.r.l., ocher-brown (up to 10.3 m) silty loam, higher: brown cryoturbated peaty loam, sharp gently undulating contact with the overlying sediments.

Parts of the buried paleo active layer horizon covering the wide ice wedges did not contain peaty inclusions. Its thickness was here reduced to about 40 cm. The upwards following deposits, located above the buried paleo active layer, have a visible thickness of 7-8 m and were studied in a second profile (Fig. 12-13). The sediment is characterized by light-brown fine bedded silty fine-sand containing numerous thin and about 10 cm long grass roots often vertical oriented. Flat peat fragments of several centimeter lengths are visible. In about 11.7 m a.r.l. a horizon with bluish-grey patches (3 cm in diameter) was observed. Besides of single vertical ice veins (up to 70 cm long) the cryotexture was massive. In general, sediment and ice structure remembers the Kuchchugui Suite studied at the south coast of Bol’shoy Lyakhovsky Island (Tumskoy 2012).

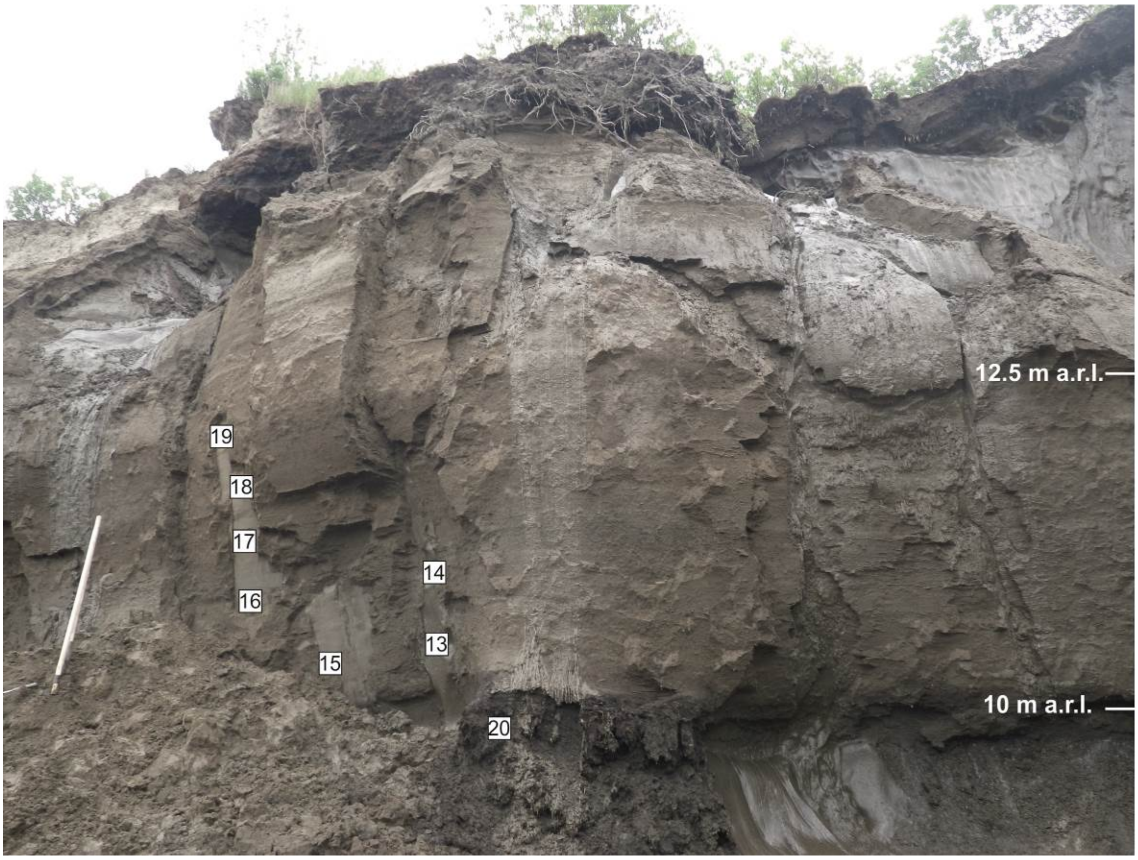

Fig. 12-13: Upper part of the exposure 12-AA-1007 with sample positions – the Achchagyskaya Suite.

13. STUDIES OF THE MONITORING SITES POK 1 IN 2013

Sebastian Wetterich & Lutz Schirrmeister

The monitoring site POK-01 (69.09510°N, 160.93877°E, Figs. 13-1) installed during the summer 2012 (see chapter 3) was again visited two times at July 20th and 29th in order to control and read the Hobo data logger and to sample bottom sediment, water, ostracodes, macrozoobenthos, phyto- and zooplankton and to measure water and air temperature, active layer and water depth.

Fig. 13-1: Photograph of the monitored pond POK-01 at July 29th 2013.

The data logger measuring air temperature, ground temperature and moisture (Tab. 13-1) at the wall of the polygon rim worked very-well and could continue the measurements because of the sufficient battery capacity for the next two years.

Tab. 13-1: Overview about location, logger type and time period of the installed data sensors.

Name	Location	Logger type	Measuring period
(T2) Air temperature	Upper polygon rim, 2 m above ground	HOBO Micro Station, HOBO 12-Bit Temperature Smart Sensor	16.07. 2012 to 29.08. 2013
(T1) Ground temperature	Upper polygon rim, depth: 3; 15; 23; 31 cm	HOBO Micro Station; HOBO 12-Bit Temperature Smart Sensor	17.07. 2012 to 29.08. 2013
(T3) Ground temperature	Upper polygon rim, depth: 25; 50; 75; 95 cm	HOBO Micro Station, HOBO 12-Bit Temperature Smart Sensor	19.07. 2012 to 29.08. 2013
(M1) Soil moisture	Upper polygon rim, depth: 2; 14; 23; 28 cm	HOBO Micro Station, Soil Moisture Smart Sensor	16.07. 2012 to 29.08. 2013

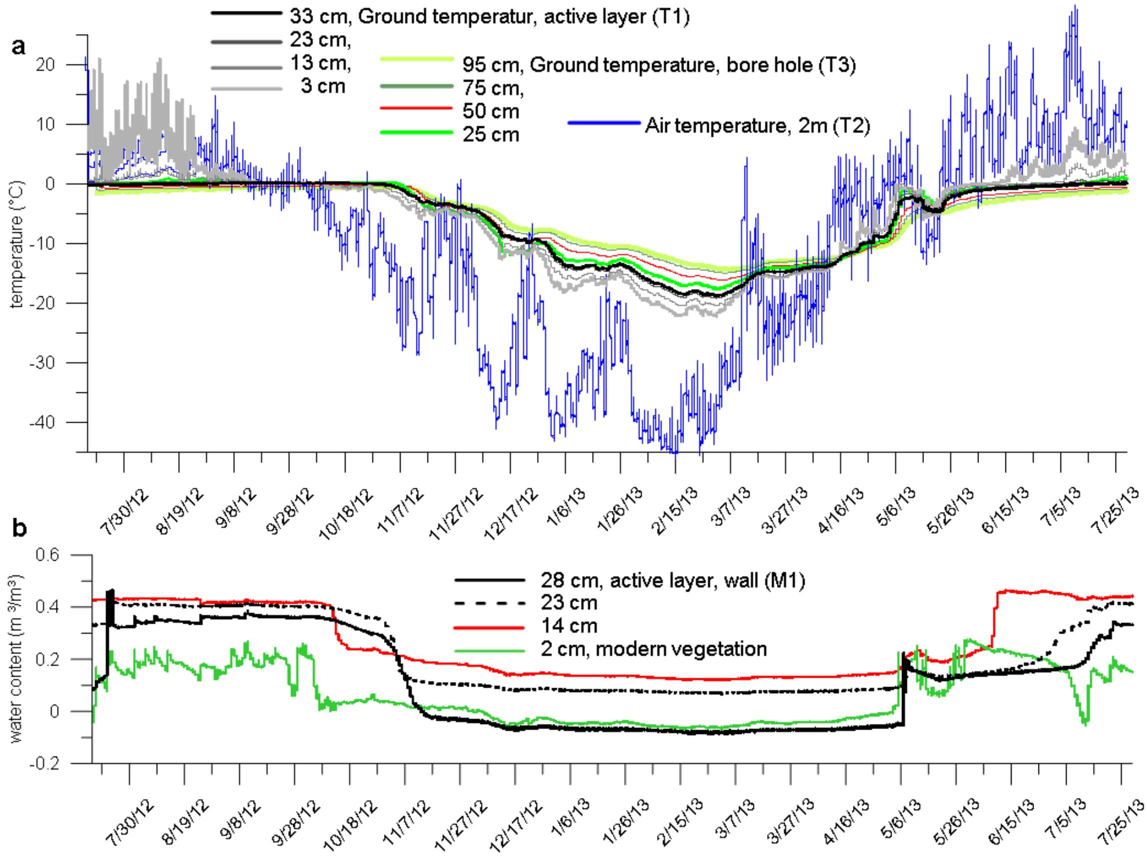

Fig. 13-2: **(a)** Air and ground temperatures, **(b)** soil moisture at the monitoring site POK-01 from July 16th 2012 until July 29th 2013.

The recorded air temperatures from four Hobo sensors (Fig. 13-2a) show an annual mean of -9.7°C with a range of. – 46.9°C and + 29.9°C. The mean annual ground temperature in the bore hole is -5.7°C and -5.8°C in the active layer (Tab. 13-2).

Tab. 13-2: Ground temperature data (annual mean, minimum, maximum) of the polygon wall.

Depth (cm)	**annual mean (°C)**	**Min (°C)**	**Max (°C)**
Active layer (T1)			
3	-5.3	-22.2	20.9
13	-6.1	-20.6	3.5
23	-5.9	-19.3	0.7
33	-5.9	-18.8	0.1
Borehole (T3)			
25	-5.7	-17.9	1.1
50	-5.8	-16.2	0.0
75	-5.6	-15.1	0.0
95	-5.6	-14.4	-0.6

The data derived from the soil moisture sensor M1 (Fig. 13-2c) reflect the freezing and thawing processes during in fall 2012 and spring 2013 respectively. During winter, when the ground was totally frozen, the moisture sensors could not measure.

Ostracods were caught from the western margin of the pond between plants and open water areas. The other samples of macrozoobenthos, zoo- and phytoplankton, of water and bottom sediment were collected in the same area with same approach as described in chapters 3 and 4. The environmental data are comparable to the data sets from the year before (see appendix 2, Tab. A 2-2).

Tab. 13-2: Physico-chemical features of the monitoring site POK 1 measured in 2013.

Date/ sample	**T air (°C)**	**T water (°C)**	**EC (µS/cm)**	**pH (wtw)**	**O_2 (mg/l)**	**Alkalinity (mmol/l)**	**Acidity (mmol/l)**	**Hardness (°dH)**	**Water depth (cm)**	**Thaw depth center (cm)**	**Thaw depth margin (cm)**	**Thaw depth wall (cm)**
20.07.13, 11:00 13POK-01a	11.4	15.3	123.7	7.0	9.0	1.0	0.4	5.0	20	50	40	18 - 35
29.07.13, 12:00 13POK-01a	11.6	16.3	110.6	7.1	10.0	1.2	0.4	5.0	22	55	55	30- 42

14. SAMPLING AND MAPPING OF THE POKHODSKAYA YEDOMA ISLAND IN 2013

Lutz Schirrmeister & Sebastian Wetterich

14.1 Background

Between and 21st and 26th July a small expedition was carried out by motor boat from Pokhodsk to the Pokhodskaya Yedoma Island in the north-western part of the Kolyma Delta. This is one of only three bedrock elevations within the delta with a maximal height of 58 m a.s.l.. According to the geological map (Aulov et al. 1998, Fig. 2-2) the island consists of Lower Cretaceous granodiorite ($\gamma\delta K_1$). The island is surrounded by the flat floodplain landscape of the delta. A small lodge located near the northeastern edge of the island (Fig. 14-1) could be used for housing.

The objectives of this trip were the study of a bedrock Yedoma type and of the covering sediments and to analyze and sample polygonal ponds in the northern Kolyma Delta with the same approach a described in chapter 4. For this reason several walks along the island's coast and across took place.

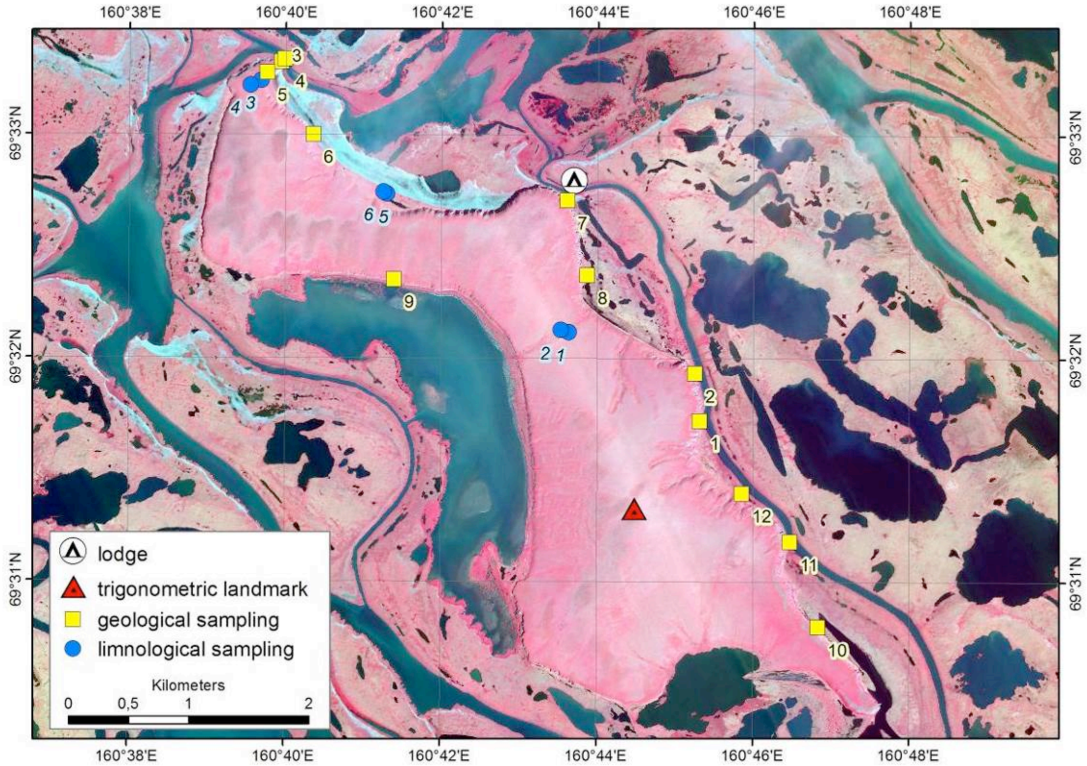

Fig. 14-1: Overview of the Pokhodskaya Yedoma Island with study sites (map compiled by F. Günther, AWI-Potsdam) Pansharpened KOMPSAT-2 satellite image with 1m geometric resolution, acquired on 26 July 2011, and displayed as false color infrared band combination. KOMPSAT-2 data were kindly provided by the European Space Agency (ESA project ID 4133, ESA ADEN, ID 3616)

14.2 Bedrock exposure along the islands coast

In the majority the observed rocky cliffs along the island's coast consist of strongly fissures and spheroidal weathered granodiorite, porphyric granodiorite and granite. In addition, porphyric rocks, aplitic and basaltic dikes crossing the granodiorite were observed (Fig. 14-2). Bedrock exposures were exemplary sampled (Tab. 14-1) in order to collect reference material e.g. for heavy mineral analyses.

Tab. 14-1: Bedrock samples and sample sites from the Pokhodskaya Yedoma.

Sample	Description
A-1, 69.55006667N°, 160.6726167°E	
13Pok-2507-1-05	granodiorite
A-2, 69.54518333°N, 160.7269167°E	
13Pok-2207-1-01	basalt, dark-grey, dense
13Pok-2207-1-02	aplite, grey, biotite inclusions
13Pok-2207-1-03	porphyric granodiorite , large feldspar crystals
A-3, 69.53958333°N 160.7311833°E	
13Pok-2207-1-04	granodiorite, spheroidal weathering
A-6, 69.51335°N, 160.7805833°E	
13Pok-2307-1-01	porphyric granodiorite, strongly weathered with large feldspars
A-8, 69.5197°N, 160.7745833°E	
13Pok-2307-2-01	Basalt, dark-grey, dense
13Pok-2307-2-02	aplite, grey
A-10, 69.52875°N 160.7553°E	
13Pok-2307-3-01	Basalt, dark-grey, dense
A-11, 69.53228333°N, 160.7542333°E	
13Pok-2307-4-01	porphyric granodiorite , large feldspar crystals
A-13, 69.55568333°N, 160.6665333°E	
13Pok-2407-2-01	granite, grey

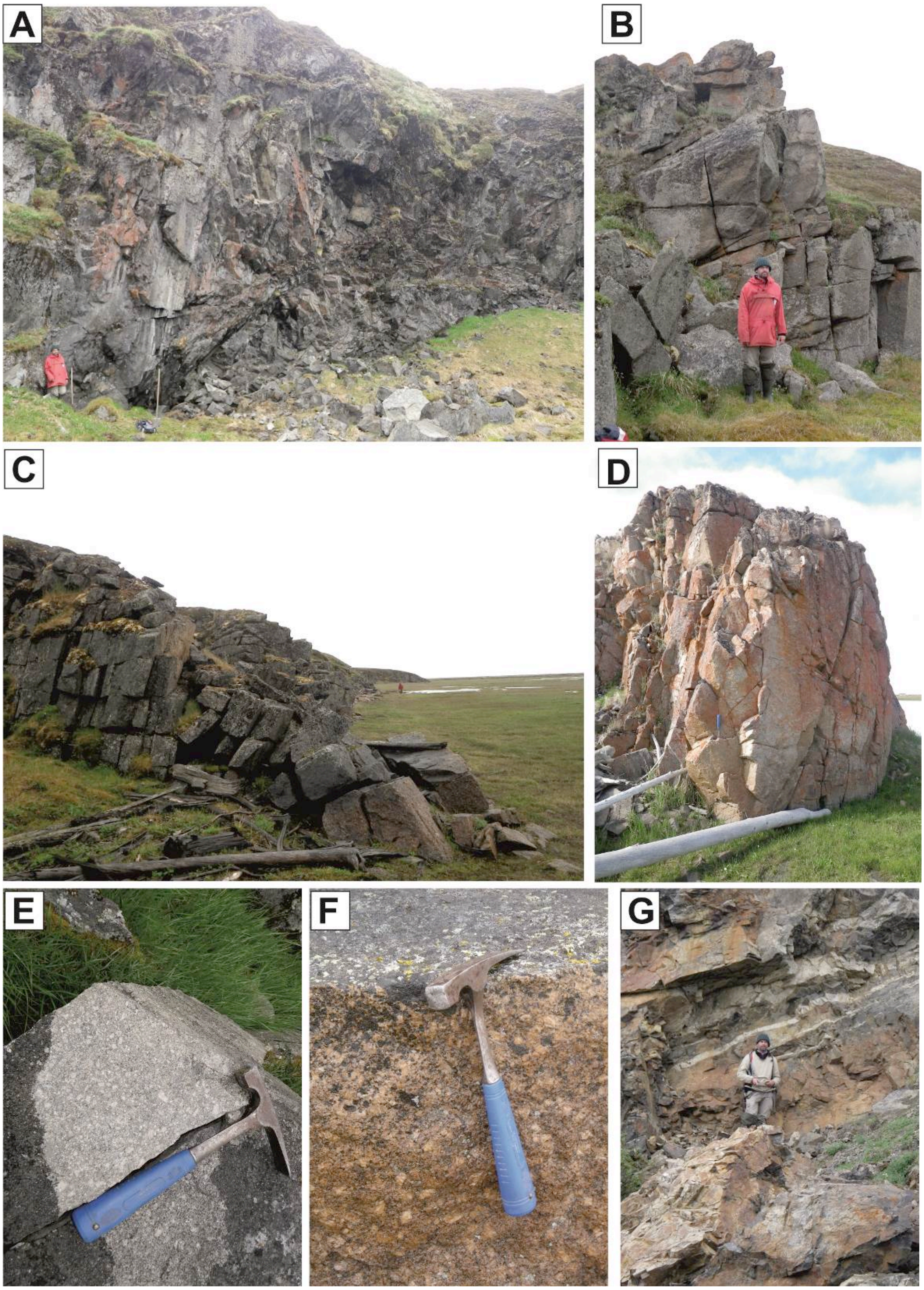

Fig. 14-2: Typical hard rock exposures and structures from the Pokhodskaya Yedoma Island
A – Basalt dike crossing diabase rock (site A-2), B - Granodiorite cliff at the east side of the island (A-3), C – Spheroidal weathering of granodiorite (A-5), D – Granodiorite cliff at the northern edge of the island (A13), E, – Example of large feldspar inclusions in porphyric granodiorite F – weathered granodiorite from the site A5, G - Alternation of light-gray aplite dikes in dark-gray basaltic rocks.

14.3 Cover deposits

Three pits dug in the cover deposits on top of the rocky island were studied and exemplarily sampled (Tab. 14-2) at the northern end of the Pokhodskaya Yedoma.
At the first site 13Pok-2407-1 (Fig. 14-3) was excavated at an erosion edge where the surface was almost free of vegetation. The active layer was about 1.3 m thick and only one frozen sample could be collected below the permafrost table. In general the studied profile consists of brown fine-grained sand and contains a lot of roots remains.

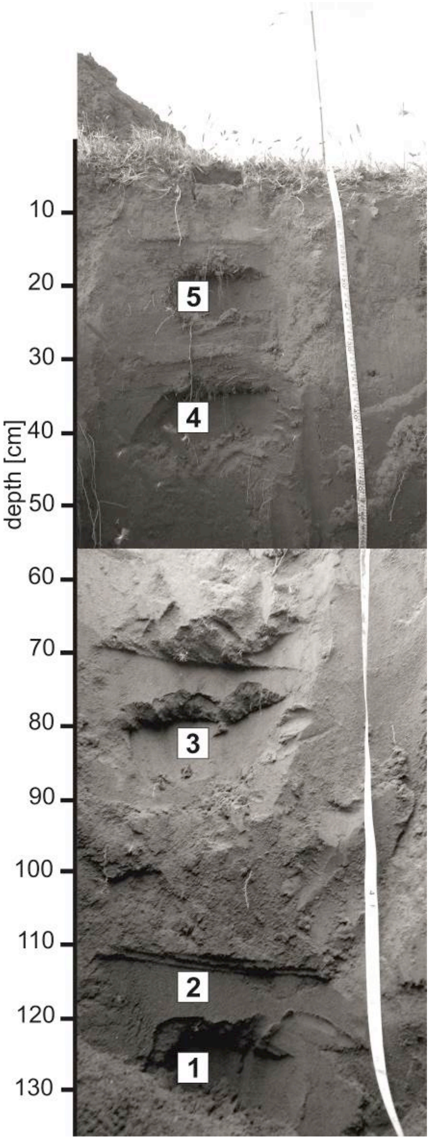

Fig. 14-3: Profile 13POK-2407-1 with sample sites.

Fig. 14-4: Profile 13POK-2407-3 below a modern frost crack with sample sites.

The second profile 13Pok-2407-3 exposed a frost crack that run in E-W-direction (Fig. 14-4) as part of initial polygons (2 to 7m in diameter) shaping the surface. The active layer was 0.3 m thick. One sample of the ice vein, filling the frost crack, was taken and one of frozen fine-grained sand. The third unfrozen sample was from the active layer.

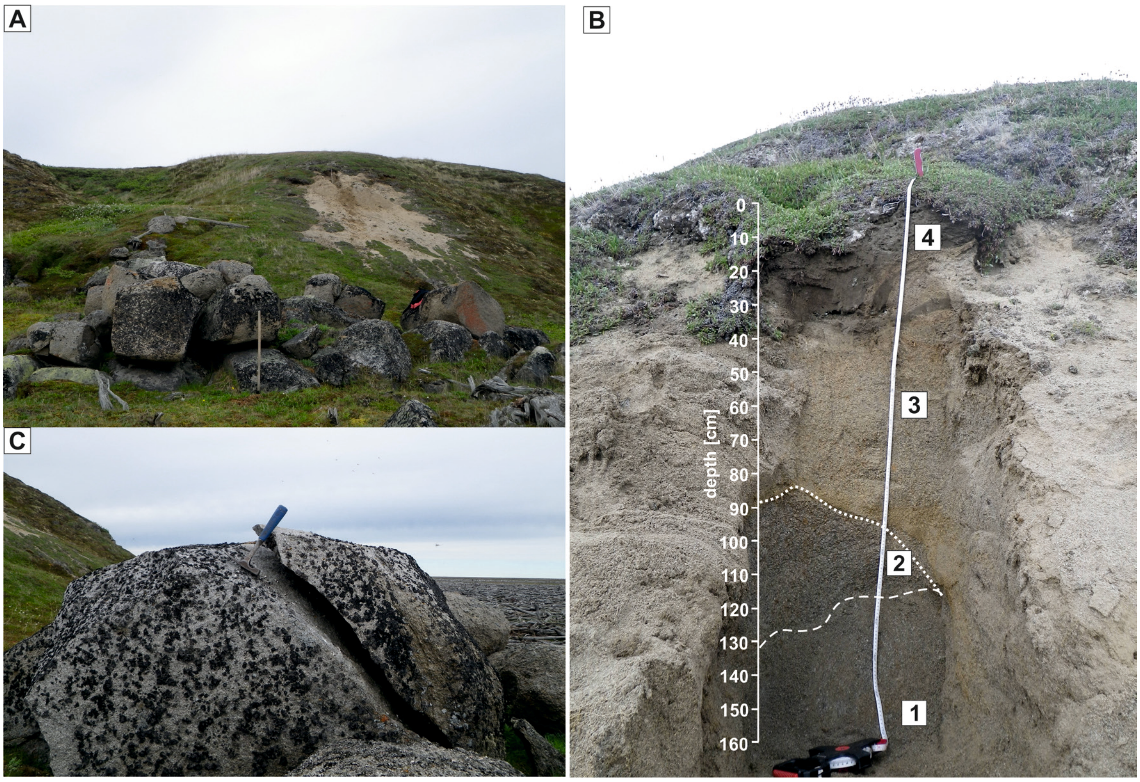

Fig. 14-4: Profile 13POK-2507-1. A-Profile location at the slope above a rock group of spheroidal weathered granodiorite, B- Frost-scattered granodiorite boulder, C-overview of the studied profile with sample positions (the dashed line presents the permafrost table; the dotted line marked the rim of a weathered granodiorite boulder).

The third profile exposed the transition from weathered rock material into sandy deposits. The exposure was located at the eastern slope of the island above a rock group that was spheroidal weathered and frost scattered (Fig. 14-4 A, C). The active layer was 1.4 m thick. The lowermost frozen sample preserved the porphyric structures of the granodiorite with coarse-grained feldspars in a darker matrix. The rock fabric is also visible the unfrozen frost weathered coarse sand below. Further up the material change into light-brown medium to coarse grained sand with yellowish iron-oxide formation at the boundary to the *in situ* weathered material. Diagonal orientated striped of darker and lighter sandy material in the upper part of the exposure reflects solifluction processes at the slope. The uppermost layer of gray-brown fine-sand presents probably an aeolian cover,

Tab. 14-2: Sample list of cover deposits from the Pokhodskaya Yedoma Island

sample	depth (cm b.s.)	cryo-texture	sediment	ice vol. (V%)	ice grav. (wt %)	ice abs. (wt %)
13-POK-2407-1, N 69.55548333		**E 160.6657667°**				
13-POK-2407-1-1	135	massive		31.2	15.7	13.6
13-POK-2407-1-2	120	unfrozen	brown, fine-sand, root remains			
13-POK-2407-1-3	80					
13-POK-2407-1-4	40					
13-POK-2407-1-5	20					
13-POK-2407-1-6	0					
13-POK-2407-3, N 69.55468333		**E 160.6626833°**				
13-POK-2407-3-1	35	ice vein, 2-5 mm				
13-POK-2407-3-2	35	massive	brown, fine-sand, root remains			
13-POK-2407-3-3	15	unfrozen				
13-POK-2507-1, N 69.55006667°		**E 160.6726167°**				
13-POK-2507-1-1	145	frozen	strongly weathered granodorite, rock fabric preserved			
13-POK-2507-1-2	120	unfrozen				
13-POK-2507-1-3	80	unfrozen	light-brown medium to coarse-sand, roots			
13-POK-2507-1-4	10	unfrozen	greyish-brown fine-sand, roots			

14.4 Studies of polygonal ponds

Seven polygon ponds located at the bottom of small valleys or depressions on the Pokhodskaya Yedoma Island as well as in the surrounding flood plain area of the Kolyma Delta were studied and sampled with the same approach as described in chapter 4. The general pond characteristics are presented below and in Tab. 14-3/4.

13POK-02
Date: 23.07.2013 **Type:** Interpolygon pond
Coordinates: 69.53535°N 160,72728333°E
Area: Pokhodskaya Yedoma, valley bottom

Size of the water body: 28.5 x 2-7 m

Water depth: 60 cm

Substrate: organic mud with undecomposed plant fragments

Vegetation
Eriophorum, moss, lichen, betula

13POK-03
Date: 23.07.2013 **Type:** Interpolygon pond
Coordinates: 69,5355°N 160,7256166667°E
Area: Pokhodskaya Yedoma

Size of the water body: 5 x 5 m
Water depth: 40 cm

Substrate: fine decomposed plant detritus with coarser undecomposed plant fragments (leaves, twigs, roots) , moss

Vegetation
Eriophorum, moss, lichen, betula

14POK-04
Date: 24.07.2013 **Type:** Interpolygon pond
Coordinates: 69,5541°N 160.6614667 °E
Area: Pokhodskaya Yedoma

Size of the water body: 22.5 x 11.5 m
Water depth: 40 cm

Substrate: fine decomposed plant detritus with coarser undecomposed plant fragments (leaves, twigs, roots)

Vegetation
Carex, Salix, moss, Rubus chamaemorus

13POK-05
Date: 24.07.2013 **Type:** Interpolygon pond
Coordinates: 69,55375°N 160,65915°E
Area: Pokhodskaya Yedoma

Size of the water body: 8 x 5 m
Water depth: 50 cm

Substrate: fine decomposed plant detritus with coarser undecomposed plant fragments (leaves, twigs, roots)

Vegetation
Carex, salix, Arctophila

13POK-06
Date: 25.07.2013 **Type:** Intrapolygon pond
Coordinates: 69,545633°N, 160,6883833°E
Area: Kolyma floodplain

Size of the water body: 5 x 1.6 m
Water depth: 30 cm

Substrate: fine decomposed plant detritus with coarser undecomposed plant fragments (leaves, twigs, roots)

Vegetation
moss, Carex, Eriophorum

13POK-07
Date: 25.07.2013 **Type:** Intrapolygon pond
Coordinates: 69,5458°N 160,6876833°E
Area: Kolyma floodplain

Size of the water body: 11.3 x 16.5 m
Water depth: 25 cm

Substrate: fine decomposed plant detritus with coarser undecomposed plant fragments (leaves, twigs, roots)

Vegetation: Ranunculus pallasii, Hippuris vulgaris, Salix sp., Betula nana, Ledum palustre, Rubus chamaemorus, Menyanthes trifoliata

15 ICE-WEDGE POLYGON PONDS IN ADVENTDALEN, SVALBARD

Andrea Schneider

15.1 Introduction and Objectives

Svalbard is located in the zone of continuous permafrost (Brown et al. 1998), which is present in valleys and mountains outside the by 60% glaciated area (Humlum et al. 2003). After the Svalbard-Barents-Ice Sheet disappeared and the archipelago was deglaciated around 10 ka BP (Mangerud et al. 1992, Forman et al. 2004), permafrost formed and reached a thickness between 100 m in valleys and 450-500 m in the mountains (Sørbel and Tolgensbakk 2002, Humlum et al. 2003).
Along with pingos, sorted stone circles and rock glaciers, ice-wedge polygons are common periglacial landforms on Svalbard. Ice wedges and ice-wedge polygons have been described mainly in large valleys such as Sassendalen, Reindalen, and Adventdalen (Sørbel and Tolgensbakk 2002). They form in cold climatic environments due to thermal contraction cracking of the underlying ground and belong to the most common morphological features of periglacial patterned ground (e.g. Minke et al. 2007, Muster et al. 2013). In low-gradient terrain where permafrost acts as a hydrological barrier to the deeper ground, and ice wedges create a heterogeneous microrelief, periglacial surface water accumulates in depressions. The formation of different types of ponds in polygon landscapes is connected to the stage of polygon development or degradation (Meyer 2003).
Permafrost is subject to intense studies and documented since beginning of the mining activities in Svalbard in the late 19th century and the first International Polar Year in 1882 (e.g. Humlum et al. 2003) and resulted in long-term observations of ground temperatures (Åkermann 2005) and active layer dynamics (Christiansen and Humlum 2003, Christiansen 2005). Previous studies of of polygonal patterned ground and ice wedges in Adventdalen include geomorphological and sedimentological surveys (e.g. Svensson 1969, 1976, Sørbel and Tolgensbakk 2002, Härtel and Christiansen 2011, Ulrich et al. 2011) to thermal contraction cracking monitoring (e.g. Matsuoka 1999, Christiansen 2005).
However, llittle is known about periglacial surface waters in Adventdalen. Hence, the objective of this field study was to explore the hydrochemical character of periglacial surface waters in lower Adventdalen during the summer season 2013 (July - September), to describe their changes, and to examine their living freshwater ostracod assemblage.

15.2 Site description

Permafrost on Svalbard is estimated to be of late Holocene age in the valleys and the coastal areas (Humlum et al. 2003). Permafrost formation initiated after the last deglaciation and postglacial uplift when large areas became exposed to subaerial temperatures (Humlum et al. 2003, Forman et al. 2004). Consequently, permafrost and periglacial features in the main valleys, such as Adventdalen, and near the present shore are about 3000 years old (Christiansen 2003, Härtel and Christiansen 2011). Sørbel and Tolgensbakk (2002) suggest that ice-wedge polygons in altitudes of more than 500 m a.s.l. may be of pre-Weichselian age and survived earlier glacial periods underneath cold-based glacier ice.
The permafrost temperature on Svalbard is −2.3 °C to −5.6 °C (Christiansen et al. 2010). The permafrost thickness in Adventdalen is estimated to be 20-30 m near the shore to Adventfjorden and increases to <100m upvalley (Humlum et al. 2003) while active-layer thicknesses are around 95–100 cm (Christiansen and Humlum 2003).

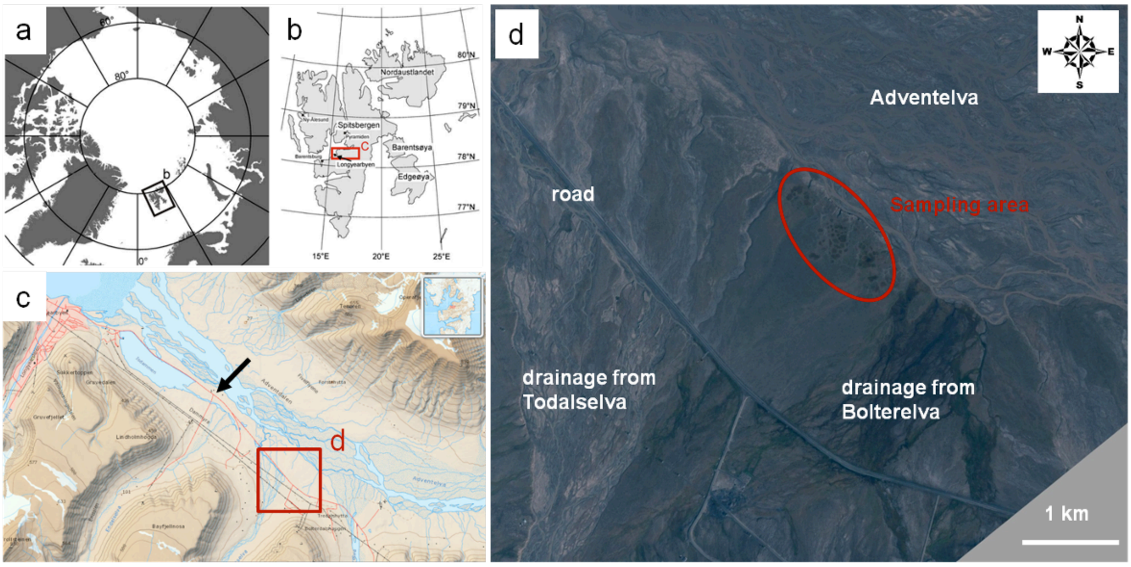

Fig. 15-1: Map of the study area with **(a)** location of the Svalbard Archipelago in the Arctic Ocean, **(b)** Svalbard and its largest island Spitsbergen with the Adventdalen area marked by the red box, **(c)** and **(d)** map/aerial photograph of the Adventdalen valley. The arrow in figure (c) marks the New Adventdalen Weather Station, run by UNIS. Figures (a) and (b) taken from Ulrich et al. 2011, (c) and (d) from TopoSvalbard/Norwegian Polar Institute, 2013.

Adventdalen is a U-shaped glacial valley located in central Spitsbergen, which is the mail island of the Svalbard archipelago, centered on 78° 120´N, 16° 200´E at around 17m a.s.l. (Fig. 15-1). The valley is ~30 km long and ~4 km wide and extends eastward from Adventfjorden where Svalbard's main town Longyearbyen is located. With a mean annual air temperature (MAAT) of -6°C at Longyearbyen Airport and an average of 190 mm of annual precipitation, the Adventdalen area is one of the driest regions on Svalbard (1961-1990; Førland et al. 1997). The MAAT maintains the presence of continuous permafrost with active growing ice wedges (Humlum et al. 2003). Strong channelized winds from the southeast are common in winter, resulting in a thin snow cover in Adventdalen (pers. comm. HH Christiansen, August 2013).

Geologically, Adventdalen is characterized by sedimentary rocks of Early Permian to Eocene age, such as Jurassic and Cretaceous sandstones, siltstones, and shales (Dallmann et al. 2001). Sørbel and Tolgensbakk (2002) observed ice-wedge polygons are typically developed in weathered rocks of Cretaceous age or older, while they are rare in areas underlain by Tertiary rocks (Fig. 15-2). Postglacial marine sediments (Dallmann et al. 2001, Forman et al. 2004) are overlying sedimentary rocks.
The valley floor of lower Adventdalen is covered by fluvial or glaciofluvial sediments with braided river floodplain deposits and terraces (Sørbel and Tolgensbakk 2002). Loess-like aeolian deposits that originate from local deflation and deposition of fine-grained fluvial sediments during dust storms blanket former river terraces (Bryant 1982). The vegetation is dominated by grasses, moss and dwarf shrubs plants (sedge-grass-moss wetland) (CAVM Team 2003).

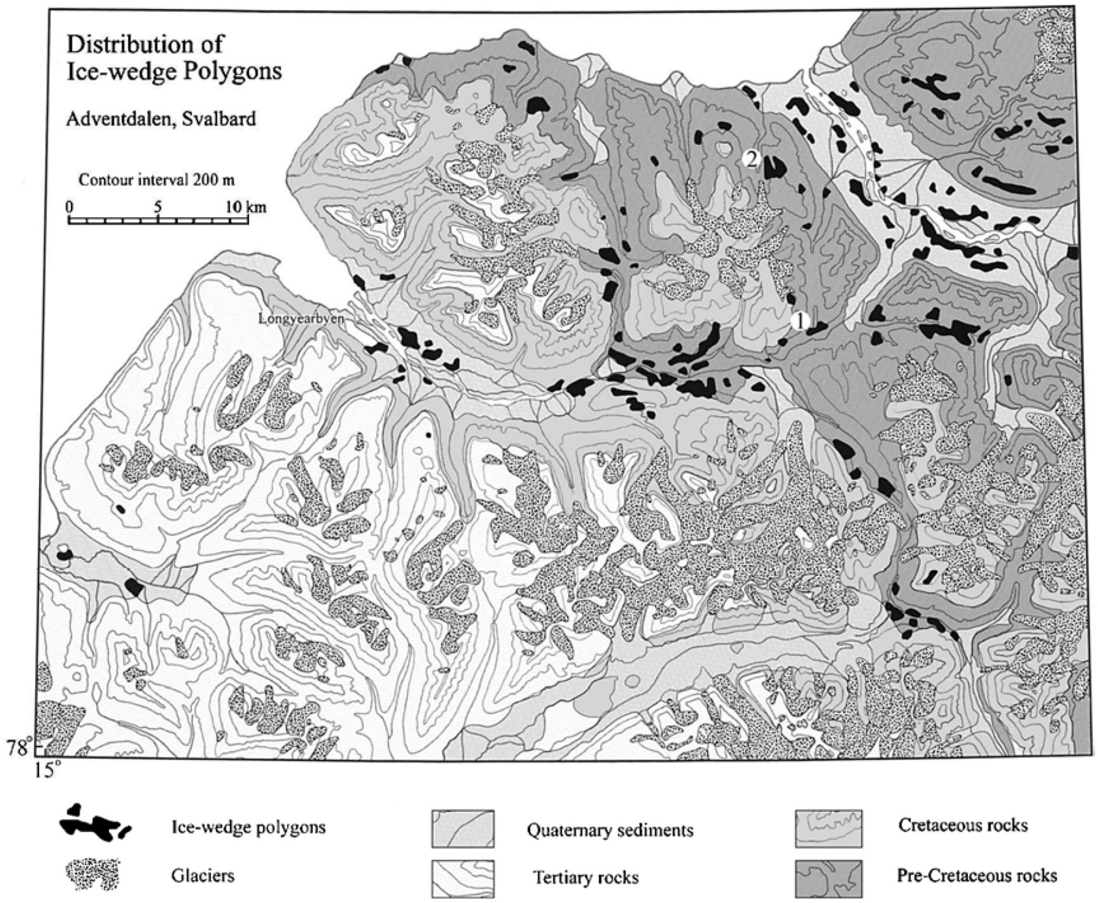

Fig. 15-2 Distribution of ice-wedge polygons and main bedrock ages within the map Adventdalen. Ice-wedge polygons occur especially in the interior Adventdalen. Figure from Sørbel & Tolgensbakk 2002.

Ice-wedge polygons occur in lower Adventdalen (Fig. 15-1a-c) on flat and slightly elevated terrain in front of an inactive alluvial fan located northwest of Bolternosa (Fig. 15-1c-d). The study site is located on the lowermost river terrace approximately 3 – 6 m above the Adventelva river bed within a network of low-centered polygons and interpolygon depressions. The polygons are widespread on the northernmost part of this terrace in the fine-grained loess. The terrace was bordered by a thermo-abrasion niche at the current river bed.

Most depressions were water-filled, but their bottom was completely vegetated with submerged growing sedges, grass, mosses and some vascular plants (e.g. *Eriophorum scheuzeri*, *Dryas octopetala*, *Pedicularis* spp.). The elevation difference between the polygon depression and the rim is 10 - 30 cm. Throughout the summer season 2013, significant changes in water level were observed with a general trend towards higher water levels in autumn. As a result, formerly dry polygon depressions turned into ponds, and some merged with neighboring ponds.
Mine 7 (Gruve 7) is Longyearbyen´s only active coal mine and located together with mine 6 (Gruve 6) close to the study site. However, river influence and acidic mine drainage can largely be ruled out as influence for the study site in Adventdalen since it is located on an elevated, inactive alluvial fan and recent drainage from Todalselva and Bolderdalselva does not cross the chosen study area.

15.3 Sampling scheme and measurements

In total 13 ponds were sampled in July/August/September 2013 (Fig. 15-3), thereof 8 intrapolygon ponds (AD-1 to -5; -9; -11; -12) and 5 interpolygon ponds (AD-6 to -8; -10; -13). For all ponds, a baseline data-set comprising the following parameters was collected (Appendix 13):

- general characteristics (coordinates, dimensions, water and thaw depth, photo collection),
- air and water temperature,
- water samples for analyzing standard water parameters (alkalinity, acidity, oxygen content, total water hardness, electrical conductivity, pH, major ion composition, stable waster isotope composition), all samples were taken ~15 cm below water table,
- freshwater ostracods (approx. 100 individuals per sample).

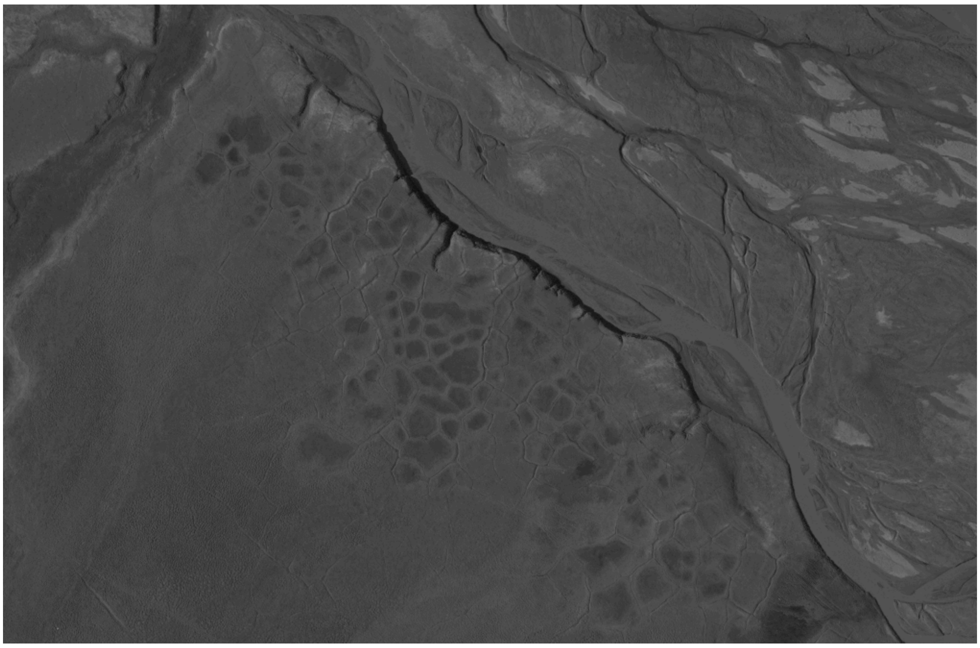

Fig. 15-3 HRSC-AX-Image of the study site in Adventdalen, Svalbard, marked pond locations (AD-01 to AD-13). Image provided by E. Hauber (DLR), and mapping by M. Ulrich (University of Leipzig).

The water samples were analyzed for pH (VWR pH 100), electrical conductivity (EC, WTW Cond3210), Sulfate (S, Hach Pocket Colorimeter II), and Chloride (Cl, Hach HQ40d). Acidity, alkalinity, oxygen content, and total hardness were analyzed with titrimetric test kits (Viscolor) after return from the field.
Samples for major ion and isotopic analyses were prepared in PE bottles or PE tubes for transport and stored cool. Kation and anion samples were filtered by a cellulose-acetate filtration set (pore size 0.45 µm) prior to conservation. Kation samples were acidified with 100 µl HNO_3 (65 %). Samples for anion and stable water isotope analyses were preserved without conservation.
Ostracods were caught from various zones in the pond: From the bottom, in the center and margin, from the water column, between plants and open water areas without vegetation. Approx. 100 animals were caught with a plankton net (mesh size 65 µm) and exhauster system according to (Viehberg 2002), and preserved in alcohol for further species identification.

15.4 Field observations

Intrapolygon ponds in lower Adventdalen had an average diameter of 10 – 15 m and a circular shape (Fig. 15-4a). In contrast, interpolygon ponds were elongated or Y-shaped, up to 1 m wide, and reached lengths of about 20 – 30m (Fig. 15-4b). The ponds were 9 – 30 cm deep. The thaw depth varied between 47 and 78 cm in the pond center, and between 39 and 103 cm at the dry pond margin. All ponds were characterized by submerged growing vegetation.

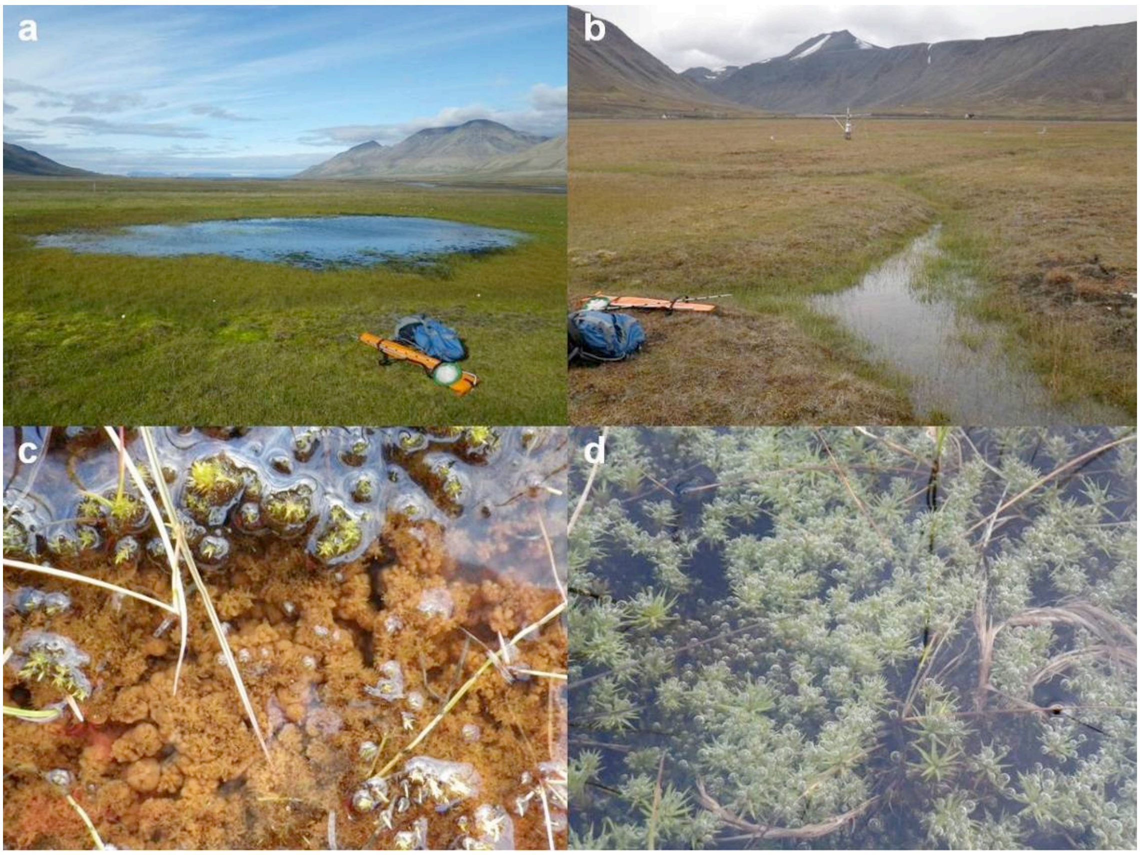

Fig.15- 4 Different types of periglacial surface waters and variations in morphology. **(a)** Intrapolygon pond (AD-2), **(b)** interpolygon pond (AD-6) with disturbed rim at its right side, **(c)** flocculate coating around submerged vegetation, **(d)** gas bubbles attached to submerged growing moss.

The pond substrate is composed of grey-brown organic-rich silty sediment below a 30 cm thick moss layer. Organic bottom substrate was rarely found, instead a soft orange-brownish layer was observed at the bottom of some ponds, or a flocculate coating around the vegetation occurred (Fig. 15-4c). Along frost cracks and polygon rims, cryoturbation processes disturbed the ground and exposed the underlying mineroganic sediment to water and air. Furthermore, gas bubbles attached submerged growing mosses were frequently observed (Fig. 15-4d).
The color of the waters was clear to brownish, at the water surface of some ponds a rainbow-colored layer occurred. The brown color of many waters is related to dissolve organic matter (DOM) and humic acids that originate from peat (Schindler et al. 1996). The abundance of benthic living species was observed to be low. When performing thaw-depth measurements, ebullition of gas occurred when probing beneath ponds and an intense H_2S-smell was recognized occasionally.

15.5 Hydrochemistry of periglacial surface waters in Adventdalen

Obtained hydrochemical characteristics and physical properties are presented in figure 15-5: The recorded air and water temperatures behave parallel and show similar patterns during the summer season. The mean air temperature was 8.4°C, with a range of min. 5.4°C and max. 11.2°C.

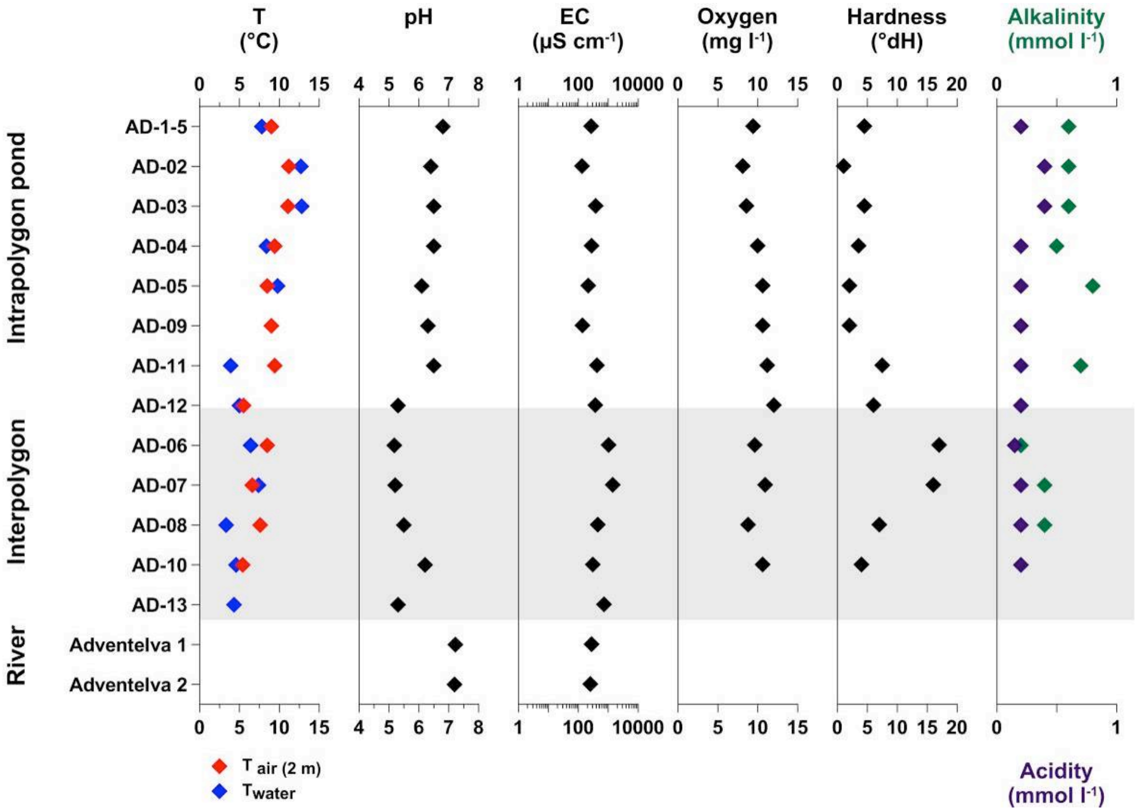

Fig. 15-5 Compilation of hydrochemical parameters of the ponds AD-1-5 to AD-13 with respect to water types. River water data from Adventelva from Rozema (2012). Note variations in scale.

The pH varied between 5 and 7. pH values were slightly acidic (around pH 5) in interpolygon ponds, while intrapolygon ponds were characterized by circumneutral ph around 7 with one exception (AD-3, pH = 5.3). EC ranged between 100 and 700 µS cm^{-1}. The EC of the interpolygon ponds AD-6 (1016 µS cm^{-1}) and AD-7 (1014 µS cm^{-1}) was slightly higher than in other ponds.
Dissolved oxygen content of the waters ranged between 8 and 14 mg l^{-1}. Oxygen content in periglacial surface waters reached the saturation level (14 mg l^{-1}) in some cases due to oxygen production from photosynthesis in submerged vegetation.
Total hardness of the pond water varied from 1.0 to 10.0°dH with a trend towards higher values in interpolygon ponds. Acidity of the studied pond waters lies between o.15 and 0.4 mm l^{-1} while alkalinity ranged from 0.2 to 0.7 mm l^{-1}. Sulfate was below detection limit (77 mg l^{-1}) in all waters.

15.6 Monitoring of a low-center polygon pond, meteorological and ground conditions

Pond AD-01 is a low-center polygon pond enclosed by a moss-sedge zone with high soil moisture, surrounded by dry polygon rims with frost cracks, and other low center polygons. The pond AD-01 is 5 m wide and 8 m long (Figs 15-6 and 15-7a). AD-01 was sampled 8 times between July 20 and September 25, 2013. A hydrochemical and biological baseline-dataset as mentioned above was obtained and the monitored pond was the only sampled site that was inhabited by a large number of freshwater ostracods.
In addition, water temperature sensors were installed directly below the water surface and at the substrate surface at the pond bottom in 25 cm water depth (Figs 15-6 and 15-7). The temperature data sensors were programmed to measure their specific value every 20 minutes between (Tab. 15-1). Temperature sensors have been calibrated by exposing them to icy water (0°C) for 24 hours.

Fig. 15-6 Photograph of the monitored pond AD-01, taken at September 7, 2013. The red stick marks the position of the water temperature sensors.

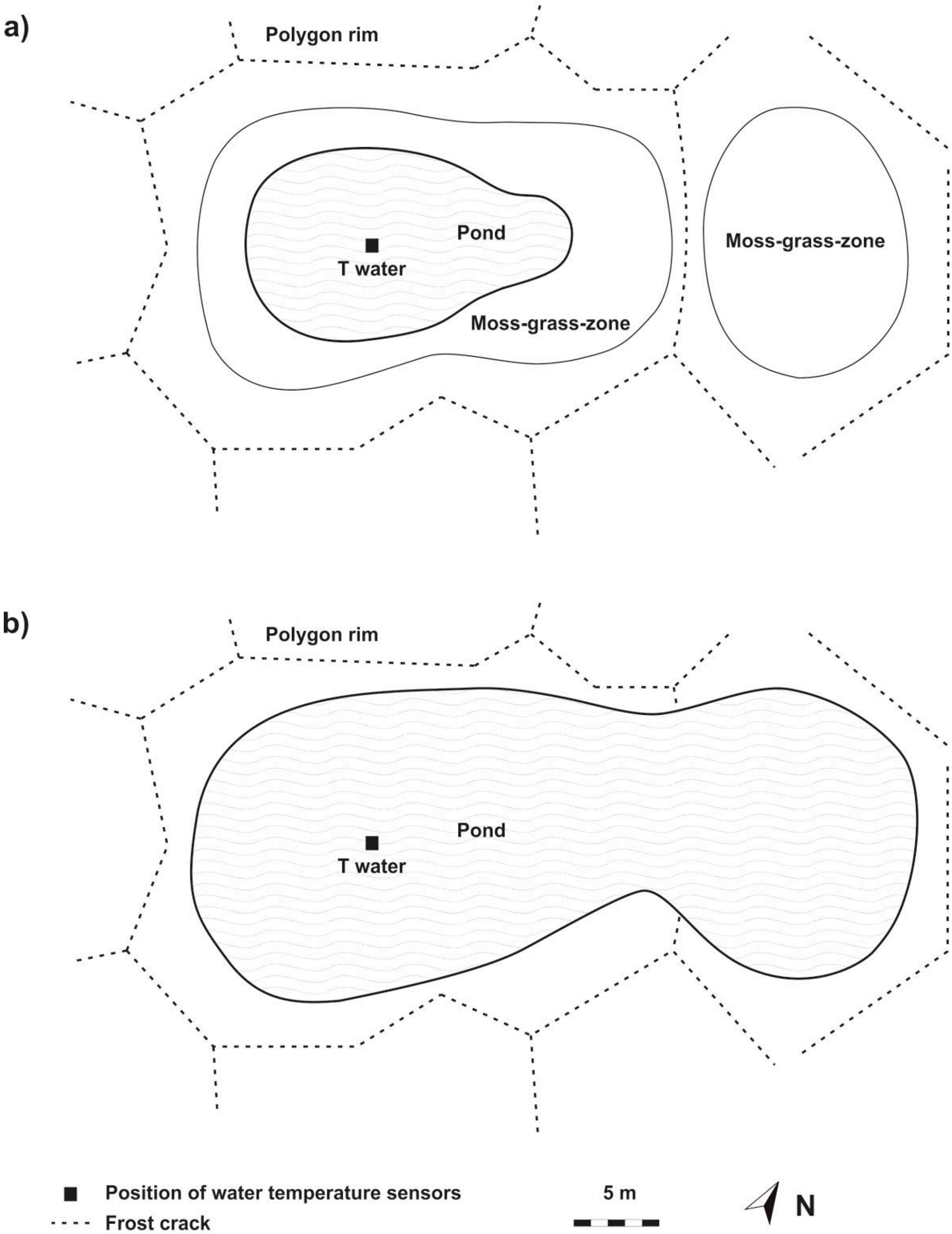

Fig. 15-7 Site scheme (top view) and location of the water temperature sensors. **(a)** Situation in July and early August, **(b)** situation from at least August 29, 2013, when AD-01 merged with a pond forming in the neighbor depression.

Tab. 15-1: Overview about location, logger type and time period of the installed data sensors.

Name	Location	Logger type	Measuring period
Data sensors installed in the pond centre for limnological conditions:			
Water temperature (Tw 6)	directly below water surface	MinidanTemp 0.1, ESYS	20.07. - 25.09. 2013, in: kl. 14:30
Water temperature (Tw 5)	at the substrate surface in ca. 25 cm water depth	MinidanTemp 0.1, ESYS	20.07. - 25.09. 2013, out: kl. 18:20

In most cases, air temperatures were slightly warmer than water temperatures (Fig. 15-8). The air and water temperatures obtained show a clear cooling trend towards autumn. At the last sampling day, September 25, 2013, the pond was covered with 2 cm thick ice.
Similar to the 12 other sampled ponds, pH values are neutral to slightly acidic (6.5 to 7.0). EC roughly doubled from 160 to 170 µS cm^{-1} to 380 µS cm^{-1} at the end of the season. The dissolved oxygen content ranged between 8 and 12 mg l^{-1}. Total water hardness also doubled (3.5 – 7°dH) while acidity and alkalinity were rather stable.

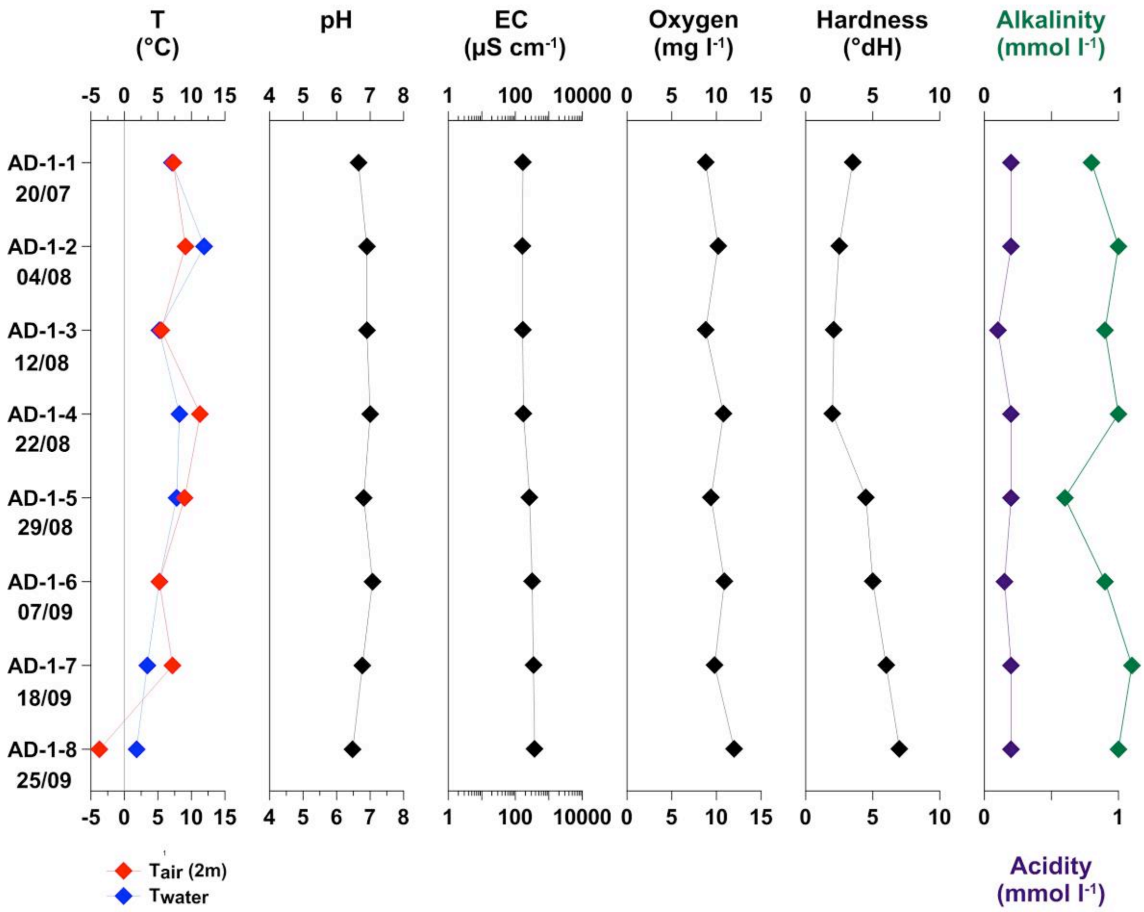

Fig. 15-8 Compilation of hydrochemical parameters of the ponds AD-1-5 to AD-13 with respect to water types. Note variations in scale.

Continuous meteorological records from Adventdalen for the monitored time period are available from a weather station hosted by the University Centre on Svalbard (UNIS). The “New Adventdalen Weather Station” (78.1210° N, 14.4941°, 15 m asl., Fig. 15-1-c) is located in ca. 3.2 km distance from the study site. Air temperature 2m above ground was recorded hourly by a Rotronic hygroclip and PT1000 temperature sensor. The recorded data are presented in figure 15-9a. They reflect daily temperature fluctuations and a sharp cooling to subzero temperatures in late September.

In August, the water level in the ponds of the entire study area rose significantly and formerly dry intrapolygon depressions turned into ponds with flooded vegetation. The water level in AD-01 increased by at least 10 cm at that time, from 26 to 35 cm (Fig. 15-9b). From monitoring event 5 (August 29, 2013) to 7 (September, 18, 2013) water depth measurements were conducted at the margin of the pond instead at its center. Therefore, the water depth plotted in figure 15-9b is slightly shallower than the actual depth was. As a result of the water level changes, in the neighboring polygon depression a pond formed and merged with AD-01. Thus, the pond size increased to a total width of 14 m and a total length of 32 m after August 29, 2013 (monitoring event 5, Fig. 15-7 b).

The thaw depth in the polygon rim and centre increased by about 20 cm from 50 to > 70 cm. As the water depth information, thaw depth was measured at the pond margin between monitoring event 5 and 7, instead at the pond center, and suffers from the same underestimation.

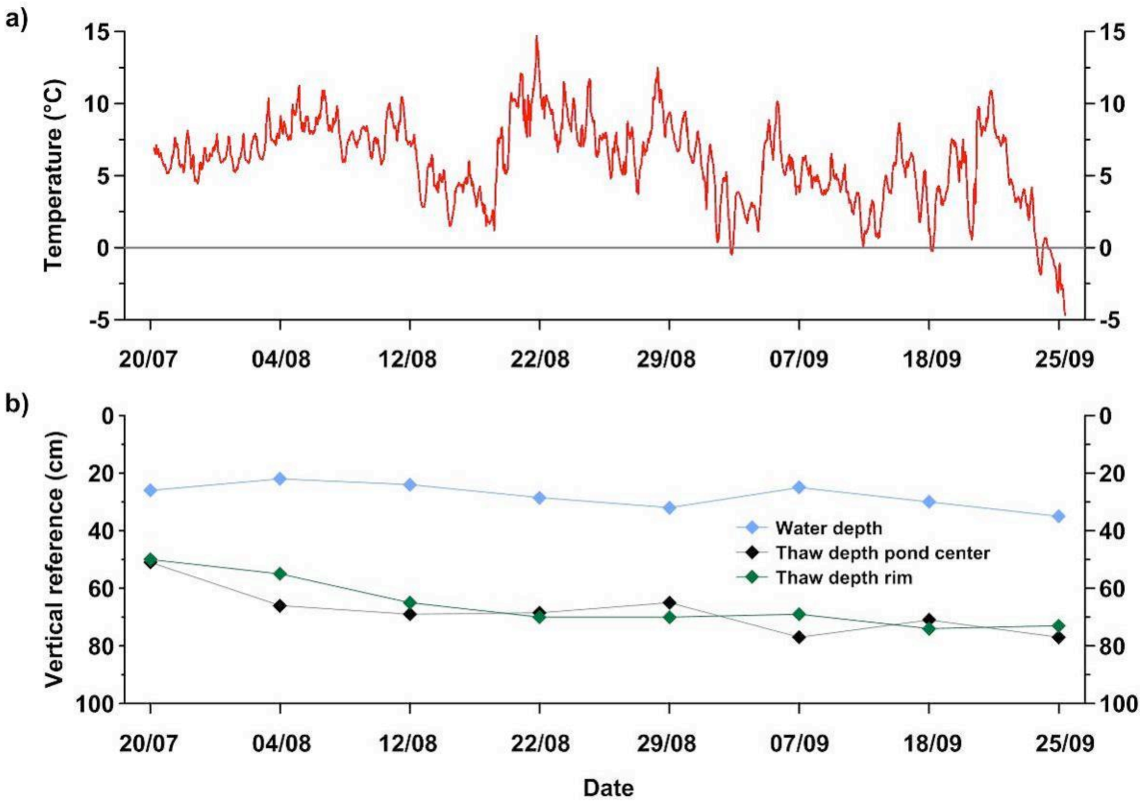

Fig. 15-9: (a) Air temperatures from July 20 until September 25, 2013. Meteorological data are from UNIS. **(b)** Water and thaw depths at the monitoring site AD-01.

15.7 Winter conditions

When the monitoring site AD-01 was visited at September 25, 2013, the pond was covered by a 2 cm thick layer of clear ice with vertical bubble structures. Under the ice, the substrate in the pond was unfrozen and living ostracods were found and sampled.
During a visit at the site at October 22, 2013, all ponds were frozen solid and covered by a 1-2 cm thin layer of loose windblown snow. The pond AD-01 was still connected to the neighboring pond.
Polygon rims were covered by ca. 3 cm of loose snow leaving parts of the vegetation uncovered and ground disturbances clearly visible, while the snow in interpolygon depressions was about 10 cm thick and the vegetation was mostly buried beneath uncompacted snow. In the snowpack, a thin layer of dust from a severe dust storm at October 14 was clearly visible. A record of snow cover duration and thickness in Adventdalen, as derived from daily automatic digital photographs installed at the site, is given in Chistiansen (2005, Fig. 15-10) for ice-wedge troughs and the adjacent polygon rims during the winter 2002 – 2003.

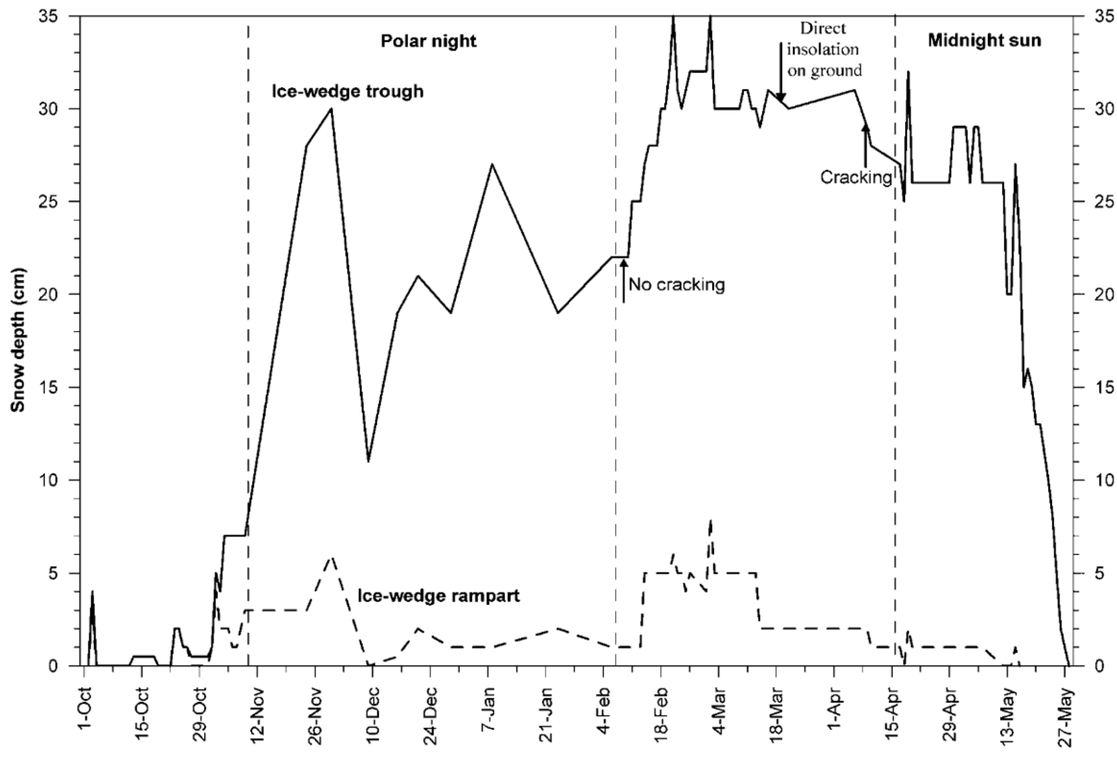

Fig. 15-10: Snow cover duration and thickness for ice-wedge troughs and the adjacent polygon rims during the winter 2002 – 2003 in Adventdalen Chistiansen (2005).

Acknowledgments

Having an own research project parallel to regular course work at UNIS has been both a challenging and fantastic experience. First of all, I want to thank Olafur Ingolfsson for his AG-332 course, which had nothing to do with the project, but was a perfect introduction to “Svalbard for beginners”, field safety awareness-wise. Otherwise, meeting white reindeers in Adventdalen on a regular base would have made me much more nervous.
Thanks to their own experience, Stefanie Härtel and Mathias Ulrich recommended a perfect study site in Adventdalen. Hanne Christiansen put me into contact with students currently working at the polygon field site, and where to find additional data. Technical support from the UNIS logistics department, especially Martin Indreiten, Jukka Pekka Ikonen and Klas Hermansson, made the field work possible, and Venke Ivarrud was always happy about sharing fresh impressions from the field and car bookings for the next sampling day.
Many thanks to Nina Friis, Anne Flink, Samuel Gauvain, Norbert Pirk, Stefano Ponti, and Krzysztof Zięba who assisted in the field, even in the worst weather! From Aga Nowak and Andy Hodson I could borrow measurement devices and lab equipment. Finding the right way to further lab work and preparing sample export was easy with the great support of Anne Hormes, Heidi Nordtømme and Gerd Irene Sigernes.
Most importantly, I thank Sebastian Wetterich, Lutz Schirrmeister and Britta Sannel for preparing a proposal for my first own research project, and borrowing equipment for field work on Svalbard. A grant through Albert and Maria Bergströms stiftelse/Stockholm University ensured that costs for field work are covered.

16 REFERENCES

ACIA (2004) Impacts of a Warming Arctic: Arctic Climate Impact Assessment. Cambridge University Press.

Åkerman, H. (2005) Relations between slow slope processes and active-layer thickness 1972-2002, Kapp Linne´. Svalbard. Norsk Geografisk Tidsskrift 59, 116-128.

Alexander, H.D., Mack, M.C., Goetz, S. et al. (2012) Carbon Accumulation Patterns During Post-Fire Succession in Cajander Larch (Larix cajanderi) Forests of Siberia. Ecosystems 15, 1065-1082.

Aulov, B.N., Potshova, M.N., Ivanenko, G.V. (1998): Map of pre Quaternary deposits (R-(55)-57 (Nizhnekolymsk) 1:1,000,000. State Geological Map of the Russian Federation. Ministry of Natural Resources of the Russian Federation.

Beermann, F., Kokhanova, L. (2012) Pedological studies of various polygon sites. Reports on Polar and Marine Research 653, 61-70.

Beyens L., Chardez D. (1995) An annotated list of testate amoebae observed in the Arctic between the longitudes 27°E and 168°W. Archiv der Protistenkunde 146, 219-233.

Billings, W.D., Luken, J.O., Mortensen, D.A., and Peterson, K.M. (1982) Arctic Tundra: A Source or Sink for Atmospheric Carbon Dioxide in a Changing Environment? Oecologia 53, 7-11.

Binney, H.A., Willis, K.J., Edwards, M.E., Bhagwat, S.A., Anderson, P.M., Andreev, A.A., Blaauw, M., Damblon, F., Haesaerts, P., Kienast, F., et al. (2009) The distribution of late-Quaternary woody taxa in northern Eurasia: evidence from a new macrofossil database. Quaternary Science Reviews 28, 2445-2464.

Blok, D., Sass-Klaassen U., Schaepman-Strub G., Heijmans M.M P.D., Sauren P., Berendse, F. (2011) What are the main climate drivers for shrub growth in Northeastern Siberian tundra? Biogeosciences 8(5), 169-1179.

Bobrov, A.A. , Siegert, C. , Andreev, A. and Schirrmeister, L. (2003) Testaceans (Protozoa: Testacea) in Quaternary permafrost sediments of Bykovsky Peninsula, Arctic Yakutia. Biology Bulletin 30, 191-206 .

Bobrov, A.A., Müller, S., Chizhikova, N.A., Schirrmeister, L., Andreev, A. (2009) Testate Amoebae in Late Quaternary Sediments of the Cape Mamontov Klyk (Yakutia). Biology Bulletin 36, 363-372.

Bobrov, A.A., Wetterich, S., Beermann, F., Schneider A., Kokhanova, L., Schirrmeister, L., Pestrykova, L.A., Herzschuh, U. (2013) Testate amoebae and environmental features of polygon tundra in the Indigirka lowland (East Siberia). Polar Biology 46, 857-870.

Bonan G.B. (2008) Forests and Climate Change: Forcings, Feedbacks, and the Climate Benefits of Forests. Science 320,1444-1449.

Bowden, W.B. Larouche, J.R., Pearce, A.R., Crosby, B.T., Krieger, K., Flinn, M.B., Kampmann, J. (2012) An Integrated Assessment of the Influences of Upland Thermal-Erosional Features on Landscape Structure and Function in the Foothills of the Brooks Range, Alaska. In K. M. Hinkel, ed. Tenth International Conference on Permafrost. Vol.1: International Contributions. Salekhard, Russia: The Northern Publisher, pp. 61–66.

Braun-Blanquet, J. (1964) Pflanzensoziologie, 3rd Edition, Vienna, Austria.

Brown, J., Ferrians, Jr. O.J., Heginbottom, J.A., Melnikov, E.S. (1998) Circum-Arctic map of Permafrost and Ground-Ice Conditions. National Snow and Ice Data Center/World Data Center for Glaciology, Boulder, CO.

Bryant, I.D. (1982) Loess deposits in lower Adventdalen, Spitsbergen. Polar Research 2, 93-103.

Campos, P.F., Willerslev, E., Sher, A., Orlando, L., Axelsson, E., Tikhonov, A., Aaris-Sørensen, K., Greenwood, A.D., Kahlke, R.-D. et al. (2010) Ancient DNA analyses exclude humans as the driving force behind late Pleistocene musk ox (Ovibos moschatus) population dynamics. Proceedings of the National Academy of Sciences 107, 5675-5680.

CAVM Team (2003) Circumpolar Arctic Vegetation Map, Scale 1:7.500.000. Conservation of Arctic Flora and Fauna (CAFF) Map No.1. U.S. Fish and Wildlife Service, Anchorage, Alaska. http://www.geobotany.uaf.edu/cavm/ finalcavm/index.html.

De Klerk, P., Donner, N., Joosten, H., Minke, M., Seifert, N., Karpov, N. S., Theuerkauf, M. (2009) Vegetation patterns, recent pollen deposition and distribution of non-pollen palynomorphs in a polygon mire near Chokurdakh (NE Yakutia, NE Siberia). Boreas 38, 39-58.

De Klerk, P., Donner, N., Karpov, N.S., Minke, M., Joosten, H. (2011) Short-term dynamics of a low-centred ice-wedge polygon near Chokurdakh (NE Yakutia, NE Siberia) and climate change during the last ca 1250 years. Quaternary Science Reviews 30, 3013-3031.

De Klerk, P., Teltewskoi, A., Theuerkauf, M., Joosten, H. (2014) Vegetation patterns, pollen deposition and distribution of non-pollen palynomorphs in an ice-wedge polygon near Kytalyk (NE Siberia), with some remarks on Arctic pollen morphology. Polar Biology 37, 1393-1412.

Chapin III, F.S. Shaver G.R., Giblin A.E., Nadelhoffer K.G., Laundre. J.A. (1995) Responses of Arctic Tundra to Experimental and Observed Changes in Climate. Ecology 76, 694-711.

Christiansen, H.H. (2003) Ice wedges in Adventdalen. In: Sollid, J.L., Christiansen, H.H. (eds.): Permafrost and periglacial features and glaciers in Svalbard. Excursion guide. VIII International Conference on Permafrost. Rapportserie i naturgeografi - Universitetet i Oslo 14,112-116.

Christiansen, H.H., Humlum, O. (2003) Active layer monitoring in Ny Ålesund and in Adventdalen in the CALM Network. In Permafrost, Periglacial Features and Glaciers in Svalbard, Excursion Guide, Sollid, J.L., Christiansen, H.H. (eds.). VIII International Conference on Permafrost. Rapportserie i naturgeografi - Universitetet i Oslo14, 97-100.

Christiansen, H.H. (2005) Thermal regime of ice-wedge cracking in Adventdalen, Svalbard. Permafrost and Periglacial Processes 16, 87-98.

Christiansen, H.H., Etzelmüller, B., Isaksen, K., Juliussen, H., Farbrot, H., Humlum, O., Johansson, M., Ingeman-Nielsen, T., Kristensen, L., Hjort, J., Holmlund, P., Sannel, A.B.K., Sigsgaard, C., Åkerman, H.J., Foged, N., Blikra, L.H., Pernosky, M.A., Ødegård, R.S. (2010) The thermal state of permafrost in the Nordic Area during the International Polar Year 2007–2009. Permafrost and Periglacial Processes 21, 156-181.

Dallmann, W.K., Kjærnet, T., Nøttvedt, A. (2001) Geomorphological and Quaternary Map of Svalbard. 1:100,000, Sheet C9G Adventdalen, Temakart No.31/32. Norwegian Polar Institute, Tromsø.

Donner, N., Minke, M., de Klerk, P., Sofronov, R., Joosten, H. (2012) Patterns in polygon mires in north-eastern Yakutia, Siberia: the role of vegetation and water. The Finnish Environment 38, 19-30.

Elser, J.J., Bracken, M.E.S., Cleland, E.E., Gruner, D.S., Harpole, W.S., Hillebrand, H., et al. (2007) Global analysis of nitrogen and phosphorus limitation of primary producers in freshwater, marine and terrestrial ecosystems. Ecology Letters 10, 1135-1142.

Flemal, R.C. (1976) Pingos and pingo scars: Their characteristics, distribution, and utility in reconstructing former permafrost environments. Quaternary Research 6, 37-53.

Flora of Siberia, Volume 5, Salicaceae – Amaranthaceae, (2003) In: Krasnoborov, I.M., Malyshev, L.I. (eds.), Enfield, New Hampshire, USA.

Flora of the Russian Arctic, Volume III, Salicaceae – Ranunculaceae, 2000. IN: Tolmachev, A.I., Packer, J.G., Griffith, G.C.D. (Eds.), Berlin, Stuttgart, Germany.

Forman, S.L., Lubinski, D.J., Ingólfsson, O., Zeeberg, J.J., Snyder, J.A., Siegert, M.J., Matishov, G.G. (2004) A review of postglacial emergence on Svalbard, Franz Josef Land and Novaya Zemlya, northern Eurasia. Quaternary Science Reviews 23, 1391–1434.

Førland, E.J., Hanssen-Bauer, I., Nordli, P.Ø. (1997) Climate statistics and longterm series of temperature and precipitation at Svalbard and Jan Mayen. DNMI rapport, 21/97 Klima.

French, H.M., (2007) The Periglacial Environment, West Sussex: John Wiley & Sons.

Geocryological Map of the USSR (1991) 1:2,500,000. Map sheet R-(55)-57 (Nizhnekolymsk). Ministry for Natural Resources of the Russian Federation.

Gebauer, R.L.E., Tenhunen, J.D., Reyonolds, J.F. (1996) Soil aeration in relation to soil physical properties, nitrogen availability, and root characteristics within an arctic watershed. Plant and Soil 178, 37-48.

Giterman, R.E., Sher, A.V., Mathewes Jr., J.V. (1982) Comparison of the development of tundra-steppe environments in East and West Beringia: pollen and macrofossil evidence from key sections, In: Hopkins, D.M., Matthews-Jr., J.V., Schweger, C.E., Young, S.B. (Eds.), Paleoecology of Beringia. Academic Press, New York, pp. 43-73.

Grosse, G., Harden, J., Turetsky, M., McGuire, A.D., Camill, P., Tarnocai, C., Frolking, S., Schuur, E.A.G., Joergenson, T., Marchenko, S. et al. (2011) Vulnerability of High-Latitude Soil Organic Carbon in North America to Disturbance. Journal of Geophysical Research 116, G00K06,

Grosse, G. Jones, B. M. (2011) Spatial distribution of pingos in Northern Asia. The Cryosphere 5, 13-33.

Grosse, G., Schirrmeister, L., Siegert, C., Kunitsky, V.V., Slagoda, E.A., Andreev, A.A., Dereviagyn, A.Y. (2007) Geological and geomorphological evolution of a sedimentary periglacial landscape in Northeast Siberia during the Late Quaternary. Geomorphology 86, 25-51.

Gurevitch, J., Scheiner, S.M., Fox, G.A. (2002) The Ecology of Plants. 2nd ed.,Sinauer Associates, Inc., Sunderland, 523 pp.

Guthrie, R.D. (2006) New carbon dates link climatic change with human colonization and Pleistocene extinctions. Nature 441, 207-209.

Harsch M.A., Hulme P.E., McGlone M.S., Duncan R.P. (2009) Are treelines advancing? A global meta-analysis of treeline response to climate warming. Ecology Letters 12,1040–1049.

Härtel, S., Christiansen, H.H. (2011) Formation and dynamics of Holocene syngenetic icewedge polygons in Adventdalen, Svalbard. Third European Conference on Permafrost. The University Center in Svalbard, Longyearbyen, Svalbard, Norway, 54 pp.

Heal, O.W. (1964) Observations on the seasonal and spatial distribution of testacea (Protozoa: Rhizopoda) in sphagnum. Journal of Animal Ecology 33, 395-412.

Holtmeier, F.-K., Broll, G. (2005) Sensitivity and response of northern hemisphere altitudinal and polar treelines to environmental change at landscape and local scales. Glob Ecol Biogeogr 14, 395-410.

Hopkins, D.M. (1982) Aspects of the Paleogeography of Beringia during the Pleistocene. In: Hopkins, D.M., Mathews Jr., J., V., Schweger, C.E., Young, S.B. (Eds.), Paleoecology of Beringia. Academic Press, London, pp. 3-28.

Humlum, O., Instanes, A., Sollid, J.L. (2003) Permafrost in Svalbard: a review of research history, climatic background and engineering challenges. Polar Research 22(1), 191–215.

Hyvärinen, H., Ritchie, J.C. (1975) Pollen stratigraphy of Mackenzie pingo sediments, N.W.T., Canada. Arctic and Alpine Research 7, 261-272.

IPCC (2007) Climate Change 2007: The Physical Science Basis: Contribution of Working Group I to the Fourth Assessment Report of the Intergovernmental Panel on Climate Change S. Solomon, D. Qin, & M. Manning (eds.), Cambridge University Press, Cambridge, UK

Ivanenko, G.V. (1998) Map of Quaternary formations. State geological map of the Russian Federation (New Series) 1: 1,00,000.

Jones, B.M., Grosse, G., Hinkel, K.M., Arp, C.D., Walker, S., Beck, R.A., Galloway, J.P. (2012) Assessment of pingo distribution and morphometry using an IfSAR derived DSM, western Arctic Coastal Plain, northern Alaska. Geomorphology 138, 1-14.

Johnson, C.N. (2009) Ecological consequences of Late Quaternary extinctions of megafauna. Proceedings of the Royal Society B: Biological Sciences 276, 2509-2519.

Joosten, H., de Klerk, P. (2007) DAMOCLES: a DAshing MOnolith Cutter for fine sectioning of peats and sediments into LargE Slices. Boreas 36, 76-81.

Kaplina, T.N., Sher, A.V., Giterman, R.E., Zazhigin, V.S., Kiselev, S.V., Lozhkin, A.V., Nikitin, V.P. (1980) Opornyi razrez pleystotsenovykh otlozheniy na reke Allaikha (nizov'ya Indigirki) (Key section of Pleistocene deposits on the Allaikha river (lower reaches of the Indigirka). In: Bulletin of Commission on Quaternary Period research, USSR Academy of Sciences, No. 50, pp. 73-95 (in Russian).

Kaplina, T.N., Giterman, R.E., Lakhtina, O.V., Abrashov, V.A., Kiselev, S.V., Sher, A.V. (1978) Duvanny Yar - key section of upper Pleistocene sediments in the Kolyma lowland. Bulletin of Quaternary Research Commission 48, 49-65 (In Russian).

Keuper, F., Bodegom van, P.M., Dorrepaal, E., Weedon, J.T., Hal van, J., Logtestijn van, R.P., Aerts, R. (2012) A frozen feast: thawing permafrost increases plant-available nitrogen in subarctic peatlands. Global Change Biology 18(6), 1998-2007.

Kienast, F., Schirrmeister, L., Siegert, C., Tarasov, P. (2005) Palaeobotanical evidence for warm summers in the East Siberian Arctic during the last cold stage. Quaternary Research 63, 283-300.

Kienast, F., Tarasov, P., Schirrmeister, L., Grosse, G., Andreev, A.A. (2008a) Continental climate in the East Siberian Arctic during the last interglacial: Implications from palaeobotanical records. Global and Planetary Change 60, 535-562.

Kienast, F., Schirrmeister, L., Wetterich, S. (2008b) Vegetation Differentiation across a topographic Yedoma – Alas Transect in the High Arctic Tundra of Oyogos Yar, East Siberia, In: Kane, D.L., Hinkel, K.M. (Eds.), 9th International Conference on Permafrost. Institute of Northern Engineering, University of Alaska Fairbanks, Fairbanks, Alaska, pp. 937-940.

Kienast, F., Wetterich, S., Kuzmina, S., Schirrmeister, L., Andreev, A.A., Tarasov, P., Nazarova, L., Kossler, A., Frolova, L., Kunitsky, V.V. (2011) Paleontological records indicate the occurrence of open woodlands in a dry inland climate at the present-day Arctic coast in western Beringia during the Last Interglacial. Quaternary Science Reviews 30, 2134-2159.

Kienast, F. (2013) Plant macrofossil records – Arctic Eurasia. In: Encyclopedia of Quaternary Science. Elias, Scott A., Mock, Cary (Editors-in-Chief), Elsevier, 2nd Edition Vol. 3, pp. 733-745.

Kuhry, P. Dorrepaal E., Hugelius G., Schuur E.A.G, Tarnocai C. (2010) Potential Remobilization of Belowground Permafrost Carbon under Future Global Warming. Permafrost and Periglacial Processes 21, 208-214.

Lavrushin, Yu.A. (1963) Allyuvii ravninnykh rek subarkticheskogo poyasa i periglyatsialnykh oblastey materikovykh oledeneniy (Alluvium of plain rivers of the subarctic zone and periglacial region of inland glaciers). Proceedings of Geological Institute of AN SSSR, 87, 264 pp. (in Russian).

Lovley, D.R., Phillips, E.J.P. (1986) Organic Matter Mineralization with Reduction of Ferric Iron in Anaerobic Sediments. Applied and Environmental Microbiology 51, 683-689.

Lovley, D.R. (1991) Dissimilatory Fe(III) and Mn(IV) Reduction. Microbiological Reviews 55, 259-287.

MacDonald, G.M., Case, R.A., Szeicz. J.M. (1998) A 538-Year Record of Climate and Treeline Dynamics from the Lower Lena River Region of Northern Siberia, Russia. Arct Alp Res 30, 334-339.

MacDonald, G., Kremenetski, K., Beilman, D. (2008) Climate change and the northern Russian treeline zone. Philos Trans R Soc B Biol Sci 363, 2283-2299.

MacDonald, G.M., Beilman, D.W., Kuzmin, Y.V., Orlova, L.A., Kremenetski, K.V., Shapiro, B., Wayne, R.K., Van Valkenburgh, B. (2012) Pattern of extinction of the woolly mammoth in Beringia. Nat Commun 3, 893.

Mack, M.C. Schuur, E.A.G., Bret-Harte , M.S., Shaver, G.R., Chapin III F.S. (2004) Ecosystem carbon storage in arctic tundra reduced by long-term nutrient fertilization. Nature 431, 440-443.

Mackay, J. R. (1962) Pingos of the Pleistocene Mackenzie Delta area. Geographical Bulletin 18, 21-63.

Mackay, J.R. (1985) Pingo ice of the western Arctic coast, Canada. Canadian Journal of Earth Sciences 22, 1452-1464.

Mackay, J.R. (1986) Growth of Ibyuk Pingo, western Arctic coast, Canada, and some implications for environmental reconstructions, Quaternary Research 26, 68-80.

Madigan, M.T., Martinko, J.M. (2006) Brock Mikrobiologie, 11th edition. Pearson Studium, München.

Mangerud, J., Bolstad, M., Elgersma, A., Helliksen, D., Landvik, J.Y., Lønne, I., Lycke, A.K., Salvigsen, O., Sandahl, T., Svendsen, J.I. (1992) The last glacial maximum on Spitsbergen, Svalbard. Quaternary Research 38, 1-39.

McGuire, A.D., Chapin III, F.S., Wirth, C., Apps, M., Bhatti, J., Callaghan, T.V., Christensen, T.R., Clein, J.S., Fukuda, M., Maximov, T., Onuchin, A., Shvidenko, A., et al. (2007) Responses of high latitude ecosystems to global change: potential consequences for the climate system. In: J. G. Canadell, Pataki, D.E., and L. F. Pitelka (eds.). Terrestrial Ecosystems in a Changing World. London, Springer, pp. 297-310.

Meyer, H. (2003) Studies on recent cryogenesis. Reports on Polar and Marine Research 466, 29-48.

Mikan, C.J., Schimel, J.P. & Doyle, A.P. (2002) Temperature controls of microbial respiration in arctic tundra soils above and below freezing. Soil Biology and Biochemistry 34, 1785–1795.

Minke, M., Donner, N., Karpov, N.S., de Klerk, P., Joosten, H. (2007) Distribution, diversity, development and dynamics of polygon mires: examples from NE Yakutia (NE Siberia). Peatlands International 2007 (1), 36-40.

Minke, M., Donner, N., Karpov, N., de Klerk, P., Joosten, H. (2009) Patterns in vegetation composition, surface height and thaw depth in polygon mires in the Yakutian Arctic (NE Siberia): A microtopographical characterisation of the active layer. Permafrost and Periglacial Processes 20, 357-368.

Muster, S., Heim, B., Abnizova, A., Boike, J. (2013) Water Body Distributions Across Scales: A Remote Sensing Based Comparison of Three Arctic Tundra Wetlands. Remote Sensing 5, 1498-1523.

Nikolskiy P.A., Basilyan A.E., Sulerzhitsky L.D., Pitulko V.V. (2010) Prelude to the extinction: Revision of the Achchagyi–Allaikha and Berelyokh mass accumulations of mammoth. Quaternary International 219, 16-25.

Nikolskiy, P.A., Sulerzhitsky, L.D., Pitulko, V.V. (2011) Last straw versus Blitzkrieg overkill: Climate-driven changes in the Arctic Siberian mammoth population and the Late Pleistocene extinction problem. Quaternary Science Reviews 30, 2309-2328.

Norsk Polarinstitut (2001) Geomorphological and Quaternary geological map of Svalbard 1: 100 000. C9G/C9Q Adventdalen. Temakart 31/32. Tromsø.

Ottow, J. (2011) Mikrobiologie von Böden. Springer, Heidelberg, 400 pp.

Owen-Smith, R.N. (1988) Megaherbivores: the influence of very large body size on ecology. Cambridge University Press, Cambridge

Prescott, G.W., Williams, D.R., Balmford, A., Green, R.E., Manica, A. (2012) Quantitative global analysis of the role of climate and people in explaining late Quaternary megafaunal extinctions. Proceedings of the National Academy of Sciences 109, 4527-4531.

Reich, P.B. Hobbie, S.E., Ellsworth, D.S., West, J.B., Tilman, D., Knops, J.M.H., Naeem, S., Trost, J. (2006) Nitrogen limitation constrains sustainability of ecosystem response to CO2. Nature 440, 922–925.

Rozema, J. (2012) Spatial variation of stable isotope ratios (δ18O and δ2H) and hydrochemical parameters within an Arctic hydrological system. A reconnaissance study of the lower Adventdalen catchment, Spitsbergen. MSc. Thesis VU University Amsterdam, 53 pp.

Schindler, D.W., Curtis, P.J., Parker, B.R., Stainton, M.P. (1996) Consequences of climate warming and lake acidificationfor UV-B penetration in North American boreal lakes. Nature 379, 705-707.

Schirrmeister, L., Pestryakova, L., Wetterich, S., Tumskoy, V. (2012) Joint Russian-German polygon project: East Siberia 2011 - 2014 ; The expedition Kytalyk 2011, Reports on Polar and Marine Research 653, 153 pp.

Schirrmeister, L., Wetterich, S. (2011) Description of the Duvanny Yar permafrost profiles. Reports on Polar and Marine Research 636, 4-18.

Schneider, A., Schirrmeister, L. (2012) Monitoring of a polygon site (KYT-1). Reports on Polar and Marine Research 653, 11-23.

Sørbel, L., Tolgensbakk, J. (2002) Ice-wedge polygons and solifluction in the Adventdalen area, Spitsbergen, Svalbard. Norsk Geografisk Tidsskrift–Norwegian Journal of Geography 56, 62–66.

Schuur, E.A.G., Crummer K.G., Vogel J.G., Mack M.C. (2007) Plant Species Composition and Productivity following Permafrost Thaw and Thermokarst in Alaskan Tundra. Ecosystems 10, 280–292.

Schuur, E.A.G., Bockheim, J., Canadell, J.G., Euskirchen, E.B.C., Goryachkin, S.V., et al. (2008) Vulnerability of Permafrost Carbon to Climate Change: Implications for the Global Carbon Cycle. BioScience 58, 701-714.

Sedlag, U., Weinert, E. (1987) Biogeographie, Artbildung, Evolution, Wörterbücher der Biologie. Gustav Fischer Verlag, Jena.

Sher, A., Kuzmina, S. (2007) BEETLE RECORDS | Late Pleistocene of Northern Asia, In: Elias, Scott A. (ed.), Encyclopedia of Quaternary Science. Elsevier, Oxford, 246-267.

Shishov L.L., Tonkonogov V.D., Lebedeva I I., Gerasimova M.I. (2004) Classification and diagnostics of soils of Russia. Oecumene, Moscow (in Russian).

Shiyatov, S., Mazepa, V. (2011) Climate-driven dynamics of the forest-tundra vegetation in the Polar Ural Mountains. Contemp Probl Ecol 4, 758-768.

Smith, L.C. Sheng, Y., MacDonald, G.M., Hinzman, L.D. (2005) Disappearing Arctic Lakes. Science 308,1429.

Soil Survey Staff (2010) Keys to Soil Taxonomy. 10th ed., US Department of Agriculture & Natural Resources Conservation Service. Washington, D.C.

Stookey, L.L. (1970) Ferrozine – A New Spectrophotometric Reagent for Iron. Analytical Chemistry 42, 779-781.

Strauss, J. (2010) Late Quaternary environmental dynamics at the Duvanny Yar key section, Lower Kolyma, East Siberia. Diploma thesis, University of Potsdam.

Sturm, M., Schimel, J., Michaelson, G., Welker, J.M., Oberbauer, S. F., Liston, G.E., et al. (2005) Winter Biological Processes Could Help Convert Arctic Tundra to Shrubland. BioScience 55, 17.

Svensson, H. (1969) Permafrost på Spetsbergen. Forskning och Framsteg 8, 20 pp. (in Swedish).

Svensson, H. (1976) Iskilar som Klimatindikator. Meddelanden från Lunds Universitets Geografiska Institutionen, No. 547. Svensk Geografisk Årsbok 52, 46-57 (in Swedish).

Teltewskoi, A., Seyfert, J., Joosten, H. (2012) Records of the model polygon LHC-11 for modern and palaeoecological studies. Berichte zur Polar- und Meeresforschung 653, 51-60.

Teltewskoi, A., Beermann, F., Beil, I., Bobrov, A., de Klerk, P., Lorenz, S., Lüder, A., Michaelis, D. & Joosten, H. (in press) 4000 years of changing wetness in a permafrost polygon peatland (Kytalyk, NE Siberia): a comparative high resolution multi-proxy study. Permafrost and Periglacial Processes.

Tumskoy, V.E. (2012) Osobennosti kriolitogeneza otlozhenii severnoi Yakutii v srednem Neopleistotsene -Golotsene (Peculiarities of cryolithogenesis in northern Yakutia from the Middle Neopleistocene to the Holocene). Kriosfera Zemli (Earths Cryosphere) 16, 12-21 (in Russian).

Ulrich M, Hauber E , Herzschuh U, Härtel S, Schirrmeister L 2011. Polygon pattern geomorphometry on Svalbard (Norway) and western Utopia Planitia (Mars) using high resolution stereo remote-sensing data. Geomorphology 134, 197-216.

UNIS new weather station in Adventdalen, online resource: http://www.unis.no/20_RESEARCH/2060_Online_Env_Data/weatherstations.htm, last accessed on October 30, 2013.

van Everdingen, R.O. (1998) Multi-language glossary of permafrost and related ground-ice terms. Boulder, CO: National Snow and Ice Data Center/World Data Center for Glaciology, 233 pp.

VDLUFA (1991) Methodenbuch. Verband Deutscher Landwirtschaftlicher Untersuchungs- und Forschungsanstalten, Darmstadt.

Viehberg, F.A. (2002) A new and simple method for qualitative sampling of meiobenthos communities. Limnologica 32, 350-351.

Vincke, S., Van de Vijver, B, Nijs, I., Beyens. L. (2006) Changes in the Testacean Community Structure Along Small Soil Profiles. Acta Protozoologica 45, 395-406.

Viollier E. Inglett P.W., Hunter K., Roychoudhury A.N., Van Cappellen P. (2000) The ferrozine method revisited: Fe(II)/Fe(III) determination in natural waters. Applied Geochemistry 15, 785-790.

Wagner, D., Gattinger, A., Embacher, A., Pfeiffer, E.-M., Schloter, M., Lipski, A. (2007) Methanogenic activity and biomass in Holocene permafrost deposits of the Lena Delta, Siberian Arctic and its implication for the global methane budget. Global Change Biology 13, 1089-1099.

Wagner, D. (2008) Microbial Communities and Processes in Arctic Permafrost Environments. Soil Biology 13, 133-154.

Walker, M.D., Everett, K.R., Walker, D.A., Birkeland, P.W. (1996) Soil development as an indicator of relative pingo age, Northern Alaska, U.S.A. Arctic and Alpine Research 28, 352-362.

Weintraub, M.N., Schimel, J.P. (2005) Nitrogen Cycling and the Spread of Shrubs Control Changes in the Carbon Balance of Arctic Tundra Ecosystems. BioScience 55, 408-415.

Wetterich, S., Schirrmeister, L., Kholodov, A. (eds., 2011) The joint Russian-German expedition BERINGIA/KOLYMA 2008 during the International Polar Year (IPY) 2007/2008. Reports on Polar and Marine Research 636, 48 pp.

Wetterich, S., Grosse, G., Schirrmeister, L., Andreev, A.A., Bobrov, A.A., Kienast, F., Bigelow, N.H., Edwards, M.E. (2012) Late Quaternary environmental and landscape dynamics revealed by a pingo sequence on the northern Seward Peninsula, Alaska. Quaternary Science Reviews 39, 26-44.

Yoshikawa, K., Leuschen, C., Ikeda, A., Harada, K., Gogineni, P., Hoekstra, P., Hinzman, L., Sawada, Y., Matsuoka, N. (2006) Comparison of geophysical investigations for detection of massive ground ice (pingo ice). Journal of Geophysical Research 111, E06S19.

Yurtsev, B.A., (1982) Relics of the xerophyte vegetation of Beringia in Northeastern Asia, In: Hopkins, D.M., Matthews-Jr., J.V., Schweger, C.E., Young, S.B. (eds.), Paleoecology of Beringia. Academic Press, New York, pp. 157-177.

Zanina, O.G., Gubin, S.V., Kuzmina, S.A., Maximovich, S.V., Lopatina, D.A. (2011) Late-Pleistocene (MIS 3-2) palaeoenvironments as recorded by sediments, palaeosols, and ground-squirrel nests at Duvanny Yar, Kolyma lowland, Northeast Siberia. Quaternary Science Reviews 30, 2107-2123.

Zimov, S.A. (2005) Pleistocene park: return of the mammoth's ecosystem. Science 308, 796-798.

Zimov, S.A., Zimov, N.S., Tikhonov, A.N., Chapin III, F.S. (2012) Mammoth steppe: a high-productivity phenomenon. Quaternary Science Reviews 57, 26-45.

Zubrzycki, S. (2012) Drilling Frozen Soils in Siberia. Polarforschung 81, 150-152.

APPENDIX 1

List of expedition participants 2012 and 2013

Lutz Schirrmeister

Participant	Competence	Affiliation	E-mail
Evgeny Arbatsky	Logistics	Pokhodsk	
Valery Arbatsky	Logistics	Pokhodsk	boss.arbatskiy@mail.ru
Mikhail Cherosov	Population botany	IBPC	cherosov@mail.ru
Mikhail Gepetnikov	Population zoology	IBPC	
Alexey Kolmogorov	Dendrochronology	NEFU	kilatrooon@mail.ru
Inokentii Koselov	Population zoology	IBPC	
Anastasia Kuzmina	Zoobenthos	NEFU	
Anatoly Nikolaev	Dendrochronology	NEFU	yktnan@rambler.ru
Liudmila Pestryakova	Phytoplankton	NEFU	lapest@mail.ru
Lilith Pogosyan	Soil science	MSU	lilit-tos@yandex.ru
Dayana Popova	Population botany	NEFU	
Sergei Pristaezhnyuk	Population zoology	IBPC	
Evgeny Sakharov	Population zoology	IBPC	
Viktor Sitalo	Limnology	Herzen University	sitalo_viktor@mail.ru
Elena Troeva	Population botany	IBPC	etroeva@mail.ru
Vladimir Tumskoy	Cryolithology	MSU	vtumskoy@rambler.ru
Evgenya Zhukova	Geomorphology	MSU	checkedz@gmail.com
Fabian Beermann	Soil science	UHH	fabian.beermann@uni-hamburg.de
Enrico Behrens	Mire ecology	EMAU	enrico.behrens@googlemail.com
Nils Hanke	Soil science	UHH	nils.hanke@gmail.com
Inga Jacobsen	Forest ecology	AWI	IngaJacobsen@gmx.de
Hans Joosten	Mire ecology	EMAU	joosten@uni-greifswald.de
Frank Kienast	Vegetation studies	Senckenberg	frank.kienast@senckenberg.de
Stefan Kruse	DNA analyses	AWI	stefan.kruse@awi.de
Andrea Schneider	Monitoring, ostracods	AWI	andrea.schneider@uit.no
Lutz Schirrmeister	Quaternary geology	AWI	lutz.schirrmeister@awi.de
Sebastian Wetterich	Monitoring, ostracods	AWI	sebastian.wetterich@awi.de
Mareike Wieczorek	Vegetation mapping	AWI	mareike.wieczorek@awi.de

APPENDIX 2

Coordinates of study sites around Pokhodsk

Lutz Schirrmeister

A 2-1: Coordinates of ecological study sites (see chapters 3 and 4).

Site	N	E
POK-1	69.09510	160.93876
POK-2	69.09165	160.93838
POK-3	69.09460	160.93855
POK-4	69.09401	160.94266
POK-5	69.09400	160.94534
POK-6	69.09536	160.93726
POK-7	69.10400	160.99977
POK-8	69.10322	160.99982
POK-9	69.10347	161.00114
POK-10	69.09303	160.94013
POK-11	69.09504	160.93744
POK-12	69.06686	160.94519
POK-13	69.06486	160.92007
POK-14	69.06491	160.93496
POK-15	69.06529	160.94134
POK-16	69.09352	160.94231
POK-17	69.09253	160.94439
POK-18	69.09295	160.94480
POK-19	69.11090	160.88188
POK-20	69.11073	160.88734
POK- 21	69.11007	160.88716
POK-22	69.12644	160.87907
POK-23	69.12644	160.87907
POK-24	69.10908	161.00141
POK-25	69.10789	161.00181
POK-27	69.05436	160.86234
POK-26	69.06082	160.86558
POK-28	69.07071	160.98106
POK-29	69.07005	160.97991
POK-30	69.06607	160.94453
POK-31	69.06575	160.94201

A 2-2: Coordinates of limnological study sites (see chapter 5)

Labels in Figs. 2-4. 2-5	Site	N	E
L-4	4	69.095050	160.939017
L-6	6	69.093450	160.942783
L-36	36	69.067883	160.943967
L-38	38	69.059083	160.936033
L-8	8	69.094017	160.945267
L-20	20	69.093033	160.945083
L-24	24	69.111367	160.882700
L-25	25	69.110767	160.887917
L-36	34	69.070683	160.981267
L-62	62	69.113850	160.984717
L-66	66	69.057600	160.853183
L-69	69	69.067367	160.796467
L-70	70	69.067133	160.816200
L-31	31	69.125450	160.677550
L-248	248	69.095050	160.939017
L-259	259	69.094596	160.938554
L-309	309	69.095043	160.937442
L-80	80	69.044533	161.011383

A 2-3: Coordinates of the collapsed polygon complex MNP12 (see chapter 6)

Site	N	E
MNP 12	69.093539	160.932125

A 2-4: Coordinates of permafrost cores (see chapters 7 and 9)

Labels in Figs. 2-4. 2-5	Core label	N	E
XII	12P-1607-1 (POK1 W)	69.095150°	160.938733°
XIII	12P-1707-1 (POK1 C)	69.095033	160.938900
XIV	12P-1907-1 (POK 3W)	69.094783	160.940700
XIV	12P-1907-2 (POK3 C)	8 m distance from 12P-1907-1	
XV	12P-2107-1 (POK4 W)	69.103750	161.002417
XV	12P-2107-2 (POK4 C)	8 m distance from 12P-2107-1	
XVI	12P-2707-1 (POK5)	69.103733	161.003900
XVII	12P-2707-2 (POK6)	69.103483	161.005517
XVIII	12P-2707-3	69.102917	161.008283
XIX	12P-3007-1 (POK7)	69.076583	160.970367
XX	12P-3007-2 (POK8)	69.076483	160.969300
V	12P-1008	69.05617	160.85904

A 2-5: Coordinates of soil pits (see chapters 7 and 8)

Pits at the "Polygon site"	N	E
P1	69.097472	160.940472
P2	69.097417	160.940611
P3	69.097417	160.940667
P4	69.097333	160.940500
P5	69.097278	160.940500
P6	69.095722	160.941028
P7	69.095722	160.941028
P8	69.095750	160.941139
P9	69.095694	160.941444
P10	69.095806	160.941861
P11	69.095917	160.941444
P12	69.095972	160.941556
P13	69.096056	160.941778
P14	69.096167	160.941722
P15	69.096250	160.941639
P16	69.096333	160.941750
P17	69.096250	160.942028
P18	69.096333	160.940417
P19	69.096389	160.940417
P20	69.096667	160.940389
P21	69.096556	160.940361
P22	69.096444	160.940167
P23	69.096750	160.940333
P24	69.097222	160.940111
P25	69.097139	160.940000
P26	69.097111	160.940222
P27	69.097111	160.940528
P28	69.097083	160.940778
P29	69.096972	160.940861
P30	69.096972	160.940750
P31	69.096917	160.940528
P32	69.096722	160.940889
P33	69.096639	160.940833
P34	69.096500	160.940833
P35	69.096611	160.941222
P36	69.096417	160.941333
P37	69.096361	160.941194
P38	69.096028	160.941250
P39	69.096167	160.941444
P40	69.096222	160.940917
P41	69.096278	160.941167

Pits at the pingo site	N	E
Pi01	69.038500	161.005306
Pi02	69.038139	161.005528
Pi03	69.038306	161.005333
Pi04	69.038361	161.005111
Pi05	69.038556	161.004889
Pi06	69.038306	161.006444
Pi07	69.037694	161.006222
Pi08	69.037250	161.005583
Pi09	69.037444	161.007167
Pi10	69.038111	161.008306
Pi11	69.038056	161.008361
Pi12(islet1)	69.039917	161.004694
Pi13(islet2.wall)	69.039972	161.004694
Pi14(islet2.center)	69.038361	161.005111

Pits at the MNP site	N	E
1	69.093944	160.932444
2	69.093917	160.932333
3	69.094028	160.932722
5	69.094194	160.932528
7	69.094167	160.932639
14	69.094083	160.932028

A 2-6: Coordinates of permafrost pits and exposures (see chapter 9)

Labels in Fig. 2-4, 2-5	Site label	N	E
I	12P-2007-1	69.063860	160.878890
II	12P-2007-2	69.063550	160.866040
III	12P-2007-3	69,064070	160.861890
IV	12P-2007-4	69.063500	160.866700
XXI	12P-2507-1 12P-0708-1	69.09503292	160.937147
XI	12P-2308	69.11288	160.76570

APPENDIX 3

Technical information, sampling and measuring data from the monitoring site Pok-01

Lutz Schirrmeister, Andrea Schneider, Sebastian Wetterich

A 3-1: Overview about location, logger type and time period of the installed data sensors.

Name	Location	Logger type	Measuring period
Data sensor installed for meteorological conditions:			
Air temperature (Ta)	2 m above ground	MinidanTemp 0.1, ESYS	16.07. - 25.08. 2012
Data sensors installed for ground conditions:			
Ground temperature (T1)	Upper polygon rim, depth: 3; 15; 23; 31 cm	HOBO Micro Station; HOBO 12-Bit Temperature Smart Sensor	17.07. - 25.08. 2012
Ground temperature (T2)	Lower polygon rim, depth: 3; 13; 23; 33 cm	HOBO Micro Station, HOBO 12-Bit Temperature Smart Sensor	17.07. - 25.08. 2012
Ground temperature (T3)	Upper polygon rim, depth: 25; 50; 75; 95 cm	HOBO Micro Station, HOBO 12-Bit Temperature Smart Sensor	19.07. - 25.08. 2012
Soil moisture (M1)	Upper polygon rim, depth: 2; 14; 23; 28 cm	HOBO Micro Station, Soil Moisture Smart Sensor	16.07. - 25.08. 2012
Soil moisture (M2)	Lower polygon rim, depth: 5; 14; 23; 30 cm	HOBO Micro Station, Soil Moisture Smart Sensor	17.07. - 25.08. 2012
Data sensors installed in the pond centre for limnological conditions:			
Water temperature (Tw)	directly below water surface	MinidanTemp 0.1, ESYS	17.07. - 25.08. 2012
Water level (WL)	10 cm below water surface	HOBO Water Level/ Temp (U20-001-04)	17.07. - 25.08. 2012
Electrical Conductivity (EC)	20 cm below water surface	HOBO U24 Conductivity/Temp Logger	17.07. - 25.08. 2012
Water temperature (Tw)	60 cm below water surface	MinidanTemp 0.1, ESYS	17.07. - 25.08. 2012

A 3-2: General characteristics, sampling depths and hydrobiological samples of the monitoring site POK-01.

Sample code	Date	Water depth at Logger (cm)	thaw depth center (cm)	Thaw depth M1/T1/AT (cm)	Thaw depth M2/T2 (cm)	Sample depth Hydrochemistry (cm)	Sample depth Exhauster (cm)	Ostracodes	Phytoplankton	Zooplankton	Makrozoobenthos	Testate amoeba	Sediment	Stable isotopes	Hydrochemistry
1-1	16/07	21	40	26 - 31	20 - 25	15	20 - 30	x	x	x	x	x	x	x	x
1-2	07/22	20	40	18 - 31	22 - 30	15	20 - 30	x	x	x				x	x
1-3	07/28	21	48	29 - 32	35 - 39	15	20 - 25	x	x	x	x			x	x
1-4	04/08	20	40	30 - 35	35	15	15 - 20	x	x	x	x			x	x
1-5	11/08	43	35	36 -40	38 - 40	20	20	x	x	x	x			x	x
1-6	17/08	55	20	40-50	35-40	10	10	x	x	x	x	x		x	x
1-7	24/08	60	12	25-30	40	10	10	x	x	x	x	x		x	x

A 3-3: Physico-chemical features of the monitoring site POK-01.

Sample code	T Air	T Water (near surface)	EC	pH	NH_4	NO_3	PO_4^{3}	Oxygen	Alkalinity	Acidity	Total hardness
Unit	°C	°C	µS/cm		mg/l	mg/l	mg/l	mg/l	mmol/l	mmol/l	°dH
Detection limit					0.015 mg/l	0.23 mg/l	0.05 mg/l				
1-1	15.9	23.3	114	7.6	0.107	0.156	0.102	8.8	0.7	0.4	3.0
1-2	21.3	16.2	110	7.6	0.010	0.125	0	9.2	0.8	0.4	3.0
1-3	7.6	7.1	85	7.4	0.039	0.139	0.004	9.8	0.6	0.6	3.0
1-4	10.2	10	90	7.4	0.029	0.163	0.012	11.0	0.6	0.3	3.5
1-5	16.8	14.2	93	6.7	0.040	0.257	0.021	9.0	0.8	0.4	3.5
1-6	5.9	6 (surface) 4.3 (bottom)	102	7.1	0.027	0.337	0	9.6	1.0	0.4	3.0
1-7	7.1	7.8 (surface) 4.0 (bottom)	107	7.4	0.027	0.307	0	11.8	1.0	0.4	3.5

APPENDIX 4

List of hydrobiological samples

Andrea Schneider

A 4-1: Location, type, and general characteristics of the studied ponds and lakes POK-02 to POK-31. LC – Intrapolygon pond in low-centered polygon, I – Interpolygon pond/collapsed ice wedge, TL – Thermokarst lake, V – Viska floodplain, K – Kolyma floodplain, H – Hummocky tundra southwest of Pokhodsk, NO – near Naumovskoje Osero, KT – Khalerchinskaya Tundra, SK – Southern Kolyma floodplain near pingo outcrop.

Sample code	Date	Coordinates	Type	Area	Size of water body (m)	Water depth (cm)	Thaw depth center (cm)	Thaw depth margin (cm)	Thaw depth polygon rim (cm)
POK-02	15/7	69.09165 °N 160.93837°E	I	V	8 x 1.4	50 - 64	0		35 - 40
POK-03	18/7	69.09460°N 160.93855°E	I	V	3 x 4	20 - 30	25		50 - 69
POK-04	19/7	69.09401°N 160.94266°E	LC	V	17.3 x 16	70.0		33 - 37	27 - 31
POK-05	19/7	69.09400°N 160.94534°E	I	V	10 x 16			39 - 40	48 - 51
POK-06	19/7	69.09537°N 160.93726°E	LC	V	11.5 x 9	59	0	35 - 36	18 - 20
POK-07	21/7	69.10400°N 160.99977°E	LC	K	17.10 x 6.0	80	10	45 - 60	51
POK-08	21/7	69.10322°N 160.99983°E	LC	K	25.8 x 22.5	margin: 80	10	40	20
POK-09	21/7	69.10347°N 161.00114°E	I	K	9 x 7 x 11, width: 1.5	62			20 - 21
POK-10	25/7	69.09303°N 160.94014	LC	V	11 x 10	7	43	43	25
POK-11	25/7	69.09504°N 160.93744°E	LC	V	4.30	21	42	39 - 42	20 - 30
POK-12	26/7	69.06686°N 160.94519°E	I	H	10.2 x 5.1, width: 1	52	8		27 - 31
POK-13	27/7	69.06633°N 160.93851°E	LC	H	10.6 x 7.20	52	27		20 - 33
POK-14	27/7	69.06490°N 160.93497°E	LC	H	7.8 x 5.2	31	19		23 - 29
POK-15	27/7	69.06528°N 160.94135°E	I	H	7.8 x 3.5	49	13		18 - 22
POK-16	30/7	69.09351°N 160.94231°E	LC	V	24 x 18	center: 210, margin: 31	margin: 58	48 - 51	41 - 45
POK-17	30/7	69.09253°N 160.94440°E	TL	V	8 x 6,5	margin: 50	margin: 35	47	34 - 40
POK-18	30/7	69.09295°N 160.94479°E	TL	V	96 x 30.5 x 35.7	center: 240, margin: 35	margin: 40	44 - 49	19 - 20

Sample code	Date	Coordinates	Type	Area	Size of water body (m) (m)	Water depth (cm) (cm)	Thaw depth center (cm) (cm)	Thaw depth margin (cm) (cm)	Thaw depth polygon rim (cm) (cm)
POK-19	1/8	69.11090°N 160.88188°E	LC	NO	14.50 x 10.90	17 - 25	33 - 38		18 - 20
POK-20	2/8	69.11073°N 160.88734°E	TL	NO	72.1 x 26.5 m	0.7 - 1.1	margin: 45	31 - 39	20 - 30
POK-21	2/8	69.11008°N 160.88716°E	I	NO	6.8 x 1.2	58	10		17 - 20
POK-22	5/8	69.12644°N 160.87906°E	LC	NO	21 x 21 m	10	60		22 - 28
POK-23	5/8	69.12675°N 160.88002°E	LC	NO	14.5 x 6.5	21	44		45
POK-24	8/8	69.10909°N 161.00142°E	LC	K	20 x 30	center: > 100, margin: 38		53	52 - 54
POK-25	8/8	69.10789°N 161.00182°E	LC	K	6 x 7	15	49		36
POK-26	10/8	69.06082°N 160.86557°E	I	KT	7.4 x 1.0	30	15		42 - 55
POK-27	10/8	69.05436°N 160.86235°E	I	KT	7 x 7 x 2.4	30	25		42 - 53
POK-28	15/8	69.07072°N 160.98106°E	I	SK	32 x 2	75	0	10	60
POK-29	15/8	69.07005°N 160.97990°E	LC	SK	25 x 14	1	12	45	32 - 50
POK-30	26/8	69.06606°N 160.94453°E	I	H	9 x 32	55	10	40	
POK-31	26/8	69.06575°N 160.94202°E	I	H	2 x 9	70	5	25 - 40	

A 4-2: Sampling depths and hydrobiological samples of the studied ponds and lakes POK-02 to POK-31.

Sample code	Sample depth Hydrochemistry (cm)	Sample depth Sediments (cm)	Sample depth Exhauster (cm)	Ostracodes	Phytoplankton	Zooplankton	Makrozoobenthos	Testate amoeba	Sediment	Stable isotopes	Hydrochemistry
POK-02	15	50 - 64	50 - 64	x	x	x	x	x	x	x	x
POK-03	15	20 - 30	20 - 30	x	x	x	x	x	x	x	x
POK-04	15	20	30 - 70	x	x	x	x	x	x	x	x
POK-05	15	20	50 - 70	x	x	x	x	x	x	x	x
POK-06	15	20 - 30	20 - 30	x	x	x	x	x	x	x	x
POK-07	15	80	80	x	x	x	x	x	x	x	x
POK-08	15	60	60	x	x	x	x	x	x	x	x
POK-09	15	20 - 30	20 - 30	x	x	x	x	x	x	x	x
POK-10	3 - 5	7	7	x	x	x	x	x	x	x	x
POK-11	15	20	20	x	x	x	x	x	x	x	x
POK-12	15	50 - 60	50 - 60	x	x	x	x	x	x	x	x
POK-13	15	55	55	x	x	x	x	x	x	x	x
POK-14	15	30	30	x	x	x	x	x	x	x	x
POK-15	15	50	20 - 50	x	x	x	x	x	x	x	x
POK-16	20	20 - 30	20 - 30	x	x	x	x	x	x	x	x
POK-17	15	20 - 30	20 - 30	x	x	x	x	x	x	x	x
POK-18	15	30 - 40	30 - 40	x	x	x	x	x	x	x	x
POK-19	10	20 - 25	20 - 25	x	x	x	x	x	x	x	x
POK-20	15	30	30	x	x	x	x	x	x	x	x
POK-21	15	50 - 60	50 - 60	x	x	x	x	x	x	x	x
POK-22	5	10 - 15	10 - 15	x	x	x	x	x	x	x	x
POK-23	15	20 - 25	20 - 25	x	x	x	x	x	x	x	x
POK-24	30	30	30 - 50	x	x	x	x	x	x	x	x
POK-25	15	15	/	/	x	x	x	x	x	x	x
POK-26	30	30	/	/	x	x	x	x	x	x	x
POK-27	15 - 20	15 - 20	/	/	x	x	x	x	x	x	x
POK-28	20	50 - 60	20 - 60	x	x	x	x	x	x	x	x
POK-29	20	50	20 - 50	x	x	x	x	x	x	x	x
POK-30	20	50	20 - 50	x	x	x	x	x	x	x	x
POK-31	10	60 - 30	60 - 31	x	x	x	x	x	x	x	x

A 4-3: Physico-chemical features of the studied ponds and lakes POK-02 to POK-31. Negative values for NH_4, NO_3 and PO_4^{3} are below the detection limits.

Sample code	**T Air**	**T Water (near surface)**	**T Water (bottom water)**	**EC**	**pH**	**NH_4**	**NO_3**	**PO_4^{3}**	**Oxygen**	**Alkalinity**	**Acidity**	**Total hardness**
Unit	°C	°C	°C	µS/cm		mg/l	mg/l	mg/l	mg/l	mmol/l	mmol/l	°dH
Detection limit						0.015 mg/l	0.23 mg/l	0.05 mg/l				
POK-02	24.6	15.2	6.8	113	6.6	0.040	0.287	0.030	5.2	0.6	1.3	4.5
POK-03	6.5	6.7	0.0	132	6.8	0.054	1.710	0.107	5.0	1.0	1.6	4.0
POK-04	16.3	11.1	10.5	124	7.1	0.032	0.438	0.031	8.4	0.8	0.4	3.5
POK-05	17.5	11.9	10.6	118	7.2	0.033	0.224	0.030	8.4	1.2	0.8	3.5
POK-06	19.9	19.8	0.0	102	7.4	0.036	0.239	0.023	6.4	1.0	0.4	3.5
POK-07	15.0	11.2	8.0	65	6.2	0.029	0.408	0.018	7.5	0.8	1.0	3.0
POK-08	18.0	14.3	0.0	126	7.3	0.030	0.307	0.027	8.6	1.8	0.4	4.0
POK-09	19.9	8.7	3.5	77	7.0	0.036	0.526	0.036	6.2	0.7	1.0	3.0
POK-10	2.0	4.8	0.0	69	7.4	0.008	0.175	0.000	11.8	0.6	0.4	6.0
POK-11	2.8	5.4	0.0	55	7.4	0.005	0.168	0.002	11.8	0.8	0.4	4.5
POK-12	3.7	4.0	0.0	61	6.8	0.013	0.932	0.006	8.6	0.6	1.0	3.0
POK-13	6.8	4.9	3.9	60	6.9	0.200	0.303	-0.001	9.6	0.4	0.2	2.2
POK-14	8.8	5.9	0.0	61	6.7	0.014	0.732	0.001	7.6	0.3	0.2	2.0
POK-15	9.5	4.4	1.3	52	6.5	0.011	0.655	0.004	5.0	0.3	0.2	2.0
POK-16	6.8	7.2	7.1	96	7.4	0.014	0.145	0.003	10.0	0.8	0.4	3.0
POK-17	7.9	7.6		118	7.4	0.013	0.186	0.003	10.0	0.8	0.6	3.0
POK-18	10.0	7.2		108	7.4	0.012	0.198	-0.003	10.6	0.8	0.4	2.0
POK-19	10.1	8.6		38	6.3	0.038	0.304	-0.001	7.8	0.4	0.4	3.0
POK-20	6.4	8.0		71	6.7				9.0	0.6	0.3	3.0
POK-21	7.1	5.4	2.9	43	6.2	0.023	0.837	0.000	7.0	0.2	1.0	2.0
POK-22	19.3	16.4		74	6.8				9.6	0.6	0.6	2.0
POK-23	16.7	16.0		53	6.9				9.4	0.4	0.4	2.0
POK-24	6.7	9.3	8.9 (in 0.5m)	64	6.9				10.0	0.4	0.4	4.0
POK-25	7.2	9.7		23	7.3				10.6	0.4	0.4	3.5
POK-26	19.0	8.0		48	4.8				2.4	0.0	4.0	
POK-27	19.3	13.0	5.8	42	4.7				7.8	0.0	1.8	
POK-28	15.0	12.0	6.5	54	6.7				7.4	0.8	0.8	3.5
POK-29	14.4	15.0	11.5	61	6.6				9.5	0.8	0.4	4.0
POK-30	6.0	5.6	5.1	66	7.0				7.0	0.8	0.8	3.0
POK-31	6.3	5.4	3.5	80	6.6				8.0	0.8	0.8	3.0

APPENDIX 5

List of limnological samples

Viktor Sitalo, Lutz Schirrmeister

A 5-1: Water samples and field results

Date	Sample	Depth (m)	EC (µS/cm)	pH (wtw)	Hydro-chemistry	Stable Isotopes
26.07.2012	36-1	0	90	7.4	x	
	36-2	1	70	7.3	x	x
	36-3	3	66	7.2	x	
27.07.2012	38-1	0	69	7.2	x	x
	38-2	1	63	7.2	x	x
	38-3	3.5	60	7.1	x	x
28.07.2012	06-1 (POK-16)	0			x	x
31.07.2012	24-1	0	127	6.5	x	x
	24-2	2	126	6.6	x	x
	24-3	2.5	128	6.6	x	x
02.08.2012	25-1 (POK-20)	0	71	6.7	x	x
03.08.2012	34-1	0.5	80	6.8	x	x
	34-2	3.0	57	6.7	x	x
08.08.2012	62-1	0.5	99	7	x	x
	62-2	3.7	85	6.72	x (H_2S !)	x
	62-3	1.5	98	7.05	x	x
10.08.2012	66-1	0.5	48	7.3	x	x
	66-2	3	33	6.5	x	x
	66-3	1	47	7.5	x	x
16.08.2012	31-1		178	6.82	x	x
	31-2		183	6.91	x	x
21.08.2012	80-1	0	51	6.42	x	x
	80-2	1	52	6.81	x	x
	80-3	2.4	51	6.84	x	x

A 5-2: Lake and pond sediment samples from short cores

Site, Date, Corer	Sample	Depth (cm)	Description
Pond 36 26.07.2012 Gravity Corer	S-36-1-1	0 - 1	highly decomposed plant material, fine, brown
	S-36-1-2	1 - 2	highly decomposed plant material, fine, brown
	S-36-1-3	2 - 3	highly decomposed plant material, fine, brownish-greyish
	S-36-1-4	3 – 4.5	silty fine sand, dark grey
	S-36-1-5	4.5 - 5.5	silty fine sand with rootlets, dark grey
	S-36-1-6	5.5 - 7.5	silty fine sand with rootlets, dark grey
	S-36-1-7	7.5 - 9	silty fine sand with rootlets, dark grey
Lake 038 27.07.2012 Gravity Corer	S-38-1-1	0 - 1	dark muddy plant material
	S-38-1-2	1 - 2	dark muddy plant material, slightly silty
	S-38-1-3	2 - 3	dark muddy plant material, slightly silty
	S-38-1-4	3 - 4	dark muddy plant material, slightly silty, coarser plant material
	S-38-1-5	4 - 5	dark muddy plant material, slightly silty, grey, coarser plant material
	S-38-1-6	5 - 6	grey, silty with plant fragments
	S-38-1-7	6 - 7	grey, silty with plant fragments
	S-38-1-8	7 - 8	grey, silty with plant fragments
	S-38-1-9	8 - 9	grey, silty with plant fragments
Lake 038 27.07.2012 Gravity Corer	S-38-2-1	0 - 1	living plant material
	S-38-2-2	1 - 2	living plant material, fine decomposed plant material, dark brown, soft
	S-38-2-3	2 - 3	fine decomposed plant material
	S-38-2-4	3 - 4	fine decomposed plant material
	S-38-2-5	4 - 5	fine decomposed plant material
	S-38-2-6	5 - 6	fine decomposed plant material with coarse plant fragments
	S-38-2-7	6 - 7	fine decomposed plant material, soft, brownish-greyish
	S-38-2-8	7 - 8	fine decomposed plant material, soft, brownish-greyish
	S-38-2-9	8 - 9	fine decomposed plant material, soft, brownish-greyish
	S-38-2-10	9 - 10	fine decomposed plant material, soft, light brownish-greyish
	S-38-2-11	10 - 11	fine decomposed plant material with coarse plant material, soft, light brownish-greyish
	S-38-2-12	11 - 12	fine decomposed plant material with coarse plant material, more dense, light brownish-greyish
	S-38-2-13	12 - 13	fine decomposed plant material with coarse plant material, dense, light brownish-greyish
	S-38-2-14	13 - 14.5	fine decomposed plant material with coarse plant material, dense, light brownish-greyish
	S-38-2-15	14.5 - 16	fine decomposed plant material with coarse plant material, dense, light brownish-greyish
12-POK-4 30.07.2012 Russian Corer	S-08-1-1	0 - 5	
	S-08-1-2	5 - 10	
	S-08-1-3	10 - 15	
	S-08-1-4	15 - 20	
	S-08-1-5	20 - 25	

Site, Date, Corer	Sample	Depth (cm)	Description
	S-08-1-6	25 - 30	
	S-08-1-7	30 - 35	
	S-08-1-8	35 - 40	
	S-08-1-9	40 - 45	
	S-08-1-10	45 - 47.5	
	S-08-1-11	47.5 - 50	
12-POK-18 30.07.2012 Russian Corer	S-20-1-1	0 - 4	decomposed plant material, fine, brown, soft
	S-20-1-2	4 - 13	decomposed plant material, fine, brown, soft
	S-20-1-3	13 - 15	decomposed plant material, fine, brown, soft
	S-20-1-4	15 - 20	decomposed plant material, fine, brown, soft
	S-20-1-5	20 - 25	decomposed plant material, fine, brown
	S-20-1-6	25 - 30	decomposed plant material, fine, brown
	S-20-1-7	30 - 35	decomposed plant material, fine, brown
	S-20-1-8	35 - 38	decomposed plant material, fine, brown
	S-20-1-9	38 - 40	decomposed plant material, fine, brown
	S-20-1-10	40 - 42	
	S-20-1-11	42 - 44	decomposed plant material with silty fine sand, greyish-brown, compact
	S-20-1-12	44 - 46	decomposed plant material with silty fine sand, greyish-brown, compact
	S-20-1-13	46 - 48	decomposed plant material with silty fine sand, greyish-brown, compact
	S-20-1-14	48 - 50	decomposed plant material with silty fine sand, greyish-brown, compact
12-POK-16 28.07.2012 Russian Corer	S-06-1-1	0 - 10	
	S-06-1-2	10 - 20	
	S-06-1-3	20 - 30	
12-POK-16 30.07.2012 Russian Corer	S-06-2-1	0 - 1	
	S-06-2-2	1 - 5	
	S-06-2-3	5 - 10	
	S-06-2-4	10 - 15	
	S-06-2-5	15 - 20	
	S-06-2-6	20 - 25	
	S-06-2-7	25 - 30	
	S-06-2-8	30 - 35	
	S-06-2-9	35 - 40	
Naumovskoje Osero 31.07.2012 Gravity Corer	S-24-1-1	0 - 1	fine decomposed plant material with coarse plant fragments, soft, brown
	S-24-1-2	1 - 3	fine decomposed plant material with coarse plant fragments, soft, brown
	S-24-1-3	3 - 5	fine decomposed plant material with coarse plant fragments, soft, brown
	S-24-1-4	5 - 7	fine decomposed plant material with coarse plant fragments, soft, brown
	S-24-1-5	7 - 9	fine decomposed plant material, soft, brown
	S-24-1-6	9 - 11	fine decomposed plant material, soft, brown
	S-24-1-7	11 - 13	fine decomposed plant material, soft, brown
	S-24-1-8	13 - 15	fine decomposed plant material, soft, brown

Site, Date, Corer	Sample	Depth (cm)	Description
	S-24-1-9	15 - 16	fine decomposed plant material, soft, brown
	S-24-1-10	16 - 17	matrix: fine decomposed plant material, coarse fragments, compact, less water, brown
	S-24-1-11	17 - 18	matrix: fine decomposed plant material, coarse fragments, compact, less water, brown
	S-24-1-12	18 - 19	matrix: fine decomposed plant material, coarse fragments, compact, less water, brown
	S-24-1-13	19 - 20	matrix: fine decomposed plant material, coarse fragments, compact, less water, brown
	S-24-1-14	20 - 21	matrix: fine decomposed plant material, coarse fragments, compact, less water, brown, greyish
	S-24-1-15	21 - 22	matrix: fine decomposed plant material, coarse fragments, compact, less water, brown, greyish
	S-24-1-16	22 - 23	matrix: fine decomposed plant material, no coarse fragments, compact, less water, brown, greyish
	S-24-1-17	23 - 24	matrix: fine decomposed plant material, no coarse fragments, compact, less water, brown, greyish
Naumovskoje Osero, 31.07.2012, Gravity Corer	S-24-2-1	0 - 2	fine decomposed plant material, soft, brown
	S-24-2-2	2 - 4	fine decomposed plant material with coarse plant fragments, soft, brown
	S-24-2-3	4 - 6	fine decomposed plant material with coarse plant fragments, soft, brown
	S-24-2-4	6 - 8	fine decomposed plant material with coarse plant fragments, soft, brown
	S-24-2-5	8 - 10	fine decomposed plant material with coarse plant fragments, soft, brown
	S-24-2-6	10 - 12	fine decomposed plant material with coarse plant fragments, brown, little silty fine sand
	S-24-2-7	12 - 14	fine decomposed plant material with coarse plant fragments, brown, little silty fine sand
	S-24-2-8	14 - 16	fine decomposed plant material with coarse plant fragments, brown, little silty fine sand
	S-24-2-9	16 - 17	fine decomposed plant material with very little coarse plant fragments, compact, brown, little silty fine sand
	S-24-2-10	17 - 18	fine decomposed plant material with very little coarse plant fragments, compact, brown, little silty fine sand
	S-24-2-11	18 - 19	fine decomposed plant material with very little coarse plant fragments, compact, brown, little silty fine sand
	S-24-2-12	19 - 20	fine decomposed plant material, compact, brown, little silty fine sand
	S-24-2-13	29 - 21	fine decomposed plant material, compact, brown, little silty fine sand
	S-24-2-14	21 - 22	fine decomposed plant material, compact and dry, brown, little silty fine sand
	S-24-2-15	22 - 23	fine decomposed plant material, compact and dry, brown, little silty fine sand
	S-24-2-16	23 - 24	fine decomposed plant material, compact and dry, brown, little silty fine sand
	S-24-2-17	24 - 25	fine decomposed plant material with coarse plant fragments, compact and dry, brown, very little silty fine sand
	S-24-2-18	25 - 26	fine decomposed plant material with coarse plant fragments, compact and dry, brown, very little silty fine sand
	S-24-2-19	26 - 27	fine decomposed plant material with coarse plant fragments, compact and dry, brown, very little silty fine sand

Site, Date, Corer	Sample	Depth (cm)	Description
	S-24-2-20	27 - 28	fine decomposed plant material with very coarse plant fragments, compact and dry, brown, very little silty fine sand
Naumovskoje Osero, 31.07.2012, Gravity Corer	S-24-3-1	0 - 1.5	modern plant material, fine decomposed plant material, soft, brown, mussel
	S-24-3-2	1.5 - 3	fine decomposed plant material with coarse fragments, brown, greyish sandy-silt, compact
	S-24-3-3	3 - 4	fine decomposed plant material with more coarse fragments, brown, greyish sandy-silt, compact
	S-24-3-4	4 - 5	fine decomposed plant material with more coarse fragments, brown, greyish sandy-silt, compact
	S-24-3-5	5 - 6	fine decomposed plant material with more coarse fragments, twig, brown, greyish sandy-silt, compact
	S-24-3-6	6 - 7	fine decomposed plant material with more coarse fragments, brown, greyish sandy-silt, compact
	S-24-3-7	7 - 8	fine decomposed plant material with more coarse fragments, brown, greyish sandy-silt, compact
	S-24-3-8	8 - 9	fine decomposed plant material with more coarse fragments, twig, brown, greyish sandy-silt, compact
	S-24-3-9	9 - 10.5	fine decomposed plant material with more coarse fragments, brown, greyish sandy-silt, compact
12-POK-20 Russian Corer A = "outer core	S-25-1a-1	0 - 5	grey silty fine sand with fine plant detritus, moist
	S-25-1a-2	5 - 10	grey silty fine sand with fine plant detritus, moist
	S-25-1a-3	10 - 15	grey silty fine sand with fine plant detritus, moist
	S-25-1a-4	15 - 17	grey silty fine sand with fine plant detritus, moist
	S-25-1a-5	17 - 19	light grey silty fine sand with fine plant detritus, dryer and more compact
	S-25-1a-6	19 - 21	light grey silty fine sand with fine plant detritus, dryer and more compact
	S-25-1a-7	21 - 23	light grey silty fine sand with fine plant detritus, dryer and more compact
	S-25-1a-8	23 - 25	light grey silty fine sand with fine plant detritus, dryer and more compact
	S-25-1a-9	25 - 28	light grey silty fine sand with fine plant detritus, dryer and more compact
12-POK-20 Russian Corer B = "inner core"	S-25-1b-1	0 - 5	decomposed plant material, small roots, brownish-grey
	S-25-1b-2	5 - 10	gradual transition from brownish plant material - more greyish silty fine sand, weakly layered
	S-25-1b-3	10 - 12	dryer, greyish, small plant fragments visible, short thin roots
	S-25-1b-4	12 - 14	dryer, greyish, small plant fragments visible, short thin roots
	S-25-1b-5	14 - 16	dryer, greyish, small plant fragments visible, short thin roots
	S-25-1b-6	16 - 18	dryer, greyish, small plant fragments visible, short thin roots
	S-25-1b-7	18 - 20	silty fine sand, light grey, dry
	S-25-1b-8	20 - 22	silty fine sand, light grey, dry
	S-25-1b-9	22 - 24	silty fine sand, light grey, dry
	S-25-1b-10	24 - 26	silty fine sand, light grey, dry
	S-25-1b-11	26 - 28	silty fine sand, light grey, dry
south of Pokhodsk, 27.07.2012 Gravity Corer	S-55-1-1	0 - 2	grey-brown fine decomposed plant material, water saturated
	S-55-1-2	2 - 3	grey-brown fine decomposed plant material, water saturated, ostracodes

Site, Date, Corer	Sample	Depth (cm)	Description
	S-55-1-3	3 - 4	grey-brown fine decomposed plant material, less water content
	S-55-1-4	4 - 5	grey-brown fine decomposed plant material, less water content
	S-55-1-5	5 - 6	grey-brown fine decomposed plant material, less water content
	S-55-1-6	6 - 7	greyish fine material with plant roots
	S-55-1-7	7 - 8	greyish fine material, silty, compact and dry
	S-55-1-8	8 - 9	greyish fine material, more silt, fine sand?, compact and dry
	S-55-1-9	9 - 10	greyish fine material, more silt, fine sand?, compact and dry
	S-55-1-10	10 - 11	greyish silty fine sand, compact and dry
	S-55-1-11	11 - 12	light grey silty fine sand, compact and dry
	S-55-1-12	12 - 13	light grey silty fine sand, compact and dry, bubbles with 1mm diameter
	S-55-1-13	13 - 14	dark grey, silty fine sand, compact and dry, bubbles with 2-3mm diameter
	S-55-1-14	14 - 15	grey silty fine sand, more compact and dry
	S-55-1-15	15 - 16	grey silty fine sand, more compact and dry
	S-55-1-16	16 - 17	grey silty fine sand, very compact, dry, sticky
	S-55-1-17	17 - 18	grey silty fine sand, very compact, dry, sticky
	S-55-1-18	18 - 19	grey silty fine sand, greyish-blueish, very compact, dry, sticky
	S-55-1-19	19 - 20	grey silty fine sand, greyish-blueish, very compact, dry, sticky
south of Pokhodsk, 27.07.2012 Gravity Corer	S-56-1-1	0 - 2	light brown, fine decomposed, small amount of plant material, water saturated
	S-56-1-2	2 - 4	light brown, fine decomposed, small amount of plant material, water saturated
	S-56-1-3	4 - 6	light brown, fine decomposed, small amount of plant material, water saturated
	S-56-1-4	6 - 8	light brown, fine decomposed, no plant material visible
	S-56-1-5	8 - 9	light greyish-brownish fine decomposed material, silty, dry, roots 0.5 mm in diameter
	S-56-1-6	9 - 10	light greyish-brownish fine decomposed material, silty, dry, roots 0.5 mm in diameter
	S-56-1-7	10 - 11	light greyish-brownish fine decomposed material, silty, dry, roots 1 mm in diameter
	S-56-1-8	11 - 12	grey, silty, dry, compact, roots 0.5 mm in diameter, bubbles 3-5 mm in diameter
	S-56-1-9	12 - 13	grey, silty, dry, compact, roots 0.5 mm in diameter, bubbles 3-5 mm in diameter
	S-56-1-10	13 - 14	grey, silty, dry, compact, roots 0.5 mm in diameter and 6-7 mm long, bubbles 3-5 mm in diameter
	S-56-1-11	14 - 15	grey, silty, dry, compact, roots 0.5 mm in diameter and 6-7 mm long, bubbles 3-5 mm in diameter
	S-56-1-12	15 - 16	grey, silty, dry, compact, roots 0.5 mm in diameter and 6-7 mm long, bubbles 3-5 mm in diameter
	S-56-1-13	16 - 17	grey, silty, dry, compact, roots 0.5 mm in diameter and 6-7 mm long, bubbles 3-5 mm in diameter
	S-56-1-14	17 - 18	grey, silty, dry, compact, roots 0.5 mm in diameter and 6-7 mm long, bubbles 3-5 mm in diameter
	S-56-1-15	18 - 19	dark grey sandy silt, bubbles 3-5 mm in diameter

Site, Date, Corer	Sample	Depth (cm)	Description
	S-56-1-16	19 - 20	dark grey sandy silt, bubbles 3-5 mm in diameter
	S-56-1-17	20 - 21	dark grey sandy silt, small amount of plant material, bubbles 3-5 mm in diameter
	S-56-1-18	21 - 22	dark grey sandy silt, bubbles 3-5 mm in diameter
	S-56-1-19	22 - 23	dark grey sandy silt, more compact and dry, bubbles 2-3 mm in diameter
	S-56-1-20	23 - 24	light grey sandy silt, more compact and dry, bubbles 2-3 mm in diameter
	S-56-1-21	24 - 25	light grey sandy silt, more compact and dry, bubbles 2-3 mm in diameter, small roots
	S-56-1-22	25 - 26	light grey sandy silt, more compact and dry, bubbles 2-3 mm in diameter, small black plant fragments
	S-56-1-23	26 - 27	light grey sandy silt, more compact and dry, bubbles smaller
	S-56-1-24	27 - 28	satin grey sandy silt, more compact and dry
	S-56-1-25	28 - 29	satin grey sandy silt, fine sand, more compact and dry
	S-56-1-26	29 - 30	greyish-blueish sandy silt with weakly decomposed plant material, brown
	S-56-1-27	30 - 31	greyish-blueish sandy silt with weakly decomposed plant material, brown
09.08.2012 Gravity corer	S-62-1-01	0 - 2	water-saturated plants, dark grey
	S-62-1-02	2 - 4	dark grey, strongly decomposed
	S-62-1-03	4 - 6	grey, silty fine-sand with plant detritus
	S-62-1-04	6 - 8	grey, silty fine-sand with plant detritus, more decomposed
	S-62-1-05	8 - 10	grey, silty fine-sand with black plant detritus, less compact
	S-62-1-06	10 - 12	grey, silty fine-sand with black plant detritus, less water content
	S-62-1-07	12 - 14	light-grey, silty fine-sand with black plant detritus, less compact
	S-62-1-08	14 - 16	light-grey, silty fine-sand with black plant detritus, compact
	S-62-1-09	16 - 17	light-grey, less sandy, clayish-silty, small black plant fragments
	S-62-1-10	17 - 18	dark-grey, fine-silty, dark-grey - black plant fragments
	S-62-1-11	18 - 19	dark - medium grey silty fine-sand, dark parts with black plant fragments, medium grey with gas bubbles
	S-62-1-12	19 - 20	dark - medium grey silty fine-sand, dark parts with black plant fragments, medium grey with gas bubbles
	S-62-1-13	20 - 21	dark - medium grey silty fine-sand, dark parts with black plant fragments, medium grey with gas bubbles
	S-62-1-14	21 - 22	grey, sandy silty, small black plant fragments
	S-62-1-15	22 - 23	grey, sandy silty, small black plant fragments, compact
	S-62-1-16	23 - 24	grey, sandy silty, small black plant fragments, compact
	S-62-1-17	24 - 25	grey, silty sand, compact, dense
	S-62-1-18	25 - 26	grey, silty sand, compact, dense
	S-62-1-19	26 - 27	grey, sand, many plant fragments, compact
09.08.2012 Gravity corer	S-62-2-01	0 - 2	brown-grey, sandy silt, water saturated plant material
	S-62-2-02	2 - 4	brown-grey, sandy silt, water saturated plant material
	S-62-2-03	4 - 6	brown-grey, sandy silt
	S-62-2-04	6 - 8	brown-grey, sandy silt with thin white roots
	S-62-2-05	8 - 10	brown-grey, sandy silt with thin white roots

Site, Date, Corer	Sample	Depth (cm)	Description
	S-62-2-06	10 - 12	brown-grey, sandy silt, more thin white roots
	S-62-2-07	12 - 14	brown-grey, sandy silt, compact
	S-62-2-08	14 - 16	brown-grey, sandy silt, compact, more sandy
	S-62-2-09	16 - 18	brown-grey, sandy silt, compact, more sandy
	S-62-2-10	18 - 19	brown-grey, sandy silt, compact
	S-62-2-11	19 - 20	brown-grey, sandy silt, compact
	S-62-2-12	20 - 21	brown-grey, sandy silt, compact
	S-62-2-13	21 - 22	brown-grey, sandy silt, thin white roots
	S-62-2-14	22 - 23	brown-grey, sandy silt, thin white roots
	S-62-2-15	23 - 24	brown-grey, sandy silt, thin white roots
	S-62-2-16	24 - 25	brown-grey, sandy silt, thin white roots
	S-62-2-17	25 - 26	coarse plant fragments, no sand, well-decomposed, thin roots
	S-62-2-18	26 - 27	coarse plant fragments, no sand, well-decomposed, thin roots
	S-62-2-19	27 - 28	grey, fine-sand, roots
	S-62-2-20	28 - 29	grey, fine-sand, roots
	S-62-2-21	29 - 30,3	greyish-blue, fine-sand
Ozero Sednoe 10.08.2012 Gravity Corer	S-66-1-01	0 - 2	black, fine sand, plant fragments
	S-66-1-02	2 - 4	black, fine sand, plant fragments, aggegates (2-3 mm)
	S-66-1-03	4 - 6	dark grey, fine sand, plant fragments, no aggregates
	S-66-1-04	6 - 8	dark grey, fine sand, plant fragments, no aggregates
	S-66-1-05	8 - 10	dark grey, fine sand, plant fragments, no aggregates
	S-66-1-06	10 - 11	grey, medium - fine sand, no plant remains
	S-66-1-07	11 - 12	grey, medium - fine sand, no plant remains
	S-66-1-08	12 - 14	grey, compact, aggregates (4-5 mm) with white points
	S-66-1-09	14 - 16	grey, dryer, sandy, compact, stinky, aggregates
	S-66-1-10	16 -n18	grey, sandy, aggregates (1 x 1,5 mm), transition zone - homogenous part
	S-66-1-11	18 - 19	grey, fine sand, withe points, homogenous, no aggregates
	S-66-1-12	19 - 20	grey, fine sand, withe points, homogenous, no aggregates, wood fragments (twigs)
	S-66-1-13	20 - 21	grey, fine sand, plant fragments, aggregates
	S-66-1-14	21 - 22	grey, fine sand, plant fragments, aggregates
	S-66-1-15	22 - 23	grey, fine sand, plant fragments, aggregates
	S-66-1-16	23 - 24	light grey, fine sand, no plant material, white points, large aggregates (1,5 x 1 cm)
	S-66-1-17	24 - 25	light grey, fine sand, no plant material, white points (1-2 mm)
	S-66-1-18	25 - 26	light grey, fine sand, no plant material, white points (1-2 mm)
	S-66-1-19	26 - 27	light grey, fine sand, no plant material, white points (1-2 mm)
	S-66-1-20	27 - 28	light grey, fine sand, no plant material, white points (1-2 mm)
	S-66-1-21	28 - 29,5	
Ozero Sednoe	S-66-2-01	0 - 2	modern plants, green, no decomposed
	S-66-2-02	2 - 4	dark brown, weakly decomposed plant material, water

Site, Date, Corer	Sample	Depth (cm)	Description
10.08.2012 Gravity Corer			saturated
	S-66-2-03	4 - 6	dark brown, weakly decomposed plant material (5-8 mm), water saturated
	S-66-2-04	6 - 8	dark brown, small palnt fragments, silty, water saturated
	S-66-2-05	8 - 10	dark brown, small palnt fragments, silty, water saturated
	S-66-2-06	10 - 12	dark brown, compact, silty, small plant fragments
	S-66-2-07	12 - 14	dark grey, silty fine sand, without plants
	S-66-2-08	14 - 16	dark grey, silty fine sand, without plants
	S-66-2-09	16 - 18	dark grey, silty, small wood fragments
	S-66-2-10	18 - 20	grey, silty fine sand, air bubbles /1-2 mm), dryer, plant fragments (leafs, short roots)
	S-66-2-11	20 - 22	dark grey, silty fine sand, many roots and leaf fragments, weakly decomposed
	S-66-2-12	22 - 24	dark grey, silty fine sand, many roots and leaf fragments, weakly decomposed
	S-66-2-13	24 - 26	dark grey, silty fine sand, many roots and leaf fragments, weakly decomposed
	S-66-2-14	26 - 27	grey, fine sand, weakly decomposed plant fragments
	S-66-2-14	27 - 28	grey, medium - fine grained sand, small root fragments
	S-66-2-16	28 - 29	grey, medium - fine grained sand, small root fragments, with aggregates (2 x 10 mm)
	S-66-2-17	29 - 30	grey, medium - fine grained sand, small root fragments, with aggregates (2 x 10 mm)
	S-66-2-18	30 - 31	grey, medium - fine grained sand, small root fragments, with aggregates (2 x 10 mm)
	S-66-2-19	31 - 32	grey, fine sand, more decomposed, short thin roots, shells (1,5 mm)
Ozero Sednoe 10.08.2012 Gravity Corer	S-66-3-01	0 - 2	modern water plants
	S-66-3-02	2 t0 4	dark brown, silty, water saturated, decomposed plant fragments
	S-66-3-03	4 - 6	dark brown, silty, water saturated, decomposed plant fragments
	S-66-3-04	6 - 8	dark brown, silty, water saturated, decomposed plant fragments
	S-66-3-05	8 - 10	dark brown, silty, water saturated, decomposed plant fragments
	S-66-3-06	10 - 12	dark brown, silty, water saturated, without plant fragments
	S-66-3-07	12 - 14	brown grey, silty, leafs
	S-66-3-08	14 - 16	brown grey, short thin plant fragments, more decomposed, silty
	S-66-3-09	16 - 18	dark grey, peat, well-decomposed
	S-66-3-10	18 - 20	dark grey, peat, well-decomposed
	S-66-3-11	20 - 22	dark grey, peat, well-decomposed
	S-66-3-12	22 - 24	dark grey, peat, well-decomposed
	S-66-3-13	24 - 26	dark grey, peat, well-decomposed
	S-66-3-14	26 - 28	brown grey, peat, well-decomposed
	S-66-3-15	28 - 30	brown grey, peat, well-decomposed
	S-66-3-16	30 - 32	grey, silty fine sand, peaty
	S-66-3-17	32 - 33	grey, silty fine sand, peaty
	S-66-3-18	33 - 34	grey, silty fine sand, peaty

Site, Date, Corer	Sample	Depth (cm)	Description
	S-66-3-19	34 - 36	grey, silty fine sand, peaty
	S-66-3-20	35 - 37	grey, silty fine sand, peaty
Ozero Bol'shoe Pokhodskoe, 15.08.2012, Gravity Corer	S-31-1-01	0 - 2	dark-grey, fine sand, wet, no organics, ostracods (?)
	S-31-1-02	2 - 3	grey, fine sand, moist, no organics, ostracods (?)
	S-31-1-03	3 - 4	grey, fine sand, moist, no organics
	S-31-1-04	4 - 5	grey, fine sand, moist, no organics
	S-31-1-05	5 - 6	grey, fine sand, moist, single plant fragments, light-brown (2-3 mm)
	S-31-1-06	6 - 7	grey, fine sand, moist, single plant fragments
	S-31-1-07	7 - 8	grey, fine sand, moist, single moss fragments, leafs, roots
	S-31-1-08	8 - 9	grey, fine sand, moist, single root fragments
	S-31-1-09	9 - 10	grey, fine sand, moist, single root fragments
	S-31-1-10	10 - 11	grey, fine sand, moist, single root fragments
	S-31-1-11	11 - 12	grey, fine sand, moist, single wood fragments (Ø 3 mm, length 5 mm)
	S-31-1-12	12 - 13	grey, fine sand, moist, single wood fragments (Ø 5 mm, length 5 mm)
	S-31-1-13	13 - 14	grey, fine sand, moist, single wood fragments (Ø 5 mm, length 10 mm)
	S-31-1-14	14 - 15	grey fine-sand, brownish spot, moist, single root fragments
Ozero Bol'shoe Pokhodskoe, 15.08.2012, Gravity Corer	S-31-2-01	0 - 2	grey, fine-sand with micas, green fresh plant fragments
	S-31-2-02	2 - 4	grey, fine-sand with micas, brownish patches
	S-31-2-03	4 - 5	grey, fine-sand with micas, brownish patches
	S-31-2-04	5 - 6	grey, fine-sand, compact, small bubbles
	S-31-2-05	6 - 7	grey, fine-sand, compact, small bubbles
	S-31-2-06	7 - 8	grey, fine-sand with micas, compact, dry
	S-31-2-07	8 - 9	grey, fine-sand with micas, compact, dry
	S-31-2-08	9 - 10	grey, fine-sand with micas, compact, dry
	S-31-2-09	10 - 11	grey, fine-sand with micas, compact, dry
	S-31-2-10	11 - 12	grey, fine-sand with micas, compact, dry
	S-31-2-11	12 - 13	grey, fine-sand with mica, less compact, wet
Ozero Bol'shoe Pokhodskoe, 15.08.2012, Gravity Corer	S-31-3-01	0 - 2	green-brown, medium-sand, moist, no organics
	S-31-3-02	2 - 4	green-brown, medium-sand, moist, no organics
	S-31-3-03	4 - 6	green-brown, medium-sand, moist, no organics
	S-31-3-04	6 - 7	green-brown, medium-sand, moist, no organics
	S-31-3-05	7 - 8	green-brown, medium-sand, moist, no organics
	S-31-3-06	8 - 9	grey (margin), brown (center), medium-sand, dry, no organics
	S-31-3-07	9 - 10	bluish-grey, medium sand with small micas, no organics, dry,
	S-31-3-08	10 - 12	bluish-grey, medium sand with small micas, no organics, dry,
	S-31-3-09	12 - 14	bluish-grey, medium sand with small micas, no organics, dry,
	S-31-3-10	14 - 16	bluish-grey, medium sand with small micas, no organics, dry,
	S-31-3-11	16 - 18	bluish-grey, medium sand with small micas, single plant fragments

Site, Date, Corer	Sample	Depth (cm)	Description
	S-31-3-12	18 - 20	grey, medium sand with small micas, single plant fragments
	S-31-3-13	20 -22	grey, medium sand with small micas, dry, no organics
	S-31-3-14	22 - 24	grey, medium sand with small micas, dry, no organics
	S-31-3-15	24 - 26	grey, medium sand with small micas, dry, no organics
	S-31-3-16	26 - 28	grey, medium sand with small micas, dry, no organics
	S-31-3-17	28 - 30	grey, medium sand with small micas, dry, no organics
	S-31-3-18	30 - 32	grey, medium sand with small micas, dry, no organics
	S-31-3-19	32 - 33	grey, medium sand with brownish fine-sand at the margin, no organics, dry
	S-31-3-20	33 - 34	dark-brown, fine-sand, dry, no organics
	S-31-3-21	34 - 35	dark-brown, fine-sand, dry, small organic fragments
	S-31-3-22	35 - 37	dark-brown, fine-sand, dry, grey medium-sand, small organic fragments
	S-31-3-23	37 - 38	dark grey, medium-sand, no organics
	S-31-3-24	38 - 39	grey, fine-sand, dry, no organics, small micas
	S-31-3-25	39 - 40	grey, fine-sand, dry, no organics, small micas
	S-31-3-26	40 - 41	grey, fine-sand, dry, no organics, small micas
	S-31-3-27	41 - 42	grey, fine-sand, dry, no organics, small micas
monitoring site 12-Pok-01 21.08.2012	POK-259-1	0 - 2	dark-greyish-brown, strong decomposed , wet, some organic inclusions, no sand, no silt
	POK-259-2	2 - 3	dark-brown, compact, 1mm organic inclusions and 1.5-2 cm long roots
	POK-259-3	3 - 4	brown, weakly decomposed, some sand
	POK-259-4	5 - 5	brown, weakly decomposed, some sand
	POK-259-5	5 - 6	grey-brown, organic, some fine sand
	POK-259-6	6 - 7	grey-brown, dense organic, root remains
	POK-259-7	7 - 8	grey-brown, dense organic, root remains
	POK-259-8	8 - 9	grey-brown, dense organic, root remains
	POK-259-9	9 - 11	grey-brown, dense organic, root remains
monitoring site 12-Pok-01 21.08.2012	POK-309-1	0 - 2	light-brown, weakly decomposed, wet
	POK-309-2	2 - 4	dark-brown, wet, weakly decomposed, plant fragments,
	POK-309-3	4 - 6	brown, more compact, well decomposed, some lighter plant remains, wet
	POK-309-4	6 - 8	light-brown, well-decomposed, light roots, vertical twigs (4.5 cm, ø 4 mm)
	POK-309-5	8 - 10	light-brown, dense organic, light roots
	POK-309-6	10 - 12	light-brown, dense organic, light roots
	POK-309-7	12 - 13,5	dark-brown, various decomposed, roots and other plant fragments
Thermokarst lake at the pingo site 21.08.2012 Gravity corer	S-80-2-1	0 - 2	dark-grey, not decomposed plant matter, water saturated
	S-80-2-2	2 - 4	dark-grey, wet, sandy, small plant fragments, moderate decomposed
	S-80-2-3	4 - 6	dark-grey, wet, sandy, more compact, wet, less organic
	S-80-2-4	6 - 8	dark-grey, wet, sandy, more compact, wet, less organic
	S-80-2-5	8 - 10	dark-grey, wet, sandy, compact, no organic visible
	S-80-2-6	10 - 12	dark-grey, wet, sandy, some plant fragments, weakly decomposed
	S-80-2-7	12 - 14	dark-grey, silty, wet no plant remains

Site, Date, Corer	Sample	Depth (cm)	Description
	S-80-2-8	14 - 16	grey, silty, dark-brown root fragments, wet
	S-80-2-9	16 - 18	grey, silty, dark-brown root fragments, wet
	S-80-2-10	18 - 20	grey, sandy, thing long plant fragments, not decomposed
	S-80-2-11	20 - 22	light-grey, sandy, more compact, more plant fragments
	S-80-2-12	22 - 24	light-grey, silty sand, plant fragments
	S-80-2-13	24 - 26	grey, silty sand, compact, small dark plant fragments
	S-80-2-14	26 - 28	light-grey, silt, less decomposed, leafs and other plant fragments
	S-80-2-15	28 - 30	grey, silty sand, compact, dryer, numerous small plant fragments
	S-80-2-16	30 - 32	light-grey, silt, compact, dry, not decomposed plant fragments
	S-80-2-17	32 - 33	light-grey, silty sand, compact, dry, inclusions of dark less decomposed plant fragments
	S-80-2-18	33 - 34	light-grey, silty sand, compact, dry, inclusions of dark less decomposed plant fragments, with aggregates
	S-80-2-19	34 - 35	light-grey, silty, compact, dry, with aggregates, some small plant fragments
	S-80-2-20	35 - 36	light-grey, silty sand, compact, dry, with aggregates, thin short roots
	S-80-2-21	36 - 37	light-grey, silty sand, dryer, small leaf fragments
	S-80-2-22	37 - 38	light-grey, silty sand, dryer, small leaf fragments
Thermokarst lake at the pingo site, 21.08.2012, Gravity corer	S-80-1-1	0 - 2	greenish-grey, water saturated, organic
	S-80-1-2	2 - 4	grey, silt, water saturated, plant remains, various decomposed
	S-80-1-3	4 - 6	grey, silty sand, few organic, various decomposed, water saturated, thin black roots
	S-80-1-4	6 - 8	grey, silty sand, , water saturated, few organic, various decomposed thin black roots
	S-80-1-5	8 - 10	grey, silty sand, water saturated, few organic, various decomposed, thin black roots
	S-80-1-6	10 - 12	grey, silty sand, water saturated, few organic, various decomposed , thin black roots
	S-80-1-7	12 - 14	grey, silty sand, organic, water saturated decomposed,
	S-80-1-8	14 - 16	grey-brown silt, water saturated, organic, decomposed
	S-80-1-9	16 - 18	grey-brown silt, water saturated, organic, decomposed, thin black roots
	S-80-1-10	18 - 20	grey-brown silt, water saturated, organic, decomposed, thin black roots and some plant macro remains
	S-80-1-11	20 - 22	grey-brown silt, water saturated, organic, decomposed, thin black roots and some plant macro remains
	S-80-1-12	22 - 24	brown, silt, less water saturated, no plant macro remain
	S-80-1-13	24 - 26	brown, silt, less water saturated, no plant macro remain
	S-80-1-14	26 - 28	brown, silt, less water saturated, no plant macro remain
	S-80-1-15	28 - 30	brown, silt, less water saturated, no plant macro remain
	S-80-1-16	30 - 32	brown, silt, small organic remains, less water saturated, small gas bubbles (2 mm)
	S-80-1-17	32 - 34	brown, silt, small organic remains, less water saturated, small gas bubbles (2 mm)
	S-80-1-18	34 - 36	brown, silt, small organic remains, less water saturated, small gas bubbles (2 mm)
	S-80-1-19	36 - 38	brown, silt, small organic remains, less decomposed, less water saturated, small gas bubbles (2 mm)

Site, Date, Corer	Sample	Depth (cm)	Description
	S-80-1-20	38 - 40	brown, silty sand, not decomposed, less water saturated, leaf fragments, organic detritus
	S-80-1-21	40 - 42	brown, silty sand, not decomposed, less water saturated, leaf fragments, organic detritus
	S-80-1-22	42 - 44	brown, silty sand, less water saturated, decomposed organic detritus
	S-80-1-23	44 - 46	gray, silty sand, rather dry, decomposed organic detritus
Thermokarst lake at the pingo site, 21.08.2012, Gravity corer	S-80-3-1	0 - 2	light-brown, well-decomposed organic, small plant remains, water saturated, ostracods
	S-80-3-2	2 - 4	brown, silty sand, well decomposed, water saturated, small plant remains
	S-80-3-3	4 - 6	brown, silty sand, well decomposed, water saturated, small plant remains
	S-80-3-4	6 - 8	brown, silty sand, well decomposed, water saturated, small plant remains
	S-80-3-5	8 - 10	core segment with brown margin and dark-gray center, silty sand, dark small plant remains, water saturated
	S-80-3-6	10 - 12	core segment with brown margin and dark-gray center, silty sand, dark small plant remains, water saturated
	S-80-3-7	12 - 14	light-brown, silty sand. less water saturated, small plant remains
	S-80-3-8	14 - 16	light-brown, silty sand. less water saturated, less decomposed, small and larger plant remains
	S-80-3-9	16 - 18	light-brown, silty sand. less water saturated, less decomposed, small and larger plant remains
	S-80-3-10	18 - 20	light-brown, silty sand. less water saturated, less decomposed, small and larger plant remains
	S-80-3-11	20 - 22	light-brown, less decomposed, plant macro-remains visible
	S-80-3-12	22 - 24	light-brown, less decomposed, plant macro-remains visible
	S-80-3-13	24 - 26	light-brown, less decomposed, plant macro-remains visible
	S-80-3-14	26 - 28	light-brown, less decomposed plant macro-remains visible
	S-80-3-15	28 - 30	gray silt, many less decomposed plant macro-remains, rather dry
	S-80-3-16	30 - 32	gray silt, many less decomposed plant macro-remains, rather dry

APPENDIX 6

Plant taxa in the collapsed polygon complex MNP12

Enrico Behrens, Pim de Klerk & Hans Joosten

Vascular and lycophyte plants:

Asteraceae: Asteraceae spec.
Betulaceae: *Betula exilis*, *Duschekia fruticosa*
Caryophyllaceae: Caryophyllaceae spec.
Cyperaceae: *Carex chordorrhiza*, *Carex* spec., *Eriophorum angustifolium*, *E*. *vaginatum*, *E*. cf. *callitrix*, *E*. spec.
Ericales: *Andromeda polifolia*, *Arctostaphylos uva-ursi*, *Chamaedaphne calyculata*, *Empetrum nigrum*, *Ledum decumbens*, *Pyrola* cf. *rotundifolia*, *Vaccinium uliginosum*, *V*. *vitis-ideae*
Grossulariaceae: *Ribes* cf. *triste*
Huperziaceae: *Huperzia* spec.
Juncaceae: *Luzula* spec.
Lentibulariaceae: *Utricularia intermedia*
Orobanchaceae: cf. *Boschniakia rossica*, *Pedicularis* spec.
Poaceae: Poaceae spec.
Ranunculaceae: *Caltha* spec., *Ranunculus pallassii*, *Ranunculus* spec.
Rosaceae: *Comarum palustre*, *Rubus chamaemorus*
Salicaceae: *Salix* spec.
Valerianaceae: *Valeriana capitata*

Mosses

Bryales: *Aulacomnium* spec.
Hypnales: *Calliergon* spec., *Campylium* spec., *Drepanocladus* spec., *Homalothecium nitens*
Marchantiales: *Marchantia* spec.
Sphagnales: *Sphagnum* spec.
Splachnales: *Meesia triquetra*

APPENDIX 7

Soil samples for rhizopode and nutrient analyses

Lillith Pogasyan, Fabian Beermann

A 5-1: Soil samples for rhizopode analyses

Site	Relief	Sample	Horizon	pH	Soil Name (American/Russian)	Depth (cm)	N	E
P1	Highl wall	1	Oi	5,6	Typic Histoturbels /Peat Cryozem homogeneous	0-5	69˚05'50,9"	160˚56'25,7"
		2	Oe	6,7		5-10		
		3	Oa	6,9		10-16		
		4	Bh	6,1		16-20		
P2	Centre	5	Oi	5,9	Fluvaquentic Sapristels /Peat Eutrothic typic	0-15	69˚05'50,7"	160˚56'26,2"
		6	Oe	5,9		15-25		
		7	Oa	6,0		25-45		
P3	Small wall	8	Oi	6,3	Fluvaquentic Hemistels /Peat Eutrothic typic	0-8	69˚05'50,7"	160˚56'26,4"
		9	Oe	5,7		8-15		
		10	Oa	5,8		15-40		
P4	Small wall	11	Oi	6,5	Typic Hemistels /Peat Eutrothic typic	0-9	69˚05'50,4"	160˚56'25,8"
		12	Oe	5,7		9-20		
		13	Oa	5,7		20-45		
P5	Centre	14	Oe	5,8	Typic Hemistels /Peat Eutrothic typic	0-8	69˚05'50,2"	160˚56'25,8"
		15	Oe2	5,9		8-38		
P6	Highl wall	16	Oa	4,6	Typic Aquiturbels /Peat Cryozem gley	0-4	69˚05'44,6"	160˚56'27,4"
		17	Bg	6,2		4-26		
P7	Small wall	18	Oi	4,3	Sphagnic Fibristels /Peat Eutrothic typic	0-12	69˚05'44,6"	160˚56'27,7"
		19	Oe	5,2		12-19		
		20	Oa	5,3		19-24		
P8	Centre	21	moss	5,2	Typic Fibristels /Peat Eutrothic typic	10-0	69˚05'44,7"	160˚56'28,1"
		22	Oi	5,5		0-23		
		23	Oa	5,6		23-40		
P9	Small wall	24	Oi	4,5	Typic Historthels /Peat Cryozem gley	0-10	69˚05'44,5"	160˚56'29,2"
		25	Oa	5,3		10-20		
		26	Bg	6,2		20-25		
P10	Small wall	27	Oi	5,4	Typic Historthels /Peat Cryozem gley	0-12	69˚05'44,9"	160˚56'30,7"
		28	Oi2	5,8		12-29		
		29	Oa/Bg	5,8		29-35		
		30	Bg	6,1		35-42		
P11	Highl wall	31	Oa	5,5	Typic Histoturbels /Peat Cryozem gley	0-9	69˚05'45,3"	160˚56'29,2"
		32	Oa/Bg	5,9		9-14		
		33	Bg	6,0		14-25		
P12	Centre	34	Oi	5,3	Typic Historthels /Peat Cryozem gley	0-23	69˚05'45,5"	160˚56'29,6"
		35	Oi2	5,8		23-30		
		36	Bg	6,1		30-33		

Site	Relief	Sample	Horizon	pH	Soil Name (American/Russian)	Depth (cm)	N	E
P13	Highl wall	37	Oi	6,2	Typic Histoturbels /Peat Cryozem gley	0-5	69˚05'45,8"	160˚56'30,4"
		38	Bh	6,6		5-8		
		39	Oa	6,3		8-13		
		40	Bg	5,8		13-16		
P14	Small wall	41	moss	4,2	Typic Historthels /Peat Cryozem gley	5-0	69˚05'46,2"	160˚56'30,2"
		42	Oi	4,7		0-10		
		43	Oe	5,3		10-16		
		44	Oa	5,3		16-22		
		45	Bg	5,6		22-30		
P15	Centre	46	Oi	5,4	Typic Historthels /Peat Cryozem gley	0-13	69˚05'46,5"	160˚56'29,9"
		47	Oe	5,7		13-33		
		48	Bg	6,1		33-36		
P16	Highl wall	49	moss	4,9	Sphagnic Fibristels /Peat Cryozem gley	2-0	69˚05'46,8"	160˚56'30,3"
		50	Oi	4,3		0-11		
		51	Oe	4,7		11-18		
		52	Bg	5,7		18-21		
P17	Small wall	53	Oi	5,2	Typic Hemistels /Peat Eutrothic typic	0-6	69˚05'46,5"	160˚56'31,3"
		54	Oe	4,8		6-15		
		55	Oa	5,1		15-20		
P18	Highl wall	56	Oi	4,4	Typic Aquiturbels /Peat Cryozem gley	0-3	69˚05'46,8"	160˚56'25,5"
		57	Oa	4,4		3-7		
		58	Bg(top)	4,7		7-50		
		58(2)	Bg(depth)	6,3		40-50		
P19	Small wall	59	Oi	4,2	Sphagnic Fibristels /Peat Eutrothic typic	0-10	69˚05'47,0"	160˚56'25,5"
		60	Oe	4,7		10-20		
		61	Oi	5,4		20-28		
P20	Highl wall	62	Oi	4,2	Typic Histoturbels /Peat Cryozem gley	0-6	69˚05'48,0"	160˚56'25,4"
		63	Oa	4,8		6-11		
		64	Bg	4,3		11-26		
P21	Small wall	65	moss	5,8	Typic Historthels /Peat Cryozem gley	4-0	69˚05'47,6"	160˚56'25,3"
		66	Oi	5,8		0-6		
		67	Oe	5,3		6-20		
		68	Oa	5,5		20-24		
		69	Bg	6,0		24-33		
P22	Highl wall	70	Oi	3,9	Typic Folistels /Dry peaty typic	0-20	69˚05'47,2"	160˚56'24,6"
		71	Oe	3,9		15-20		
		72	Oa	4,1		20-35		
P23	Small wall	73	Oi	4,5	Typic Sapristels /Peat Eutrothic typic	0-8	69˚05'48,3"	160˚56'25,2"
		74	Oe	5,5		8-12		
		75	Oa	5,9		12-25		
P24	Small wall	76	Oi	6,2	Fluvaquentic Hemistels /Peat Cryozem homogeneous	0-6	69˚05'50,0"	160˚56'24,4"
		77	Oa	6,0		6-10		
		78	Bh	6,4		10-16		

Site	Relief	Sample	Horizon	pH	Soil Name (American/Russian)	Depth (cm)	N	E
		79	Oe	6,0		16-30		
		80	Oa	6,1		30-35		
P25	Small wall	81	Oi	4,8	Typic Historthels /Peat Cryozem homogeneous	0-2	69˚05'49,7"	160˚56'24,0"
		82	Oe	4,6		2-11		
		83	Oa	5,6		11-19		
		84	Bh	5,4		19-22		
P26	Small wall	85	moss	6,2	Typic Historthels /Peat Cryozem gley	8-0	69˚05'49,6"	160˚56'24,8"
		86	Oi	6,2		0-8		
		87	Oe	5,7		8-16		
		88	Bg	6,2		16-34		
P27	Small wall	89	Oi	4,9	Typic Hemistels /Peat Eutrothic typic	0-10	69˚05'49,6"	160˚56'25,9"
		90	Oa	6,5		10-15		
		91	Oe	5,8		15-25		
P28	Small wall	92	Oe	5,1	Typic Hemistels /Peat Eutrothic typic	0-4	69˚05'49,5"	160˚56'26,8"
		93	Oa	6,5		4-12		
		94	Oe	6,0		12-18		
P29	Small wall	95	moss	5,0	Typic Historthels /Peat Cryozem gley	10-0-5	69˚05'49,1"	160˚56'27,1"
		96	Oi	4,8		0-10		
		97	Oa	6,4		10-16		
		98	Bh	6,3		16-26		
P30	Centre	99	Oi	5,4	Typic Fibristels /Peat Eutrothic typic	0-29	69˚05'49,1"	160˚56'26,7"
P31	Highl wall	100	Oi	4,4	Typic Historthels /Peat Cryozem homogeneous	0-2	69˚05'48,9"	160˚56'25,9"
		101	Oe	4,4		2-8		
		102	Oa	4,9		8-25		
		103	Bh	5,7		25-28		
P32	Small wall	104	moss	5,7	Typic Sapristels /Peat Eutrothic typic	4-0	69˚05'48,2"	160˚56'27,2"
		105	Oi	5,4		0-6		
		106	Oa	5,6		6-19		
P33	Highl wall	107	Oe	4,5	Typic Aquiturbels /Peat Cryozem gley	0-10	69˚05'47,9"	160˚56'27,0"
		108	Bg	5,7		10-26		
P34	Small wall	109	Oi	4,8	Typic Historthels /Peat Cryozem homogeneous	0-5	69˚05'47,4"	160˚56'27,0"
		110	Oa	6,1		5-20		
		111	Bh	6,0		20-35		
P35	Highl wall	112	Oe	4,4	Typic Aquiturbels /Peat Cryozem gley	0-8	69˚05'47,8"	160˚56'28,4"
		113	Bg	6,3		8-44		
P36	Centre	114	Oe	5,5	Typic Historthels /Peat Cryozem gley	0-23	69˚05'47,1"	160˚56'28,8"
		115	Oe2	5,5		23-29		
		116	Oa	5,6		29-33		
		117	Bg	5,9		33-37		
P37	Small wall	118	Oe	5,6	Typic Historthels /Peat Cryozem homogeneous	0-7	69˚05'46,9"	160˚56'28,3"
		119	Oa	6,1		7-18		
		120	Bh	5,7		18-24		

Site	Relief	Sample	Horizon	pH	Soil Name (American/Russian)	Depth (cm)	N	E
P38	Centre	121	Oi	4,0	Typic Aqiturbels /Peat Cryozem gley	0-9	69˚05'45,7"	160˚56'28,5"
		122	Bg	4,9		9-48		
P39	Small wall	123	Oi	5,6	Fluvaquentic Fibristels /Peat Cryozem gley	0-13	69˚05'46,2"	160˚56'29,2"
		124	Bg	5,3		13-27		
		125	Oa	5,6		27-31		
P40	Small wall	126	Oi	4,4	Typic Historthels /Peat Cryozem gley	0-4	69˚05'46,4"	160˚56'27,3"
		127	Oe	4,9		4-14		
		128	Oa	6,9		14-20		
		129	Bh	6,4		20-29		
		130	Bg	6,6		29-35		
P41	Small wall	131	Oi	6,0	Fluvaquentic Hemistels /Peat Cryozem homogeneous	0-6	69˚05'46,6"	160˚56'28,2"
		132	Bh	6,0		6-10		
		133	Oe	5,8		10-26		

A 5-2: Soil samples for nutrient analyses

Sample	Nr	Type	Area	Date	Water content (wt %)	pH	EC (µS/cm)
POKF2 Wall 1507 I Oi	301	Monitoring	1	15.07.2012	67.74	6.3	58
POKF2 Wall 1507 I Oe	302	Monitoring	2	15.07.2012	68.29	5.9	39
POKF2 Wall 1507 I Oa	303	Monitoring	3	15.07.2012	73.85	6.1	35
POKF2 Wall 1507 II Oi	304	Monitoring	1	15.07.2012	75.76	6.3	50
POKF2 Wall 1507 II Oe	305	Monitoring	2	15.07.2012	74.47	6.0	31
POKF2 Wall 1507 II Oa	306	Monitoring	3	15.07.2012	72.09	6.0	37
POKF2 Wall 1507 III Oi	307	Monitoring	1	15.07.2012	67.57	5.5	70
POKF2 Wall 1507 III Oe	308	Monitoring	2	15.07.2012	67.86	5.8	39
POKF2 Wall 1507 III Oa	309	Monitoring	3	15.07.2012	76.00	5.8	36
POKF2 Centre 1507 I Oi	310	Monitoring	4	15.07.2012	89.47	5.5	31
POKF2 Centre 1507 I Oe/Oa	311	Monitoring	5	15.07.2012	86.89	6.0	49
POKF2 Centre 1507 II Oi	312	Monitoring	4	15.07.2012	88.00	5.8	28
POKF2 Centre 1507 II Oe/Oa	313	Monitoring	5	15.07.2012	89.61	5.9	27
POKF2 Centre 1507 II Oi	314	Monitoring	4	15.07.2012	90.48	5.8	23
POKF2 Centre 1507 II Oe/Oa	315	Monitoring	5	15.07.2012	88.24	5.8	29
POKF1 Wall Oi	316	Limitation	-	16.07.2012	NA	NA	NA
POKF1 Wall Oe	317	Limitation	-	16.07.2012	NA	NA	NA
POKF1 Wall Bh	318	Limitation	-	16.07.2012	NA	NA	NA
POKF1 Centre Oi	319	Limitation	-	16.07.2012	NA	NA	NA
POKF1 Centre Oa1	320	Limitation	-	16.07.2012	NA	NA	NA
POKF1 Centre Oa2	321	Limitation	-	16.07.2012	NA	NA	NA
POKF1 Wall 0-5	322	Core	0-50	17.07.2012	70.27	4.5	68
POKF1 Wall 5-10	323	Core	0-50	17.07.2012	76.74	4.9	35
POKF1 Wall 10-15	324	Core	0-50	17.07.2012	75.56	5.3	21
POKF1 Wall 15-20	325	Core	0-50	17.07.2012	26.32	6.4	11
POKF1 Wall 20-25	326	Core	0-50	17.07.2012	23.64	6.5	12
POKF1 Wall 25-30	327	Core	0-50	17.07.2012	21.24	6.8	17
POKF1 Wall 30-35	328	Core	0-50	17.07.2012	22.73	6.8	15
POKF1 Wall 40-45	329	Core	0-50	17.07.2012	28.95	7.0	17
POKF1 Wall 45-50	330	Core	0-50	17.07.2012	22.62	6.9	21
POKF1 Wall 50-54	331	Core	50-100	17.07.2012	28.00	6.6	25
POKF1 Wall 54-60	332	Core	50-100	17.07.2012	65.22	6.3	47
POKF1 Wall 60-65	333	Core	50-100	17.07.2012	71.70	6.2	48
POKF1 Wall 65-70	334	Core	50-100	17.07.2012	78.38	6.4	54
POKF1 Wall 70-75	335	Core	50-100	17.07.2012	73.42	6.1	56
POKF1 Wall 75-80	336	Core	50-100	17.07.2012	82.35	6.0	47
POKF1 Wall 80-86	337	Core	50-100	17.07.2012	52.46	6.3	63
POKF1 Centre Al I	338	Core	0-50	17.07.2012	77.60	6.1	30
POKF1 Centre AL II	339	Core	0-50	17.07.2012	86.75	5.9	24
POKF1 Centre AL III	340	Core	0-50	17.07.2012	73.46	6.0	29
POKF1 Centre 50-55	341	Core	0-50	17.07.2012	80.29	5.7	32
POKF1 Centre 55-60	342	Core	50-100	17.07.2012	56.54	5.8	36

Sample	Nr	Type	Area	Date	Water content (wt %)	pH	EC (µS/cm)
POKF1 Centre 60-65	343	Core	50-100	17.07.2012	75.79	5.6	43
POKF1 Centre 65-70	344	Core	50-100	17.07.2012	74.25	5.6	40
POKF1 Centre 70-75	345	Core	50-100	17.07.2012	72.66	5.9	26
POKF1 Centre 75-80	346	Core	50-100	17.07.2012	80.00	5.7	19
POKF1 Centre 80-85	347	Core	50-100	17.07.2012	79.87	5.7	19
POKF1 Centre 85-90	348	Core	50-100	17.07.2012	82.94	5.7	28
POKF1 Centre 90-95	349	Core	50-100	17.07.2012	69.38	5.9	24
POKF1 Centre 95-100	350	Core	50-100	17.07.2012	76.58	5.9	27
POKF1 Centre 100-105	351	Core	100+	17.07.2012	75.08	5.7	34
POKF1 Centre 105-110	352	Core	100+	17.07.2012	74.24	5.9	37
POKF1 Centre 110-115	353	Core	100+	17.07.2012	71.21	6.0	45
POKF1 Centre 115-120	354	Core	100+	17.07.2012	62.66	5.7	56
POKF1 Centre 120-125	355	Core	100+	17.07.2012	60.59	5.6	60
POKF3 Wall 0-5	356	Core	0-50	19.07.2012	89.00	6.1	130
POKF3 Wall 5-10	357	Core	0-50	19.07.2012	84.87	5.7	31
POKF3 Wall 10-15	358	Core	0-50	19.07.2012	76.51	5.3	37
POKF3 Wall 15-20	359	Core	0-50	19.07.2012	76.28	5.3	34
POKF3 Wall 20-25	360	Core	0-50	19.07.2012	75.99	5.5	56
POKF3 Wall 25-30	361	Core	0-50	19.07.2012	80.99	5.6	63
POKF3 Wall 35-40	362	Core	0-50	19.07.2012	31.76	5.8	38
POKF3 Wall 40-45	363	Core	0-50	19.07.2012	36.22	5.9	36
POKF3 Wall 45-50	364	Core	0-50	19.07.2012	48.49	5.7	41
POKF3 Wall 50-55	365	Core	0-50	19.07.2012	58.98	5.8	48
POKF3 Wall 55-60	366	Core	50-100	19.07.2012	61.67	6.1	64
POKF3 Wall 60-65	367	Core	50-100	19.07.2012	63.80	5.5	159
POKF3 Wall 65-70	368	Core	50-100	19.07.2012	70.26	5.7	149
POKF3 Wall 70-75	369	Core	50-100	19.07.2012	97.80	5.8	71
POKF3 Wall 75-80	370	Core	50-100	19.07.2012	98.23	6.3	30
POKF3 Wall 80-85	371	Core	50-100	19.07.2012	87.40	6.2	34
POKF3 Wall 85-90	372	Core	50-100	19.07.2012	40.72	6.9	46
POKF3 Wall 90-95	373	Core	50-100	19.07.2012	28.69	7.3	156
POKF3 Wall 30-35	374	Core	0-50	19.07.2012	39.89	7.6	30
POKF3 Center 0-5	375	Core	0-50	19.07.2012	92.48	6.3	125
POKF3 Center 5-10	376	Core	0-50	19.07.2012	83.40	5.8	63
POKF3 Center 10-15	377	Core	0-50	19.07.2012	79.25	5.6	62
POKF3 Center 15-20	378	Core	0-50	19.07.2012	75.66	5.7	62
POKF3 Center 20-25	379	Core	0-50	19.07.2012	83.07	5.5	38
POKF3 Center 25-30	380	Core	0-50	19.07.2012	83.16	5.8	35
POKF3 Center 30-35	381	Core	0-50	19.07.2012	81.22	5.7	32
POKF3 Center 35-40	382	Core	0-50	19.07.2012	75.27	5.7	38
POKF3 Center 40-45	383	Core	0-50	19.07.2012	77.30	5.8	32
POKF3 Center 45-50	384	Core	0-50	19.07.2012	72.63	5.6	40
POKF3 Center 50-55	385	Core	50-100	19.07.2012	76.01	5.7	28
POKF3 Center 55-60	386	Core	50-100	19.07.2012	74.14	5.8	24

Sample	Nr	Type	Area	Date	Water content (wt %)	pH	EC (µS/cm)
POKF3 Center 60-65	387	Core	50-100	19.07.2012	79.75	5.7	24
POKF3 Center 65-70	388	Core	50-100	19.07.2012	82.31	5.7	24
POKF3 Center 70-75	389	Core	50-100	19.07.2012	84.61	5.9	21
POKF3 Center 75-80	390	Core	50-100	19.07.2012	82.75	5.8	23
POKF3 Center 80-85	391	Core	50-100	19.07.2012	75.21	6.0	23
POKF3 Center 85-90	392	Core	50-100	19.07.2012	77.09	5.7	27
POKF3 Center 90-95	393	Core	50-100	19.07.2012	77.41	5.8	28
POKF3 Center 95-100	394	Core	50-100	19.07.2012	75.00	6.0	32
POKF3 Center 100-105	395	Core	100+	19.07.2012	NA	6.0	37
POKF3 Center 105-110	396	Core	100+	19.07.2012	NA	6.1	56
POKF3 Center 110-115	397	Core	100+	19.07.2012	NA	6.1	50
POKF4 Wall 0-5	398	Core	0-50	21.07.2012	17.14	5.9	84
POKF4 Wall 5-10	399	Core	0-50	21.07.2012	55.49	5.0	61
POKF4 Wall 10-15	400	Core	0-50	21.07.2012	47.30	5.8	24
POKF4 Wall 15-20	401	Core	0-50	21.07.2012	37.53	6.5	19
POKF4 Wall 20-25	402	Core	0-50	21.07.2012	38.45	6.7	18
POKF4 Wall 25-30	403	Core	0-50	21.07.2012	52.33	6.6	31
POKF4 Wall 30-35	404	Core	0-50	21.07.2012	48.68	6.0	30
POKF4 Wall 35-40	405	Core	0-50	21.07.2012	54.30	5.7	27
POKF4 Wall 40-45	406	Core	0-50	21.07.2012	57.70	5.7	27
POKF4 Wall 45-50	407	Core	0-50	21.07.2012	66.18	6.0	20
POKF4 Wall 50-55	408	Core	50-100	21.07.2012	75.65	5.9	33
POKF4 Wall 55-60	409	Core	50-100	21.07.2012	76.43	6.0	31
POKF4 Wall 60-65	410	Core	50-100	21.07.2012	76.19	5.9	18
POKF4 Wall 65-70	411	Core	50-100	21.07.2012	75.15	5.9	36
POKF4 Wall 70-75	412	Core	50-100	21.07.2012	87.18	5.9	21
POKF4 Wall 75-80	413	Core	50-100	21.07.2012	83.38	5.7	24
POKF4 Wall 80-85	414	Core	50-100	21.07.2012	75.26	5.8	26
POKF4 Wall 85-90	415	Core	50-100	21.07.2012	71.96	5.9	22
POKF4 Wall 90-95	416	Core	50-100	21.07.2012	91.33	5.9	21
POKF4 Wall 95-100	417	Core	50-100	21.07.2012	78.37	5.8	17
POKF4 Wall 100-105	418	Core	100+	21.07.2012	NA	5.9	19
POKF4 Wall 105-110	419	Core	100+	21.07.2012	NA	5.9	21
POKF4 Center 0-5	420	Core	0-50	21.07.2012	68.09	5.2	21
POKF4 Center 5-10	421	Core	0-50	21.07.2012	60.12	5.1	13
POKF4 Center 10-15	422	Core	0-50	21.07.2012	46.03	5.2	14
POKF4 Center 15-20	423	Core	0-50	21.07.2012	65.89	5.3	17
POKF4 Center 20-30	424	Core	0-50	21.07.2012	62.08	5.3	18
POKF4 Center 30-40	425	Core	0-50	21.07.2012	79.23	5.5	18
POKF4 Center 40-45	426	Core	0-50	21.07.2012	78.34	5.7	22
POKF4 Center 45-50	427	Core	0-50	21.07.2012	61.02	5.7	22
POKF4 Center 50-55	428	Core	0-50	21.07.2012	71.14	5.7	17
POKF4 Center 55-60	429	Core	50-100	21.07.2012	76.48	5.8	19
POKF4 Center 60-65	430	Core	50-100	21.07.2012	90.27	5.7	15

Sample	Nr	Type	Area	Date	Water content (wt %)	pH	EC (µS/cm)
POKF4 Center 65-70	431	Core	50-100	21.07.2012	93.77	5.8	13
POKF4 Center 70-75	432	Core	50-100	21.07.2012	96.31	5.7	15
POKF4 Center 75-80	433	Core	50-100	21.07.2012	90.45	5.4	27
POKF4 Center 80-85	434	Core	50-100	21.07.2012	90.12	5.8	18
POKF4 Center 85-90	435	Core	50-100	21.07.2012	76.84	5.6	15
POKF4 Center 90-95	436	Core	50-100	21.07.2012	90.39	5.8	15
POKF2 Wall 26.07. I Oi	437	Monitoring	1	26.07.2012	78.22	7.1	66
POKF2 Wall 26.07. I Oe/Bh	438	Monitoring	2	26.07.2012	67.26	6.6	21
POKF2 Wall 26.07. I Oa	439	Monitoring	3	26.07.2012	79.12	6.4	21
POKF2 Wall 26.07. II Oi	440	Monitoring	1	26.07.2012	74.03	6.2	58
POKF2 Wall 26.07. II Oe/Bh	441	Monitoring	2	26.07.2012	70.86	6.1	32
POKF2 Wall 26.07. II Oa	442	Monitoring	3	26.07.2012	76.86	6.0	21
POKF2 Wall 26.07. III Oi	443	Monitoring	1	26.07.2012	68.79	5.7	86
POKF2 Wall 26.07. III Oe/Bh	444	Monitoring	2	26.07.2012	63.65	6.1	34
POKF2 Wall 26.07. III Oa	445	Monitoring	3	26.07.2012	64.75	6.0	32
POKF2 Wall 26.07. I Oi	446	Monitoring	4	26.07.2012	86.53	5.7	28
POKF2 Wall 26.07. I Oe	447	Monitoring	5	26.07.2012	85.09	5.9	29
POKF2 Wall 26.07. II Oi	448	Monitoring	4	26.07.2012	87.39	6.0	27
POKF2 Wall 26.07. II Oe	449	Monitoring	5	26.07.2012	85.33	6.0	20
POKF2 Wall 26.07. III Oi	450	Monitoring	4	26.07.2012	88.79	5.9	21
POKF2 Wall 26.07. III Oe	451	Monitoring	5	26.07.2012	86.38	5.9	21
POKF5 0-5	452	Core	0-50	27.07.2012	79.52	5.3	44
POKF5 5-10	453	Core	0-50	27.07.2012	59.94	5.5	14
POKF5 10-15	454	Core	0-50	27.07.2012	67.50	5.5	17
POKF5 15-20	455	Core	0-50	27.07.2012	41.75	6.2	14
POKF5 20-25	456	Core	0-50	27.07.2012	41.75	6.3	17
POKF5 25-30	457	Core	0-50	27.07.2012	32.52	6.4	19
POKF5 30-40	458	Core	0-50	27.07.2012	42.66	6.3	17
POKF5 40-45	459	Core	0-50	27.07.2012	36.56	6.5	28
POKF5 45-50	460	Core	0-50	27.07.2012	37.72	6.6	39
POKF5 50-55	461	Core	50-100	27.07.2012	28.46	6.3	39
POKF5 55-60	462	Core	50-100	27.07.2012	34.88	6.2	43
POKF5 60-65	463	Core	50-100	27.07.2012	31.39	6.5	42
POKF5 65-70	464	Core	50-100	27.07.2012	38.96	6.6	60
POKF5 70-75	465	Core	50-100	27.07.2012	37.17	6.5	50
POKF5 75-80	466	Core	50-100	27.07.2012	59.20	6.0	80
POKF5 80-85	467	Core	50-100	27.07.2012	62.54	5.7	120
POKF5 85-90	468	Core	50-100	27.07.2012	72.50	5.8	127
POKF5 90-95	469	Core	50-100	27.07.2012	62.88	6.2	48
POKF5 95-100	470	Core	50-100	27.07.2012	69.56	6.3	31
POKF7 0-5	471	Core	0-50	30.07.2012	60.00	5.1	250
POKF7 5-10	472	Core	0-50	30.07.2012	56.58	5.0	115
POKF7 10-15	473	Core	0-50	30.07.2012	55.38	5.3	63

Sample	Nr	Type	Area	Date	Water content (wt %)	pH	EC (µS/cm)
POKF7 15-20	474	Core	0-50	30.07.2012	53.93	5.5	49
POKF7 20-25	475	Core	0-50	30.07.2012	50.64	5.5	64
POKF7 25-30	476	Core	0-50	30.07.2012	46.30	5.4	32
POKF7 30-35	477	Core	0-50	30.07.2012	51.27	5.6	55
POKF7 35-40	478	Core	0-50	30.07.2012	55.20	5.6	37
POKF7 40-45	479	Core	0-50	30.07.2012	63.50	5.7	52
POKF7 45-50	480	Core	0-50	30.07.2012	58.02	5.5	69
POKF7 50-55	481	Core	50-100	30.07.2012	55.46	5.4	67
POKF7 55-60	482	Core	50-100	30.07.2012	61.96	5.9	12
POKF7 60-65	483	Core	50-100	30.07.2012	47.25	5.7	19
POKF7 65-70	484	Core	50-100	30.07.2012	63.54	5.8	24
POKF7 70-75	485	Core	50-100	30.07.2012	34.74	6.1	51
POKF7 75-80	486	Core	50-100	30.07.2012	51.87	6.3	57
POKF7 80-85	487	Core	50-100	30.07.2012	55.49	6.0	65
POKF7 85-90	488	Core	50-100	30.07.2012	60.29	6.2	56
POKF7 90-95	489	Core	50-100	30.07.2012	44.09	6.1	50
POKF7 95-100	490	Core	50-100	30.07.2012	56.15	6.1	47
POKF8 0-5	491	Core	0-50	30.07.2012	60.59		
POKF8 5-10	492	Core	0-50	30.07.2012	43.18		
POKF8 10-15	493	Core	0-50	30.07.2012	55.68		
POKF8 15-20	494	Core	0-50	30.07.2012	69.64		
POKF8 20-25	495	Core	0-50	30.07.2012	74.67		
POKF8 25-30	496	Core	0-50	30.07.2012	69.70		
POKF8 30-35	497	Core	0-50	30.07.2012	87.58		
POKF8 35-40	498	Core	0-50	30.07.2012	87.51		
POKF8 40-45	499	Core	0-50	30.07.2012	89.09		
POKF8 45-50	500	Core	0-50	30.07.2012	94.88		
POKF8 50-55	501	Core	50-100	30.07.2012	96.55		
POKF8 55-60	502	Core	50-100	30.07.2012	96.10		
POKF8 60-65	503	Core	50-100	30.07.2012	96.51		
POKF8 65-70	504	Core	50-100	30.07.2012	95.16		
POKF8 70-75	505	Core	50-100	30.07.2012	89.35		
POKF8 75-80	506	Core	50-100	30.07.2012	91.83		
POKF8 80-85	507	Core	50-100	30.07.2012	91.41		
POKF8 85-90	508	Core	50-100	30.07.2012	77.01		
POKF8 90-95	509	Core	50-100	30.07.2012	82.97		
POKF8 95-100	510	Core	50-100	30.07.2012	81.23		
POKF2 Wall 9.08 I Oi	511	Monitoring	1	09.08.2012	76.56		
POKF2 Wall 9.08 I Oe	512	Monitoring	2	09.08.2012	72.10		
POKF2 Wall 9.08 I Bh	513	Monitoring	3	09.08.2012	70.08		
POKF2 Wall 9.08 II Oi	514	Monitoring	1	09.08.2012	70.51		
POKF2 Wall 9.08 II Oe	515	Monitoring	2	09.08.2012	69.10		
POKF2 Wall 9.08 II Bh	516	Monitoring	3	09.08.2012	64.87		
POKF2 Wall 9.08 III Oi	517	Monitoring	1	09.08.2012	76.07		

Sample	Nr	Type	Area	Date	Water content (wt %)	pH	EC (µS/cm)
POKF2 Wall 9.08 III Oe	518	Monitoring	2	09.08.2012	73.27		
POKF2 Wall 9.08 III Bh	519	Monitoring	3	09.08.2012	68.16		
POKF2 Center 9.08 I Oi	520	Monitoring	4	09.08.2012	79.56		
POKF2 Center 9.08 I Oe	521	Monitoring	5	09.08.2012	85.53		
POKF2 Center 9.08 II Oi	522	Monitoring	4	09.08.2012	84.22		
POKF2 Center 9.08 II Oe	523	Monitoring	5	09.08.2012	84.50		
POKF2 Center 9.08 III Oi	524	Monitoring	4	09.08.2012	87.84		
POKF2 Center 9.08 III Oe	525	Monitoring	5	09.08.2012	90.69		

APPENDIX 8

List of ice, sediment and soil samples from the pingo site

Sebastian Wetterich, Lutz Schirrmeister & Lilith Pogosyan

Appendix 8-1: Sample description of the pingo exposure 'Shirokovsky Kholm'. * Relative distance from the landing site (see also Fig. 8-1).

Sample code	Depth [m b.s]	Height [m l.l.]	Relative distance* [m]	Material	Description (CS - Cryostructures)
12P-1908-A					
12P-1908-A-00		7.2	44	sediment	unfrozen, surface (dune ?), light grey-brown, peaty
12P-1908-A-01-IW	0.5	6.5	45.5	ice	syngenetic ice wedge on slope of the pingo, 1.8 m in width and 1.2 m in length exposed, shoulders, milky white ice, irregular vertical elongated and round bubbles 1 mm in diameter, samples taken every 0.2 m in horizontal transect
12P-1908-A-02-IW	0.5	6.5	45.2	ice	see above
12P-1908-A-03-IW	0.5	6.5	45.4	ice	see above
12P-1908-A-04-IW	0.5	6.5	45.6	ice	see above
12P-1908-A-05-IW	0.5	6.5	45.8	ice	see above
12P-1908-A-06-IW	0.5	6.5	46	ice	see above
12P-1908-A-07-IW	0.5	6.5	46.2	ice	see above
12P-1908-A-08	0.1	6.9	46.4	sediment	unfrozen, active layer, grey-brown, silt, modern roots
12P-1908-A-09	0.5	6.5	45	sediment	grey-brown, silty fine-sand, peaty, plant remains, coarse lens-like reticulated CS, clear ice lenses up to 1 cm thick with air bubbles up to 1 mm in diameter
12P-1908-A-10	1	6	45	sediment	grey-brown, silty fine-sand, no organic remains, coarse lens-like CS, clear ice lenses up to 2 cm thick with air bubbles less than 1 mm in diameter
12P-1908-A-11	1.5	5.5	45	sediment	grey-brown, silty fine-sand, no organic remains, coarse lens-like CS, clear ice lenses up to 2 cm thick with air bubbles less than 1 mm in diameter
12P-1908-A-12	1.8	5.2	45	sediment	bedded alternations of dark grey and light grey silty fine-sand (20 mm thick), ripple bedding, ataxitic CS, ice lenses up to 1 mm thick and 0.5 to 2 cm long
12P-1908-A-13	2.4	4.6	45	sediment	light brown, moss peat, allochtonous (?), fine lens-like CS, single diagonal ice lenses
12P-1908-A-14	3	4	45	sediment	light grey-brown, silt, no organic remains, coarse lens-like CS, vertical and subvertical lenses up to 1 mm thick and up to 1.5 cm long
12P-1908-A-15	3.5	3.5	45	sediment	bedded alternations of dark grey silty fine-sand (10 mm thick) and light grey-brown plant detritus (5 mm thick), ataxitic CS, ice lenses up to 1 mm thick and 0.5

Sample code	Depth [m b.s]	Height [m l.l.]	Relative distance* [m]	Material	Description (CS - Cryostructures)
					to 2 cm long
12P-1908-A-16	4	3	45	ice	clear ice lens, 20 cm thick, no bubbles
12P-1908-A-17	4.5	2.5	45	sediment	light brown, moss peat, silt, coarse lens-like CS, single bubbles
12P-1908-A-18	4.8	2.2	45	ice	ice belt between 4.7 and 5.0 m b.s., clear ice, irregular bubbles 1 to 2 mm in diameter, no sediment
12P-1908-A-19	5.3	1.7	45	sediment	light brown, red-brown peat, signs of cryoturbation, coarse lens-like CS, lenses 1 to 2 cm thick
12P-2008-A					
12P-2008-A-01	1	3.7	28.5	sediment	brown moss peat, allochtonous (?), compact, massive CS
12P-2008-A-02	1.2	3.5	28.5	sediment	light grey-brown, middle to fine sand, massive CS
12P-2008-A-03	1.65	3.05	27	sediment	bedded alternations of grey fine-sand (5 to 10 mm thick) and brownish plant detritus (1 to 2 mm thick), peat inclusions (5 to 15 cm long and 2 to 4 cm thick), diagonal ice veins (1 to 1.5 mm thick and 5 to 30 cm long)
12P-2008-A-04	1.9	2.8	27	sediment	bedded alternations of grey fine-sand (5 to 10 mm thick) and brownish plant detritus (1 to 2 mm thick), peat inclusions (5 to 15 cm long and 2 to 4 cm thick), diagonal ice veins (1 to 1.5 mm thick and 5 to 30 cm long)
12P-2008-A-05	2.1	2.6	27	sediment	bedded alternations of grey fine-sand (5 to 10 mm thick) and brownish plant detritus (1 to 2 mm thick), peat inclusions (5 to 15 cm long and 2 to 4 cm thick), diagonal ice veins (1 to 1.5 mm thick and 5 to 30 cm long)
12P-2008-A-06	1.5	3.2	27	ice	bubble-rich ice, bubbles (0.2 to 2 mm in diameter) non-regularly distributed, dirty-yellowish at surface due to organic matter from overlying peat (?)
12P-2008-A-07	1.5	3.2	28	ice	bubble-poor clear ice, bubbles (1 mm in diameter) distinct ice crystals (5 x 5 mm)
12P-2008-A-08	1.5	3.2	29	ice	clear ice, no bubbles, distinct ice crystals (5 x 5 mm to 30 to 50 mm)
12P-2008-A-09	2.6	2.1	28.5	ice	clear ice, no bubbles, distinct ice crystals (5 x 5 mm to 30 to 50 mm)
12P-2008-A-10	2.4	2.3	26	ice	bubble-poor clear ice with bubbles (1 to 2 mm in diameter) in subvertical and horizontal layers
12P-2008-A-11	3	1.7	26	ice	bubble-rich clear ice with vertical elon-gated bubbles (1 to 2 mm in diameter, up to 10 mm long) in vertical layers, horizontal grey fine-sand inclusions (2 mm thick, 10 mm long) in layers

Sample code	Depth [m b.s]	Height [m l.l.]	Relative distance* [m]	Material	Description (CS - Cryostructures)
12P-2008-A-12	3.2	1.5	26	ice	bubble-rich clear ice with bubbles (1 mm in diameter) in vertical layers, horizontal grey fine-sand inclusions (2 mm thick, 10 mm long) in layers
12P-2008-A-13	3.4	1.3	26	ice	bubble-rich clear ice with vertical elongated bubbles (1 to 2 mm in diameter, up to 10 mm long) in vertical stripes, horizontal grey fine-sand inclusions (2 mm thick, 10 mm long) in layers
12P-2008-A-14	2.4	2.3	25	ice	bubble-poor clear ice with bubbles (1 to 2 mm in diameter) in subvertical and horizontal layers
12P-2008-A-15	3	1.7	25	ice	bubble-poor clear ice with bubbles (1 to 2 mm in diameter) in subvertical and horizontal layers
12P-2008-A-16	2.4	2.3	20	ice	bubble-poor clear ice with non-regular bubbles (1 to 2 mm in diameter) in vertical orientation, distict ice crystals (2 x 2 mm)
12P-2008-A-17	2.7	2	20	sediment	sediment layer with horizontal ice layers
12P-2008-A-18	3.2	1.5	20	ice	bubble-poor clear ice with non-regular bubbles (1 in diameter), distict ice crystals (2 x 2 mm)
12P-2008-A-19	3.2	1.5	19	ice	bubble-rich clear ice, bubbles (1 mm in diameter) in vertical and subvertical layers
12P-2208-A					
12P-2208-A-01	0.3	10.4	-30	sediment	grey-brown, fine-sand, in situ roots, unfrozen
12P-2208-A-02	1.3	9.4	-30	sediment	grey-brown, silty fine-sand, slightly bedded, root remains, peat inclusions (1 to 2 cm thick, 3 to 7 cm long), wood remains (1 cm in diameter, 10 cm long), reddish brown iron oxide spots, unfrozen
12P-2208-A-03	2.3	8.4	-31	sediment	grey-brown, silty fine-sand, slightly bedded, root remains, peat inclusions (1.5 cm thick, 10 to 15 cm long), wood remains (1 cm in diameter, 10 cm long), reddish brown iron oxide spots, unfrozen
12P-2208-A-04	3.6	7.1	-31	sediment	light grey, fine-sand, peat inclusions (1 to 2 cm thick, 5 to 7 cm long), wood remains (0.5 cm in diameter, 2 cm long), yellowish brown iron oxide spots, whitish (calcerous?) spots (< 1 cm in diameter), ataxic CS, single ice veins (5 mm thick, 0.5 to 2 cm long)
12P-2208-A-05	4	6.7	-31	sediment	light grey, fine-sand, peat inclusions horizontal oriented (1 to 2 cm thick, 5 to 7 cm long), wood remains (0.5 cm in diameter, 2 cm long), yellowish brown iron oxide spots, whitish (calcerous?) spots (< 1 cm in diameter), ataxic CS, single ice veins (5 mm thick, 0.5 to 2 cm long)

Sample code	Depth [m b.s]	Height [m l.l.]	Relative distance* [m]	Material	Description (CS - Cryostructures)
12P-2208-A-06	4.5	6.2	-31	sediment	light grey, fine-sand, peat inclusions horizontal oriented (1 to 2 cm thick, 5 to 7 cm long), wood remains (0.5 cm in diameter, 2 cm long), yellowish brown iron oxide spots, whitish (calcerous?) spots (< 1 cm in diameter), ataxic CS, single ice veins (5 mm thick, 0.5 to 2 cm long)
12P-2208-A-07	4.65	6.05	-31	sediment	light grey, fine-sand, slightly bedded, peat inclusions rounded (1 to 1.5 cm in diameter), ataxic CS, single ice veins (5 to 10 mm thick, 2 to 3 mm long); 5 cm thick layer directly above the underlying ice body, sample taken from unfrozen material
12P-2208-A-08	6.5	3.9	-28	ice	bubble-rich whitish ice with bubbles (0.5 to 1 mm in diameter) non-regularly distributed
12P-2208-A-09	5	5.7	-29	ice	bubble-rich whitish ice with bubbles (0.5 to 2 mm in diameter) in subvertical and horizontal layers, elongated bubbles (1 to 2 cm long) in subvertical direction
12P-2208-A-10	5	5.7	-30	ice	bubble-poor clear ice with bubbles (1 to 2 mm in diameter) non-regularly distributed
12P-2208-A-11	4.7	6	-31	ice	bubble-poor clear ice with bubbles (1 to 2 mm in diameter) non-regularly distributed
12P-2208-A-12	5	5.7	-31	ice	bubble-poor clear ice with bubbles (1 to 2 mm in diameter) non-regularly distributed
12P-2208-A-13	5.6	5.1	-31	ice	bubble-poor clear ice with bubbles (1 to 2 mm in diameter) in subvertical and horizontal layers
12P-2208-A-14	6	4.7	-31	sediment	brown, silty fine-sand, root and wood remains (2 mm in diameter, 5 cm long), red-brown iron oxide spots, lens-like CS, single veins 1 mm thick, 1 cm long)
12P-2208-A-15	6.3	4.4	-31	ice	bubble-rich whitish ice with bubbles (1 to <10 mm in diameter) in vertical bubble chains, non-regularly sediment inclusions (0.5 cm in diameter), sandy sediment layer 1 cm thick
12P-2208-A-16	6.6	4.1	-31	ice	bubble-rich whitish ice with bubbles (1 to 2 mm in diameter), non-regularly distributed, sediment inclusions
12P-2208-A-17	6.9	3.8	-31	ice	bubble-poor whitish ice with bubbles (0.5 to 2 mm in diameter), non-regularly distributed
12P-2208-A-18	5	5.7	-32	ice	bubble-rich clear ice with bubbles (1 mm in diameter) in subvertical and horizontal layers
12P-2208-A-19	5.1	5.6	-33	ice	bubble-rich clear ice with bubbles (1 mm in diameter) in subvertical and horizontal layers, ice crystals (2 x 3 cm)

Sample code	Depth [m b.s]	Height [m l.l.]	Relative distance* [m]	Material	Description (CS - Cryostructures)
12P-2208-A-20	4.7	6	-35	ice	bubble-rich clear ice with bubbles (1 mm in diameter) in horizontal layers
12P-2208-A-21	5.3	5.4	-35	ice	bubble-rich unclear ice with bubbles (0.5 mm in diameter), non-regularly distributed in spots of up to 5 cm in diameter, ice crystals (0.5 x 1 cm)
12P-2208-A-22	5.5	5.2	-35	ice	bubble-poor clear ice with bubbles (<1 mm in diameter), non-regularly distributed, large ice crystals (4 x 7 cm)
12P-2208-A-23	6.2	4.5	-35	ice	bubble-rich clear ice with bubbles (different in diameter), non-regularly distributed
12P-2208-A-24		3	-45	ice	bubble-rich clear ice with bubbles (1 mm in diameter) in subvertical and horizontal layers, ice crystals
12P-2208-A-25		2.2	-45	ice	bubble-poor clear ice with bubbles, non-regularely distributed
12P-2208-A-26		3	-25	ice	bubble-rich clear ice with bubbles (1 to 3 mm in diameter), non-regularly distributed
12P-2208-A-27		2.3	-25	ice	bubble-rich clear ice with bubbles (1 mm in diameter) in subvertical and horizontal layers
12P-2208-A-28		2.4	-15	ice	bubble-rich clear ice with bubbles (1 to 23 mm in diameter), non-regularly distributed, ice crystals 1 x 2 cm
12P-2208-A-29		2	-15	ice	bubble-rich clear ice with bubbles (1 mm in diameter) in horizontal layers
12P-2208-A-30		1.7	-15	ice	bubble-rich clear ice with bubbles (1 mm in diameter) in subvertical and horizontal layers

Appendix 8-2: Field data and planned analytics of the pingo exposure 'Shirokovsky Kholm'

Sample code	**Field data**			**Samples**					**Planned lab**		
	EC [µS cm^{-1}]	**pH (WTW)**	**absolute ice content [wt%]**	**Sediment**	**IW ice**	**Texture ice**	**Massive ice**	**$\delta^{18}O$, δD**	**Hydro-chemistry**	**Grain size CN, δ13C**	**Fossils, sedimentology**
12P-1908-A											
12P-1908-A-00				x						x	x
12P-1908-A-01-IW					x			x			
12P-1908-A-02-IW					x			x			
12P-1908-A-03-IW					x			x			
12P-1908-A-04-IW	66	5.7			x			x	x		
12P-1908-A-05-IW					x			x			
12P-1908-A-06-IW					x			x			
12P-1908-A-07-IW					x			x			
12P-1908-A-08				x						x	x
12P-1908-A-09			87.6	x		x		x		x	x
12P-1908-A-10			66.0	x		x		x		x	x
12P-1908-A-11				x		x		x		x	x
12P-1908-A-12			75.4	x		x		x		x	x
12P-1908-A-13			93.1	x		x		x		x	x
12P-1908-A-14			78.4	x		x		x		x	x
12P-1908-A-15				x		x		x		x	x
12P-1908-A-16						x		x		x	x
12P-1908-A-17			88.3	x		x		x		x	x
12P-1908-A-18	40	5.9				x		x	x		
12P-1908-A-19			93.8							x	x
12P-2008-A											
12P-2008-A-01			91.1	x							
12P-2008-A-02			55.6	x							
12P-2008-A-03				x		x		x			
12P-2008-A-04			55.7	x		x		x			
12P-2008-A-05				x		x		x			
12P-2008-A-06	1068	7.3					x	x	x		
12P-2008-A-07	32	7.3					x	x	x		
12P-2008-A-08	32	7.3					x	x	x		
12P-2008-A-09	32	7.2					x	x	x		
12P-2008-A-10	30	7.2					x	x	x		
12P-2008-A-11	101	6.0					x	x	x		
12P-2008-A-12	174	7.5					x	x	x		
12P-2008-A-13	41	7.1					x	x	x		
12P-2008-A-14	35	7.4					x	x	x		
12P-2008-A-15	55	7.1					x	x	x		
12P-2008-A-16	74	7.0					x	x	x		
12P-2008-A-17	2020	7.0	72.7	x		x	x	x	x	x	x
12P-2008-A-18	75	7.4					x	x	x		
12P-2008-A-19	203	7.4					x	x	x		
12P-2208-A											
12P-2208-A-01				x							
12P-2208-A-02				x							
12P-2208-A-03				x							
12P-2208-A-04			57.4	x							

Sample code	**Field data**			**Samples**					**Planned lab**		
	EC [µS cm^{-1}]	**pH (WTW)**	**absolute ice content [wt%]**	**Sediment**	**IW ice**	**Texture ice**	**Massive ice**	**$\delta^{18}O$, δD**	**Hydro-chemistry**	**Grain size CN, δ13C**	**Fossils, sedimentology**
12P-2208-A-05			53.1	x							
12P-2208-A-06			50.2	x							
12P-2208-A-07			41.9	x							
12P-2208-A-08	41	6.5					x	x	x		
12P-2208-A-09	63	6.6					x	x	x		
12P-2208-A-10	67	6.6					x	x	x		
12P-2208-A-11	74	6.6					x	x	x		
12P-2208-A-12	57	6.9					x	x	x		
12P-2208-A-13	54	6.8					x	x	x		
12P-2208-A-14	251	5.8		x		x		x	x	x	
12P-2208-A-15	108	6.6					x	x	x		
12P-2208-A-16	75	6.7					x	x	x		
12P-2208-A-17	57	6.7					x	x	x		
12P-2208-A-18	42	6.8					x	x	x		
12P-2208-A-19	36	6.9					x	x	x		
12P-2208-A-20	61	6.5					x	x	x		
12P-2208-A-21	32	6.6					x	x	x		
12P-2208-A-22	24	6.8					x	x	x		
12P-2208-A-23	81	6.8					x	x	x		
12P-2208-A-24	47	6.9					x	x	x		
12P-2208-A-25	45	7.2					x	x	x		
12P-2208-A-26	42	7.0					x	x	x		
12P-2208-A-27	90	6.9					x	x	x		
12P-2208-A-28	116	6.9					x	x	x		
12P-2208-A-29	25	6.7					x	x	x		
12P-2208-A-30	80	6.7					x	x	x		

Appendix 8-3: Soil description and data of the pingo 'Shirokovsky Kholm'

Soil profile ID	Horizon	Depth [cm b.s.]	pH (WTW)	Soil Name (American/Russian)	Coordinates
Pi01	Oi	0-7	4.2	Fluvaquentic Sapristels /	N 69˚02'18,6"
	Oa1	7-19	4.7	Peat Cryozems homogeneous	E 160˚00'19,1"
	Bh	19-25	4.7		
	Oa2	25-28	4.8		
Pi02	Oi	0-5	4.2	Typic Historthels /	N 69˚02'17,3"
	Oe	5-12	4.8	Peat Cryozems homogeneous	E 160˚00'19,9"
	Oa	12-14	4.7		
	Bh	14-23	5.5		
	Bh(2)	14-23	5.0		
	Bh(3)	14-23	4.8		
Pi03	Oi	0-7	4.3	Typic Sapristels /	N 69˚02'17,9"
	Oe	7-10	4.1	Peat Eutrothic typic	E 160˚00'19,2"
	Oa	10-32	4.5		
Pi04	Oi	0-10	4.1	Typic Historthels /	N 69˚02'18,1"
	Oe	10-19	4.3	Peat Cryozems homogeneous	E 161˚00'18,4"
	Oa	19-25	4.3		
	Bh	25-33	5.3		
Pi05	Oi	0-12	4.0	Typic Hemistels /	N 69˚02'18,8"
	Oe/Oa	12-26	4.3	Peat Oligotroph typic	E 161˚00'17,6"
Pi06	Oi	0-8	4.0	Typic Historthels /	N 69˚02'17,9"
	Oe	8-15	4.5	Peat Cryozems homogeneous	E 161˚00'23,2"
	Bh	15-22	4.8		
Pi07	Oi1	0-10	4.4	Sphagnic Fibristels /	N 69˚02'15,7"
	Oi2	10-24	4.9	Peat Eutrothic typic	E 161˚00'22,4"
Pi08	Oi	0-24	4.6	Sphagnic Fibristels / Peat Eutrothic typic	N 69˚02'14,1" E 161˚00'20,1"
Pi09	Oa	0-5/13	5.9	Typic Historthels /	N 69˚02'14,8"
	Bh	5/13-75	4.9	Peat Cryozems homogeneous	E 161˚00'25,8"
Pi10	Oi	0-10	4.1	Typic Historthels /	N 69˚02'17,2"
	Bh	10-32	5.4	Peat Cryozems homogeneous	E 161˚00'29,9"
Pi11	Oi	0-8	4.3	Typic Hemistels /	N 69˚02'17,0"
	Bh	8-32	5.1	Peat Oligotroph typic	E 161˚00'30,1"
Pi12 (islet1)	Oi	0-30/80	6.0	Typic Fibristels / Peat Eutrothic typic	N 69˚02'28,5" E 161˚00'65,4"
Pi13 (islet2, wall)	Oi	0-10	4.9	Typic Hemistels / Peat Eutrothic typic	N 69˚02'23,7" E 161˚00'16,9"
	Oe	10-32	5.6		
Pi14 (islet2, center)	Oi	0-40	5.5	Typic Fibristels / Peat Eutrothic typic	N 69˚02'23,9" E 161˚00'16,9"
PiL	Oi	0-4	5.6	Typic Historthels /	N 69˚02'16,4"
	Oe	4-7	5.4	Peat Cryozems gley	E 161˚00'21,9"
	Oa	7-18	5.5		
	Bg	18-37	5.8		

APPENDIX 9

Samples from cores and pits (Pokhodsk)

Lutz Schirrmeister, Vladimir Tumskoy, Sebastian Wetterich

sample	depth (cm b.s.)	cryotexture	sediment	ice vol. (V%)	ice grav. (wt %)	ice abs. (wt %)	bulk density (g/cm^3)	TI
Monitoring site 12P-1607-1 (POK1 W), N 69.095150°, E 160.938733°								
12-P-1607-1-1	33-36	massive	silty fine-sand					
12-P-1607-1-2	36-46	horizontal lens-like	silty fine-sand	46	32	24.2	1.70	
12-P-1607-1-3	56-63	horizontal lens-like, vertical ice veins	peaty fine-sand					x
12-P-1607-1-4	64-72	horizontal layered	peaty fine-sand	82	314	75.8	0.97	x
12-P-1607-1-5	72-81		Peaty fine-sand					x
12-P-1607-1-6	81-85		weakly peaty fine-sand					x
12-P-1607-1-7	85-96		weakly peaty fine-sand					x
12-P-1607-1-8	96-103		Weakly peaty fine-sand					x
12-P-1607-1-9	104-115		weakly peaty fine-sand	88	261	72,3	1,09	x
12-P-1707-1 (POK1 C), Pond in a low-centered polygon, N 69.095033°, E 160.938900°								
12-P-1707-1-1	54-61	horizontal net-like	strong peaty silty fine-sand					x
12-P-1707-1-2	61-68	lens-like	strong peaty silty fine-sand					
12-P-1707-1-3	69-78	lens-like	strong peaty silty fine-sand	93	310	75,6	1,10	
12-P-1707-1-4	78-87	lens-like	strong peaty silty fine-sand					x
12-P-1707-1-5	87-95	lens-like	strong peaty silty fine-sand					x
12-P-1707-1-6	95-106	lens-like	strong peaty silty fine-sand					x
12-P-1707-1-7	106-116	lens-like	strong peaty silty fine-sand					x
12-P-1707-1-8	116-125	lens-like	strong peaty silty fine-sand					x
12-P-1707-1-9	125-137	lens-like	strong peaty silty fine-sand	87	250	71,4	1,10	x

sample	depth (cm b.s.)	cryotexture	sediment	ice vol. (V%)	ice grav. (wt %)	ice abs. (wt %)	bulk density (g/cm^3)	TI
12P-1907-1 (POK3 W), near the monitoring site, N 69.094783°, E 160.940700°								
12-P-1907-1-1	28-32	massive with vertical ice veins	peat					x
12-P-1907-1-2	32-42	lattice-like	brownish-grey peaty silty fine-sand					x
12-P-1907-1-3	42-57	layered, lattice-like	brownish-grey peaty silty fine-sand	82	176	63,8	1,16	x
12-P-1907-1-4	57-94	Ice wedge						
12-P-1907-1-5	57-94	Ice wedge						
12-P-1907-1-6	57-94	Ice wedge						
12-P-1907-1-7	57-94	Ice wedge						
12-P-1907-1-8	57-94	Ice wedge						
12-P-1907-1-9	80-85	Ice wedge						
12-P-1907-2 (POK3 C), 8 m distance from 12P-1907-1								
12-P-1907-2-1	33-41		thawed peat					x
12-P-1907-2-2	41-58	pseudoataxitic	peat	97	507	83,5	1,04	x
12-P-1907-2-3	58-75	pseudoataxitic	peat	87	372	78,8	0,99	x
12-P-1907-2-4	75-90	pseudoataxitic	peat	86	332	76,9	1,01	x
12-P-1907-2-5	90-103	layered, lens-like	strongly peaty , silty fine-sand	92	368	78,6	1,106	x
12-P-1907-2-6	103-106	layered, lens-like	strongly peaty , silty fine-sand					x
12-P-1907-2-7	106-115	layered, lens-like	strongly peaty , silty fine-sand					x
12-P-1907-2-8	115-120	layered, lens-like	strongly peaty , silty fine-sand					x
12-P-1907-2-9	120-130	reticulated, lens-like	weakly peaty , silty fine-sand	80	163		1,16	x
12-P-2107-1 (POK4 W), Kolyma flood plain, Pokhodskaya Channel, wall, N 69.103750°, E 161.002417°								
12-P-2107-1-2	25-29	massive	peat, lower part of the active layer					
12-P-2107-1-3	29-34	net-like	peaty silt					
12-P-2107-1-4	34-46	peat: pseudo-ataxitic, silt: horizontal net-like	silty peat	86	225	69,2	1,09	
12-P-2107-1-5	46-54	pseudoataxitic, horizontal net-like	silty peat	88	420	80,8	0,98	x
12-P-2107-1-6	54-64	pseud-ataxitic, horizontal net-like	silty peat	98	250	71,4	1,08	x
12-P-2107-1-7	64-76	pseudoataxitic, horizontal net-like	silty peat					x
12-P-2107-1-8	76-94	pseudoataxitic, horizontal net-like	silty peat	95	427	81,0	1,06	x
12-P-2107-3-1	105-118	reticulated, lense-like	peaty silt	91	450	81,8	1,00	x

sample	depth (cm b.s.)	cryotexture	sediment	ice vol. (V%)	ice grav. (wt %)	ice abs. (wt %)	bulk density (g/cm^3)	TI
12-P-2107-2 (POK4 C) Kolyma flood plain, Pokhodskaya Channel, centre, 8 m distance from 12P-2107-1								
12-P-2107-2-1	41-49	massive	peat	86	241	70,7	1,10	
12-P-2107-2-2	49-65	massive	silty peat	95	422	80,8	1,06	
12-P-2107-2-3	65-75	massive	silty peat	96	610	85,9	1,00	x
12-P-2107-2-4	75-87	pseudoataxitic, porphyric	silty peat	93	1200	92,3	0,91	x
12-P-2107-2-5	87-102	porphyric	peat with silty lenses					x
12-P-2107-2-6	102-112	porphyric	peat with silty lenses	93	941	90,4	0,93	x
12-P-2707-3, Kolyma flood plain, Pokhodskaya Channel, N 69.102917°, E 161.008283°								
12-P-2707-3-0	40-50	unfrozen	peat					
12-P-2707-3-1	50-60	unfrozen	peat					
12-P-2707-3-2	60-70	unfrozen	peat					
12-P-2707-3-3	70-80	horizontal micro streaks	sandy silt, laminated, peaty	52	39	28,1	1,67	
12-P-2707-3-4	80-88	horizontal micro streaks	sandy silt, laminated, peaty	51	34	25,4	1,79	
12-P-2707-3-5	88-92	horizontal micro streaks	sandy silt, laminated, peaty					
12-P-2707-1-1	100-108	horizontal net-like	sandy silt, laminated	75	134	57,3	1,18	
12-P-3007-1, Lake floodplain near Pokhodsk, N 69.076583°, E 160.970367°								
12-P-3007-1-1	45-58	massive, separate ice inclusions up to 1 mm	peaty silty sand, brown, at 54-63 cm - peat, interlayer dark brown to black	70	178	64,0	0,98	
12-P-3007-1-2	62-71	massive, separate ice inclusions up to 1 mm	peaty silty sand, brown, at 54-63 cm - peat, interlayer dark brown to black	53	110	52,4	0,92	
12-P-3007-1-3	76-90	horizontal lenticular; size of ice lenses varies with the depth	gray loam, with coarse (5 x 1 cm) black and light-brown plant residues	82	150	60,0	1,23	x
12-P-3007-1-4	93-100	horizontal lenticular; size of ice lenses varies with the depth	gray loam, coarse black and light-brown plant residues; peat inclusion	66	73	42,2	1,4	x
12-P-3007-1-5	105-112	horizontal lenticular; size of ice lenses varies with the depth	gray loam, coarse (5 x 1 cm) black and light-brown plant residues	69	78	43,8	1,42	x
12-P-3007-1-6	113-123	horizontal lenticular	silty sand	56	50	33,3	1,52	
12-P-3007-1-7	125-137	horizontal lentic.	silty sand					
12-P-3007-1-0	100-108	horizontal lentic.	silty sand, brown	65	63	38,7	1,5	x
12-P-3007-1-8	100-120	horizontal lentic.	silty sand, brown	92	685	87,3	0,95	x
12-P-3007-1-9	120-140	horizontal lentic.	silty sand, brown					

sample	depth (cm b.s.)	cryotexture	sediment	ice vol. (V%)	ice grav. (wt %)	ice abs. (wt %)	bulk density (g/cm³)	TI
12-P-1008-1, Khalerchinskaya Tundra, N 69.05617°, E 160.85904°								
12-P-1008-1-1	0-8	unfrozen	surface vegetation					
12-P-1008-1-2	10-20	unfrozen	soil horizon					
12-P-1008-1-3	20-30	unfrozen	soil horizon					
12-P-1008-1-5	50-60	massive	grey-brown, fine sand, not bedded		21,3	17,6		
12-P-1008-1-6	60-69	massive	grey-brown, fine sand, not bedded		22,4	18,3		
12-P-1008-1-7	69-79	massive	grey-brown, fine sand weakly bedded		24,9	19,9		
12-P-1008-1-8	79-89	massive	grey-brown, fine sand weakly bedded		25,8	20,5		
12-P-1008-1-9	89-99	massive	grey-brown, fine sand weakly bedded		26,7	21,1		
12-P-1008-1-10	99-110	massive	fine sand, alternate bedding		26,9	21,2		

Pits and exposures

12-P-2007-1, Khalerchinskaya Tundra, mud boil, N 69.063860°, E 160.878890°								
12-P-2007-1-1	surface	unfrozen	peaty sand					
12-P-2007-2, Khalerchinskaya Tundra, N 69.063550°, E 160.866040°								
12-P-2007-2-1	0-6		surface vegetation					
12-P-2007-2-2	6-8		peat					
12-P-2007-2-3	16-20		fine sand					
12-P-2007-2-4	21-25		fine sand					
12-P-2007-2-5	35-40		fine sand					
12-P-2007-2-6	40-44	massive	fine sand					
12-P-2007-3, Khalerchinskaya Tundra, mud boil, N 69,064070°, E 160.861890°								
12-P-2007-3-1	surface	unfrozen	peaty sand					
12-P-2007-4, Khalerchinskaya Tundra, mud boil, N 69.063500°, E 160.866700°								
12-P-2007-4-1	surface	unfrozen	peaty sand					
12-P-2207, outflow of Viska Channel from the Pokhodskoe lake, N 69.1269152518361°, E 160.678712725639°								
12-P-2207-1	surface	unfrozen	sand					
12-P-2507-1 / 12-P-0708-1, Ice wedge pit, near the monitoring site, N 69,09503292°, E 160,937147°								
horizontal distance								
12-P-2507-1-1	35 - 50	wedge ice						
12-P-2507-1-2	50 - 65	wedge ice						
12-P-2507-1-3-	65 - 80	wedge ice						
12-P-2507-1-4	80 - 95	wedge ice						
12-P-2507-1-5	95 - 110	wedge ice						
12-P-2507-1-6		surface ice lens						
12-P-2507-1-7		cave ice						
12-P-2507-1-8			silty loam with peat, greyish-brown		324	76,4		

sample	depth (cm b.s.)	cryotexture	sediment	ice vol. (V%)	ice grav. (wt %)	ice abs. (wt %)	bulk density (g/cm^3)	TI
12-P-2507-1-9		massive	(right) peat lens, dark brown		263	72,5		
12-P-2507-1-10		massive	(left) peat lens, dark brown		217	68,5		
12-P-2507-1-11		surface ice lens, vertically oriented needles (or bubbles)						
12-P-2507-1-12		ice vein, 2,5 cm						
12-P-2507-1-13		elementary ice vein						
12-P-0708-1-1-	15 cm	wedge ice						
12-P-0708-1-2		wedge ice						
12-P-0708-1-3		wedge ice						
12-P-0708-1-4		wedge ice						
12-P-0708-1-5		wedge ice						
12-P-0708-1-6		wedge ice						
12-P-0708-1-7		wedge ice						
12-P-0708-1-8		wedge ice						
12-P-0708-1-9		wedge ice						
12-P-0708-1-10		wedge ice						
12-P-0708-1-11		wedge ice						
12-P-0708-1-12		wedge ice						
12-P-0708-1-13		wedge ice						
12-P-0708-1-14		wedge ice						
12-P-2308, Viska flood plain, exposure, N 69.11288°, E 160.76570°								
12-P-2308-A-01	10	micro lens-like	greyish-brown, silty fine-sand, bedded, plant detritus, thin roots					
12-P-2308-A-02	40	micro lens-like	greyish-brown, silty fine-sand, bedded, plant detritus, roots					
12-P-2308-A-03	70	micro lens-like	greyish-brown, silty fine-sand, bedded, plant detritus, roots					
12-P-2308-A-04	90	micro lens-like	greyish-brown, silty fine-sand, reddish-brown patches					
12-P-2308-A-05	120	micro lens-like	greyish-brown, silty fine-sand, reddish-brown patches					
12-P-2308-B-01	5	unfrozen	peaty plant cover					
12-P-2308-B-02	30	unfrozen	brownish-grey, fine-sand					

APPENDIX 10

Sample list for paleobotanical studies

Frank Kienast

Date	Sample Code	Sample number	Depth (cm)	Sediment	Plant remains (sieved)	notes
09.08.2012	Du 12 / 9.8. / I	1	0	x	x	
09.08.2012	Du 12 / 9.8. / I	2	30	x	x	
09.08.2012	Du 12 / 9.8. / I	3	60	x	x	
09.08.2012	Du 12 / 9.8. / I	4	90	x	x	
09.08.2012	Du 12 / 9.8. / I	5	120	x		
09.08.2012	Du 12 / 9.8. / I	6	150	x	x	
09.08.2012	Du 12 / 9.8. / I	7	180	x	x	
10.08.2012	Du 12 / 9.8. / II	9	210	x	x	
10.08.2012	Du 12 / 9.8. / II	10	240	x	x	
10.08.2012	Du 12 / 9.8. / II	11	270	x	x	
10.08.2012	Du 12 / 10.8. / I	1	0	x	x	2 samples (A, B)
10.08.2012	Du 12 / 10.8. / I	2	50	x	x	4 samples (A, B, C, D)
10.08.2012	Du 12 / 10.8. / I	3	100	x	x	4 samples (A, B, C, D)
10.08.2012	Du 12 / 10.8. / I	4	150	x	x	4 samples (A, B, C, D)
10.08.2012	Du 12 / 10.8. / I	5	200	x	x	3 samples (A, B, C)
10.08.2012	Du 12 / 10.8. / I	6	250	x	x	3 samples (A, B, C)
10.08.2012	Du 12 / 10.8. / I	7	300	x	x	3 samples (A, B, C)
10.08.2012	Du 12 / 10.8. / I	8	350		x	2 samples (A, B)
10.08.2012	Du 12 / 10.8. / I	9	400	x	x	3 samples (A, B, C)
10.08.2012	Du 12 / 10.8. / I	10	450	x	x	comment: Sediment/Sand
10.08.2012	Du 12 / 10.8. / I	11	500	x	x	3 samples (A, B, C)
10.08.2012	Du 12 / 10.8. / I	12	550	x	x	3 samples (A, B, C)
10.08.2012	Du 12 / 10.8. / I	13	600	x	x	

APPENDIX 11

Photographs from dendrochronological and ecological studies in the treeline zone

Mareike Wieczorek

Appendix 11-1: Lunch at the field site

Appendix 11-2: A sudden drop in temperature of more than 20 °C led to snow covered tents

Appendix 11-3: Sampling tree cores for dendrochronological analyses

Appendix 11-4: Detailed survey of larch seedling establishment in relation to vegetation and microrelief

APPENDIX 12

Samples from cores and exposures (Kytalyk, Achchagyi Alaikha)

Lutz Schirrmeister, Andrea Schneider, Vladimir Tumskoy

sample	depth (cm b.s.)	cryotexture	sediment	ice vol. (V%)	ice grav. (wt%)	ice abs. (wt%)	bulk density (g/cm^3)	TI
12-KYT-0507-1 Upper alas level, near the station, no polygon pattern, N 70.829367°, E 147.483233E°								
12-KYT-0507-1-1	6-11	massive to horizontal lens-like	silty fine sand, greyish-brown	51	32	24.2		
12-KYT-0507-1-2	41-50	lens-like reticulated	silty fine sand, grey	64	95	48.7		
12-KYT-0607-1, Upper alas level, near the station, no polygon pattern, N 70.829483°; E 147.48305E °								
12-KYT-0607-1-1	0-14		living moss					
12-KYT-0607-1-2	14-32	unfrozen	moss peat					
12-KYT-0607-1-3	32-41	horizontal micro lens-like	silty fine sand	51	40	28.6		
12-KYT-0607-1-4	41-55	massive	moss peat		267.9	72.8		
12-KYT-0607-1-5	55-62	reticulated	silty fine sand		74.8	42.8		x
12-KYT-0607-1-6	67-72	massive	peat layer		403	80.1		x
12-KYT-0607-1-7	75-86	ice belts	silty fine sand		62.3	38.4		x
12-KYT-0607-1-8	86-98	ice belts	silty fine sand	60	73	42.2		
12-KYT-0607-2, monitoring site, dry polygon center, N 70.83121°N; E 147.48299°E								
12-KYT-0607-2-1	20-27	layered	peat unfrozen					
12-KYT-0607-2-2	29-35	reticulated	peat frozen		298.0	74.9		
12-KYT-0607-2-3	40-50	reticulated	silty fine sand		68.4	40.6		x
12-KYT-0607-2-4	61-73	diagonal lens-like	peat		224.7	69.2		
12-KYT-0607-2-5	75-79	horizontal lens-like	silty fine sand with peat inclusions		172.4	63.3		x
12-KYT-0607-2-6	81-92	diagonal net-like	silty sand	84	217	68.5		
12-KYT-0607-2-7	92-103	Ice belts	silty sand	69	196.1	66.2		x

sample	depth (cm b.s.)	cryotexture	sediment	ice vol. (V%)	ice grav. (wt%)	ice abs. (wt%)	bulk density (g/cm^3)	TI
12-KYT-0807-1, Low center polygon with a small pond, N 70.830783°; E 147.48365°								
12-KYT-0807-1-1	20-30		unfrozen condensed peat					
12-KYT-0807-1-2	30-37		dark-brown frozen peat, shrub roots					
12-KYT-0807-1-3	37-46	lattice-like	grey silty fine sand with peat inclusions	39	30	23.1		
12-KYT-0807-1-4	46-56	lattice-like	grey silty fine sand		60.4	37.7		x
12-KYT-0807-1-5	56-60	horizontal	grey silty fine sand					
12-KYT-0807-1-6	60-70	horizontal ice lenses	Peaty silty fine-sand	80	191	65.6		
12-KYT-0807-1-7	70-80	diagonal lens-like	greyish to dark-brown cryoturbated peaty silt					
12-KYT-0807-1-8	80-91	diagonal lens-like	greyish to dark-brown cryoturbated peaty silt		197.2	66.4		x
12-KYT-0807-1-9	91-95		peaty silt					
12-KYT-0807-2, surface of the western Yedoma ridge, no polygon pattern, N 70.826233°; E 147.480483°								
12-KYT-0807-2-1	10 - 20		plant cover	67	93	48.2		
12-KYT-0807-2-2	20 - 35	horizontal lens-like	greyish-brown silty fine sand		42.4	29.8		
12-KYT-0807-2-3	35 - 42	massive	greyish-brown silty fine sand, thin roots	38	22	18		
12-KYT-0807-2-4	42 - 48	diagonal lens-like	dark-brown platy peaty silty fine sand		36.6	26.8		
12-KYT-0807-2-5	48 - 52	horizontal lens-like	greyish-brown silty fine sand					x
12-KYT-0807-2-6	52 - 61	horizontal lens-like	greyish-brown silty fine sand	39	36	26.5		
12-KYT-0807-2-7	61 - 70	horizontal lens-like	light-grey silty fine sand		106.8	51.6		x
12-KYT-0807-2-8	71 - 80	horizontal fine lens-like	greyish-brown silty fine sand, small peat inclusions		184.8	64.9		x
12-KYT-0807-2-9	80 - 90	horizontal lens-like	greyish-brown silty fine sand, small peat inclusions		67.9	40.4		x
12-KYT-0807-2-10	90 - 102	ataxitic	greyish-brown silty fine sand, small peat inclusions		108.3	52.0		x
12-KYT-0807-2-11	102 - 110	ataxitic	greyish-brown silty fine sand, small peat inclusions					

sample	height (m a.r.l.)	cryotexture	sediment
12-AA-1007-2 Achchagyi-Allaikha (70.560633°N, 147.44015°E)			
12-AA-1007-2-1	8-8.5	net-like, ice veins 1 mm thick	brownish-grey silty fine sand
12-AA-1007-2-2	9.0	net-like, ice veins 1 mm thick	brownish-grey silty fine sand
12-AA-1007-2-3	9.5	net-like and ataxitic	brownish-grey silty fine sand, peat inclusions (5-10 cm)
12-AA-1007-2-4	9.9	cryoturbated	dark-brown, grey, peaty paleosol
12-AA-1007-2-5	10.3	cryoturbated, fine lens-like	greyish-brown peaty loam
12-AA-1007-2-6	10.7	massive, structure less,	brownish, loamy silty fine sand
12-AA-1007-2-7-IW	8.5	old ice wedge, 0.5 m left	
12-AA-1007-2-8-IW	8.5	old ice wedge, 1.0 m left	
12-AA-1007-2-9-IW	9.5	younger, central ice wedge, penetrating the older ice wedge	
12-AA-1007-2-10-IW	9.5	younger, central ice wedge, penetrating the older ice wedge	
12-AA-1007-2-11-IW	9.0	old ice wedge, 0.5 m right	
12-AA-1007-2-12-IW	9.0	old ice wedge, 1.0 m right	
12-AA-1007-2-13-IW	10.5	younger ice wedge, penetrating the Allaikhovskaya S. in a wall-like bulge	
12-AA-1007-2-14-IW	11.0	younger ice wedge, penetrating the Allaikhovskaya S. in a wall-like bulge	
12-AA-1007-2-15	10.5	vertical ice veins 70 cm long, 1-2 cm wide	brown weakly bedded, silty fine-sand, grass roots
12-AA-1007-2-16	11.0	vertical ice veins 70 cm long, 1-2 cm wide	brown weakly bedded, silty fine-sand, grass roots
12-AA-1007-2-17	11.5	vertical ice veins 70 cm long, 1-2 cm wide	brown weakly bedded, silty fine-sand, thin vertical grass roots, 10 cm long
12-AA-1007-2-18	12.0	massive	fine-bedded silty fine-sand, thin vertical and horizontal grass roots, 10 cm long, flat peat inclusions (“kotletki”)
12-AA-1007-2-19	12.5	massive	fine-bedded silty fine-sand, thin vertical and horizontal grass roots, 10 cm long, flat peat inclusions (“kotletki”)
12-AA-1007-2-20	10.0	massive	less decomposed peat of the paleo active layer

APPENDIX 13

Sampling and measuring data from Advendaen

Andrea Schneider

A-13-1: List of samples, type and location of the studied ponds.
A – interpolygon pond water, E – intrapolygon pond water, R – rain water

Sample Code	Water Type	Coord.	Date	Ostracods	Sediment	Isotopes	Cations	Anions	backup
AD-1-1	A	78.18629 N, 15.92238 E	7/20/2013	x		x	x	x	x
AD-1-2	A		8/4/2013	x	x	x	x	x	x
AD-1-3	A		8/12/2013	x		x	x	x	x
AD-1-4	A		8/22/2013	x		x	x	x	x
AD-1-5	A		29/8/2013	x		x	x	x	x
AD-1-6	A		7/9/2013	x		x	x	x	x
AD-1-7	A		18/9/2013	x		x	x	x	x
AD-1-8	A		25/9/2013	x		x	x	x	x
AD-02	A	78.18742 N, 15.91527 E	8/6/2013	x	x	x	x	x	x
AD-03	A	78.18581 N, 15.91954 E	8/6/2013	x (2-3)	x	x	x	x	x
AD-04	A	78.18722 N, 15.91764 E	8/22/2013		x	x	x	x	x
AD-05	A	78.18747 N, 15.91754 E	8/22/2013		x	x	x	x	x
AD-06	E	78.18576 N, 15.92589 E	3/9/2013		x	x	x	x	
AD-07	E	78.18649 N, 15.92041 E	3/9/2013		x	x	x	x	
AD-08	E	78.18522 N, 15.92097 E	3/9/2013		x	x	x	x	
AD-09	A	78.18453 N, 15.92925 E	18/9/2013	x (2-3)	x	x	x	x	x
AD-10	E	78.18364 N, 15.91032 E	7/9/2013		x	x	x	x	x
AD-11	A	78.18484 N, 15.92827 E	18/9/2013		x	x	x	x	x
AD-12	A	78.18521 N, 15.93021 E	7/9/2013		x	x	x	x	x
AD-13	E	78.11225 N, 15.55167 E	3/9/2013		x	x	x	x	x
AD-Rain-1	R		8/8/2013 22:30			x			
AD-Rain-2	R		10/8/2013 16:00			x	x	x	
AD-Rain-3	R		13/8/2013 16:00			x			
AD-Rain-4	R		22/8/2013 14:00			x	x	x	
AD-Rain-5	R		4/9/2013 9:30			x			

A-13-2: Physico-chemical features of the monitoring site AD-01 and the ponds AD-2 to AD-13.

Sample Code	T Air (°C)	T Water (°C)	pH	EC (µS/cm)	O2 (mg/l)	Alkalinity (mmol/l)	Acidity (mmol/l)	total hardness (mmol/l)	total hardness (°dH)
AD-1-1	7.3	7.1	6.7	170	8.8	0.8	0.20	0.8	3.5
AD-1-2	9.1	11.9	6.9	164	10.2	1.0	0.20	0.6	2.5
AD-1-3	5.5	5.2	6.9	166	8.8	0.9	0.10	0.5	2.1
AD-1-4	11.3	8.2	7.0	175	10.8	1.0	0.20	0.6	2.0
AD-1-5	9.0	7.80	6.81	267	9.4	0.6	0.20	1.0	4.5
AD-1-6	5.2	5.2	7.07	316	10.9	0.9	0.15	1.0	5.0
AD-1-7	7.2	3.4	6.77	347	9.8	1.1	0.20	1.2	6.0
AD-1-8	-3.7	1.8	6.48	377	12.0	1.0	0.20	1.5	7.0
AD-02	11.20	12.70	6.40	133	8.1	0.6	0.40	0.4	1.0
AD-03	11.10	12.80	6.50	378	8.6	0.6	0.40	1.0	4.5
AD-04	9.40	8.40	6.50	275	10.0	0.5	0.20	0.8	3.5
AD-05	8.50	9.80	6.10	213	10.6	0.8	0.20	0.6	2.0
AD-06	8.50	6.40	5.18	1016	9.6	0.2	0.15	3.2	17.0
AD-07	6.60	7.40	5.2	1416	10.9	0.4	0.20	3.0	16.0
AD-08	7.60	3.30	5.5	444	8.8	0.4	0.20	1.4	7.0
AD-09	9.00	4,2	6.30	137	10.6	0.2	0.20	0.6	2.0
AD-10	5.40	4.60	6.20	308	10.6	0.2	0.20	1.0	4.0
AD-11	9.40	3.90	6.50	423	11.2	0.7	0.20	1.5	7.5
AD-12	5.50	5.00	5.30	372	12.0	0.2	0.20	1.2	6.0
AD-13	8.5	4.3	5.3	714	10.1	0.2	0.20	2.0	10.0

A-13-3: Dimensions, substrate description, sampling depths of the studied ponds.

Sample Code	Diameter (m)	Depth (cm)	Thaw depth center (cm)	Thaw depth rim (cm)	Substrate	Sample depth Hydrochemistry (cm)	Sample depth Sediments (cm)	Sample depth Exhauster (cm)
AD-1-1		26	51	50	moss, submerged vegetation	15		15
AD-1-2		22	66	53-57		15	15	15
AD-1-3		24	69	62-68		15		15
AD-1-4		28	68 - 69	70		15		15
AD-1-5		32	65	70		15		15
AD-1-6		25	77	68-80		15		15
AD-1-7		30	71	74		15		15
AD-1-8		35	77	73		15		15
AD-02	10 x 14.5	15	75	39	moss, submerged vegetation	5	15	15-20
AD-03	6 x 8	9	78	50	moss, submerged vegetation	5	9	9
AD-04	18 x 20	23	72 - 75	78.00	moss, submerged vegetation	15	23	
AD-05	6 x 10	14	75 - 78	86 - 89	moss, submerged vegetation	12	15	
AD-06	1 x 16	29	68	90 - 95	moss, submerged vegetation, some minerogenic sediment	15	30	
AD-07	1 x 14	21	65	98 - 103	moss, submerged vegetation	15	25	
AD-08	1 x 8 x 21	14	47	85 - 90	moss, submerged vegetation, orange-brownish layer, some minerogenic sediment	15	15	
AD-09	7 x 13	21	81	55-60	moss, submerged vegetation	15	15	15-20
AD-10	30 x 1	23	65	82 - 89	moss, submerged vegetation	15	15	
AD-11	43 x 13	30	63	58-60	moss, submerged vegetation	15	15	
AD-12	10 x 7	22	69.0	77-80	moss, submerged vegetation	15	15	
AD-13	0.5 x 25	30	60.0	93 - 98	moss, submerged vegetation, some minerogenic sediment	15	30	

Die **Berichte zur Polar- und Meeresforschung** (ISSN 1866-3192) werden beginnend mit dem Band 569 (2008) als Open-Access-Publikation herausgegeben. Ein Verzeichnis aller Bände einschließlich der Druckausgaben (ISSN 1618-3193, Band 377-568, von 2000 bis 2008) sowie der früheren **Berichte zur Polarforschung** (ISSN 0176-5027, Band 1-376, von 1981 bis 2000) befindet sich im electronic Publication Information Center **(ePIC)** des Alfred-Wegener-Instituts, Helmholtz-Zentrum für Polar- und Meeresforschung (AWI); see http://epic.awi.de. Durch Auswahl "Reports on Polar- and Marine Research" (via "browse"/"type") wird eine Liste der Publikationen, sortiert nach Bandnummer, innerhalb der absteigenden chronologischen Reihenfolge der Jahrgänge mit Verweis auf das jeweilige pdf-Symbol zum Herunterladen angezeigt.

The **Reports on Polar and Marine Research** (ISSN 1866-3192) are available as open access publications since 2008. A table of all volumes including the printed issues (ISSN 1618-3193, Vol. 377-568, from 2000 until 2008), as well as the earlier **Reports on Polar Research** (ISSN 0176-5027, Vol. 1-376, from 1981 until 2000) is provided by the electronic Publication Information Center **(ePIC)** of the Alfred Wegener Institute, Helmholtz Centre for Polar and Marine Research (AWI); see URL http://epic.awi.de. To generate a list of all Reports, use the URL http://epic.awi.de and select "browse"/ "type" to browse "Reports on Polar and Marine Research". A chronological list in declining order will be presented, and pdf-icons displayed for downloading.

Zuletzt erschienene Ausgaben:

Recently published issues:

697 (2016) Studies of Polygons in Siberia and Svalbard**,** edited by Lutz Schirrmeister, Liudmila Pestryakova, Andrea Schneider and Sebastian Wetterich

696 (2016) The Expedition PS88 of the Research Vessel POLARSTERN to the Atlantic Ocean in 2014, edited by Rainer Knust and Frank Niessen

695 (2016) The Expedition PS93.1 of the Research Vessel POLARSTERN to the Arctic Ocean in 2015, edited by Ruediger Stein

694 (2016) The Expedition PS92 of the Research Vessel POLARSTERN to the Arctic Ocean in 2015, edited by Ilka Peeken

693 (2015) The Expedition PS93.2 of the Research Vessel POLARSTERN to the Fram Strait in 2015, edited by Thomas Soltwedel

692 (2015) Antarctic Specific Features of the Greenhouse Effect: A Radiative Analysis Using Measurements and Models by Holger Schmithüsen

691 (2015) Krill in the Arctic and the Atlantic Climatic Variability and Adaptive Capacity by Lara Kim Hünerlage

690 (2015) High latitudes and high mountains: driver of or driven by global change? 26th Intern. Congress on Polar Research, 6 – 11 September 2015, Munich, Germany, German Society for Polar Research, edited by Eva-Maria Pfeiffer, Heidemarie Kassens, Christoph Mayer, Mirko Scheinert, Ralf Tiedemann and Members of the DGP Advisory Board

689 (2015) The Expedition PS89 of the Research Vessel POLARSTERN to the Weddell Sea in 2014/2015, edited by Olaf Boebel

688 (2015) The Expedition PS87 of the Research Vessel POLARSTERN to the Arctic Ocean in 2014, edited by Rüdiger Stein

ALFRED-WEGENER-INSTITUT
HELMHOLTZ-ZENTRUM FÜR POLAR-
UND MEERESFORSCHUNG

BREMERHAVEN

Am Handelshafen 12
27570 Bremerhaven
Telefon 0471 4831-0
Telefax 0471 4831-1149
www.awi.de

HELMHOLTZ
GEMEINSCHAFT